Cartilage Wear simulation models for Surface and Spacer Hemiarthroplasty and Tissue Engineering

Ewen Jody Northwood MEng (Hons)

Submitted in accordance with the requirements for the degree of

Doctor of Philosophy

School of Mechanical Engineering
University of Leeds
Leeds, UK

April 2007

Acknowledgements

First and foremost I would like to thank my wife to be, Emma. She is my rock, my guild and my best friend, without her I would not have started this PhD let alone finished it.

Secondly, I would like to thank my supervisor Professor John Fisher for allowing me the freedom to explore new ideas, having the confidence in me to give me the initial project and for the immense technical and general support he has provided to me over the last three years. In addition, I would also like to thank Professor Jin and Professor Ingham for their additional support and advice. An extra special thank you should also go to Professor Fellows (Aunty) who took the time to read my work and helped beyond measure.

I would also like to express a huge thank you to all the technical and laboratory support within the mechanical engineering department, in particularly Devon Derby, Phil Wood, Adrian Eagles and Lee Wetherill. For their patient, understanding and willingness to help, it made it an experience.

Additionally, a huge thank you should go to my parents and the boys (you know who you are!), whose support, guidance and sense of humour made me laugh, see the positive side when things were down, brought a poor student beers when we were out and helped make the last 3 years seem more like my undergraduate again than real work.

I would also like to thank Diane Baker and Rick Kowalski at DePuy CMW for providing me with the help and samples I needed, even at very short notice.

Finally, I would like to acknowledge all the PhD students past and present who have helped to make it an enjoyable experience.

Abstract

Understanding the wear of the biomaterial/cartilage interface is vital in the development of more satisfactory materials for use in the clinical repair of worn or damaged synovial joints. The aims of this study were to investigate a wide range of biphasic hydrogels as potential chondroplasty materials and to further the understanding of natural joint tribology. The mechanical properties of each potential chondroplasty material were quantified and their tribological performance investigated by means of a series of simple geometry friction and wear studies in Ringer's solution and a protein-containing lubricant. Also uni- and multi-directional continuous sliding tests in a protein-containing lubricant were conducted under various loading conditions to evaluate the friction and degradation of each material and that of the opposing articular cartilage surface. A number of potential chondroplasty materials were also evaluated as defect repair materials when implanted using a proposed clinical method. Selected biphasic hydrogel materials showed a marked reduction in dynamic friction, degradation and articular cartilage pin damage when compared with single-phase materials. Following continuous wear studies, alterations in opposing cartilage surface topography were found to be associated with increased levels of dynamic friction.

The protocols devised in this study are the first to yield objective and quantifiable data demonstrating a reduction in friction and opposing cartilage surface degradation following the implantation of certain biphasic hydrogel defect repair materials. They also demonstrate the potential of biphasic hydrogels to act as superior chondroplasty materials compared with currently available materials. Future work will focus on the optimisation of biphasic hydrogel properties, including the long-term durability and immunogenicity of each material following implantation, in order that materials will more closely mimic the tribology of natural articular cartilage.

Table of Contents

Table of Figures

Abbreviations

γ	Coefficient of Friction
Ø	Diameter
μm	micrometer
ACI	Autologous Chondrocyte Implantation
AEA	Acoustic Emission Analysis
BL	Boundary Layer
DPPC	Dipalmitoyl Phosphatidylcholine
E	Elastic modulus
ECM	Extra-cellular Matrix
EHL	Elastic-Hydrodynamic Lubrication
ESEM	Environmental-Scanning Electron Microscopy
EWC	Equilibrium Water Content
FCD	Fixed Charge Density
GAG	Glycosaminoglycan
HA	Hyaluronic Acid
LVDT	Linear Variable Displacement Transducer
OA	Osteoarthritis
PCM	Pericellular Matrix
PVA-H	Polyvinyl Alcohol Hydrogel
SF	Synovial Fluid
SAL	Surface Amorphous Layer
SAPL	Surface Active Phospholipid Layer
SAL	Surface Amorphous Layer
SEM	Scanning Electron Microscopy
SIPN	Semi-Interpenetrating Network
UHMWPE	Ultra High Molecular Weight Polyethylene
WLI	White Light Interferometry

1 Introduction

The understanding of synovial joint pathology and a search for effective treatments has been the objective of research for centuries. Hunter et al discussed the anatomy and pathology of articular cartilage as early as 1743 *(Hunter, 1743)* and since that time several treatments and a range of full and hemiarthroplasty treatments have been developed. However, the quest to reduce patient trauma, increase efficacy and availability of new and current treatments continues. New materials and techniques such as artificial cartilage material and the injection of high molecular weight hyaluronic acid lubricants have all been developed with these objectives in mind.

The development of effective defect repairs and hemiarthroplasty techniques requires not only the objective quantification of the potential implant material's wear and tribological performance but also the objective evaluation of degradation and wear to the surrounding and opposing cartilage surfaces following implantation. A key objective in achieving this is to understand the friction and wear of articular cartilage within normal healthy synovial joints and following a number of surgical solutions. An aim of this study was to create a viable model which will allow this understanding to be enhanced. The combination of traditional engineering disciplines such as biomechanical, tissue and biochemical studies is fundamental to further success in this kind of research.

To understanding pathology of synovial joint disease, and how disease affects normal function, it is essential to first understand the physiology, histology and relationships within healthy synovial joints. Synovial joint physiology and tribology was first studied over a century ago *(Reynolds, 1886, Macconaill, 1932)*. Today, lubrication and friction within the joint, in particular on the lubricating properties of synovial fluid and frictional characteristic of articular cartilage is a major research area.

1.1 Definition and Classification of Joints

Mammalian joints are categorised according to the joint anatomy, joint articulation and the characteristics of the joint tissue. The articulations are divided into three classes: synarthroses or immovable, amphiarthroses or slightly movable, and diarthroses or freely movable joints *(Gray, 1918)* . Of these classes it is diarthrodial (synovial) joints which will be the subject of this literary review.

1.2 Diarthrodial (Synovial) Joints

In a diarthrodial joint the interfacial bony surfaces are covered with articular cartilage, and connected by ligaments lined by a synovial membrane. The joint may be divided, completely or incompletely, by an articular disk or meniscus, the periphery of which is continuous with the fibrous capsule while its free surfaces are contained by the synovial membrane *(Gray, 1918)*. Within the knee the articulating surfaces are not congruent *(Norkin and Levingie, 1983)*, and the meniscus aids both load bearing and lubricating properties.

Like all diarthrodial joints, the knee is lined with a metabolically active tissue, the synovium, which secretes the synovial fluid providing nutrients and also removes waste products from the intra-articular tissues *(Mow and Hayes, 1997, Kingston, 2000)*. The synovium and the two articulating surfaces form the joint capsule, which contains synovial fluid forming a closed biomechanical bearing. This can be seen in Figure 1-1. The joint capsule allows a large degree of relative motion and has a remarkable potential to remain functional over the human lifetime *(Mow and Hayes, 1997, Norkin and Levingie, 1983, Forster and Fisher, 1999)*.

The joint capsule consists of two layers, the stratum fibrosum (outer layer) and the stratum synovium (inner layer) *(Norkin and Levingie, 1983)*. The fibrosum is a dense fibrous tissue which completely encloses the bony components *(Norkin and Levingie, 1983)*. It is reinforced by surrounding

muscle and tendons that cross the joint *(Norkin and Levingie, 1983, Kingston, 2000)*. This increases joint stability and allows efficient function.

The very poor vascular supply to the joint capsule *(Norkin and Levingie, 1983)* has a significant negative effect on joint regeneration. It is also believed that the nerve endings located in the fibrosum are sensitive to mechanical stimuli such as compression, tension, vibration. Studies have also suggested that the nerve endings with the fibrosum supply information about the rate and direction of the joint movement *(Wyke, 1967, Norkin and Levingie, 1983)*.

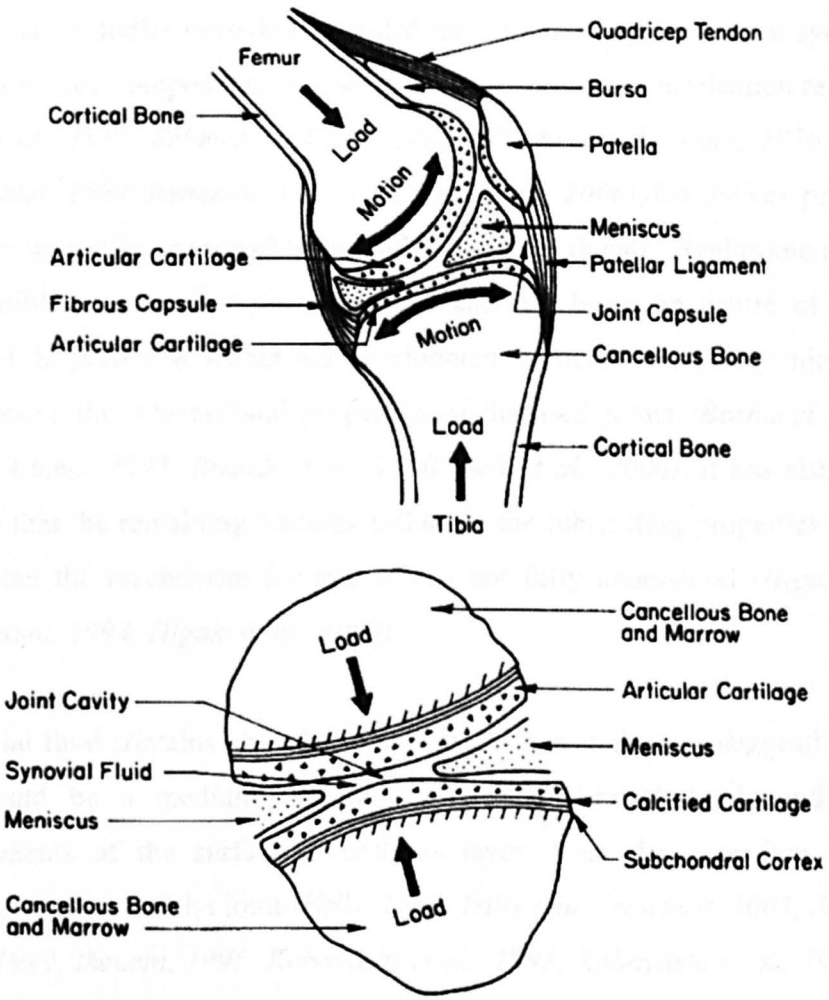

Figure 1-1: A schematic diagram of a Synovial Joint *(Mow and Hayes, 1997)*.

1.2.1 Synovial Fluid

Synovial fluid (SF) has been the topic of much research over the years but the small yields from a healthy human knee, between 0.5 to 2ml, has meant much of the research has been completed on samples from larger animals, particularly bovine. A clear or yellowish colour, SF comprises of a dialysate of blood plasma without clotting factors, and a number of proteins and phospholipids polysaccharides such as hyaluronic acid (HA) as well as erthrocytes, haemoglobin *(Mow and Hayes, 1997)*. The function of these components has been investigated in various *in vitro* studies *(Higaki and Murakami, 1994, Higaki and Murakami, 1995, Bell et al., 2006)*.

A number of studies have demonstrated the lubricating properties of synovial fluid or its key components, in particular under boundary lubrication regimes *(Jay et al., 1998, Schmidt and Sah, 2006, Wright and Dowson, 1976, Hills and Butler, 1984, Reimann et al., 1975, Bell et al., 2006)*, but the key proteins or other molecules responsible are still a source of debate. Hyaluronic acid is responsible for synovial joint viscosity and has been the centre of much research in particular within the development of hemiarthroplasty injections to improve the lubricational properties of diseased joints *(Barbucci et al., 2002, Adams, 1993, Brandt et al., 2000, Bell et al., 2006)*. It has also been shown that the remaining proteins influence the lubricating properties of the fluid, but the mechanism for this is still not fully understood *(Higaki and Murakami, 1994, Higaki et al., 1998)*.

Synovial fluid contains phospholipids and this has lead to the suggestion that SF could be a medium for the transport of phospholipids and other components of the surface amorphous layer, from the synovium to the bearing surfaces of the joint *(Hills, 1988, Hills and Crawford, 2003, Jay and Cha, 1999, Ikeuchi, 1995, Kobayashi et al., 1995, Kobayashi et al., 1996)*. It has been shown that SF deposits a layer containing phospholipids on to glass plates *in vitro (Hills, 1988)*. However the role of phospholipids lubrication is still unclear. For more information the reader is directed to Chapter 1.3.

To understand the biomechanics of the synovial joint it is essential to understand the visco-elastic properties of synovial fluid. It has been shown that at low shear rates ($0.1s^{-1}$), the viscosity of synovial fluid is in the tens of Pa s, however at higher shear rates ($1000s^{-1}$) it is in the region of a hundredth Pa s *(Cooke et al., 1978)*. This clearly shows non-Newtonian behaviour *(Massey, 1968)*. Within normal healthy *in vivo* conditions the viscosity of synovial fluid is little more than twice the viscosity of water *(Chan et al., 2000)*.

1.3 Articular Cartilage

Avascular cartilage tissue forms a thin layer on the articulating surfaces of the synovial joint resulting in protection of the bony components from wear created by the joint movement. The lubrication and wear properties associated with synovial joints are remarkable *(Unsworth, 1991)*. The main functions of this compliant tissue layer are to spread the applied load over a larger area of the joint *(Brown et al., 2001)*, and provide the mechanism to reduce friction and wear. Cartilage achieves levels of lubrication and friction reduction far beyond that seen in traditional mechanical bearings. To understand how cartilage can achieve these outstanding levels of lubrication it is necessary to understand its fundamental structure and how cartilage physiologically changes under varying loads and frequencies.

Cartilage structure can be thought of as two interacting organic matrices within a reactant fluid. Cartilage cells (chondrocytes) are surrounded by a matrix rich in collagen, called the pericellular matrix (PCM) which provides a microenvironment for the chondrocytes. Collagen is the main structural protein found in ligaments, skin and bone. It has a high content of the amino acid 'Proline' which contributes to collagens elasticity and strength. A number of PCM's combine together with proteoglycans to form an extra-cellular matrix (ECM). The collagen fibrils and the proteoglycans give articular cartilage its structure and support the internal mechanical stresses which results from loads being applied to the joint. This structure, together

with ion-filled water, gives articular cartilage its biomechanical properties *(Mow et al., 1984, Mow et al., 1980a)*. The ECM forms the bulk of the tissue and is responsible for many of its properties, especially the mechanical characteristics *(Stockwell, 1979)*.

The collagen content of articular cartilage is 10-30 % of the wet weight, with the proteoglycans accounting for 3-10% *(Muir, 1980)*. The remaining 60-87% of cartilage consists of water, inorganic salts and small quantities of other matrix proteins *(Mow and Hayes, 1997)*.

The anisotropic properties of cartilage means the reaction to loading and direction vary but these properties are not fully understood. There have been many studies to try to understand and model the properties of cartilage and other hydrated biological soft tissues. The biphasic model *(Mow et al., 1980a, Mow et al., 1990b)* assumed both the solid matrix phase and the interstitial fluid phase of the tissue to be immiscible and each phase to be separate and incompressible. The model, although very useful, does make some major assumptions including an assumption that cartilage processes two distinct phases, solid and fluid. The model was developed into a triphasic theory *(Lai et al., 1991)* which assumes a third miscible phase, an ionic phase. The triphasic theory took into account the electromagnetic interactions between the charged atoms within the ECM. The model did increase the accuracy when compared with the initial biphasic model *(Mow et al., 1980a)* but a comprehensive model still requires further development.

The structure of cartilage is inhomogeneous and traditionally has been considered as four distinct layers. The composition and structure of cartilage changes with the depth from the joint surface *(Buckwalter, 1983, Lipshitz et al., 1976)*. A schematic representation of the layered structure with percentage thicknesses can be seen in Figure 1-2. Krishnan et al suggested that the inhomogeneous structure of cartilage enhances the superficial fluid support at the surface and thus contributes to a reduction in the friction and wear at the surface *(Krishnan et al., 2004a)*. This study also demonstrated

that the inhomogeneity of the structure did not promote uniformity in the stresses and strains experienced by the material. It should be noted that the study used a finite element model with a number of theoretical assumptions, in particular the phasic nature of the internal structure.

However, recent research has suggested an additional mono or multi-layer membrane on the cartilage surface. This Surface Amorphous Layer (SAL) is itself thought to comprise of two layers. Above the superficial tangential zone is a layer of glycosaminoglycans (GAGs) and proteins, void of collagen fibrils and chondrocytes with proportionally high water content. This portion of the SAL is thought to vary in thickness between 2- 200μm across the tibial and femoral surfaces *(Hills and Butler, 1984, Hills and Crawford, 2003, Pickard et al., 1998b, Graindorge et al., 2005)*. Additional studies have suggested a primary layer above the GAG and protein layer composed of phospholipids called the Surface Active Phospholipid Layer (SAPL), thought to be approximately 10μm thick *(Kobayashi et al., 1996, Kobayashi et al., 1995)*.

The SAL can be irregular and visualisation methods can make distinguishing between the main collagenous layer and the SAL very difficult *(Kobayashi et al., 1995, Graindorge et al., 2005, Kobayashi et al., 1996)*. Earlier studies using SEM and TEM have demonstrated a layer of non-collagenous tissue with a proportionally higher water content *(Gardner and McGillivray, 1971, Kobayashi et al., 1995, Hills and Butler, 1984)*. However, sample preparation required dehydration which would affect the water content and geometry of the surface layers. It is therefore vital to visualise the surface in a fully hydrated state.

Recent studies have demonstrated the removal of this SAL using Indian ink staining and other visualisation techniques. The subsequent analysis showed the SAL comprised of 37% proteins (lubricin), 33.3% GAGs and 29.7% phospholipids *(Ferrandez and Graindorge, 2003)*. Recent work has also suggested a regeneration of the SAL from the underlying collagenous layer.

This regeneration could be a reason for the variation in results friction studies. This membrane of phospholipids, glycosaminoglycans and proteins and its contribution to lubrication is still a source of debate.

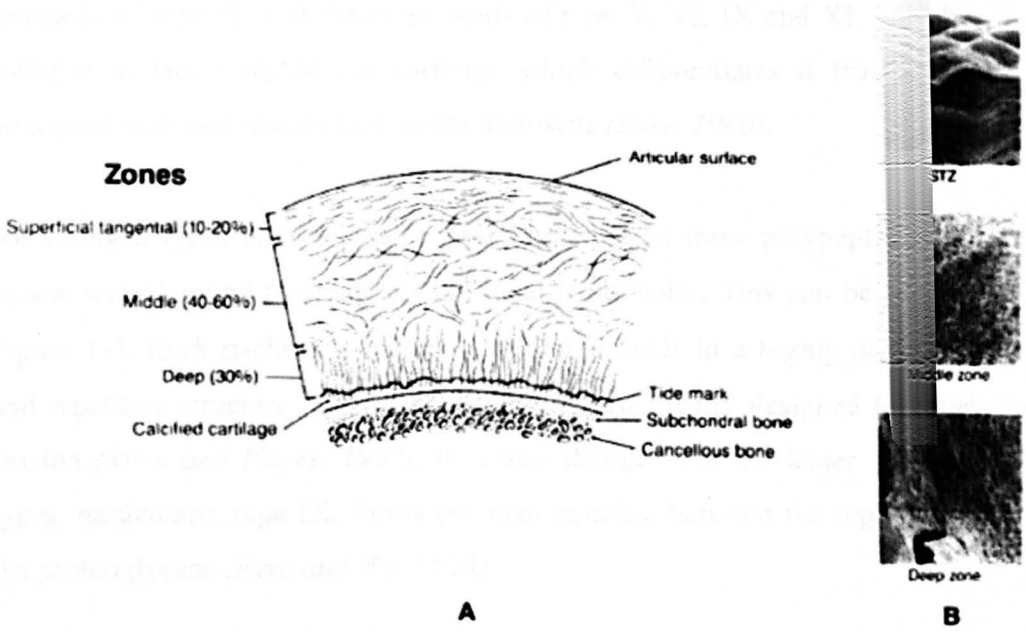

Figure 1-2: A schematic diagram showing the traditional four distinct layers of the articular cartilage structure *(Mow and Hayes, 1997)*.

The highly complex nature of articular cartilage means that it is very difficult to apply traditional engineering properties to the material. However, using biphasic models and experimental results, research does state a representative range of the effective Young's Modulus for physiological loading frequencies to be 10-20MNm^{-2} *(Freeman, 1979)*. It has also been demonstrated that articular cartilage is exposed to contact pressure of between 3-5 MPa during normal walking and up to 18 MPa during other activities such as stair climbing and rising from a chair *(Morrell et al., 2005, Freeman, 1979, Mow and Hayes, 1997)*.

The use of enzymatic degradation to simulate the onset of clinical diseases or to isolate potential key lubricating components of the articular cartilage structure has been widely used. The use of Chondroitinase ABC to selectively degrade the proteoglycan structure has demonstrated alterations in the mechanical properties such as Young's modulus *(Lyyra et al., 1999)* and friction *(Pickard et al., 1998a, Jin et al., 2000, Katta et al., 2006)*

1.3.1 Collagen

The protein collagen is the largest molecular component in the ECM. There are 18 different types of collagen, with articular cartilage being made up primarily of type II, with lesser amounts of type V, VI, IX and XI. It is the collagen variation within the cartilage which differentiates it from other biological hydrated tissues such as the meniscus *(Eyre, 1980)*.

All collagen types have the same basic structure of three polypeptide (α-) chains wound round to create a right hand triple helix. This can be seen in Figure 1-3. Each α-chain is made up of amino acids in a highly organized and repetitive structure. This structure seems specifically designed to resist tension *(Mow and Hayes, 1997)*. It is also thought that the lesser collagen types, particularly type IX, forms covalent bonding between the type II and the proteoglycans *(Eyre and Wu, 1995)*.

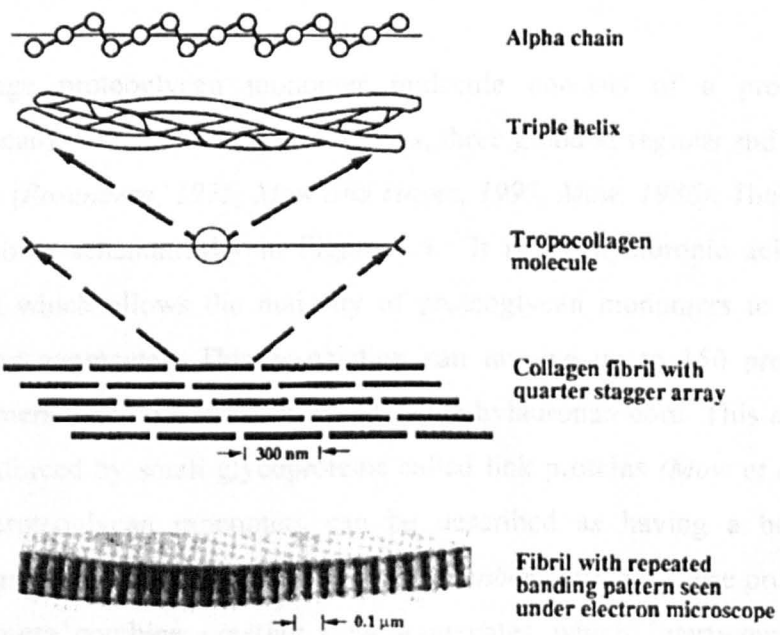

Figure 1-3: Diagram of Collagen helix and its components *(Mow and Hayes, 1997)*.

Collagen fibres have a high tensile strength, approximately 15 -30 Nm^{-2}, weight to weight which is equivalent to steel *(Harkness, 1968)*. Therefore, the density of the fibres, fibre size, orientation and the crosslink bonding

gives cartilage its overall mechanical stability and high tensile strength *(Nimni, 1988)*. The high tensile strength is also important in maintaining the internal swelling pressure, which allows the cartilage to resist relatively high compressive loads *(Hardingham et al., 1986)*. More detail on the osmotic swelling pressure is given below.

1.3.2 Proteoglycans

A main component of the ECM, proteoglycans are complex molecules build from monomer which consist of a protein core to which one or more glycosaminoglycans (GAGs) are covalently attached *(Mow and Hayes, 1997)*. Cartilage proteoglycans are protein–polysaccharide molecules which exist as a monomers or aggregates *(Muir, 1980)*. Aggregates form from monomers creating large macromolecules. Both contribute to the material properties. In cartilage large aggregating proteoglycans (aggrecan and versican) form 50-85% of the proteoglycan content, while the smaller proteoglycans probably contribute 10% *(Mow and Hayes, 1997)*.

Cartilage proteoglycan monomer molecule consists of a protein core (aggrecan) with several distinct regions, three globular regions and a binding region *(Rosenberg, 1975, Mow and Hayes, 1997, Mow, 1986)*. These regions are shown schematically in Figure 1.4. It is the hyaluronic acid binding region which allows the majority of proteoglycan monomers to associate, forming aggregates. This association can involve up to 150 proteoglycan monomers, non-covalently attached to the hylauronan core. This attachment is reinforced by small glycoproteins called link proteins *(Mow et al., 1992)*. The proteoglycan monomers can be described as having a bottle bush structure, see Figure 1-4 *(Mow, 1986, Rosenberg, 1975)*. These proteoglycan monomers combine creating long aggregates which intertwine with the collagen matrix.

Within the ECM there are a number of complex reactions or interactions taking place which all contribute to the overall properties. *In vivo* the sulphate (SO4) and carboxyl (COOH) groups of the chondroitin sulphate and keratan

sulphate, shown in Figure 1-4, have a negative charge. This creates a swelling pressure or fixed charge density (FCD) in two ways. Firstly the GAGs have an overall negative charge and tend to repel each other and this electromagnetic force is increased when the ECM is under a compressive load. It has also been shown that within interfibullar space, proteoglycans are compressed to approximately 20% of their none constrained dimensions. This also increases the reaction forces between the negatively charged GAGs. *(Muir, 1983, Rosenberg, 1975, Mow et al., 1990b)*

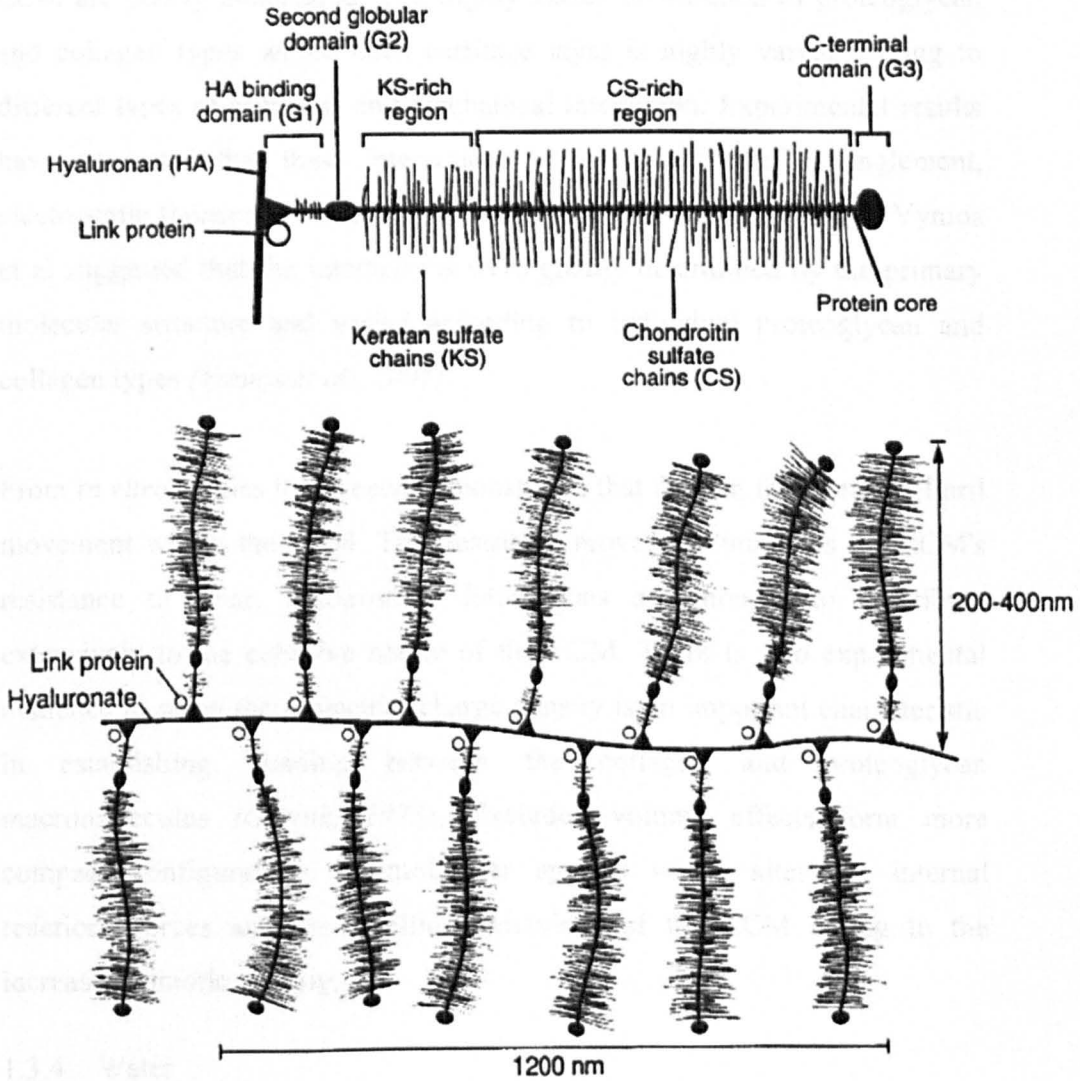

Figure 1-4: Schematic representation of an aggregating proteoglycan monomer molecule composed of an extended protein core with several distinct domains (top), and a proteoglycan aggregate with many proteoglycan monomers attached to a chain of hylauronate (bottom). ***(Mow and Hayes, 1997)***

Secondly to maintain an overall neutral charge, the GAGs attract positively charged ions e.g., Na+. This leads to a higher concentration of total ions within the ECM than in the ambient environment. This charge imbalance also causes a pressure gradient across the ECM. This pressure gradient is known at the Donnan Osmotic pressure *(Donnan, 1924, Mow and Hayes, 1997, Edwards, 1966)*.

1.3.3 Proteoglycan and Collagen Interactions

The interactions between proteoglycan and collagen macromolecules in the ECM are poorly understood. The highly varied distribution of proteoglycan and collagen types within each cartilage layer is highly varied leading to different types of chemical and mechanical interaction. Experimental results have suggested that these interactions involve mechanical entanglement, electrostatic forces and excluded volume effects *(Mow et al., 1990c)*. Vynios et al suggested that the interactions were greatly determined by the primary molecular structure and varied according to individual proteoglycan and collagen types *(Vynios et al., 2001)*.

From *in vitro* studies it has been demonstrated that friction forces retard fibril movement within the ECM. This restricted movement increases the ECM's resistance to wear. Electrostatic interactions are thought to contribute extensively to the cohesive nature of the ECM. There is also experimental evidence to show the molecular charge density is an important characteristic in establishing bonding between the collagen and proteoglycan macromolecules *(Obrink, 1973)*. Excluded volume effects form more compact configurations of molecular species which alter the internal reactions forces and the swelling behaviour of the ECM owing to the increased osmotic activity.

1.3.4 Water

The major component by weight in the ECM is water, 20-30% of collagen weight is associated water as is also approximately 80% of the wet weight of cartilage *(Mow, 1986, Mow and Hayes, 1997)*. The water provides a medium which allows the movement of gases, nutrients and waste products between

chondrocytes to the synovium *(Mankin and Thrasher, 1975)*. Positive ions in the water are attracted to the negative charge on the proteoglycans. This attraction of positive ions to the ECM gives the water within it an overall positive charge. These ions include sodium, potassium and calcium. This strong relationship between the proteoglycans and the ion filled water is very important within ECM and has major effects on mechanical loading properties of cartilage.

Approximately 30% of water within the ECM occupies the intrafibrillar space of collagen, and appears to be excluded from mechanical and proteoglycan charge effects. The remaining water can be transported by charge variation or mechanical loading through the interstitial network *(Mow, 1986, Mow et al., 1990b, Mow et al., 1990a, Stockwell, 1979)*. This transportation of fluid is affected by three factors;

a) the Fixed Charge Density (FCD) and associated swelling pressure.
b) the organisation of the collagen matrix.
c) the mechanical properties of the network *(Mow and Hayes, 1997)*.

The expulsion of the interstitial fluid affects the overall properties in a number of ways, firstly the removal of the ion filled water causes an increase in the repulsion forces between the negatively charged proteoglycans. Secondly, the interstitial water flow through the ECM exerts a nonlinear compression effect on the ECM. This strain-dependent permeability means an increased resistance to prolonged compression forces *(Mow and Hayes, 1997, Maroudas, 1976, Wachtel and Maroudas, 1998)*.

1.3.5 Chondrocytes

Accounting for approximately 10% by volume of mature cartilage, these cells are embedded in lacunae within the cartilage matrix. Surrounding each chondrocyte is a highly organised network of collagen, proteoglycans and other proteins forming the PCM. It has been demonstrated that the presence and interaction of the PCM and chondrocytes is an important factor in ECM production and maintenance *(Stockwell, 1979)*.

Chondrocytes are responsible for creation, maintenance and remodelling the ECM structure. Chondrocytes control the synthesis and balance of matrix proteins by the use of enzymes such as the collagenase group, which breakdown the collagen structure. Chondrocytes constantly vary in size, shape and distribution within the defined layers of cartilage *(Stockwell, 1979)*, with higher concentrations within the Deep Zone and a flatter elongated shape towards the Superficial Tangential Zone (STZ). This is shown in Figure 1-5. Chondrocytes have been shown to maintain considerable metabolic activity essential in physiological maintenance of the ECM and its components *(Stockwell, 1979, Shepherd, 1997)*.

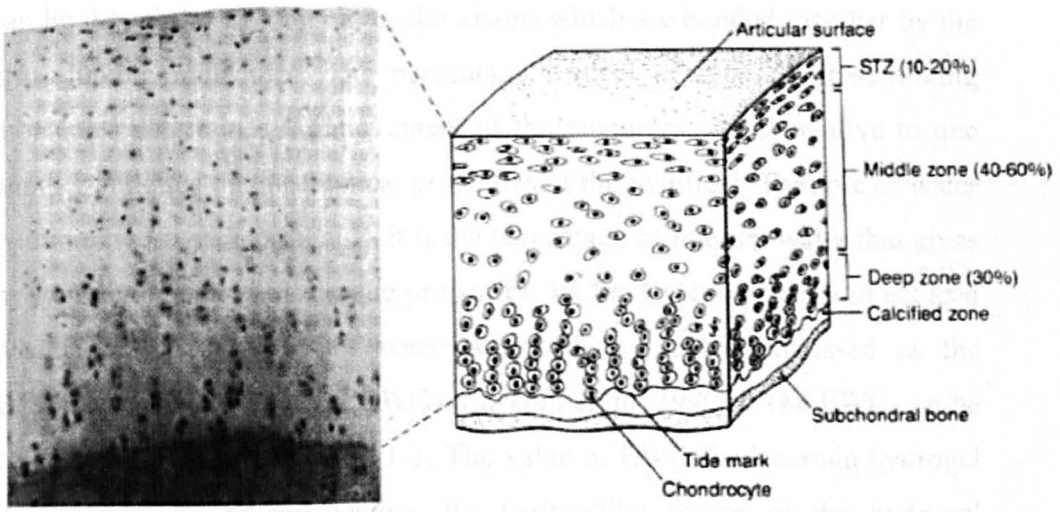

Figure 1-5: A schematic representation of the distribution of chondrocytes within the articular cartilage layer ***(Mow et al., 1990c)***

Chondrocyte activity within the ECM is thought is be stimulated by cyclic loading and the associated stress and strain *(Stockwell, 1979, Murakami et al., 2003)*. Loading frequencies associated with normal actively such as walking have been shown to stimulate chondrocyte synthesis and encourage movement of chondrocytes to the deeper layers of the ECM. These responses to external stimuli allow greater resistance to compressive loading and efficient recovery from excessive deformation *(Murakami et al., 2003,*

Urban, 1994). Finite Element Model (FEM) studies have shown that initial high values of strain are likely to give a large stimulus to the chondrocytes of the surface layer, which is capable of controlling the metabolic activity of the chondrocytes *(Murakami et al., 2003)*.

1.4 Hydrogel Polymers

1.4.1 Hydrogel Structure and Internal Bonding

The use of hydrogel polymers within the health care industry has been investigated for over 50 year and their use has infiltrated a wide range of areas from contact lenses to skin graft scaffolding. A hydrogel polymer comprises fundamentally of three main parts; monomer chains, cross-linking molecules and water molecules. The monomer or backbone to the hydrogel can be thought of as long molecular chains which are bonded together by the cross-linking molecules. The percentage content or type of cross-linking molecules determines the movement of the monomer chains relative to one another and thus the mechanical properties of the hydrogel. The role of water within a hydrogel is critical as it is the percentage of internal water that gives hydrogel polymers their unique properties. Its fundamental role is to act as a plasticizer. The amount of water absorbed is usually expressed as the Equilibrium Water Content (EWC) *(Corkhill et al., 1990a)*. The EWC can be calculated using the Equation 1-1. The value of EWC for a certain hydrogel is governed by several factors, the hydrophilic nature of the hydrogel monomer, the type and percentage content of cross-linking agents, and external factors such as temperature, tonicity and the hydration medium itself *(Corkhill et al., 1990a)*.

$$\mathrm{EWC} = \frac{\text{Weight of water in the gel}}{\text{Total weight of hydrated gel}} \times 100\% \qquad (1\text{-}1)$$

Equilibrium Water Content (EWC) Equation

Water within the hydrogel is thought to exist in a number of states. Water molecules which are an integral part of the polymer structure, bonded usually by strong hydrogen bonding are refereed to as 'non-freezing' or 'bound'

water. Water molecule that are not a integral part of the polymer structure and are free to move throughout the network are described as 'freezing' or 'free' water. The ratio of bound to free water has a strong influence on the properties of a certain hydrogel.

1.4.2 Hydrogel Polymers within Arthroplasty and Hemi-arthroplasty Implants

The role of hydrogels within arthroplasty and hemiarthroplasty implants can be split into three distinct areas; tissue engineering scaffolds, synthetic implants for hemiarthroplasty or defect repair and as a component of a conforming total joint replacement. The area most relevant to this study is the use of hydrogel polymers as an articular cartilage replacement material. In the past thirty years improvements in the mechanical properties of hydrogels has lead to their use as the load bearing material for full and hemiarthroplasty implants. The porosity and biocompatibility of hydrogel materials has also made these materials very suitable as a mechanical scaffold for tissue engineered components such as tissue engineered articular cartilage and tendons. Tissue engineered components are the combination of cells, synthetic or tissue scaffolds, and suitable biochemical factors to improve or replace biological functions.

It has long been suggested that the optimum way to eliminate wear problems from arthroplasty and hemi-arthroplasty implants would be the use of materials which promote and maintain fluid film lubrication *(Walker and Gold, 1971)*. Studies on various hydrogel materials for use as cartilage replacements began with McCutchen et al *(McCutchen, 1969)*, who investigated Hydron, a water swollen polyhydroxyalkacrylic ester and the same material polymerised about a reinforcing polyester structure. The weeping properties of this polymer were an advantage as a cartilage replacement possibility. The study concluded that the friction coefficient of Hydron against a polyester surface maintained a value of 0.02 until the lubricant, in this case distilled water was drawn away from the contacting surfaces.

Other hydrogel polymers such as a Polyvinyl alcohol (PVA) gel used by Sasada et al., showed fundamental mechanical properties similar to that of cartilage but within this study the PVA gel showed a high failure rate of 85% when tested as the bearing material within a full arthroplasty hip simulator *(Sasada et al., 1985)*. This study highlighted the main concerns for hydrogel polymers; the long term wear and mechanical stability under cyclic loading.

Drawing on the experience within other engineering disciplines, soft materials were also investigated as a hemiarthroplasty implant by Medley et al., who used a polyurethane chosen to have visco-elastic and hydrophilic properties in the range of natural articular cartilage *(Medley, 1980)*. This *in vitro* study showed a high correlation between increased velocity and reduced wear. This indicated that the wear was highly dependent on the lubrication regime present. The use of soft materials within full arthroplasty implants was also suggested by Unsworth et al *(Unsworth, 1987)*.

The situation was reviewed by Corkhill et al, who studied the use of a conventional synthetic homogeneous hydrogel based on 2-hydroxyethyl methacrylate (HEMA) and a number of composite hydrogels, based on a semi-interpenetrating network, (SIPN) *(Corkhill et al., 1990b)*. The SIPN formulation produces a network which is stiffer and stronger than conventional hydrogels as well as mimicking the layered structure of cartilage more closely. The results showed that SIPN's possessed an increase in mechanical properties but still fell short of the values of natural cartilage. The study also revealed the key factors influencing the mechanical properties of SIPN's, such as the filler polymer structure, molecular weight and the glass transition temperature of the filler polymer. By optimising these factors the authors were able to create SIPN formulations with fundamental mechanical properties similar to the lower figures stated for articular cartilage and thus increase the potential for the use of hydrogel polymers as arthroplasty and hemiarthroplasty implantation materials.

The continued improvement in the mechanical properties and stability of these materials, in conjunction with the limitations of conventional materials used with hemiarthroplasty solutions, has meant the tribology of one surface soft material arthroplasty implants has been studied extensively. In particular theoretical optimisation and computer modelling of contact areas, stresses and elasto-hydrodynamic film thickness have been advanced *(Dowson et al., 1991, Jin et al., 1991)*.

The lubrication and subsequent wear improvement of polyvinyl alcohol-hydrogel (PVA-H) over ultra high molecular weight polyethylene (UHMWPE) were investigated by Oka et al in a number of studies *(Oka et al., 1990, Oka et al., 2000, Oka, 2001)*. The initial study *(Oka et al., 1990)* demonstrated PVA-H showed distinct improvement over UHMWPE in three distinct areas. By measuring the existence and thickness of a fluid film present between the test material and a glass plate, it was shown that PVA-H maintained a thicker fluid film for longer, thus increasing the proportion of fluid film lubrication and reducing the percentage of load carried by surface to surface contact. This reduction reduces the wear of the opposing materials.

The study also showed that under impact loading UHMWPE experienced higher stresses for a shorter time period than PVA-H. This suggested that PVA-H had a better damping effect than UHMWPE and PVA-H would prove better at resisting impact fatigue than UHMWPE. The biocompatibility of PVA-H and UHMWPE was also validated by *in vivo* testing and a subsequent histological study. The results showed a marked reduction in inflammation with the PVA-H materials thus suggesting a better biocompatibility than UHMWPE.

It should however be pointed out that this study did not take into account the long term wear resistance of the PVA-H formulations nor evaluated the boundary lubrication properties of each material. It is therefore difficult of predict the true lubrication and wear properties to PVA-H and UHMWPE until tested under *in vivo* conditions and within a mixed lubrication regime.

The frictional behaviour of two hydrogel materials and a number of other soft polyurethane polymers against a hard counter face were studied by Caravia et al., *(Caravia et al., 1993a, Caravia et al., 1993b)*. These studies investigated the start up and dynamic friction of each material within a mixed and boundary lubrication regime.

A trepolymer hydrogel and a SIPN were compared against a medical grade polyetherurethane *(Caravia et al., 1993a)*. The lubricants used within the study were deionised water or bovine calf serum. The hydrogels did not show the characteristics of other soft polymers *(Caravia et al., 1993b)*, as the soft polyurethane materials produced higher friction at low velocity than UHMWPE. Hydrogels with high water content produced the lowest value of friction within both the static and dynamic studies. This would suggest that the water content of the hydrogel is released during low velocity loading which overcomes the high contact areas present between soft polyurethane and a rigid counter face.

This series of studies clearly demonstrates the advantages of using water soluble polymers as soft cushion bearing materials. It should be noted however that the hydrogels used did not possess the mechanical properties suitable for survival *in vivo* and the study did not validate the hydrogels performance over extended time periods. Possible *in vivo* issues such a water re-absorption and static friction performance during cyclic loading need to be investigated before conclusions can be made regarding the comparison of soft polymers and hydrogels.

1.5 Knee Anatomy and Kinematics

Each joint has a particular sequence of motion, with timing, magnitudes and direction varying with demand and individuals. The knee performs four arcs of motion during each gait cycle. At initial contact flexion varies from 0 to 5°. During loading the knee then flexes to about 15° at the Loading Response.

There is then a progressive extension during mid-stance and on to full extension at Pre-swing, at about 40% through the cycle. This is followed by a relatively rapid flexion to approximately 60° at Initial Swing. Knee flexion. then decreases in Mid-swing, and full extension is achieved in the Terminal Swing *(Lafortune et al., 1992, Mow and Hayes, 1997).*

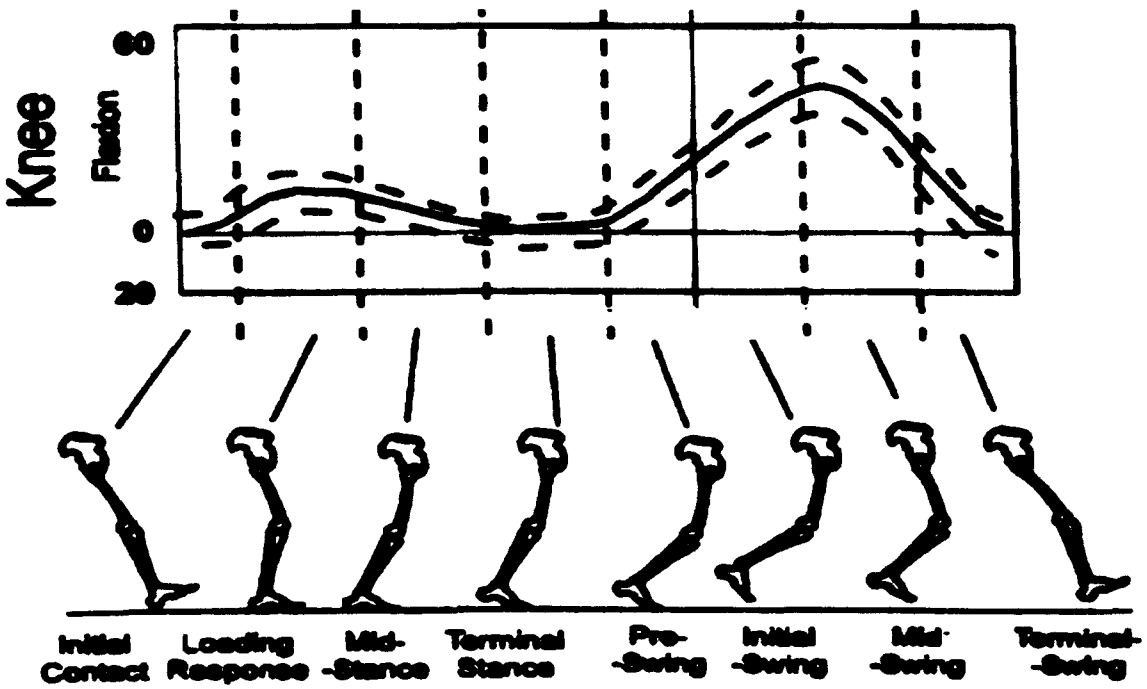

Figure 1-6: Knee flexion over the gait cycle *(Mow and Hayes, 1997).*

The maximum loading on the knee during normal walking occurs when the heal strikes at Initial Contact or just before the toe leaves contact at Pre-swing. The loading can reach up to 3000N, occur for 0.1 – 0.15 seconds and corresponds to the position of lowest bearing surface velocity. Fluid film lubrication can not be maintained under this combination of low velocity and high load and thus mixed and boundary lubrication are thought to be dominant *(Unsworth, 1991, Mow and Hayes, 1997, Wright and Radin, 1993).*

1.6 Diarthrodial Joint Lubrication Studies

It is important to understand the methodology used in studies investigating current joint lubrication theory. Lubrication theory was developed using

friction testing and *in vitro* compression testing in an attempt to understand joint behaviour under various conditions.

1.6.1 Entire Joint Pendulum Studies

The first study of this kind was performed by Jones et al., measuring the static friction of equine stifle joints *(Jones, 1934, Jones, 1936)*. Other studies have followed over the last 80 years, for example *(Unsworth et al., 1975, Mabuchi et al., 1994, Higaki and Murakami, 1995)*. The use of whole joint friction testing allows the joint contact geometry to remain intact and *in vivo* lubrication flow dynamics to be achieved.

Subtle differences in methodology, such as variability in surface to surface contact, oscillating angles and lubrication, means that the results are very difficult to repeat and compare. In most cases the complete joint capsule was tested with associated muscles, tendons etc removed. This common practice alters joint stability and kinematics which can lead to varying results. It should also be stated that there is little known about the differences between living and dead tissue and how lack of metabolic activity could influence the results. This variation in results can be seen in Table 1-1.

1.6.2 Small Sample Studies

The complication of frictional coefficient calculations and the lack of control of variables within whole joint testing can be overcome by using small effectively flat predefined samples. The natural curvature of synovial joints means that the samples can have only relatively small dimensions. Other disadvantages are that the unnatural contact area profile and shorter flow path means the lubrication flow within a small sample may differ from the whole joint *in vivo (Forster et al., 1995, Pickard et al., 1998a, Murakami et al., 2003, Bell et al., 2006)*. Small samples studies also induced experimental variations, which would not occur within whole joint studies, such as collagen matrix orientation.

The advantages of using small samples are the greater control and understanding of tribological conditions, and the ability to measure cartilage

against a known engineering material *(Forster et al., 1995, Ikeuchi, 1995).* Small sample testing also allows easy evaluation of lubricants, biochemical degradation assays and the variation of the cartilage make up, such as water and hyaluronic acid content *(Pickard et al., 2000, Bell et al., 2006, Katta et al., 2006).* A collection of results from whole joint and small sample studies are shown in Table 1-1.

Whole Joint Testing			
Reference	Joint Type	Lubricant	Coefficient of Friction
(Jones, 1934)	Horse Stifle	SF	0.02
(Unsworth et al., 1975)	Human hip	SF + HA	0.021-0.039
(Mabuchi et al., 1994)	Canine hip	SF	0.007 (± 0.004)
Small Specimen Testing			
Reference	Bearing Surfaces	Lubricant	Coefficient of Friction
(Dowson et al., 1969)	Cartilage/ Glass	SF	0.1-0.9
(Stachowiak et al., 1994)	Cartilage/ Metal	SF	0.02-0.065
(Forster et al., 1995)	Cartilage/ Metal	SF	0.010-0.27

Table 1-1: Coefficient of friction measured during Whole Joint and Small Specimen Studies. (SF = Synovial Fluid, HA = Hyaluronic Acid Solution)

1.6.3 Compression Test Studies

A vast amount of work has been directed towards the study of cartilage properties by compression or indentation testing. This is due to the ease of calculation and experimental procedure. In most studies the cartilage is put under compression and allowed to creep to a final equilibrium. Creep is caused by the compression of the ECM and exudation of the interstitial fluid. Cartilage is also under compression *in vivo* and therefore it is vital to understand how the material and its environment react under compressive loading. The creep and fluid exudation allows the calculation of the engineering properties of cartilage by the use of standard mathematical theories.

Early work tested dehydrated or un-immersed samples leading to varying results. Elmore et al were the first to highlight the importance of the interstitial fluid and cartilage interaction *(Elmore and Sokoloff, 1963)*. Most early indentation studies assumed cartilage to be an elastic material but later studies have incorporated the biphasic viscoelastic theory *(Mow et al., 1990c, Mow et al., 1980a)* and tri-phasic theories within the calculations *(Lai et al., 1991, Mow et al., 1989)*. In a number of studies the cartilage interaction with the compression apparatus, such as frictional effects of internals walls, has been assumed negligible. However, these effects do alter the mechanical loading on the cartilage sample.

1.7 Diarthrodial Joint Lubrication

Lubrication of synovial joints has been and continues to be an area of much research and controversy. The primary function of a lubricant is to separate the bearing surfaces *(Massey, 1968)*. The highly complex nature of synovial joints means it is highly unlikely that the varied properties and demands on diarthrodial joints will be surmised and explained by a single lubrication theory *(Dowson et al., 1969)*. Currently lubrication theory can be split into two main categories, fluid film lubrication and boundary lubrication. A schematic representation of the main lubrication theories can be seen in Figure 1-7.

1.7.1 Fluid film Lubrication

Fluid film lubrication can be found in all areas of engineering. A film of fluid completely separates opposing surfaces and thus allows relative motion. To achieve the separation the minimum film thickness needs to be greater than the combined surface roughness of the opposing bearing surfaces. The method of how the fluid film is created varies dependent on fluid properties, loading and motion. Within synovial joint research there are a number of fluid film lubrication theories.

1.7.1.1 Hydrodynamic lubrication

The high viscosity of synovial fluid and relative motion of the articulating surfaces creates a wedge shaped fluid layer which by generating a hydrodynamic pressure causes a separation of the microscopic surface contacts. This type of lubrication requires continuous relatively high speed motion to create the pressures needed to separate the contacting surfaces to a distance greater than the surface roughness. The ability of the speeds experienced by diarthrodial joints to provide these necessary pressures has been questioned and thus it is generally accepted that this method of lubrication does not act exclusively *(Dowson et al., 1969, Hou et al., 1989, Mow and Hayes, 1997, Mow et al., 1980a, Wright and Radin, 1993).*

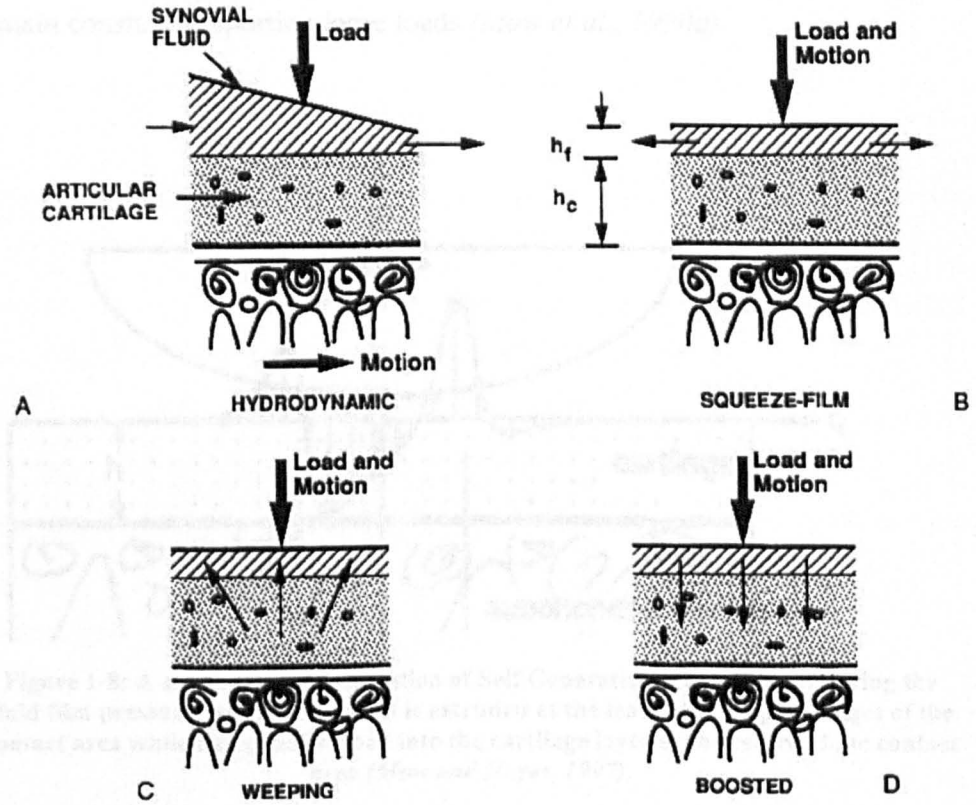

Figure 1-7 : A schematic diagram showing the four main theories of fluid film lubrication within synovial joints *(Mow and Hayes, 1997).*

1.7.1.2 Elastic-hydrodynamic Lubrication (EHL) and Micro-Elastichydrodynamic Lubrication (micro-EHL)

The theory uses the same basic idea as Hydrodynamic but suggests that within the elastic surfaces of a diarthrodial joint the pressure generated could

deform the surfaces. This deformation would reduce the Ra and mean lower articulating speeds would be required to separate the surfaces.

Micro-EHL is an extension of this theory which described the pressure development and subsequent ability to smooth the cartilage surface at a local macroscopic level *(Dowson and Jin, 1986)*.

1.7.1.3 Squeeze- film Lubrication

When two bearing surfaces come together, the fluid is forced out. As this can not occur instantaneously a pressure gradient is built up and thus applies a reacting force on to the bearing surfaces. As cartilage is deformable, this pressure gradient compresses the bearing surface and causes a local depression of trapped fluid. As fluid can not escape, the pressure gradient can remain constant supporting large loads *(Mow et al., 1990a)*.

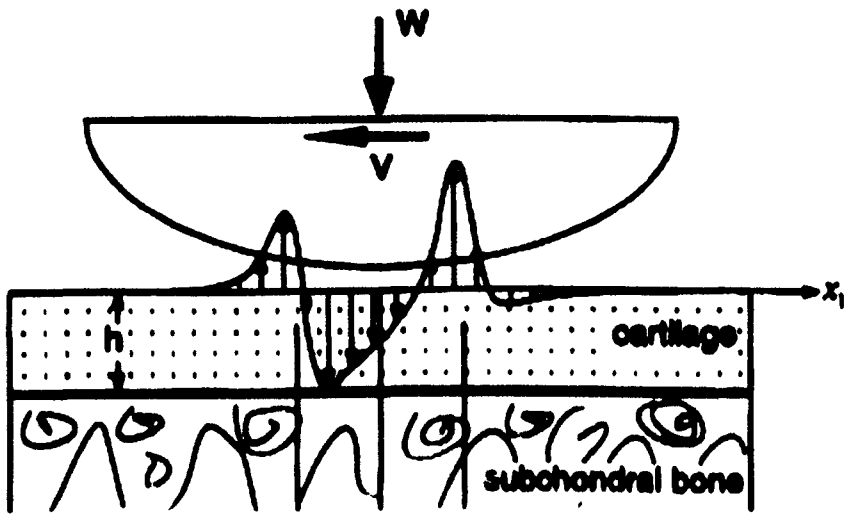

Figure 1-8: A schematic representation of Self Generating lubrication. Showing the fluid film pressure gradients as fluid is extruded at the leading and tailing edges of the contact area while being reabsorbed into the cartilage layer at the centre of the contact area *(Mow and Hayes, 1997)*.

1.7.1.4 Boosted Lubrication

Boosted lubrication theory states that the permeable cartilage surfaces act as a filter. As the surfaces come together the increase in pressure forces the smaller molecules in the synovial fluid (water and various electrolytes) to filter through into the ECM. This leaves a high concentration of hyaluronic

acid proteins between the two surfaces to act as lubricant *(Longfield et al., 1969, Walker et al., 1970)*. The increased viscosity of the hyaluronic gel also leads to pockets of gel being trapped in the natural surface roughness of the cartilage, thus creating a squeeze film effect *(Ikeuchi, 1995)*. Various studies have shown the filtration using mathematical models and experimental results. However, a full understanding of how hyaluronic acid-linked proteins act as a lubricant is still to be achieved *(Mow and Hayes, 1997, Bell et al., 2006)*.

1.7.1.5 Weeping and Self Generating Mechanism

An extension of the EHL theory was first put forward by McCutchen et al *(McCutchen, 1959, McCutchen, 1962)*. The theory of 'a weeping bearing' states that cartilage will surrender a percentage of fluid when under an applied pressure. The fluid then acts or assists the synovial fluid in hydrodynamic lubrication *(Unsworth et al., 1975, McCutchen, 1959)*.

From an understanding that cartilage can be modelled as a hydrated biphasic material and from experimental evidence that shows fluid absorption at the centre point of the contact area, a fluid extrusion and re-absorption theory was suggested. This so called 'self generation' mechanism suggests that the fluid is surrendered at the preceding edge of the contact, reabsorbed around the centre point of contact and surrendered again at the tail edge *(Mow and Hayes, 1997, Hou et al., 1989, Mow et al., 1980b)*. Figure 1-8 *(Mow and Hayes, 1997)* shows the suggested hydrodynamic pressures gradients across the point of contact.

Although demonstrated by experimental results, there still remain questions regarding the time taken for the exudation and re-absorption of the fluid and whether the properties of the expelled fluid could maintain the necessary lubrication. Weeping lubrication, which described the extraction of fluid from the cartilage surface, evolved into 'Biphasic lubrication', which as discussed below, described the influence of both the fluid and solid components of articular cartilage on synovial joint lubrication.

1.7.2 Biphasic Lubrication

To understand synovial joint lubrication is it important to understand the phasic nature of cartilage and how this effects lubrication. When loaded the collagen network and proteoglycans within the cartilage structure transmit the mechanical stresses. By the evolution of 'weeping' and 'self generated' lubrication it was possible to explain that under load, cartilage also expels fluid from the loaded areas to unloaded areas and the joint capsule itself *(Forster et al., 1995, Forster and Fisher, 1996, Mow et al., 1984, Mow et al., 1990c, Mow and Hayes, 1997, McCutchen, 1959, McCutchen, 1962)*. During this exudation phase the pressure gradients created by the fluid flow through the solid structure causes the fluid to act as the load bearing structure. When the load is removed the tissue reabsorbs the fluid due to the inherent charge induced swelling pressures *(Lai et al., 1991, Mow et al., 1990c, Forster and Fisher, 1999)*.

The accepted biphasic theory assumes both the solid matrix phase and the interstitial fluid phase of the tissue to be immiscible and each phase to be separate and incompressible *(Mow et al., 1980a, Mow et al., 1990b)*. These biphasic properties and the elastic deformable nature of cartilage means that the lubrication of synovial joints is a combination of EHL and boundary lubrication. However, the transition from one lubrication form to another is not clearly understood. The transition phase or 'mixed lubrication' regime is vital during *in vivo* joint lubrication. This 'mixed lubrication' can be seen schematically in Figure 1-9.

It has been estimated that the human knee spends over 95% of its time with the joint undergoing significantly high loading but with little movement *(Forster et al., 1995)*. It is at these conditions that biphasic lubrication enables the joint to achieve minimum friction with a combination of EHL and boundary lubrication.

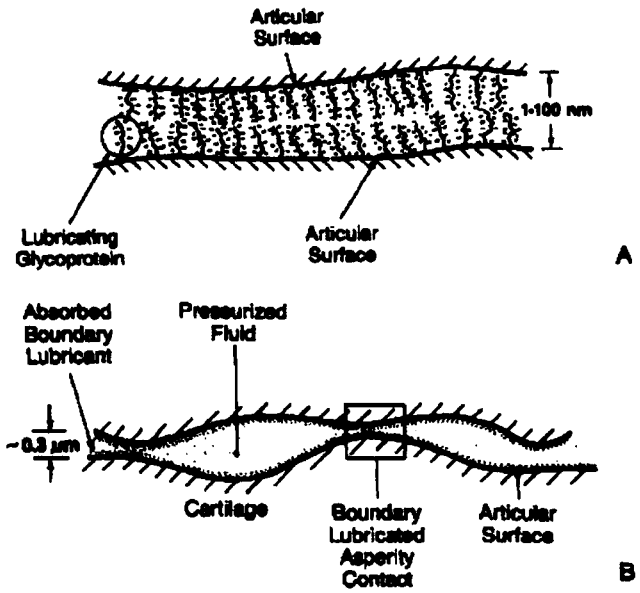

Figure 1-9: A schematic diagram showing Boundary Lubrication and its combination with Fluid film Lubrication. ***(Mow and Hayes, 1997)***

The importance of interstitial fluid pressurisation within the mixed lubrication regime has also been demonstrated both theoretically and experimentally by Krishnan et al who provided experimental data showing the distinct linear relationship between the interstitial fluid pressure and the frictional coefficient of articular cartilage *(Krishnan et al., 2004b)*. The study concluded that the interstitial fluid pressure within the cartilage was the primary mechanism for load support, reducing the load on the collagen-proteoglycan matrix. The study did however possess a number of limitations, e.g. the interstitial fluid was inferred from the rear of the sample and not from the surface face experiencing the frictional force. There were also limitations within the quantification of the frictional value for the solid to solid contact. The study also assumed a homogeneous structure during the testing but the in-homogeneity of the cartilage structure will cause the fluid pressure to vary with depth and thus cause the load support on the collagen –proteoglycan matrix to vary also.

1.7.3 Boundary Lubrication

Boundary lubrication (BL) occurs when the fluid film thickness is less than the surface roughness of the cartilage. It is the interface between the surface layers that prevents or reduces the surface contact that results in a high

friction value. Natural kinematics of the joint support the idea of BL as the relatively slow speeds are not enough to enable effective hydrodynamic lubrication theory *(Unsworth, 1991)*. Many conventional engineering materials experience BL within the synovial joint BL occurs by the interaction between a variety of chemical additives and the cartilage surface. It is generally acknowledged that the main lubricating factors are glycoproteins, including lubricin or hyaluronic acid and phospholipids. However, which exactly and in what proportions is still a source of debate. Both protein complexes are found in synovial fluid with hyaluronic acid also found in the cartilage surface *(Mow and Hayes, 1997)*.

Studies using cartilage on cartilage samples *(Linn, 1968, Linn, 1967, Linn and Radin, 1968)* and polymer on glass, *(McCutchen, 1966, Hills and Butler, 1984, Jay, 1992b, Jay, 1992a)* indicated the existence of boundary layer lubrication and the ability of the synovial fluid to play a part in it. The role of synovial fluid in changing the physiochemical nature of the cartilage surfaces and the independence of synovial fluid viscosity in BL has also been demonstrated *(Jay et al., 1998, Jay, 1992b, Hills and Butler, 1984, Hills, 2000)*. Other studies have suggested that synovial fluid has a minor role and that boundary lubrication is the result of the natural reaction between the cartilage layers and the water molecules between these surface layers *(Swann et al., 1981a, Swann et al., 1985, Forster et al., 1995)*.

Currently it is generally accepted that the major lubricants for BL are glycoproteins, phospholipids or a combination of both. Research has demonstrated lipid depletion samples show an increased friction at lower loading time but no effect at longer loading times *(Ozturk et al., 2004b, Pickard et al., 1998b)*. Protein removed samples showed no effects at lower loading times but reduced the friction over long loading times, and both lipid and protein removed samples showed both characteristics. This would suggest that proteins and lipids have degrees of lubricating ability *(Pickard et al., 1998b)*.

A number of studies have demonstrated the ability of glycoproteins, particularly lubricin, to act as the lubricating medium within BL. *(Swann et al., 1981b, Jay, 1992b, Jay, 1992a, Jay et al., 2001a, Jay and Cha, 1999, Higaki et al., 1998).* However in most studies the testing was completed on non-biological materials *in vitro*, thus the influence of cartilage and its reaction with synovial fluid could not be assessed. Within some early studies, the lack of phospholipid removal from the test medium means their effects can not be discounted. Jay et al attempted to determine whether the primary lubricant was phospholipid or protein based. They concluded that phospholipids do not play a predominant role and that lubricin was the major lubricate *(Jay and Cha, 1999).* This test however was *in vitro* and tested at a condition ideal for lubricin to act as a lubricant.

The consideration of hyaluronic acid (HA) as the major boundary lubricant was based on its ability to influence synovial fluid (SF) viscosity. Bell et al demonstrated that HA was an effective boundary lubricant when compared with Ringer's solution and phosphate-buffered saline *(Bell et al., 2006).* However other studies showed that the removal of HA from SF had little effect on BL, suggesting that HA does not have the dominant role *in vivo (Jay et al., 1998, Higaki and Murakami, 1994, Higaki et al., 1998, Hills and Thomas, 1998).* It has however been shown HA is important in maintaining fluid film lubrication under heavy loading *(Higaki and Murakami, 1994).*

Owing to their hydrophilic and hydrophobic regions phospholipids can be considered as 'surfactants', which react with the two bearing surfaces and have the ability to modify the surface properties *(Hills, 1988).* Phospholipids that participate in these reactions are called surface active phospholipids (SAPL). SAPLs are known to act as boundary lubricants within the lungs and pericardium *(Hills, 2002b).* SAPL possess a number of molecular properties that would aid their ability to provide BL. They possess fatty acids in the non-polar hydrophobic moieties which are the ideal length for lubrication. They also contain phosphate groups which in their ionised state can initiate strong polar ionised linkages *(Hills, 1988, Hills and Butler, 1984, Sarma et*

al., 2001). It is these forces, and the ability to creates layers *(Hills, 1990)*, which researchers believe is how phospholipids create BL *(Higaki et al., 1998)*.

There are three main phospholipids found on the surface of bovine cartilage, phosphatidylcholine, phosphatidylethanolamine and sphingomylein *(Sarma et al., 2001)*. Of these the most common is a derivative of phosphatidylcholine, dipalmitoyl phosphatidylcholine (DPPC). This possesses a strong positive charge allowing surface bonding and a structure that allows close 'packing' of the molecules. These are properties defined vital for good boundary lubrication *(Hills, 1988)*.

Within the research into phospholipids, most studies have concentrated on proving their lubrication ability on glass / glass or other mechanical materials. This *in vitro* work failed to take into account the complete nature of cartilage and synovial fluid and the important interactions which have been shown to exist.

In summary, the final model for BL and it elements it still the source of debate, although it has been shown that both proteins and phospholipids have lubricating ability. However, with little variation in methodologies, a lack of *in vivo* studies and very few direct comparative studies, it is impossible to form overall conclusions.

1.8 Cartilage Wear

The engineering definition of wear states that wear is the 'progressive' loss of material from the surface as a result of mechanical action *(Ashby and Jones, 1995)*. In the case of cartilage, this definition does not give a full picture. The complex nature of cartilage and the mechanical and biochemical relationships within it mean that a great number of factors contribute to its wear and degradation. However, its importance in the creation of effective arthroplasty and hemiarthroplasty implants can not be understated. Cartilage wear can be split into two areas, mechanical wear and biochemical degradation *(Mow and*

Hayes, 1997). It is generally considered that the wear of cartilage is initially low owing to the very efficient lubrication of synovial joints. However wear increases as the superficial lubrication layer is progressively removed by normal aging, excessive loading or pathological effects *(Stachowiak et al., 1994, Mow and Hayes, 1997)*.

It should be noted that wear over the surface of the femoral and tibial condyles is unique to each case *(Weidow et al., 2002, Wang et al., 1997)*. The position on the surface and cause of wear means the shape, size or amount of material removed varies. In a number of studies the possibility was investigated that the properties of wear particles can show from which layer of cartilage they originated from and help to determine the cause *(Kuster et al., 1998, Stachowiak and Podsiadlo, 1997)*. These studies gave encouraging results but the individual patient response to pain, lack of adhesion wear measurement and variation within wear patterns associated with a cause of wear such as osteoarthritis (OA) means that conclusions could not be determined.

1.8.1 Mechanical Wear

There are two main areas of mechanical wear; fatigue and interfacial. Both occur within all engineering tribological systems.

1.8.1.1 Fatigue wear

The cyclic stresses and strains generated within a structure under repetitive loading such as walking or running cause microscopic damage to the material structure. Within cartilage it can cause collagen fibres to buckle or loosen. This loosening of the collagen network affects the ECM interactions and changes how the cartilage reacts under loading. Over time this can cause cracks and even the loss of tissue fragments. This type of wear is independent of lubrication and surface contact area *(Berrien et al., 2000, Mow and Hayes, 1997)*.

1.8.1.2 Interfacial wear

The area of most research, interfacial wear can be split into two distinct areas, adhesive wear and abrasive wear. Adhesive wear occurs when the lubrication, fluid film or boundary breaks down and surface to surface contact forms microscopic welds *(Hutchings, 1992)*. When a junction is formed between opposing surfaces, and if the weld is stronger than the cohesive strength of the material, fragments may be torn off and may adhere to the stronger material. This exchange of material radically alters the microscopic contact points and changes the stress and strain profiles throughout the cartilage layer.

Abrasive wear is when a soft material comes into contact with a significantly harder material. The harder material may cut into the soft material causing removal of the bearing surface and an addition of particles between the surfaces *(Hutchings, 1992)*. This addition of material within the joint cavity leads to an increase in surface to surface contact and an increase in all types of wear *(Forster and Fisher, 1999, Hayes et al., 1993, Mow and Hayes, 1997, Mow et al., 1999)*.

1.8.2 Biochemical Degradation

It has long been suggested that mechanical effects are not the only form of degradation within cartilage wear *(Mow and Hayes, 1997)*. However, other causes have been the subject of very little research. The complex chemical interactions within the cartilage structure means that an alteration in the biochemical balance would cause a radical change in response to stress and strain. To maintain a balance within the ECM, enzymes such as the collegenase group which can break the cross-linkage covalent bonding and separate the triple helix of collagen are generated. Variations in production of these enzymes can vastly alter the mechanical properties of collagen *(Clark, 2000)*. The cause of alterations in production can be aging, excessive strain on the joint or a number of clinical diseases *(Maroudas and Holborow, 1980)*.

It is this alteration to the biochemical balance, which can be initiated *in vitro* and thus created the chemical changes associated with OA and other degenerative disease. A number of studies has suggested that the cytokine Interleukin-1α has a key influence on the progression of OA *(Shibakawa et al., 2003, Lotz, 2001, Patwari et al., 2003, Pratta et al., 2003, Ellis et al., 1994)*. The artificial addition to cartilage of Interleukin-1α *in vitro* has been considered as a method to induce biochemical degradation for evaluation of friction and wear properties *(Forsey, 2003)*.

An early sign of tissue degradation is the loss of proteoglycans. This is thought to be caused by the action of proteinases, and other biochemical agents released from the synovial membrane or the chondrocytes themselves. The loss of proteoglycans from the ECM exposes the collagen fibres to attack from collagenases, by facilitating their entry to the ECM and possibly promotes the removal of collagenases inhibitors. This is thought to be one of the initial factors of rheumatoid arthritis *(Panayi, 1982)*.

The natural aging of cartilage and the ECM also produces significant changes in the structure and stoichiometric orientation of proteoglycan aggregates causing shortening of chains and changes in stability throughout the varying cartilage layers. This alters the osmotic swelling pressure and other vital interactions that affect the properties of cartilage *(Wells et al., 2003)*.

There have also been a number of studies into the friction and wear of chemically modified cartilage. Enzymes such as papain, chondroitinase or trypsin have been used to damage or remove certain elements of the cartilage structure *(Forsey, 2003, Lipshitz et al., 1980, Jin et al., 2000, Basalo et al., 2004)*. These studies have demonstrated how chemical elements within the ECM have influence on its tribological properties. However in each case the studies were completed *in vitro* and the lack of metabolic activity within the ECM and lubricant could have affected the reaction of cartilage to any chemical changes.

1.8.3 Wear Measurement Techniques

One of the major issues within biomechanical wear research is the methodology employed to quantify wear of cartilage and synovial joints. It is vital to understand the advantages and limitations to each technique such that a full understanding of the results can be achieved.

1.8.3.1 Material Removal Measurement

The material removed techniques involve the quantification of changes in sample mass or the filtration of the lubricating medium and then the analysis of the filtrate. Ferrography *(Stachowiak and Podsiadlo, 1997, Graindorge and Stachowiak, 2000)*, scanning electron microscopy (SEM) and more recently environmental-SEM have all been used to analyse material of interest. These techniques do not however take into account adhesion wear or biochemical wear both of which play an important role within the wear of cartilage.

1.8.3.2 Friction

A very common technique is to infer wear degradation from changes in friction. Friction is defined as 'the resistance encountered by one body in moving over another body' *(Hutchings, 1992)*. There are two main types of friction, static and dynamic. Static friction is the force that will cause initial relative movement of one body against another. This force is dependent on the pressure between the two bodies and the relative amount of surface to surface contact. Dynamic or Sliding friction is the force to maintain the relative movement of one body against another. The force is dependent on the pressure between the two bodies, the surface to surface contact and the lubrication modes that are present. The frictional coefficient is calculated using Equation 2-2.

However it should be stated that there is no clear relationship between measured friction, surface roughness and wear for different materials and systems. Friction testing of articular cartilage also fails to measure chemical or mechanical degradation below the first cartilage layer. It is also very

reliant on lubrication, which if unrepresentative of *in vivo* synovial joint lubrication could alter the results.

1.8.3.3 Acoustic Emissions and Quantitative Ultrasound Techniques

The technique called acoustic emission analysis (AEA) is used to measure friction within the joint. Internal joint friction causes energy which is given off in the form of acoustic emissions. The ease of measurement and the unique output created by various joint wear patterns and pathological phenomena allow a high degree of understanding within *in vivo* measurement *(Schwalbe et al., 1999).*

It should be stated that this technique is used mainly for clinical diagnosis. The measurement of interfacial friction as an implication of wear has the advantages and disadvantages stated above. However, for *in vivo* joint studies or the analysis of a whole joint in a simulator, non-intrusive techniques for the measurement of wear could prove very useful.

Ultrasound backscatter techniques are commonly used as diagnostic tools within the medical care industry. However, the effects of cartilage degradation on ultrasound backscatters and the possible use as a quantitative wear measurement technique are in the early stages of research. Although the speed of wave propagation, attenuation and focal positioning through a number of biological tissues have been studied *(Toyras et al., 2003)* the fundamental acoustic properties of cartilage remain to be identified. A number of ultrasound studies *(Cherin et al., 1998, Jaffre et al., 2003, Pellaumail et al., 2002)* have investigated the effects of chemically degraded cartilage and healthy cartilage on ultrasound backscatter properties with some success. Pellaumail et al and Saarakkala et al *(Saarakkala et al., 2004, Pellaumail et al., 2002)* showed that collagen does have a distinct echo signature but the ability to detect proteoglycan degradation is still at a very early stage.

The fundamental properties of ultrasound and current techniques impose limits the use of ultrasound as a wear quantification technique. A balance is required between the wave frequency, which is directly proportional to the image detail, and the depth of penetration of the tissue. Achieving balance between these two variables can restrict the type of tissue this technique can be used with.

1.8.3.4 Surface Topography

A number of technique including optical microscopy, transmission electron microscopy and surface profilometry have been used to quantify the surface profile of healthy and worn articular cartilage *(Forster and Fisher, 1999, Hunter, 1743, Barnett, 1961, Sayles et al., 1979, Krishnan et al., 2004a)*. Further information on the quantification of articular cartilage surface topography can be found in Chapter 5.2.

1.9 Cartilage Defects and Associated Surgical Defect Repair Procedures

Damage to the articular cartilage surface has been demonstrated *in vitro* to occur at contact pressures of 25 MPa and above, under single high impact loading *(Buckwalter, 2002)*. However, continuous cyclic loading at far lower contact pressures has been shown to disrupt the surface integrity and to result in surface fibrillations *(Weightman et al., 1973, Buckwalter, 2002)*.

The mode of cartilage injury can be split into three main types;

1) cartilage defect including matrix and cell injuries resulting in no visible damage to the mechanical structure.
2) focal chondral injuries resulting from acute or repetitive trauma that results in focal mechanical tears, flaps or defects which lack the depth to reach the underling subchondral bone *(Buckwalter, 2002, Minas and Nehrer, 1997, Newman, 1998)*.
3) osteochondral injuries extended to the subchondral bone and which result in haemorrhage, clot formation and an active inflammatory immune response *(Buckwalter, 2002, Minas and Nehrer, 1997, Gross, 2003, Hangody et al., 2001, Newman, 1998)*.

There are three main areas of surgical intervention for osteochondral injuries. Abrasion and microfracture techniques penetrate the subchondral bone stimulating an inflammatory immune response and vascular repair at the surface of the defect. These treatments are of relatively low cost and can be performed arthroscopically. These are best suited to small cartilage defects with no bone involvement *(Buckwalter, 2002, Gross, 2003, Minas and Nehrer, 1997)*. The resultant repair is fibrocartilage which does not process the mechanical and chemical properties of articular cartilage and has been shown to become more fibrous and deteriorate over time and usage *(Minas and Nehrer, 1997, Gross, 2003, Newman, 1998)*.

Autologous osteochondral transplantation is replacement of an cartilage defect by the transplantation of a cartilage/bone plug from an unload area of the joint. The development of this technique, which uses a number of small plugs to fill a larger defect, is termed Mosaicplasty. This technique reduces the risk of disease transmission and leads to high cell survival rates when compared with allograft transplantation. This technique has also shown the greatest clinical success with defects less than 3mm diameter. However, the limited supply of autogenous tissue and the requirement for matching surface topography and joint geometry means there are limitations to the process. Another key concern is the ongoing monitoring for donor site morbidity *(Minas and Nehrer, 1997, Gross, 2003, Hangody et al., 2001, Buckwalter, 2002, Newman, 1998)*.

Introduced within the last 20 years, autologous chondrocyte implantation (ACI) uses the patient's cartilage for harvesting chondrocytes that are then grown in cell culture for between 4-8 weeks. The resultant cells are implanted back into the patient's defect and covered with a peristeum flap harvested from the patient *(Minas and Nehrer, 1997, Bentley et al., 2003, Clar et al., 2005, Hangody et al., 2001, Buckwalter, 2002, Newman, 1998)*. The technique has produced a number of clinical successes with several of clinical papers reporting relative clinical success for both mosaicplasty and ACI

(Bentley et al., 2003, Hangody et al., 2001, Clar et al., 2005). However, it has been suggested that the mosaicplasty does demonstrate deterioration over time *(Bentley et al., 2003).* ACI does require two operations although one can be performed arthroscopically. The associated cell culture also requires specialist knowledge and equipment not available in all health centres. These factors result in a far higher relative cost when compared with microfracture and autologous osteochondral transplantation, which has lead to ACI procedure not being implemented by certain health authorities *(Clar et al., 2005).*

1.10 Common Knee Diseases

To complete an extensive study of natural cartilage degradation and the pathological effects it is important to understand known disease and associated effects.

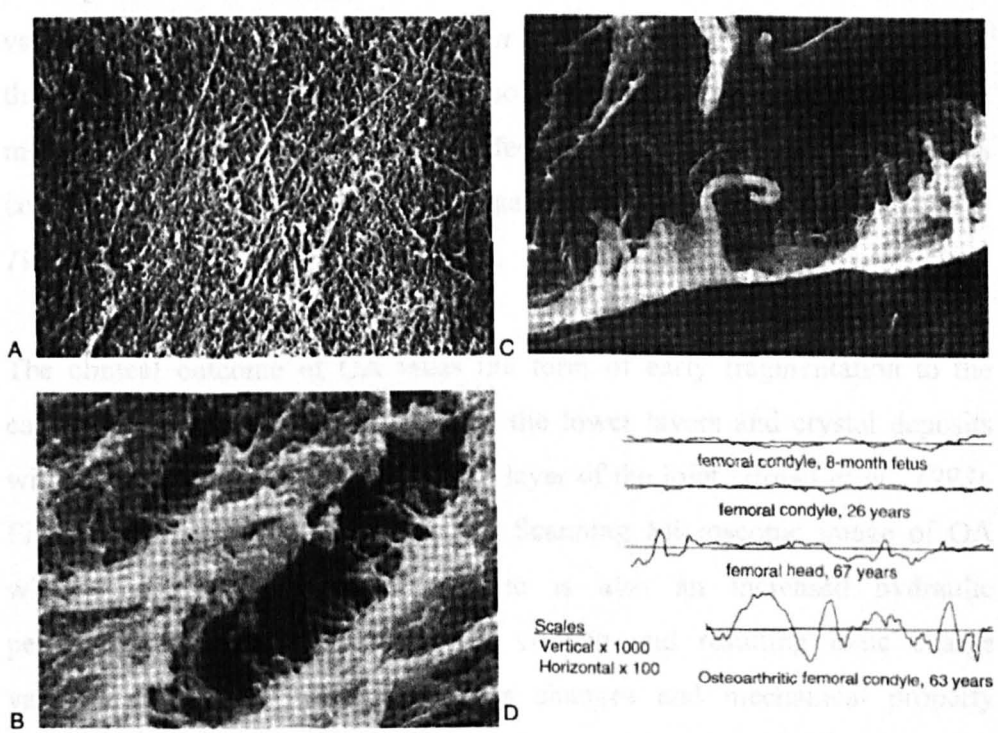

Figure 1-10: Environmental Scanning Microscopic images, (A) Normal healthy articular cartilage surface (B) Typical appearance of articular cartilage surface form a osteoarthritis human specimen (C) Aged femoral head surface retrieved from a fracture neck of a femur (D) Talysurf tracing of surface roughness from normal, aged and osteoarthritic samples *(Mow and Hayes, 1997).*

1.10.1 Rheumatoid arthritis/ Lupus

Rheumatoid arthritis is an inflammatory disease that can affect linings of joints and internal organs. This disease attacks collagenous tissue, softens bone and it is thought the tissues own immunological mechanisms plays an important role. Lupus is a specific inflammatory disease, which attacks the collagen fibres contained within soft tissue. This can also affect the majority of the major organs.

1.10.2 Osteoarthritis

There has been a large amount of controversy regarding the causes of osteoarthritis (OA). Owing to the lack of clinical understanding it has been very difficult to categorised OA in a formal definition. Current thinking states "OA is the group of overlapping distinct diseases, which may have different etiologist but similar biologic, morphologic and clinical outcomes" *(Flores and Hochberg, 1998)*. The pathological effects of OA are irregular loss of cartilage within synovial joints, sclerosis of the bone, subchondral cysts, and variable synovial inflammation *(Felson et al., 2000)*. It has also been noted that OA commonly effects only one compartment of the knee typically the medial condyle, with little or no effect to other areas, which again has contributed to conflicting theories regarding the causes of OA *(Freeman, 1979)*.

The clinical outcome of OA takes the form of early fragmentation to the cartilage surface with lacerations into the lower layers and crystal deposits within synovial fluid and the cartilage layer of the joint *(Hayes et al., 1993)*. Figure 1-10 shows an Environmental Scanning Microscopic image of OA within the cartilage structure. There is also an increased hydraulic permeability, this increase in water content and resulting ionic charge variation, leads to swelling pressure changes and mechanical property alterations within the ECM. There is eventual loss of the cartilage layer leading to bone on bone contact and an increased rate of wear.

1.11 Summary

The development of multi-disciplined *in vitro* cartilage friction and wear models and the development of novel clinical solutions for articular cartilage defect repair and trauma damage will increase available solutions to the clinical community and improve patient care. The majority of past studies have concentrated on one of the traditional engineering disciplines, mechanical, chemical and tissue. The combinations of different disciplines within a comprehensive experimental model will allow detailed understanding of synovial joint properties and the complex interactions that occur within the joint and with the external environment.

2 Methods and Materials

2.1 Introduction

This chapter describes materials, methods and apparatus developed and used in this thesis.

2.2 Materials

2.2.1 Procurement of the Bovine Articular Cartilage Specimens

Bovine femurs with the patella and part of the knee capsule still attached were collected from an abattoir within 36 hours of commercial slaughter. The collected specimens were obtained from 18 month old skeletally mature animals and were of a healthy and normal appearance. The specimens were 'deboned' in a cold room, stored in medical grade bags and transported to the University of Leeds. On arrival, excess muscle, tendons and the patella were removed and the patella-femoral head sprayed with 100% Ringer's Solution every 2 minutes to maintain hydration. Ringer's solution is a crystalloid isotonic solution used for intravenous hydration within the medical industry and it composition is given in Table 2-1.

Composition of 100% Ringer's Solution within a body fluid
147 mmol/l Na^+
4 mmol/l K^+
156 mmol/l Cl^-
2.2 mmol/l Ca^{2+}

Table 2-1: Composition of Ringer's Solution used in this studies

2.2.1.1 Determination of Superficial Layer Collagen Fibre Orientation

The structure of bovine cartilage has been well documented *(Buckwalter, 1983, Moss and Moss, 1983, Freeman, 1979, Lewis and McCutchen, 1959, Mow and Hayes, 1997)*. The orientation of the superficial collagen fibre layer was determined to control this variable during the study.

Indian ink staining has been used as a standard method for determining the superficial collagen structure *(Meachim et al., 1974, Bullough and Goodfellow, 1968, Freeman, 1979)*. Indian ink was applied below the superficial layer which then followed the orientation of the collagen fibres to create a visible line between 1 and 2 mm in length and 0.2mm thick, along the direction of the collagen fibre.

A size 3 needle was dipped in 100% black Indian ink (Windsor and Newton, UK) to a minimum depth of 3mm. The needle was then inserted into the cartilage surface until it struck the subchondral bone. Care was taken to make sure the needle was perpendicular to the cartilage surface. The needle was then rotated a minimum of 360^0 making sure the insertion was circular in shape and thus any orientation shown by ink migration would not be influenced by needle concentric tolerances.

In order to validate the method, three bovine cartilage specimens of 30mm long by 20mm wide were taken from the patella-femoral canal. The collagen fibre orientation within the outer region of the specimen surface was investigated using the Indian ink method. The orientation shown by ink migration was then used to infer the orientation across the entire surface. The Indian ink staining method was then applied to the entire surface. The resultant collagen fibre orientation was then compared visually with the inferred orientation of the surrounding tissue. It was found that the fibre orientation at the outer edge of the specimen surface, as revealed by the Indian ink method could be used to reliably predict the collagen fibre orientation over the entire surface. The Indian ink migration on the cartilage pin and surrounding area can be seen in Figure 2-1.

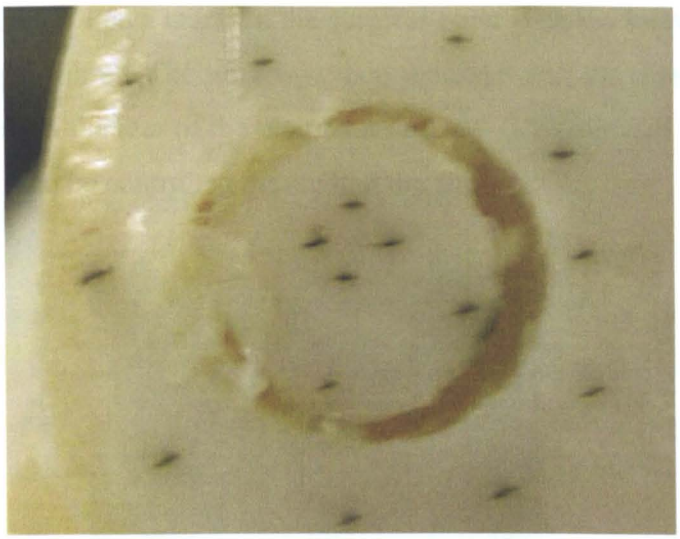

Figure 2-1: Validation test for the Indian Ink Process as a Bovine cartilage plug and surrounding area are treated with Indian ink to define the collagen fibre direction.

2.2.1.2 Harvesting of the Osteochondral Plugs

Excess tissue was removed from femurs and the cartilage surface inspected for any signs of visible damage. The plugs were harvested from the patella-femoral canal as this is the area mostly to yield a flat contact face to the plug *(Staubli et al., 1999)*.

The femur was clamped in place with the patella-femoral grove facing upwards. Using a surgical hand corer the plugs were cut out of the patella-femoral canal, down to the subchondral bone, as shown Figure 2-2(A). It was important to record the direction of the surface collagen fibres at this point before the plugs were removed and the orientation lost. In the area directly surrounding the circular mark made by the corer, Indian ink was applied around the circumference at 30° intervals, using the method stated above. After 2 minutes the surface was then washed with 100% Ringer's solution and the ink lines inspected. Approximately 95% of pins marked out with Indian ink indicated a distinct direction of fibre orientation.

For the specimens with distinct Indian ink alignment, a surgical corer attached to a 12V portable drill was used to create the osteochondral plug. The corer was inserted to a minimum depth of 12mm before being removed.

Care was taken to line a mark on the surgical corer with the known direction of the collagen fibres. The plug was then removed and the direction of the fibres marked on the rear of the plug by a saw cut. This allowed the collagen fibre direction to be controlled throughout the study.

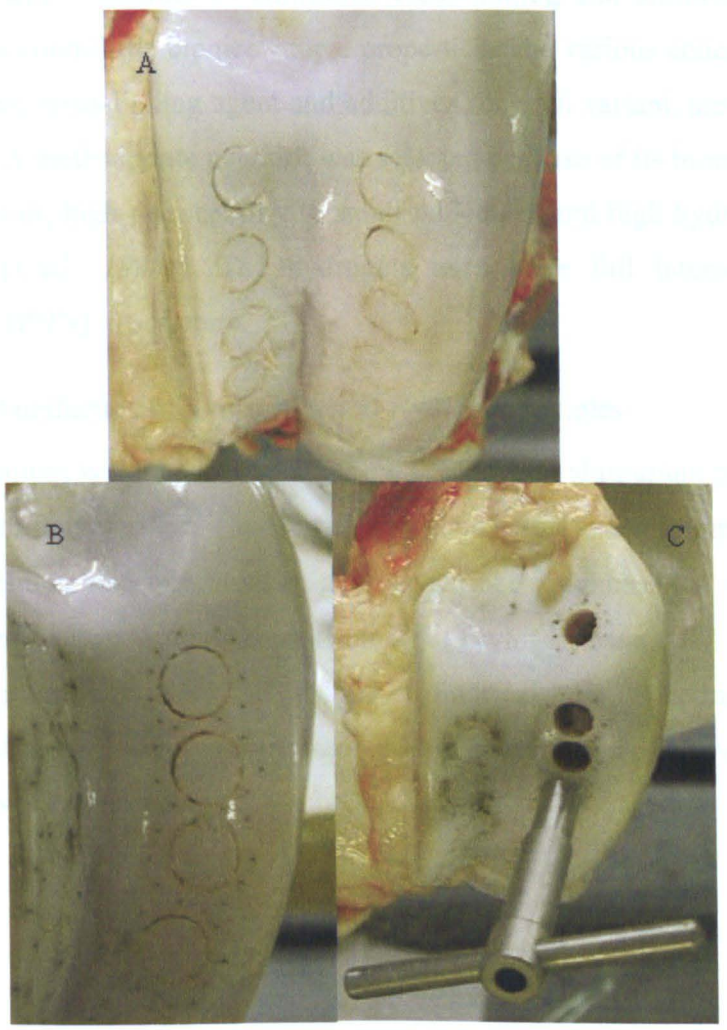

Figure 2-2: (A) The initial stage of the pin harvesting process as the pins are marked out on the patella-femoral cannel, (B) The application of the Indian ink as described in section 3.3.1, (C) The extraction of the Bovine cartilage pins at the final stage.

The osteochondral plugs were then stored in 100% Ringer's solution and frozen at -20°C. During this study frozen and fresh plugs where tested to determine the effects of the freezing process and as in previous literature *(Pickard et al., 1998b, Forster and Fisher, 1999)*, no difference was detected between fresh and frozen /re-thawed samples.

2.2.2 Chondroplasty Hydrogel Materials

Hydrogels can be defined as polymer networks, which are water swollen but do not dissolve in water *(Corkhill et al., 1990b, Corkhill et al., 1990a)*. The hydrogels within this study were methyl methacrylate acid (MMA) based, combined with a number of additional cross-linking and antibiotic agents designed to control the biomechanical properties. The various concentrations of monomer, cross-linking agent and additives for each variant, are shown in Table 2-2. A methacrylate network was selected because of its biocompatible characteristics, high permeability to small molecules and high hydrophilicity *(Corkhill et al., 1990a)*. The hydrogels used were full interpenetrating network (FIPN's) in structure.

2.2.2.1 Manufacture of Single Material Hydrogel Samples

Plate specimens were created by applying 0.75ml into aluminium planchettes to be photo-polymerised. The aluminium planchettes were stamped out of sheet aluminium and possessed an average surface roughness Ra $\approx$ 0.015μm (n=5) quantified using a stylus profilometry (Taylor Hobson, UK). For more detail see section 2.5.1. Hydrogel cylindrical pin specimens were manufactured by filling custom made 10mm internal diameter which were then photo-polymerised.

	1A	1D	1E	1G	1J	1K	1AG	2A	2D	2E	2G	2J	
Hydroxyethyl Methacrylate (HEMA)	98	88	88	88	78	78	96						
Tetrahydrofurfuryl Methacrylate (THFMA)								98	88	88	88	78	
Hydroxypropyl Methacrylate (HPMA)													
Ethylene glycol dimethacrylate (EGMDA)		10			10				10			10	
Polyethylene glycol-400-dimethacrylate (PED-400-DMA)			10			10				10			
Methacrylic Acid				10	10	10					10	10	
2,3-butadione	2	2	2	2	2	2	2	2	2	2	2	2	
Gentamicin							2						
Total %	100	100	100	100	100	100	100	100	100	100	100	100	
	2K	2AG	3K	4A	4D	4E	4G	4J	4K	4AG	4L	4M	4N
Hydroxyethyl Methacrylate (HEMA)			39								39		26
Tetrahydrofurfuryl Methacrylate THFMA	78	96	39									39	26
Hydroxypropyl Methacrylate (HPMA)				98	88	88	88	78	78	96	39	39	26
Ethylene glycol dimethacrylate (EGMDA)					10			10					
Polyethylene glycol-400-dimethacrylate (PED-400-DMA)	10		10			10			10		10	10	10
Methacrylic Acid	10		10				10	10	10		10	10	10
2,3-butadione	2	2	2	2	2	2	2	2	2	2	2	2	2
Gentamicin		2								2			
Total %	100	100	100	100	100	100	100	100	100	100	100	100	100

Table 2-2: Percentage content by weight of monomer, cross-linking agents and additional additives for each hydrogel variant test.

Photo-polymerisation was initiated by incorporating 2,3-butanedione as the photo-initiator, which absorbs at a maximum wavelength of 419nm. The light source used was visible light emitted at a wavelength of 420nm. All samples were given a 15 minute standardized exposure to the light source. Once completed, samples were stabilised for 72 hours in the 37°C oven. The

completed dehydrated samples were either circular disc-shaped with a diameter of 22mm, and a layer thickness of between 1mm and 1.25mm, or cylindrical in shape measuring 10mm diameter by 5cm in length. The cylindrical pins were then machined as described in section 2.2.2.3.

2.2.2.1.1 Equilibrium Water Content of Biphasic Materials

The quantification of equilibrium water content (EWC) was performed using six specimens of each hydrogel. All specimens were weighed to the nearest 0.0001 g at 20°C within an environmentally controlled room. The samples were then placed into individual containers full of distilled water pre-heated at 37°C and placed in an oven at 37°C (± 2°C). At set time points over 3 months, the discs were removed from the solution, blotted dry with standard laboratory tissue paper, weighed to the nearest 0.0001g, and returned to the solution. The final EWC value was determined when the calculated EWC value remained constant (±0.5%) for 6 reading over a 1 month time period and are shown in Table 2-3. The percentage EWC was calculated using equation 2-1.

$$EWC = \{(Mt - Mo)/Mo\} \times 100\% \qquad (2\text{-}1)$$

Equilibrium Water Content (EWC) Equation
M_o = initial dry weight, M_t = weight of swollen gel

Hydrogel Variant	Percentage Equlibrium Water Content (EWC)
1D	37
3K	19
4A	53
4E	20
4M	14
4N	25

Table 2-3: Percentage equilibrium water content values for a selection of Hydrogel Variant

2.2.2.2 Manufacture of Composite hydrogel Samples

Cylindrical plug composite specimens comprised of two sections, a mounting layer manufactured from second generation bioactive bone cement (DePuy

CMW, UK) and a bearing surface layer composed of the hydrogel variant under investigation. Bone cement was mixed according to the manufacture's instructions. After no more than 50 seconds, a retrograde filling method was used to syringe the curing mixture into custom made moulds. A lid was applied and the bone cement left to cure for 1 hour. Following removal from the mould, the bone cement plugs were visually inspected for voids or surface cracks and 1200 grit grade wet and dry paper (Struers, Denmark) was used to create a consistence test surface on each contact face.

Each bone cement plug was then inserted vertically into a custom made mould with the appropriate internal diameter. The appropriate hydrogel monomer was injected onto the surface of the cement pin and cured using the same method as the uni-material hydrogel specimens. Following the curing process, the composite specimens were removed and machined as described in section 2.2.2.3.

2.2.2.3 Cylindrical Pin Machining

Un-hydrated cylindrical plugs were manufactured as described in section 2.2.2.1. However as each variant had individual water take up properties, in order to insure all hydrated specimens processed the same dimensions an individual hydration expansion factor was calculated for each variant. Using a 10mm diameter rod of each variant, as described in section 2.2.2.1 three pins Ø10mm (±0.02mm) by 10mm (±0.02mm) were machined. Each set of three were hydrated within 100% Ringer's solution for 8 weeks at room temperature and the new dimensions quantified using a Profile Projector (Nikon, Japan) and Vernia Calipers. The dimension alteration between the hydrated and non-hydrated pins was calculated and used to define the hydration expansion coefficient for each variant, as shown in Table 2-4.

Using the hydration factor, a set of pins for each variant was turned on a lathe to the individual un-hydrated dimensions shown in table 2-3. The samples were then hydrated with Ringer's solution for a minimum of 60 days and the dimension re-quantified. The final hydrated dimensions can be seen in Table

2-4. The results showed an acceptable tolerance. All single and composite material pins following standard manufacture, as describe above were then machined to un-hydrated dimensions using the hydration coefficient to ensure that once hydrated each variant was the desired dimensions for each test.

	Calculation of Hydration Factor		Calculation of Dehydrated Dimensions for Testing		Final Hydrated Dimensions (mm)
	Dehydrated dimension (mm)	Hydrated dimension (mm)	Hydration Factor	Dehydrated Dimensions for Testing (mm)	
Hydrogel Variant 3K	10	10.86	1.086	9.2	9.95
Hydrogel Variant 4M	10	10.59	1.059	9.44	10.05
Hydrogel Variant 1D	10	10.69	1.069	9.35	10.1
Hydrogel Variant 4N	10	10.41	1.041	9.6	9.91

Table 2-4: Average dimensions used to calculate the diameter and length of dehydrated pins for the Tri-Pin on Disc Test

2.2.3 SaluCartilage™ Specimens

To act as an additional control, SaluCartilage™ (SaluMedica™, USA), a commercially available hydrogel implant intended to treat chondral or osteochondral defects was also studied. The required number of Ø10mm by 10mm cylindrical specimens were purchased and stored at room temperature as per the manufacturer's instructions.

2.2.4 Single Phase Control Materials

To understand the effects of biphasic properties on friction response a number of single phasic materials were investigated as controls. Polished stainless steel BS316 counter face plates with an average surface roughness of 0.02(±0.002)μm were used as the positive control.

Four single phasic polymers, Delrin, GUR1120 ultra high molecular weight polyethylene (UHMWPE), a medical grade silicone elastomer (Percous Plastic, France) and a medical grade thermo-polyetherurethane (The Polymer Technology Group, USA) were also used as single phasic controls. In each case, the polymers were supplied in sheet form, cut to dimensions identical to the biphasic samples. Table 2-5 shows the elastic modulus of each single phasic material.

Single Phasic Material	Elastic Modulus (MPa)
BS316 Stainless Steel	200000 (standard value)
Ultrahigh Molecular Weight Polyethene GUR1120	600 (standard value)
Delrin	2795 (standard value)
Silicone Elastomer	97
Thermo-Polyetherurethane	3

Table 2-5: Mechanical Properties of Single Phasic Materials

2.3 Experimental Methodology and Apparatus

2.3.1 Lubrication Film Thickness Predictions

Previous literature *(Pickard et al., 1998a, Forster and Fisher, 1996, Bell et al., 2006)* record investigations into the frictional behaviour of articular cartilage pins against a number of different surfaces. In each case the frictional behaviour studied was under mixed or boundary lubrication regimes. In order to investigate the effects of a hydrated soft polymer within mixed and boundary regimes it was deemed necessary to perform this current investigation under the same lubrication regime. Details of the calculations can be found within Appendix A.

2.3.2 Friction Apparatus

2.3.2.1 Short Term Friction Test Apparatus

A flat counter face referred to as the plate specimen, was contained in a bath of the desired lubricant. The bath, mounted on a linear bearing (Schneeberger GmbH, Germany) was reciprocated by a motor and worm gear configuration (Parvalux Electrical Motors Ltd, UK) through a set distance and at the desired speed. Above the bath and perpendicular to the direction of motion was the load bearing arm. The arm was pivoted at one end with a counter weight. The pivot and weight was set such that when unloaded, the arm and pin holder assembly could move freely and would not transfer any load to the contacting surfaces. The other end of the arm was fixed to a liner piezoelectric force transducer (Kistler, Germany) mounted perpendicular to

the arm and parallel to the direction of motion. A schematic diagram of the apparatus is shown in Figure 2-3.

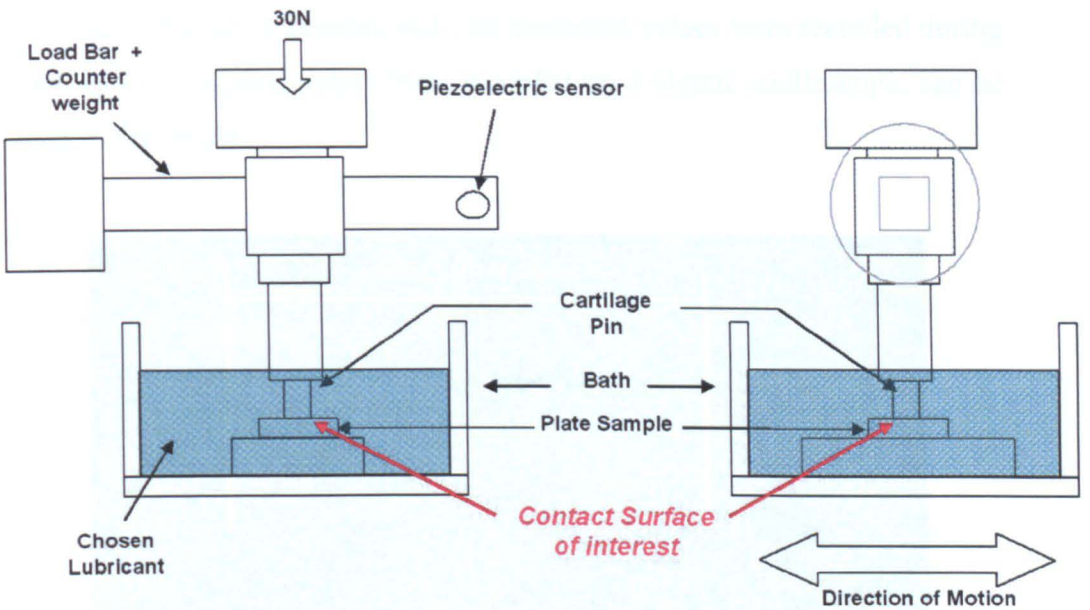

Figure 2-3: A Schematic diagram showing the key features of the test apparatus, motion direction and environment.

The pin sample was mounted within a holder such that the pin protruded by the layer of cartilage and approximately 2 mm of subchondral bone. Once loaded the holder was inserted into the plain bearing of the load bearing arm. The plain bearing was mounted such that the contact surface of a pin specimen contacted the test surface of the plate specimen. The pin holder was then loaded to the desired level, thus inducing the test level of contact stress between the two surfaces. The plain bearing within the load bearing arm allowed the pin holder to move freely in the vertical axis, which maintained a constant load and contact stress level throughout the test.

The friction force between the two test surfaces was transmitted through the pin holder, plain bearing and load bearing arm to the piezoelectric sensor, the output voltage of which could be converted to a frictional force (N) using a known calibration factor. More detail of the calibration methodology is given in section 2.3.4. The output signal from the piezoelectric sensor was

processed via an analogue to digital signal amplifier (Kistler, Germany) and recorded on a PC using LabView (National Instruments, USA). A sample rate of 100 points per second, over a duration of 10 seconds was recorded every 30 seconds throughout each test. To reduce variation in the friction value an average of the 300 maximum and 300 minimum values were recorded during each cycle. A typical output trace recorded on a digital oscilloscope, can be seen in Figure 2-4.

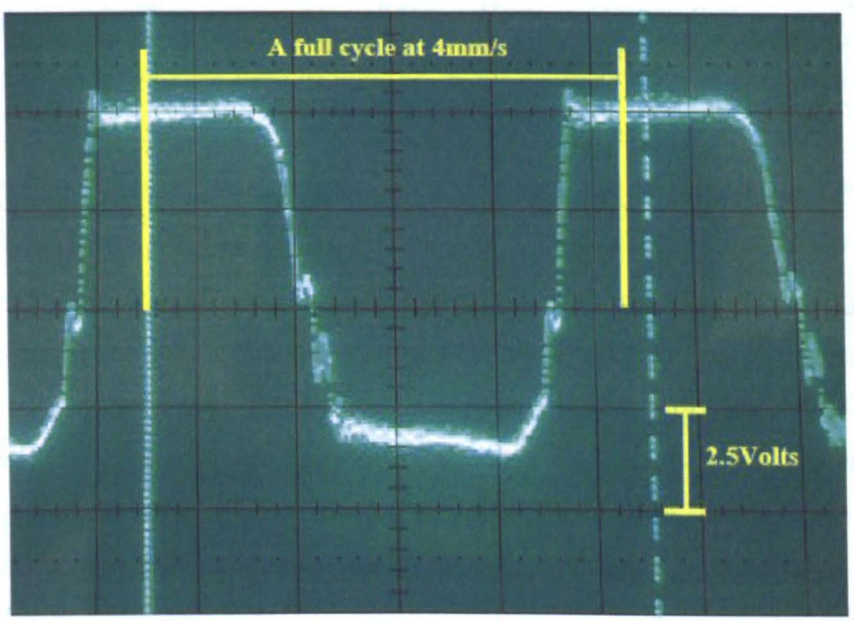

Figure 2-4: A typical output trace from the oscilloscope.

The apparatus was designed to measure low frictional values. The linear bearing produced an internal frictional coefficient of 0.0062 (± 0.0005). This loss was taken into account during the calibration calculation. Other losses may have occurred by movement of the pin holder within the plain bearing within the vertical direction owing the macroscopic changes in the surface geometry. The experimental cycle was evaluated using known engineering materials and values from the literature *(Forster, 1996, Forster et al., 1995, Forster and Fisher, 1996, Pickard et al., 1998b, Bell et al., 2006).*

2.3.2.2 Simple Geometry Wear Simulator

The short term friction apparatus had a number of limitations including, a maximum loading capacity of 30N and uni-axial directionality. As part of

this study and to fulfil the objectives of this investigation, a new simple geometry wear simulator was designed and manufactured. The simple geometry wear simulator was based on the short term friction apparatus, comprising of a flat counter face referred to as the plate specimen, mounted in a bath containing the desired lubricant. The bath, was mounted on a linear bearing (Schneeberger GmbH, Germany) which reciprocated by a motor and worm gear configuration (Parvalux Electrical Motors Ltd, UK) through a set distance and at the desired speed.

The simple geometry wear simulator was designed to run for up to four weeks, which meant overcoming piezoelectric sensor drift which is the undesirable change in output signal over time. The load bearing arm was mounted above the bath and perpendicular to the direction of motion. The arm was pivoted at one end on a bearing and could move freely, not transferring any load to the contacting surfaces. The other end of the arm was free to move over a fixed liner piezoelectric force transducer (Kistler, Germany) mounted perpendicular to the arm and parallel the direction of motion. Force was transmitted from the load bearing arm to the piezoelectric force transducer via a custom made removable Tourin washer. To reset the piezoelectric force transducer a fixation pin was inserted into the load bearing arm and the Tourin washer was disconnected, removing load from the piezoelectric force transducer without interference to the test surfaces. Following the piezoelectric force transducer reset process the washer was then replaced and the pin removed again exposing the piezoelectric force transducer to the forces and allowing continued quantification of the contact zone friction force.

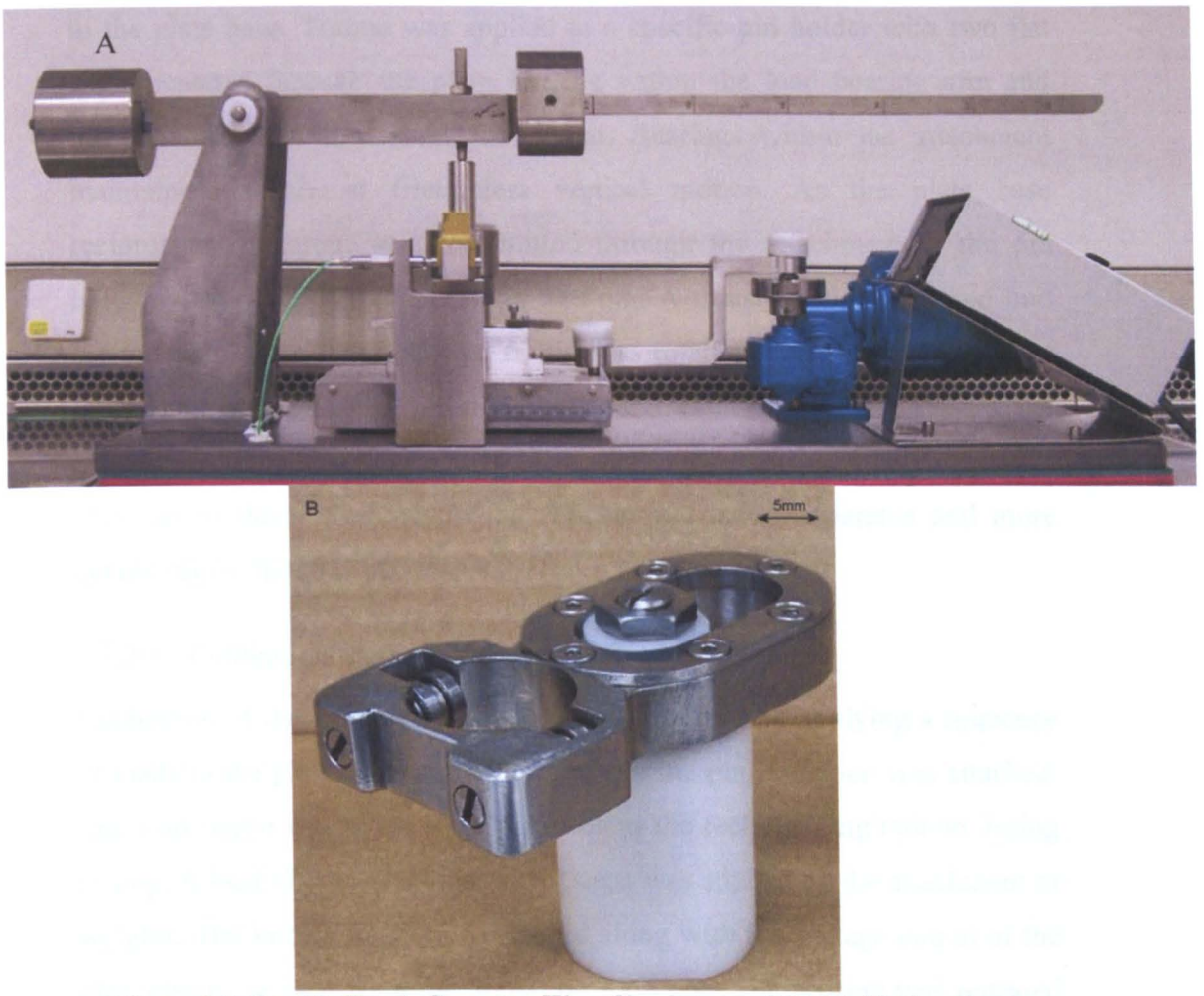

Figure 2-5: The (A) Simple Geometry Wear Simulator and (B) Multi-Directional attachment

The pin sample was mounted within a holder such that the pin protruded by the layer of cartilage and approximately 2mm of subchondral bone. The holder was inserted into the polymer plain bearing of the load-bearing arm allowing free movement in the vertical axis. Load was applied through a point contact to the top of the holder by a pivoted arm, which allowed a load range of 5N-256N to be applied. As in the short term friction apparatus, when motion was applied the friction force at the contact zone was transmitted through the pin holder, plain bearing and load bearing arm to the piezoelectric sensor.

A multi-directional attachment was also designed, which rotated the pin $\pm 20^{o}$ about the centre during a complete reciprocating stroke of 10mm in length. The attachment was made from stainless steel and placed onto a dowel fixed

to the plate base. Torque was applied to a specific pin holder with two flat edges inserted through the plain bearing within the load bearing arm and through the multi-directional attachment. Bearings within the attachment maintained an almost frictionless vertical motion. As the plate base reciprocated, a torque was transmitted through the attachment to the pin holder, rotating both the pin holder and pin. A thrust bearing mounted into the top of the pin holder allowed frictionless rotation at the point contact for load application. In the uni-directional and multi-directional set up the calibration, data logging processes and friction test methodology were identical to those used within the short-term friction apparatus and more details can be found in sections 2.3.2.

2.3.2.3 Calibration Methodology

Calibration of the friction transducer was completed by applying a sequence of loads to the pin holder at the point where the pin specimen was attached. The load vector was in the same direction as the reciprocating motion during testing. A load of 0 – 9.81N in 0.981N steps was applied by the attachment of weights. The known force was recorded along with the voltage output of the piezoelectric sensor, from the digital oscilloscope. The process was repeated four times and the four sets of results were used to produce a calibration curve, an example of which is shown in Figure 2-6. This allowed the calculation of a calibration factor for each simulator. This factor allowed the calculation of the resistance Force (Fr) between the two surfaces from the voltage output. Once Fr had been measured, Equation 2-2 was used to calculate the frictional coefficient between two interacting surfaces.

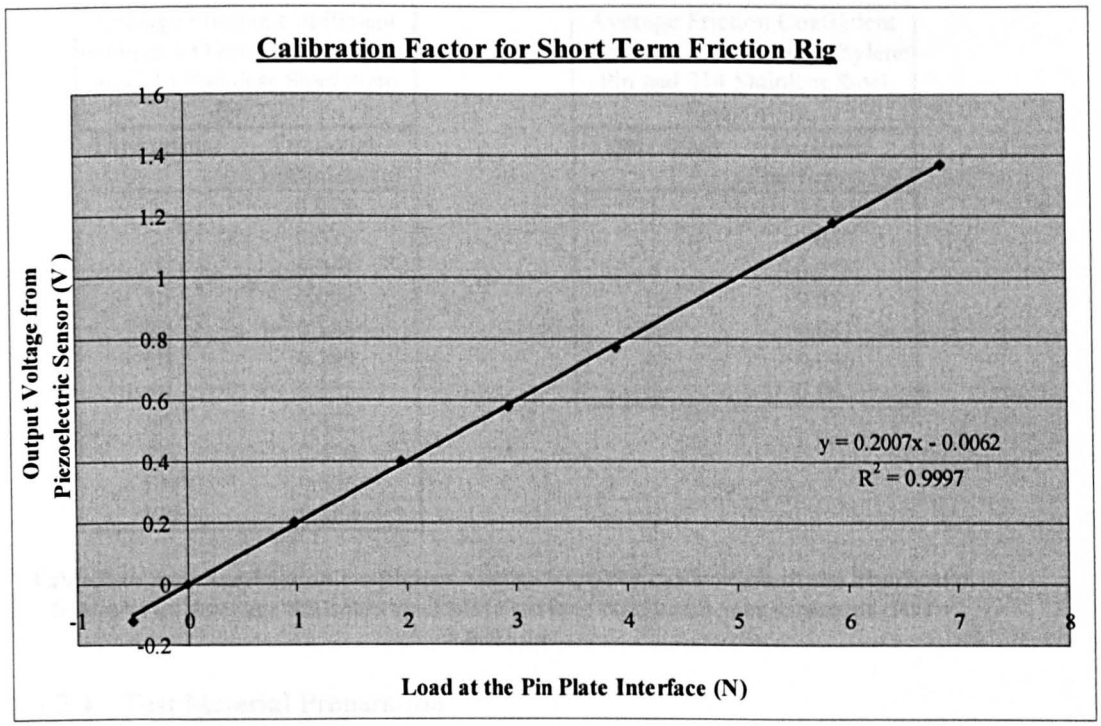

Figure 2-6: Graph showing the formula used to calculate the Calibration Factor.

$$Fr = \gamma \times Fn \qquad (2\text{-}2)$$

Equation used for the calculation of the Frictional Coefficient
Fr = Resistance Force, γ = Friction Coefficient and Fn = Force perpendicular to surface

To confirm the calibration of both simulators a number of simple pin on plate tests were completed at a various loading and speed configuration between surfaces with established frictional coefficients. The test materials chosen were a GUR1120 polyethylene pin on a BS314 stainless steel plate and a bovine articular cartilage pin on a 314 stainless steel plate. The experimental methodology used is described in section 2.3.2.4 and the bovine cartilage pins were harvested using the methodology described in section 2.1.1. A GU1120 polyethylene pin on a BS314 stainless steel plate was tested at random intervals throughout the each set of testing to confirm that each simulator was still within acceptable tolerance limits. The results from the tests were compared with in-house experimental data and data in previous literature *(Forster and Fisher, 1996, Forster and Fisher, 1999)*. Table 2-6 shows an example of the results from the short term friction apparatus.

Average Friction Coefficient between a Ø9mm Cartilage Pin and 314 Stainless Steel Plate (n=2)	
Time (mins)	Frictional Coefficient (γ)
1	0.028
2	0.035
5	0.061
10	0.094
20	0.188
30	0.269
40	0.335
60	0.422
80	0.499
100	0.535
120	0.562

Average Friction Coefficient between a Ø9mm Polyethylene Pin and 314 Stainless Steel Plate (n=3)	
Time (mins)	Frictional Coefficient (γ)
1	0.059
2	0.060
5	0.058
10	0.055
20	0.051
40	0.046
60	0.042

Table 2-6: Average friction coefficient results from the calibration of the Short term friction rig, Average Stainless steel plate surface roughness measurement (Ra) = 0.0056μm

2.3.2.4 Test Material Preparation

The bovine cartilage pins and plate specimens were defrosted for 12 hours at room temperature prior to testing. All plate materials were defined as plate specimens and tested against an articular cartilage pin. Bovine cartilage plates were mounted on stainless steel backing plates with adhesive (Loctite, USA) applied to the underside of subchondral bone. The stainless steel specimens were custom made plates with an average surface roughness (Ra) of 0.002μm quantified by a Talysurf 5 profiler (Taylor-Hobson, UK), see section 2.4.1. All hydrogel materials were hydrated in Ringer's solution for a minimum of 28 days at a constant 21°C before testing. The Ringer's solution was made using sterilised water and changed every 7days.

Single phasic polymers were soaked in sterilised water for 12 hours before testing. All polymer specimens were mounted on a stainless steel backing plate by means of a high-grade waterproof double-sided adhesive tape. This provides a clean effective method of mounting the test materials without the possibility of test surface contamination. The mounted samples were stored at 21°C in Ringer's solution.

2.3.3 Tri-pin on Disc Unconfined Uniaxial Compression Test

2.3.3.1 Tri-Pin on Disc Apparatus

A stainless steel disc was mounted into a circular stainless steel (BS303) bath containing 130ml of 25% bovine serum (0.1% sodium azide) which acted as the lubricant. The three pin specimens were placed within stainless steel (BS316) collets and fixed into the tri-pin on disc holder, which was then located such that the three specimens sat just above the stainless steel disc. To create contact, load was applied to the top rear face of the tri-pin on disc holder by a pivoted load arm making point contact to a metal bar running through a polymer plain bearing. Height variation was quantified using a depth gauge located on the tri-pin on disc holder.

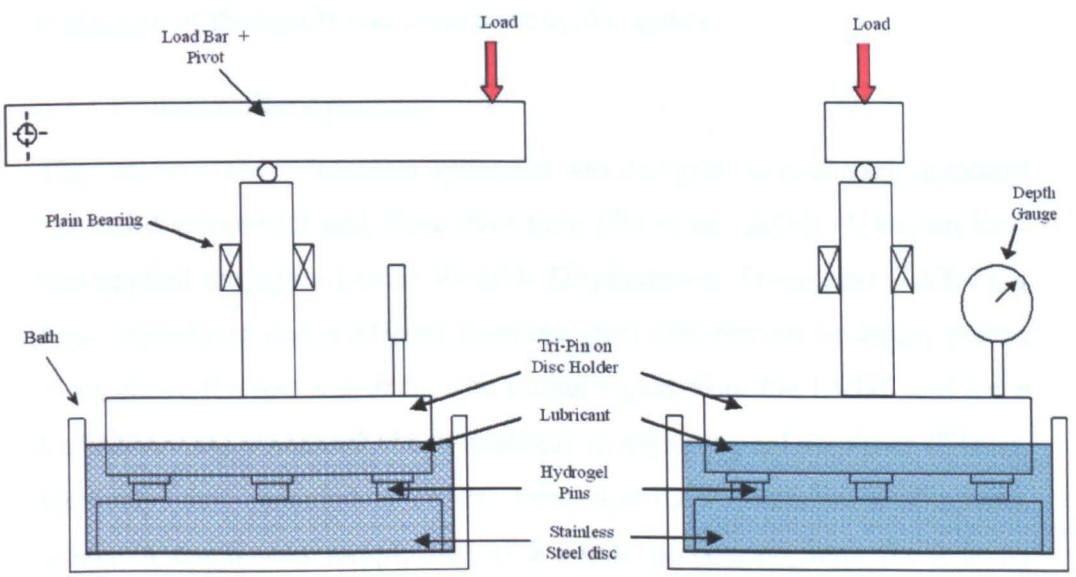

Figure 2-7: Schematic diagram of the Tri-pin on Disc Apparatus

2.3.3.2 Unconfined Uniaxial Compression Methodology

Submerged within 100% Ringer's solution, three fully hydrated hydrogel pins were mounted into the tri-pin on disc holder. The stainless steel disc was placed into the bath containing 25% bovine serum (0.1% sodium azide) to act as the lubricant. Two customised mounting blocks were used to position the tri-pin on disc holder such that the hydrogel pins were 0.5 mm above the metal disc but submerged by the lubricant. The load bar and depth gauge were then positioned and the initial position recorded. The mounting blocks

were then removed and the load applied after 30 seconds. The height variations were then recorded at set points over 24 hours. Following a final reading the pins were removed and dimensions re-recorded using the Profile Projector (Nikon, Japan).

2.3.4 Indentation and Computational Finite Element Displacement Test

A combination of an indentation test and 2 dimensional axisymmetric finite element model was used to characterise the compression modulus, biphasic properties and fluid load support characteristics for each hydrogel tested. The finite element model was written and developed by Sainath Pawaskar as part of a Master of Science Project *(Pawaskar, 2006)*. Accurate geometry and boundary conditions were supplied by the author and the model created by Sainath Pawaskar. All material property alterations, computation analysis and evaluation of the results was completed by the author.

2.3.4.1 Indentation Apparatus

The custom made indentation apparatus was designed to accurately measure vertical displacement and force over time *(Jin et al., 2000)*. A known load was applied through a Linear Variable Displacement Transducer (LVDT), a force transducer and a Ø3mm stainless steel flat bottom indenter, placed 1mm above the test specimen. The output signal from the LVDT and force transducer was processed via an analogue to digital signal amplifier (Kistler, Germany) and recorded on a PC using LabView (National Instruments, USA). A continuous sample rate of 5 points per second, over the 2 hours duration was used for each test. Using a known calibration factor the output signal from both the LVDT and force transducer could be converted to displacement and load over time.

2.3.4.2 Indentation Methodology

A fully hydrated Ø10mm uni-material hydrogel specimen was placed into a custom made collet such that 4mm of hydrogel was unconfined. The specimen and collet were then placed into a bath of Ringer's solution and positioned such that the top face of the specimen was 1mm above the indenter (Figure 2-8). The load was applied and data acquisition stated at the

point of contact between the indenter and specimen. After 2 hours, the data acquisition was stopped and the specimen inspected for any visual signs of fracture or material loss.

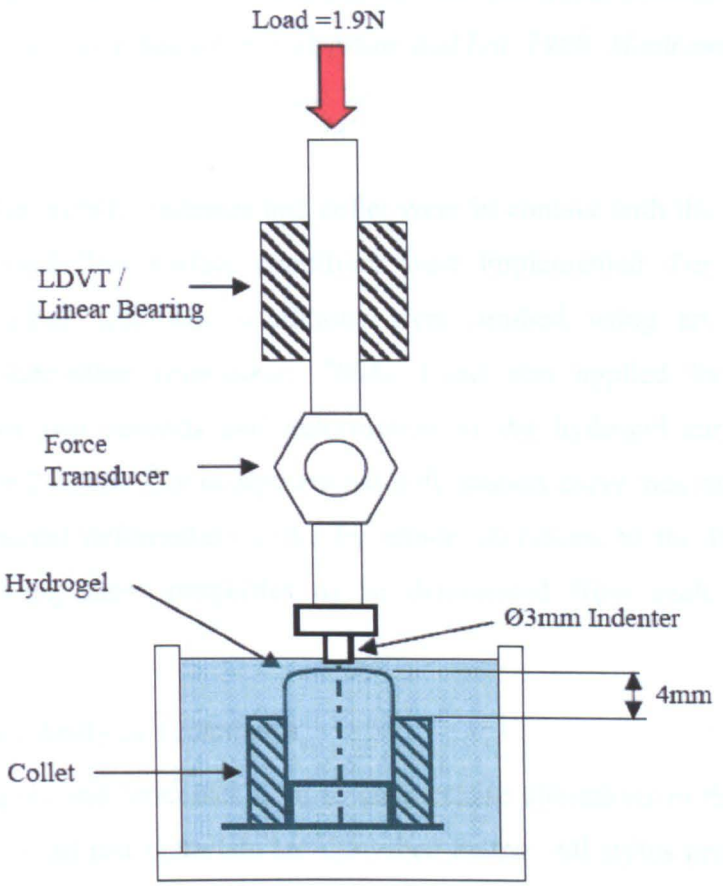

Figure 2-8: Schematic diagram of the Indentation Apparatus

2.3.4.3 Axisymmetric Poroelastic Biphasic Finite Element Model

The two dimensional axisymmetric poroelastic biphasic finite element model (ABAQUS, version 6.5-5) was used to simulate the indentation tests and derive the Aggregate modulus (Ha) and permeability (K) for each hydrogel specimen.

The Ø10mm diameter by 10mm long uni-material hydrogel pin was modelled with 800 4-node bilinear displacement and pore pressure elements (CAX4RP). A maximum compressibility was assumed such that the Poisson's ratio of each hydrogel was equal to 0.0. The indenter and collet

were modelled as analytically rigid with no permeability which meant that the contact face between the indenter and hydrogel surface was an impermeable boundary. A mesh sensitivity check on the predicted results was also performed. The friction coefficient between the metal indenter and the hydrogel pin was assumed to be 0.02 *(Mow and Lai, 1980, Macirowski et al., 1994)*.

Whenever the metallic indenter and collet were in contact with the hydrogel surface no fluid flow surface conditions were implemented. For all other hydrogel surface free-flow conditions were applied using an in-house developed subroutine *(Pawaskar, 2006)*. Load was applied by a ramp condition for two seconds and deformation of the hydrogel surface was modelled for 2 hours. The computational deformation curve was matched to the experimental deformation curve by minor alterations to the Ha and K values allowing these properties to be determined from each hydrogel material.

2.4 Surface Analysis Techniques

The techniques and processes used to characterise alterations in the surface topography of all test materials are described below. All stylus profilometry measurements were conducted by a trained technician. All other protocols described in this section were undertaken by the author following suitable training. Computer data files produced by all techniques were processed and evaluated by the author.

2.4.1 Stylus Profilometry

Stylus profilometry was a common 2-dimensional method of quantifying the surface topography on engineering materials. A stylus traversed across the surface converting its vertical movement to an electrical signal which through suitable processing, filtering and calibration can be used to build a trace of the surface profile. Modern profilometry are capable of high accuracy and reproducibility within resolution limits of ~0.001-0.002μm. The stylus profilometer used within this study was a Talysurf 5 model (Taylor-Hobson, UK) connected to a standard PC. A Gaussian cut-off filter equal to 0.8mm

was defined suitable for assessing the variety of surface textures within this study. Important specifications are listed below;

Straightness of Traverse	Within 0.5μm over 120mm
Traverse Speed	0.5mm/s ±5%
Vertical Resolution	20nm at 12mm range
Conisphere Diamond Tip Radius	2.5μm
Applied Vertical Force	0.85mN
Cut off filter	Gaussian - 0.8mm

2.4.2 White Light Interferometry

White light interferometry (WLI) was a non-contact optical method used to assess surface topography. The specimen surface was exposed through a lens to a white light source. Using the principles of interference of light, which states that when light rays are reflected between two none parallel surfaces, the different path lengths at various parts of the surface cause phase changes in the reflected light. This results in some rays being cancelled out and some augment each other resulting in alternate dark and light fringes. The shape and spacing of these fringes were dependent on the reflecting surface as irregularities were reproduced in irregularities within the interference pattern being reflected back. These irregularities within the reflection pattern were processed by a standard PC and software to give a 3D representation of the surface topography and associated data files. Accurate measurements tens of centimetres in area were created by stitching a number of readings together. The model used within this study was a WYKO® surface profiler (Veeco Instruments) running WYKO® Vision 32 software. All data acquisition within this study was taken using the Vertical Scanning Interferometry (VSI) mode. Important specifications are listed below;

Vertical Range	2mm
Vertical Resolution	1nm

Accuracy	Dependent on surface and magnification
Area of focus	Dependent on magnification
Light source wavelength	Visible Spectrum (400-700nm)

2.4.3 Laser Profilometry

Laser Profilometry was a non-contacting optical method which provided qualitative information of surface topography. The process used a single frequency infrared light source which is focused on a known area of the specimen (1μm in diameter) by an optical lens. Light reflected by the specimen surface was directed by a beam splitter, through a prism onto an arrangement of photodiodes, forming two spots. At the starting point the position of the two light spots was such that the diodes were illuminated equally. As the lens moved over the surface, changes in the reflected light resulted in a shift in the imaged focal point and the illumination of the diodes became unequal. This unequal illumination caused a focal error which through an amplifier was used to infer the surface topography of the specimen surface. For consistent measurements, the area of projected light and light distribution must be kept constant. This was completed by movement of the lens relative to the surface through a control circuit which monitored the focus error signal and moved the lens accordingly. The system used within this study was the Laser Micro-focus System, (USB Messtechnik, GMBH, Germany). Important specifications are listed below;

Vertical Measurement Ranges	±50μm & ±500μm
Vertical resolution	10nm & 100nm (respectively)
Accuracy	Dependent of surface
Light spot diameter	1μm
Minimum surface reflection	1%
Light source wavelength	780nm

3 Determination of Hydrogel Mechanical Properties

3.1 Introduction

The aims of this study were to investigate and quantify the fundamental mechanical properties of a number of potential chondroplasty materials. Once completed this would allow the objective material properties to be compared with the tribological performance, providing a greater understanding of each material when assessed as a potential chondroplasty material. The mechanical properties of hydrogels are best understood using rubber elasticity and viscoelastic theory *(Anseth et al., 1996, Benham PP et al., 1996)*. A number of standard processes including Shore 'A' hardness, uniaxial tensile, unconfined compression and indentation tests were used to quantify a number of mechanical properties thus allowing a greater understanding of each potential chondroplasty materials *(British Standards, 2006, British Standards, 1996)*. All strain quoted within this study is 'Engineering Strain'

3.2 Shore 'A' Hardness and Uniaxial Tensile Testing

3.2.1 Materials

All hydrogel materials as shown in Table 2-2, were investigated using the Shore 'A' methodology *(British Standards, 2006)*. All hydrogel materials shown in Table 3-1, were investigated using the uni-axial tensile test. More information regarding all test materials can be found in Chapter 2.2.

Uniaxial Tensile Test - Biphasic Hydrogel Materials Tested	
1A	4E
1D	4G
1K	4K
2K	4L
3K	4M
4A	4N
4D	

Table 3-1: Biphasic Materials Tested using Uniaxial Tensile Method

3.2.2 Method

3.2.2.1 Shore 'A' Hardness Testing Method

The relationship between Shore hardness and Elastic modulus was demonstrated by Gent et al *(Gent, 1958)*. However, although no Shore hardness scale was specified, hard vulcanised rubber was studied indicating the use of a Shore 'D' hardness scale. Therefore, the Shore 'A' hardness model used statistically determinate data from known single phasic elastomers with quantified Shore 'A' hardness and elastic modulus which was then validated against previous literature *(Gent, 1958, George et al., 1987)*. Figure 3-1 shows the 2nd order polynomial line plotted at a 95% confidence limit from data of 25 elastomer materials, which was used to determine the equivalent elastic modulus (E_d) of each hydrogel material. By assuming an isotropic single phasic response for all materials, the model was used to determine the initial viability of each potential chondroplasty material. However, the hardness calculated within this study was an empirical test and not a material property.

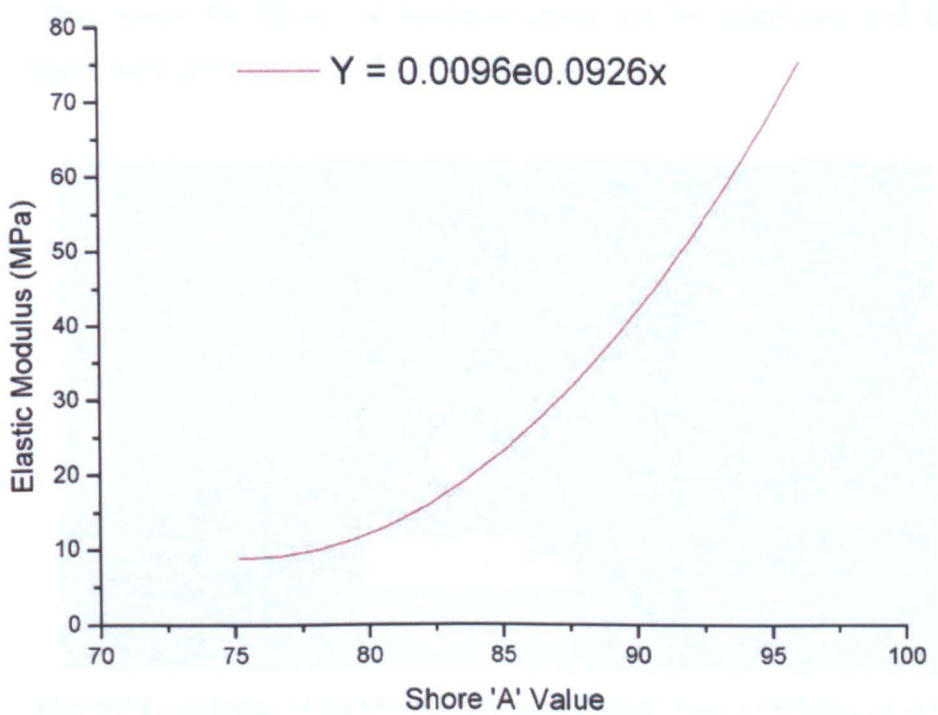

Figure 3-1: Shore 'A' Model - 2nd Order Polynomial line fitted to data from known Elastomer database

Following fourteen days hydration within distilled water at 20°C, excess water was removed from the circular hydrogel specimens using standard laboratory tissue. The specimens were then placed on to the Shore 'A' tester (Model No, 3123.01, Zwick Testing Machines Ltd, Ulm, Germany) consisting of a hardened indenter, an accurately calibrated spring and a depth indicator, shown in Figure 3-2. The indenter was mounted such that it extended 2.5mm from the surface of the sample. In the fully extended position, the indicator displayed zero and when fully depressed with a known force of 10N, the indicator displayed 100. Therefore, every shore 'A' point was equal to 0.0025 mm penetration. A deeper indentation would indicate a softer material and produce a lower indicator reading *(Ashby and Jones, 1995)*. The Shore 'A' reading was taken over a period of 10 seconds and the sample returned to the hydration medium within a maximum time limit of 30 seconds.

Three measurements were taken on three samples of each hydrogel. A small number of the hydrogel variants shattered during testing as shown in Table 3-2. This meant the Shore 'A' hardness could not be calculated and these variants were removed from the investigation.

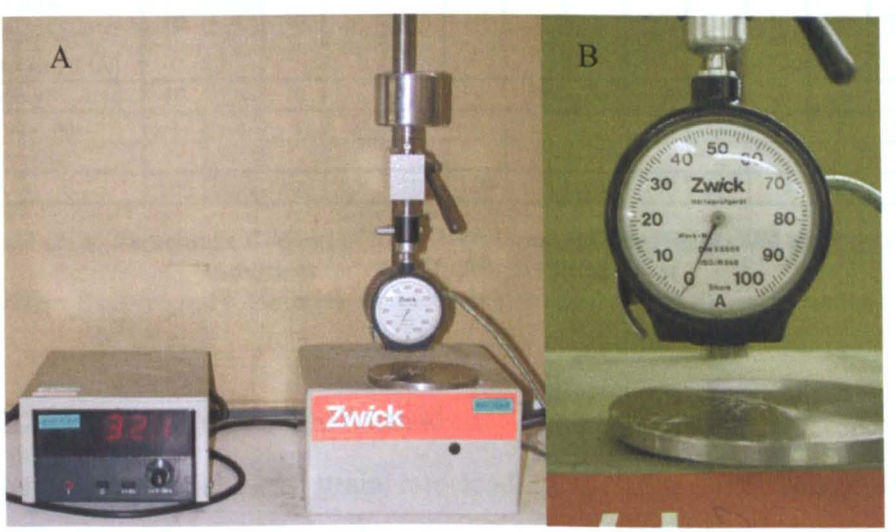

Figure 3-2: (A) Image of the Shore A tester and Digital Output, (B) Close up of the indenter, and a depth indicator

	1A	1D	1E	1G	1J	1K	1AG	2A	2D	2E	2G	2J	
Hydroxyethyl Methacrylate (HEMA)	98	88	88	88	78	78	96						
Tetrahydrofurfuryl Methacrylate THFMA								98	88	88	88	78	
Hydroxypropyl Methacrylate (HPMA)													
Ethylene glycol dimethacrylate (EGMDA)		10			10				10			10	
Polyethylene glycol-400-dimethacrylate (PED-400-DMA)			10			10				10			
Methacrylic Acid				10	10	10					10	10	
2,3-butadione	2	2	2	2	2	2	2	2	2	2	2	2	
Gentamicin							2						
Total %	100	100	100	100	100	100	100	100	100	100	100	100	
	2K	2AG	3K	4A	4D	4E	4G	4J	4K	4AG	4L	4M	4N
Hydroxyethyl Methacrylate (HEMA)			39								39		26
Tetrahydrofurfuryl Methacrylate THFMA	78	96	39									39	26
Hydroxypropyl Methacrylate (HPMA)				98	88	88	88	78	78	96	39	39	26
Ethylene glycol dimethacrylate (EGMDA)					10			10					
Polyethylene glycol-400-dimethacrylate (PED-400-DMA)	10		10			10			10		10	10	10
Methacrylic Acid	10		10				10	10	10		10	10	10
2,3-butadione	2	2	2	2	2	2	2	2	2	2	2	2	2
Gentamicin		2								2			
Total %	100	100	100	100	100	100	100	100	100	100	100	100	100

Table 3-2: Percentage Content of Monomer, Cross-linking Agents and additional Additives for each Hydrogel Variant Test
(Grey Background = Materials that tore or shattered during Shore'A' testing)

3.2.2.2 Uniaxial Tensile Test Method

A standard uni-axial 'low strain rate loading to failure test' was used to quantify material properties under uniaxial tension. Data from each test was used to determine the elastic modulus, yield point, yield strength, ultimate tensile strength and other material properties. Procedures for tensile testing of

rubber and plastics are well defined within previous literature and British standards *(Ashby and Jones, 1995, British Standards, 1996, Oka et al., 2004)*.

The thickness of each dehydrated specimen was quantified using Vernia Calipers, which allowed the selection of specimens with an un-hydrated thickness of 1 mm (±0.05mm). The specimens were then hydrated for fourteen days in distilled water at 20°C. Standard geometry test specimens were cut using a hardened steel tensile test sample cutter (Wallace and Crompton, UK) (Figure 3-3), then return the hydration medium.

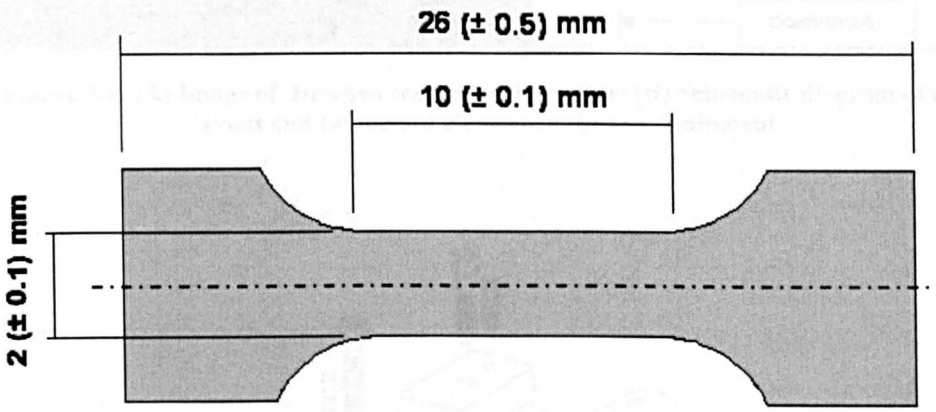

Figure 3-3: Diagram showing the relevant dimension of the Tensile Test Specimen.

The tensile testing was performed in a screw driven Howden tensile testing system, shown in Figure 3-4. The system comprised of a screw driven Howden Machine, a digital controller (Howden Model EDC100), a power amplifier (Howden Model DDA06) and a personal computer.

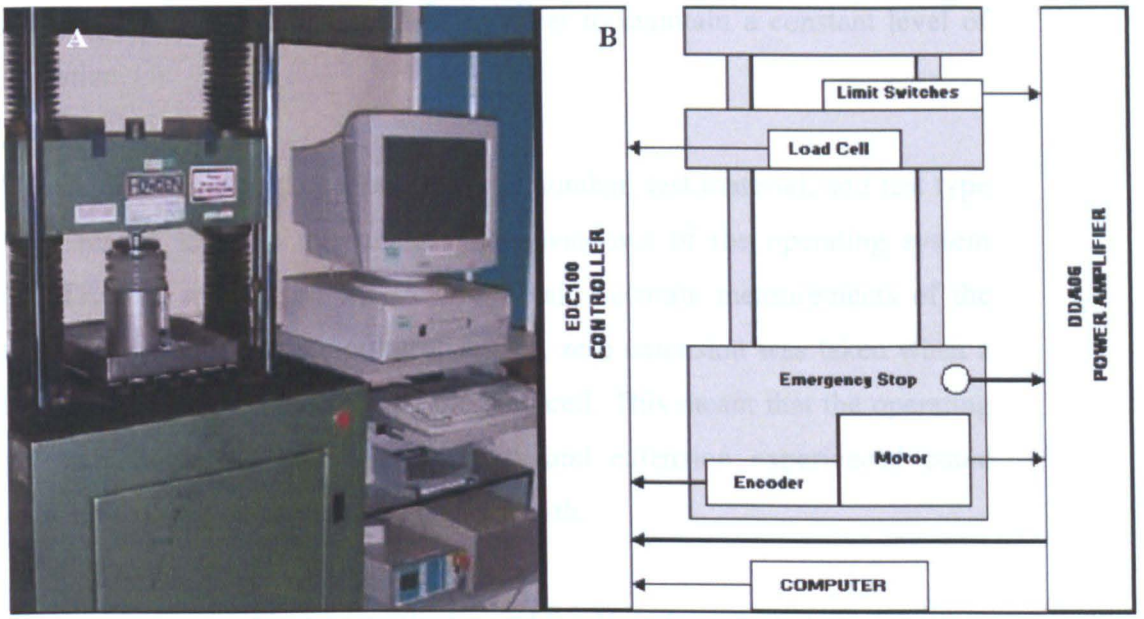

Figure 3-4: (A) Image of Howden tensile testing system (B) Schematic diagram of the layout and Important element to the test equipment

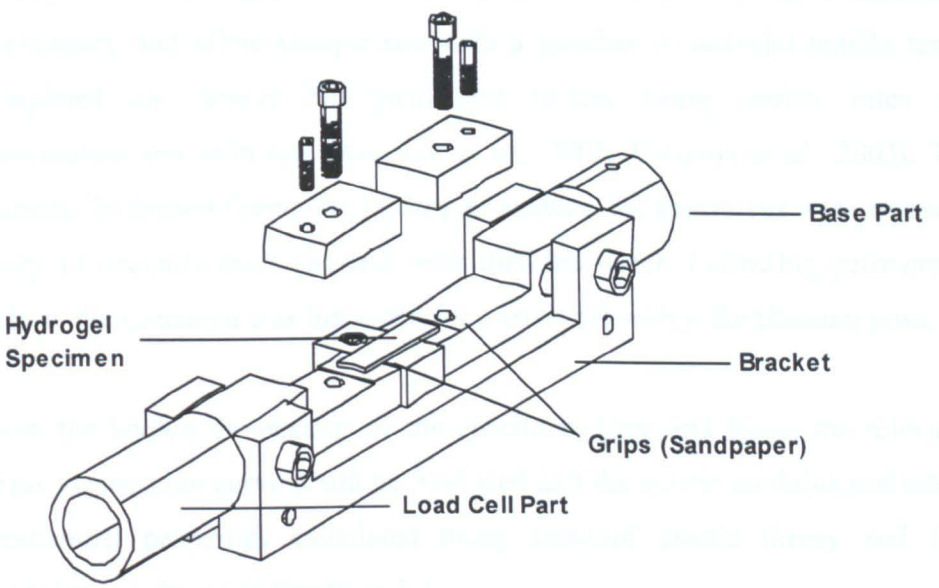

Figure 3-5: Diagram showing the purpose built aluminium and titanium jig.

Before testing the gauge length and sample thickness were measured at three different points along the test specimen, using Vernia Calipers. Each test sample was loaded with the aid of a purpose built aluminium and titanium jig, shown in Figure 3-5. The titanium jaws held the sample at the correct point indicated in Figure 3-5, and the aluminium bracket meant the jaws were aligned, removing any chance of multi-axial stress. The loading process was

completed submerged within distilled water to maintain a constant level of hydration.

Specimen thickness, gauge length, serial number, test material, and test type were loaded into the relevant dialogue windows of the operating system (MTTE.exe), running on the PC. To obtain accurate measurements of the tissue gauge length at the point of failure, zero extension was taken when a force of 0.005N was detected by the load cell. This meant that the operating program from the initial gauge length and extension experienced could automatically calculate the final gauge length.

The specimen was placed into the jig and the Howden tensile testing system. The aluminium bracket was removed and the test started. The time dependent mechanical properties of each hydrogel were considered and a test speed of 10mm/min at a data acquisition rate at 20Hz was used. This was to maintain consistency and allow comparison with a number of uniaxial tensile tests completed on various biological soft tissues using similar rates of deformation and stain rate *(Korossis et al., 2002, Korossis et al., 2005)*. To maintain hydration during the loading procedure, the specimens were sprayed every 15 seconds front and rear with distilled water. Following permanent failure, the specimen was inspected for movement within the titanium jaws.

From the known dimensions of the specimen, time and force, the relevant stress verses stain curve could be produced and the elastic modulus and other mechanical properties calculated using standard elastic theory and the formulations shown in Equation 3-1.

$$\sigma_{TS} = F_{TS} / A$$

$$\varepsilon_{TS} = \Delta L / L \qquad (3\text{-}1)$$

$$E = \sigma_{TS} / \varepsilon_{TS}$$

Tensile Stress (σ_{TS}), Tensile Strain (ε_{TS}), Elastic Modulus (E), F_{TS} = Uniaxial Tensile Force, A = Cross sectional Area of the sample, L = None Constrained Sample Length, ΔL = Uniform extension of None Constrained Sample Length in the uniaxial direction and ε_{NS}= Nominal Strain.

3.2.3 Non-confined Indentation and Finite Element Analysis

3.2.3.1 Experimental

Three samples of each hydrogel specimen (Table 3-3) were hydrated for a minimum of 4 weeks within Ringer's solution. Figure 3-6 shows the final dimensions and the position when placed into a custom made collet. Each collet was then mounted into a bath filled with 100% Ringer's solution and placed into the indentation apparatus as described in section 2.3.4. The specimen was then left for 2 minutes to acclimatise. A load of 1.9 N was then applied to the indenter resulting in a contact pressure between the Ø3 mm flat faced indenter and the hydrogel pin of 0.27 MPa.

	Ø10mm by 10mm Diameter Hydrogel Pin
Hydrogel Variant	1D
	4M
	4N
	3K
	SaluCartilage™

Table 3-3: The hydrogel specimen tested using the indentation and finite element methodology

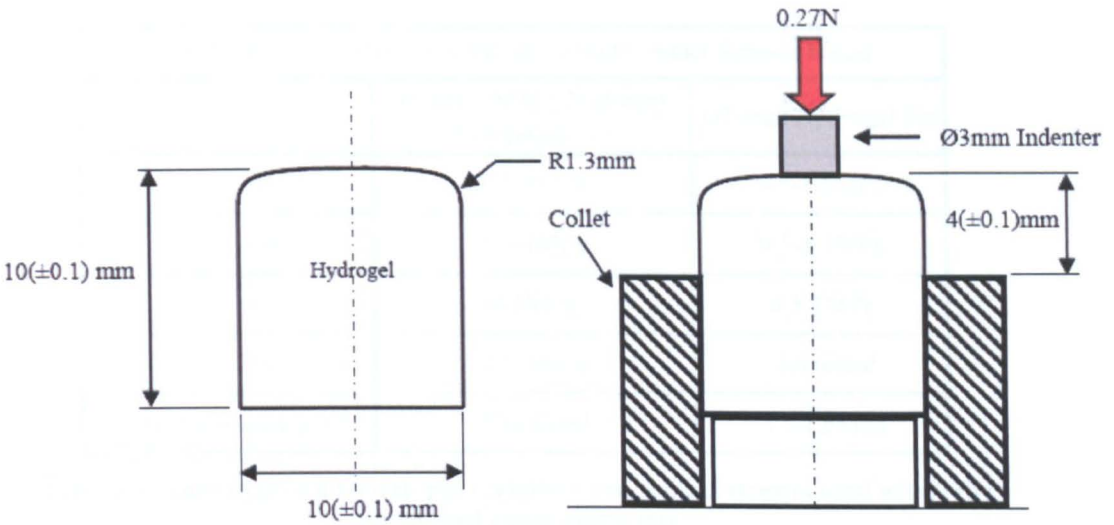

Figure 3-6: Hydrated hydrogel pin dimensions and experimental configuration within the collet fixtures for the indentation test

Deformation of the specimen was recorded for 2 hours at a sample rate of 5 Hertz, at which point the data acquisition was stopped and the load removed. The specimen was inspected for any visual signs of fracture or material loss and stored a +4°C for further analysis.

3.2.3.2 Computational

Using the finite element model described in section 2.3.4.3, a theoretical deformation curve was produced for each hydrogel variant and compared with the average indentation displacement curve. The computational deformation curve was matched to the indentation displacement curve by minor alterations to the aggregate modulus (Ha) of the solid phase *(Mow and Hayes, 1997, Mow et al., 1980a, Ateshian et al., 1994)* and permeability (K) values allowing these properties to be determined for each hydrogel material. The water content for SaluCartilage™ was assumed to be 75% *(Stammen et al., 2001)*.

3.2.4 Uniaxial Unconfined Compression Tests of Hydrogel Materials

Table 3-4 shows the hydrogel materials testing within two different pin formats, a Ø5mm by 10mm bi-material polymethylmethacrylate (PMMA) Hydrogel composite and a Ø10mm by 10mm uni-material hydrogel pin, as described in the section 2.3.

The Range on Materials, Pin Variations and Contact Stresses tested			
		Ø5mm PMMA/Hydrogel Composite Pin	Ø10mm Hydrogel Pin
Hydrogel Variant	1D	0.5-1MPa	0.5-1.5MPa
	4M	0.5-1MPa	0.5-1.5MPa
	4N	0.5MPa	0.5-1MPa
	3K	0.5-1MPa	Not tested
	SaluCartilage™	Not tested	0.5-1.5MPa

Table 3-4: The range of materials pin variations and contact stresses used within the unconfined compression test

Three pins of each specimen were mounted into three collets as shown in Figure 3-7. Each collet was then loaded into the tri-pin and disc holder and positioned 0.5 mm above the stainless steel disc making sure that the pins were full submerged within a bath of 25% bovine serum. The depth gauge was then positioned and the appropriate load applied. The initial value was taken at the point when the pins contacted the stainless steel disc. The height variation was recorded at set points for 24 hours. The pins were removed and inspected for any visible sign of damage.

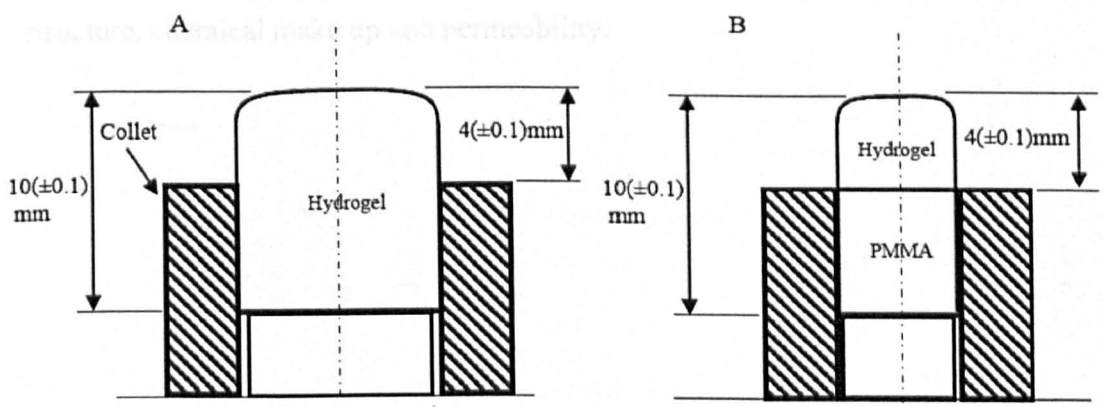

Figure 3-7: A schematic diagram showing the position of each pin Variant when placed within the collet, (A) shows Ø10mm Hydrogel Pins, (B) shows Ø5mm Hydrogel/PMMA Variant

3.3 Hydrogel Mechanical Properties Results

3.3.1 Elastic and Biphasic Properties

Figure 3-8 shows a number of tensile stress versus stain results for hydrogel 4M obtained using the uniaxial tensile test methodology. The Shore 'A' determined equivalent elastic modulus (E_d) and the uniaxial tensile test determined equivalent elastic modulus (E_{ts}) for each hydrogel (Figure 3-9) demonstrated a wide variation between both methodologies. The correlation between both sets of results and a linear regression line were plotted (Figure 3-10), demonstrating a R^2 number = 0.22896 thus a low correlation and a large variation between evaluation methodologies

Despite processing different monomers, hydrogel variants 2K and 4D produced stress /strain curves with three distinct regions as seen in biological tissue such as cartilage and heart values *(Freeman, 1979, Broom, 1977)*, indicating an initial unfolding of the long monomer chains, a secondary phase of gradual monomer realignment and orientation and an final third phase in which the load is support by the long monomers chain entirely. This three phase stress /strain curve was not seen within the other hydrogels indicating a variation in load resistance, dependent of the movement of the molecular structure, chemical make up and permeability.

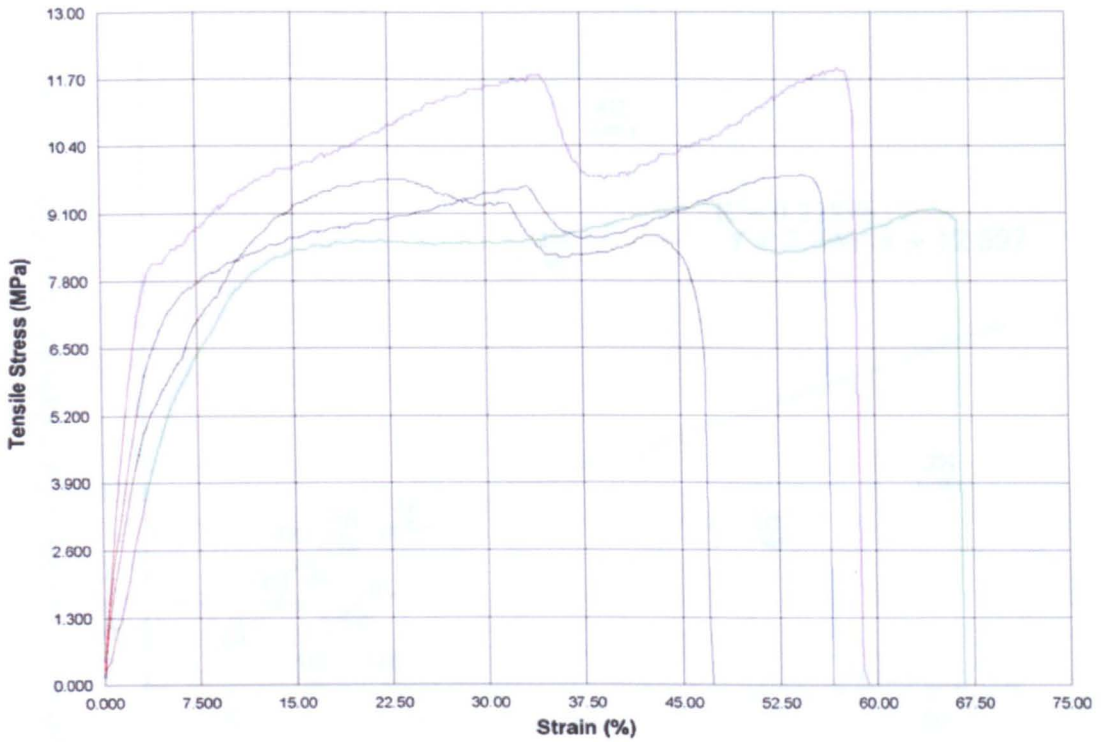

Figure 3-8: Tensile Stress against Tensile Strain Plots for Hydrogel 4M acquired during the Uniaxial Tensile Test

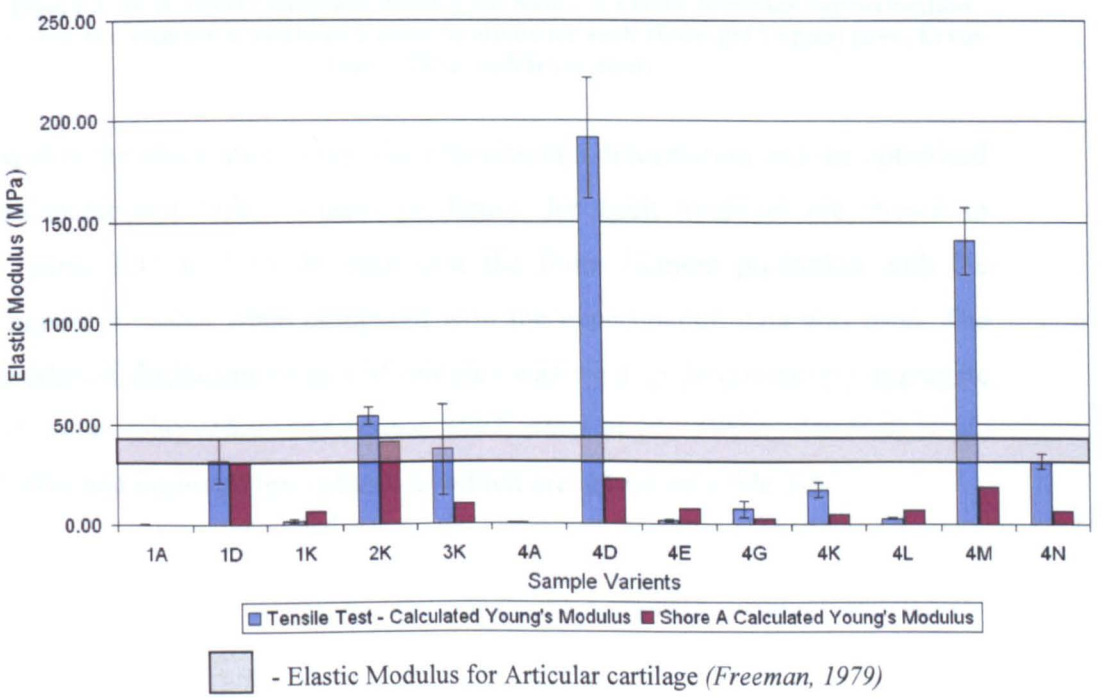

Figure 3-9: Determination of the Elastic Modulus of Hydrogel variants from Shore A' and Uniaxial Tensile Testing (n=6, Error bars = 95% confidence limit)

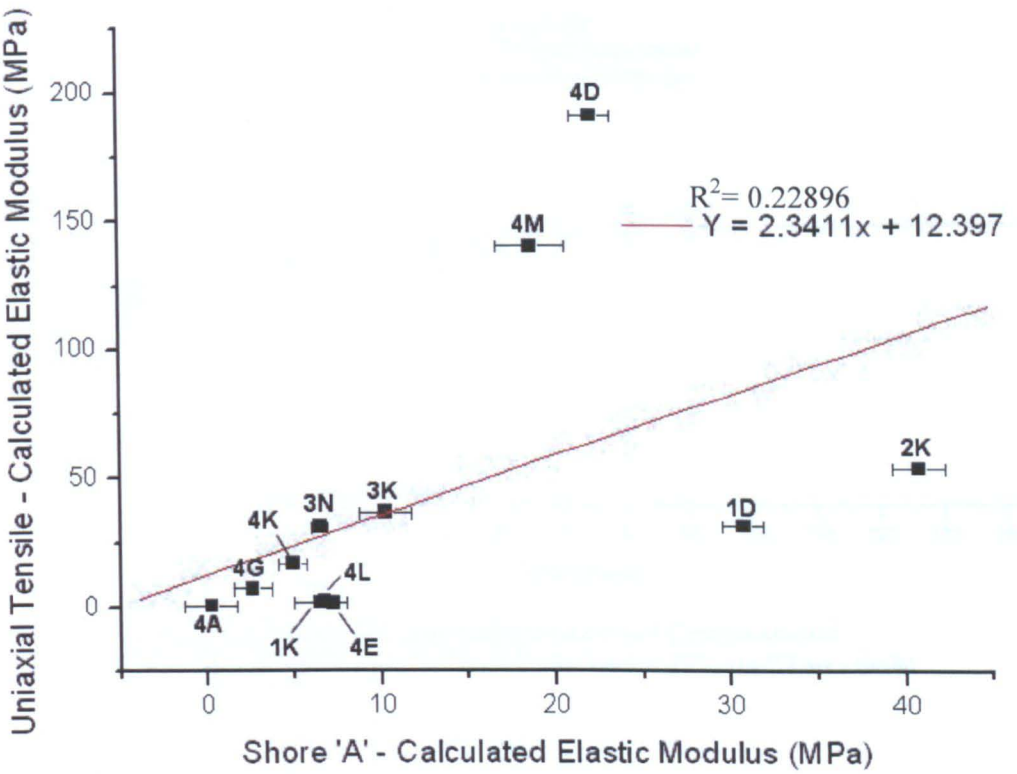

Figure 3-10: A Scatter Diagram showing the Shore A Elastic Modulus approximation against the Uniaxial Calculated Elastic Modulus for each Hydrogel Variant (n=6, Error bars = 95% confidence limit)

Within the indentation study, the experimental deformation and the optimised computational finite element prediction for each hydrogel are shown in Figures 3-11 to 3-15. In each case the finite element prediction with the highest R^2 value when compared with the experimental data was used. The predicted displacement at 150 minutes was used to determine the aggregate Modulus (Ha) *(Mow and Hayes, 1997, Mow et al., 1980a, Ateshian et al., 1994)* and permeability values (K) which are shown in Table 3-5.

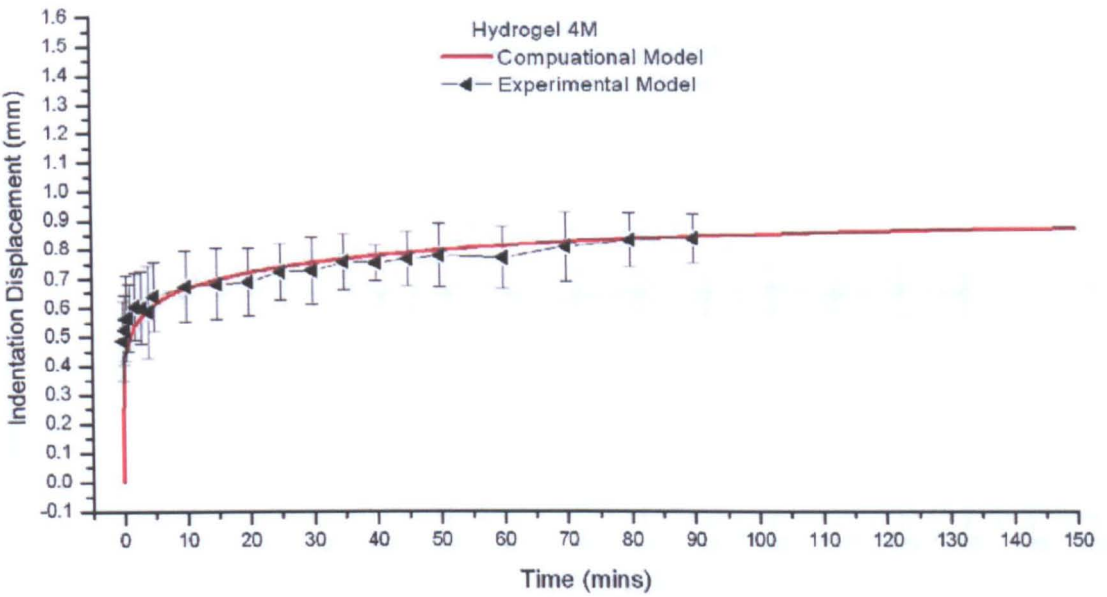

Figure 3-11: Indentation Test Experimental and Computational Height Reduction for Hydrogel 4M, (n=3, Error bars = 95% confidence limit)

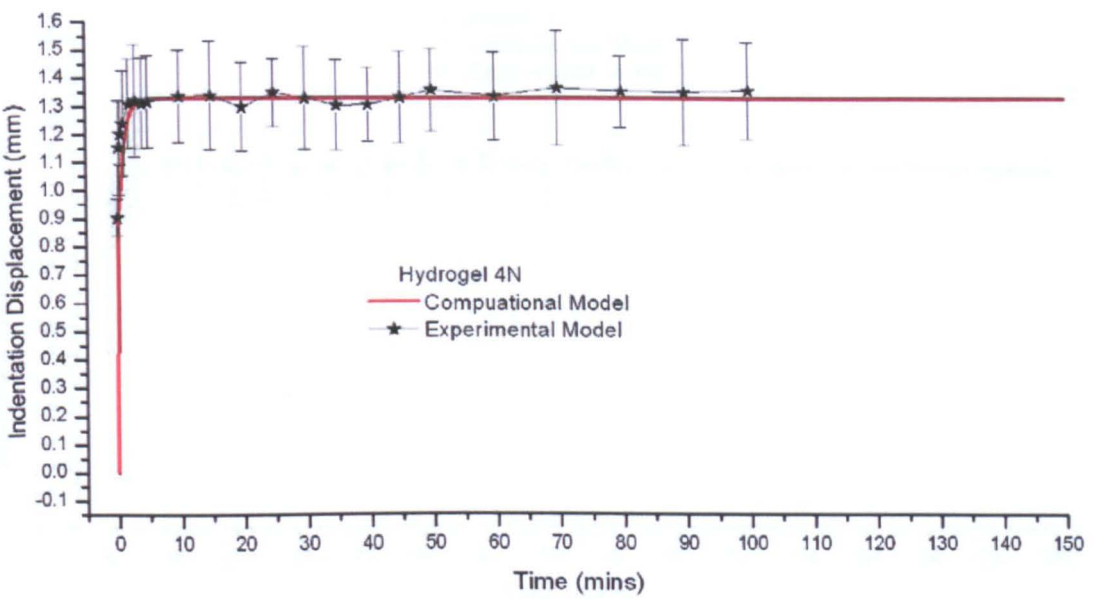

Figure 3-12: Indentation Test Experimental and Computational Height Reduction for Hydrogel 4N (n=3, Error bars = 95% confidence limit)

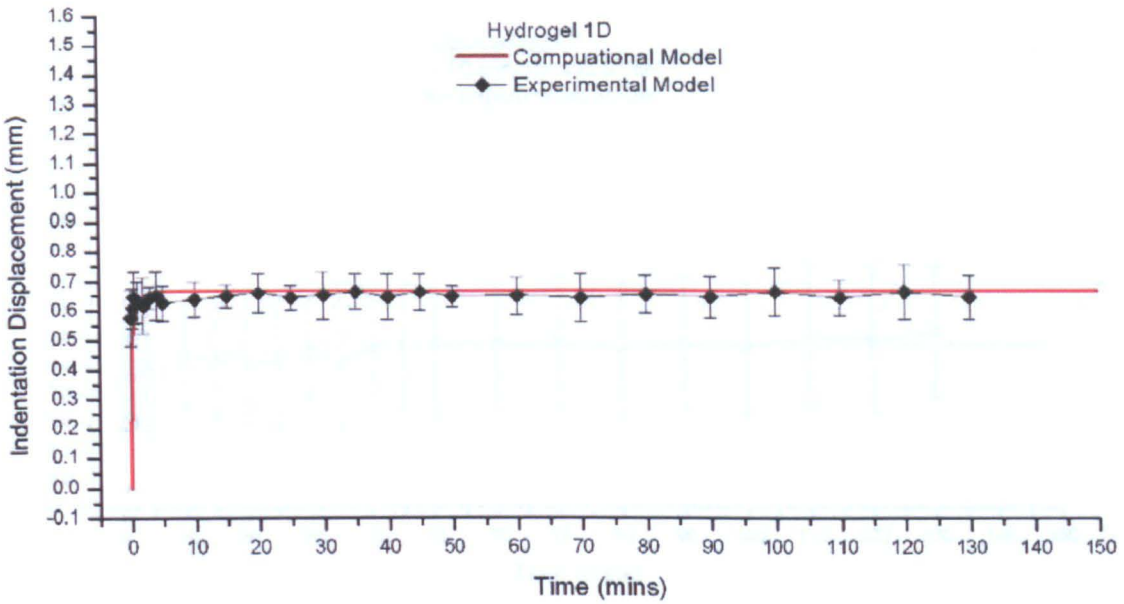

Figure 3-13: Indentation Test Experimental and Computational Height Reduction for Hydrogel 1D (n=3, Error bars = 95% confidence limit)

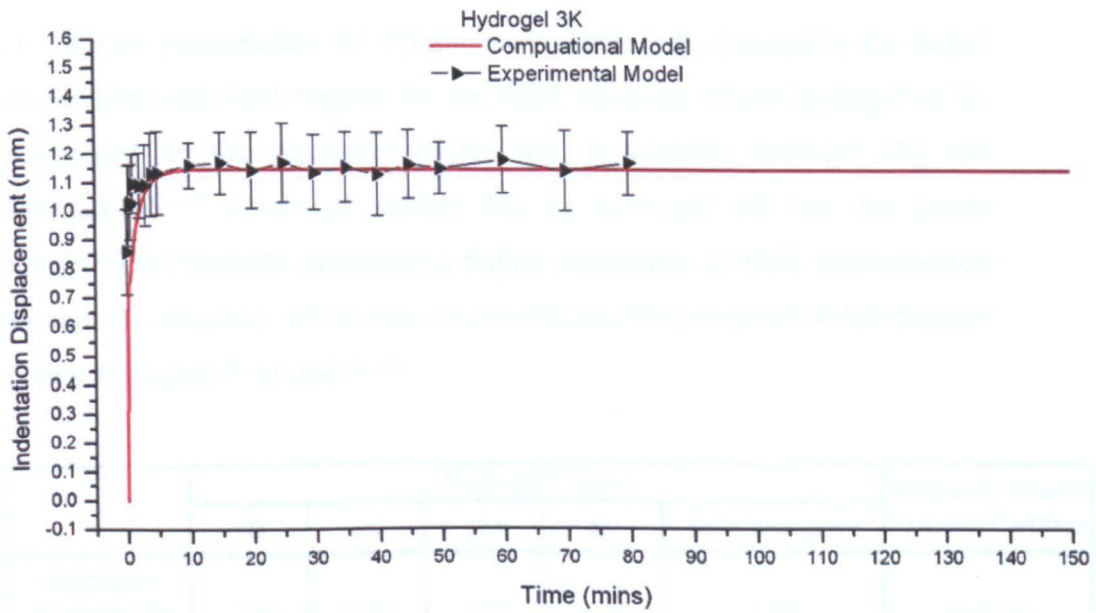

Figure 3-14: Indentation Test Experimental and Computational Height Reduction for Hydrogel 3K (n=3, Error bars = 95% confidence limit)

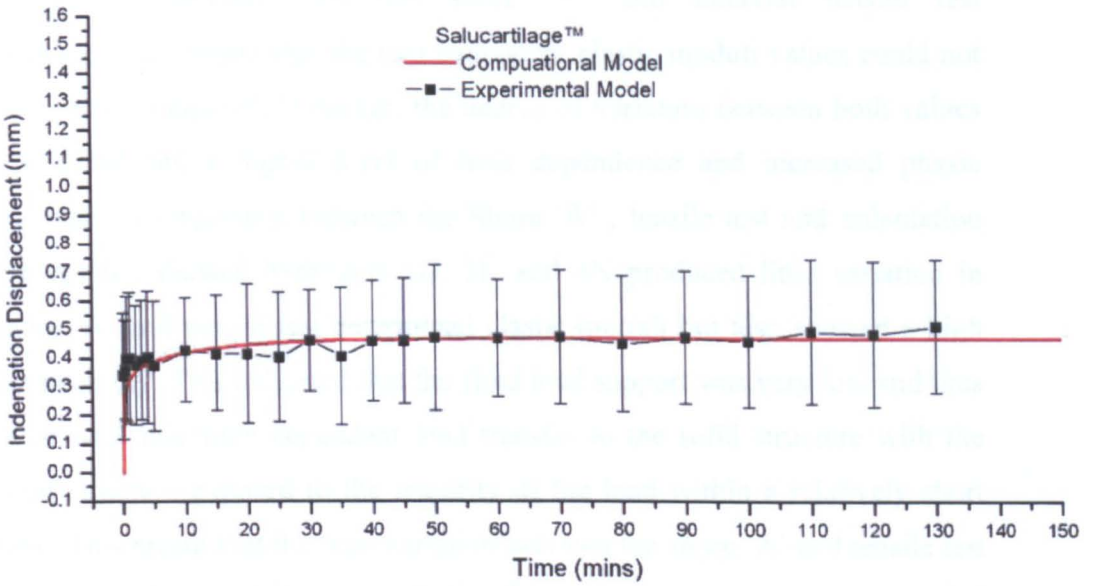

Figure 3-15:Indentation Test Experimental and Computational Height Reduction for Salucartilage™ (n=3, Error bars = 95% confidence limit)

This higher permeability for 1D shown in Table 3-5, resulted in the initial deformation and load support by the solid structure of the hydrogel to be maintained for the remainder of the test. In contrast hydrogel 4M and SaluCartilage™ processed similar Ha to hydrogel 1D but far lower permeability constants indicating a higher percentage of fluid pressurisation through the structure, which could have dictated the progressive deformation shown in Figures 3-11 and 3-15.

	Hydrogel Variant					Range for Natural Articular Cartilage
	1D	3K	4M	4N	SaluCartilage™	
Aggregate Modulus, Ha (MPa)	1.00	0.50	0.72	0.44	1.50	0.47-15
Permeability K ($x10^{-15} m^4/Ns$)	0.50	0.50	0.01	1.50	0.02	0.004 -0.019

Table 3-5: Summary of Model Derived Compression Modulus and Permeability for each Hydrogel Variant ***(Mow et al., 1989, Swann and Seedhom, 1989, Jin et al., 2000).***

The fundamental mechanical properties for a biphasic or viscoelastic material are time dependent until an equilibrium state is reached *(Mak et al., 1987, Mow et al., 1980a, Ateshian, 1997, Ateshian et al., 1994)*. The time load

application between both the Shore 'A' and uniaxial tensile test methodologies meant that the two equivalent elastic moduli values could not be directly compared. However, the degree of variation between both values would indicate a higher level of time dependence and increased phasic response. Comparison between the Shore 'A' , tensile test and indentation test results, showed hydrogels 1D, 3K and 4N produced little variation in shore 'A' and tensile test determined elastic moduli but also showed a high permeability. This indicated that the fluid load support was very low and thus there was little time dependent load transfer to the solid structure with the solid structure exposed to the majority of the load within a relatively short time. This meant that the time variation between the shore 'A' and tensile test methodologies would have had little effect on the equivalent elastic moduli values calculated.

In contrast, hydrogel 4M produced a large difference in shore 'A' and tensile test determined elastic moduli, a low permeability and thus a more dominant phasic response. This phasic response indicates high levels of initial fluid load support and time dependent load transfer between the fluid phase and solid phase. Thus, the time variation between the Shore 'A' and tensile test methodologies had a far greater influence on the calculated elastic moduli value and thus resulted in the large variation demonstrated between the two methods.

3.3.2 Ultimate Tensile and Compressive Strength Results

The tensile strength (σ_{ts}) for each hydrogel, shown in Figure 3-16, demonstrated that although the E_{ts} for the number of hydrogels was within the range of articular cartilage, the σ_{ts} was considerably lower. The majority of hydrogel specimens have σ_{ts} values in the order of 500% lower than the presented range for articular cartilage *(Freeman, 1979)*. The presented data including the 1% proof stress of each hydrogel (Figure 3-17), clearly showed the fundamental mechanical property differences between each hydrogel polymer and the complex un-homogeneous structure of articular cartilage.

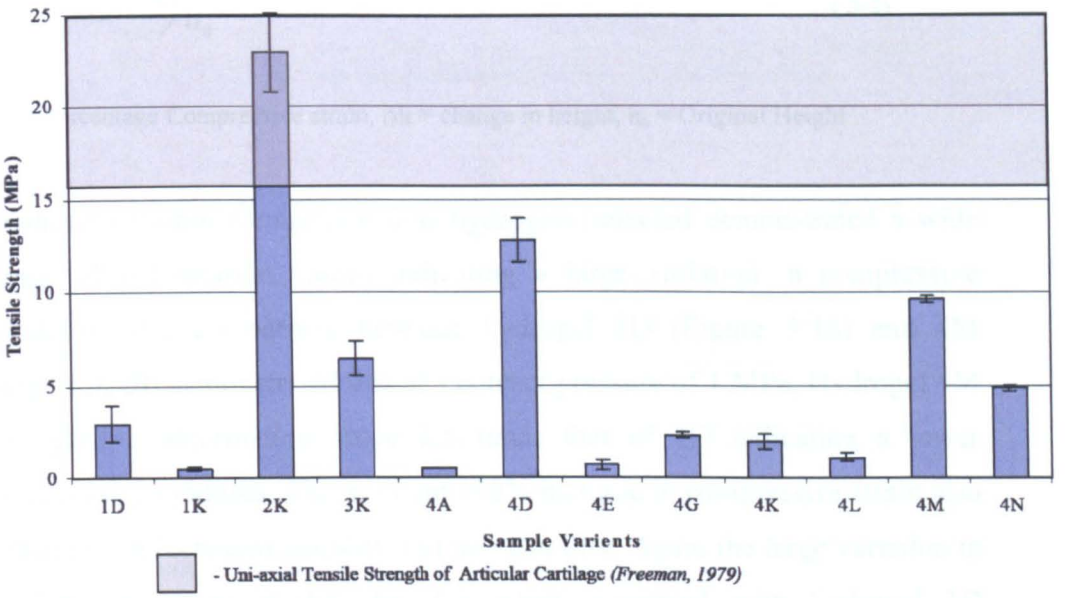

Figure 3-16: Uniaxial Tensile Strength calculated using Uniaxial Tensile Testing (n=6, Error bars = 95% confidence limit)

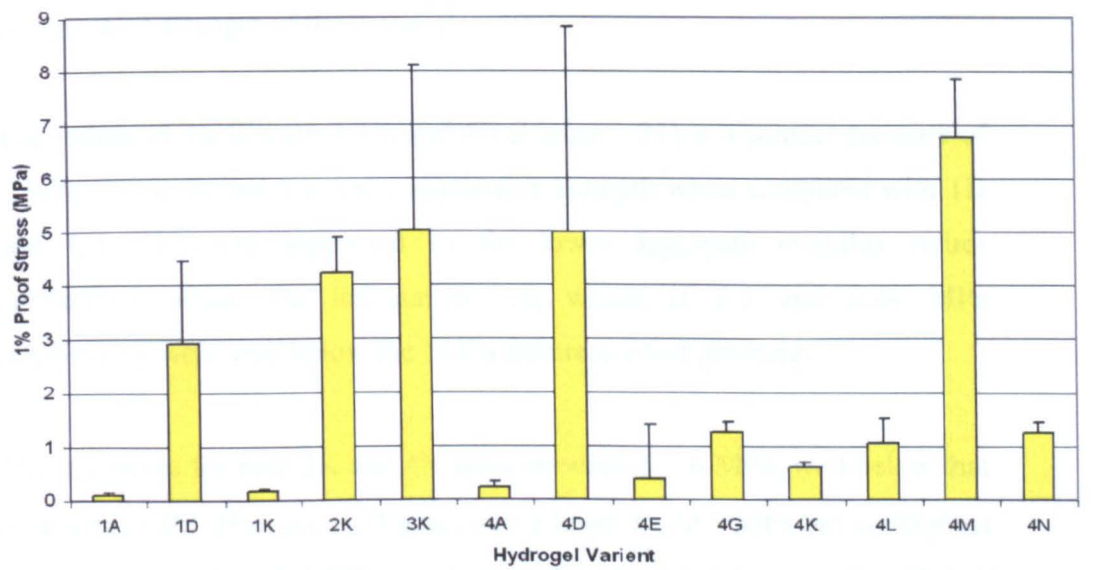

Figure 3-17: Hydrogel Variant 1% Proof Stress Calculated from Uniaxial Tensile Testing (n=6, Error bars = 95% confidence limit

Considering both uni-material and bi-material pins, the compression test produced a wide variation in height deformation between individual hydrogels and material configuration. By assuming a contact stress and using Equation 3-2, the percentage compressive strain (ε_{Cs}) was also calculated allowing further evaluation of each hydrogel material.

$$\varepsilon_{Cs} = \Delta h / h_0 \qquad (3\text{-}2)$$

ε_{Cs} = Percentage Compressive strain, Δh = change in height, h_0 = Original Height

Within the bi-pin format, the four hydrogels selected demonstrated a wide range of deformation values indicating a large variation in compressive modulus. The comparison between hydrogel 1D (Figure 3-18) and 4M (Figure 3-20) demonstrated that at a contact pressure of 1 MPa, Hydrogel 4M produced a deformation value 2.5 times that of 1D indicating a lower compressive modulus. The resultant 150% increase in compressive strain also indicated an increased ductility and permeability. Again the large variation in determined elastic moduli for 4M when compared with hydrogel 1D indicated the importance of viscoelastic and biphasic effects in the compression strength of the material.

The failure of 3K (Figure 3-19) and 4N (Figure 3-21) at a contact pressure of 1 MPa also indicated a lower compressive strength when compared with 1D and 4M. This was supported by the lower aggregate modulus values determined within the indentation test which at 0.5 and 0.44 MPa respectively were well below the 1MPa failure contact pressure.

The σ_{ts} values for both 3K and 4N were between 5 – 6 MPa, well below that of hydrogel 4M. However, 1D processed a lower σ_{ts} of 3 MPa but the highest aggregate modulus of 1 MPa, indicating that the compressive strength and resistance to failure for each material was related to the internal stresses generated by fluid dissipation and the fluid like realignment of the molecular structure. As viscoelastic materials, the time variation between the Shore 'A', uni-axial tensile test and compression test means a fundamental variation in stress distribution throughout the material *(Benham PP et al., 1996)* which could explain the variation in results for hydrogel 1D. However, as demonstrated in section 3.3.1, the high level of permeability and low phasic nature of 1D means this effect would be small.

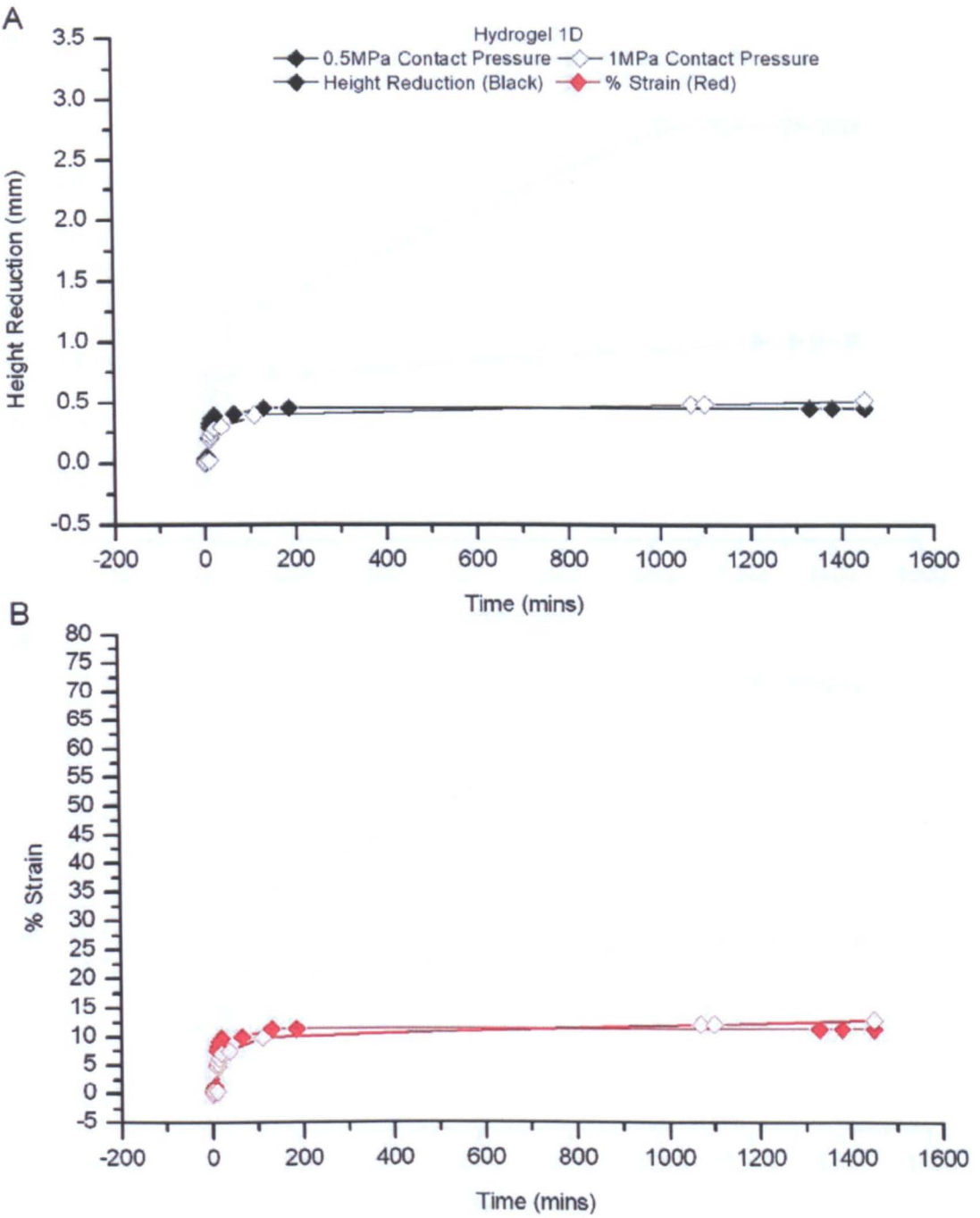

Figure 3-18: Ø5mm by 10mm Bi-material Cement/Hydrogel Height reduction (A) and % Stain (B) for hydrogel Variant 1D

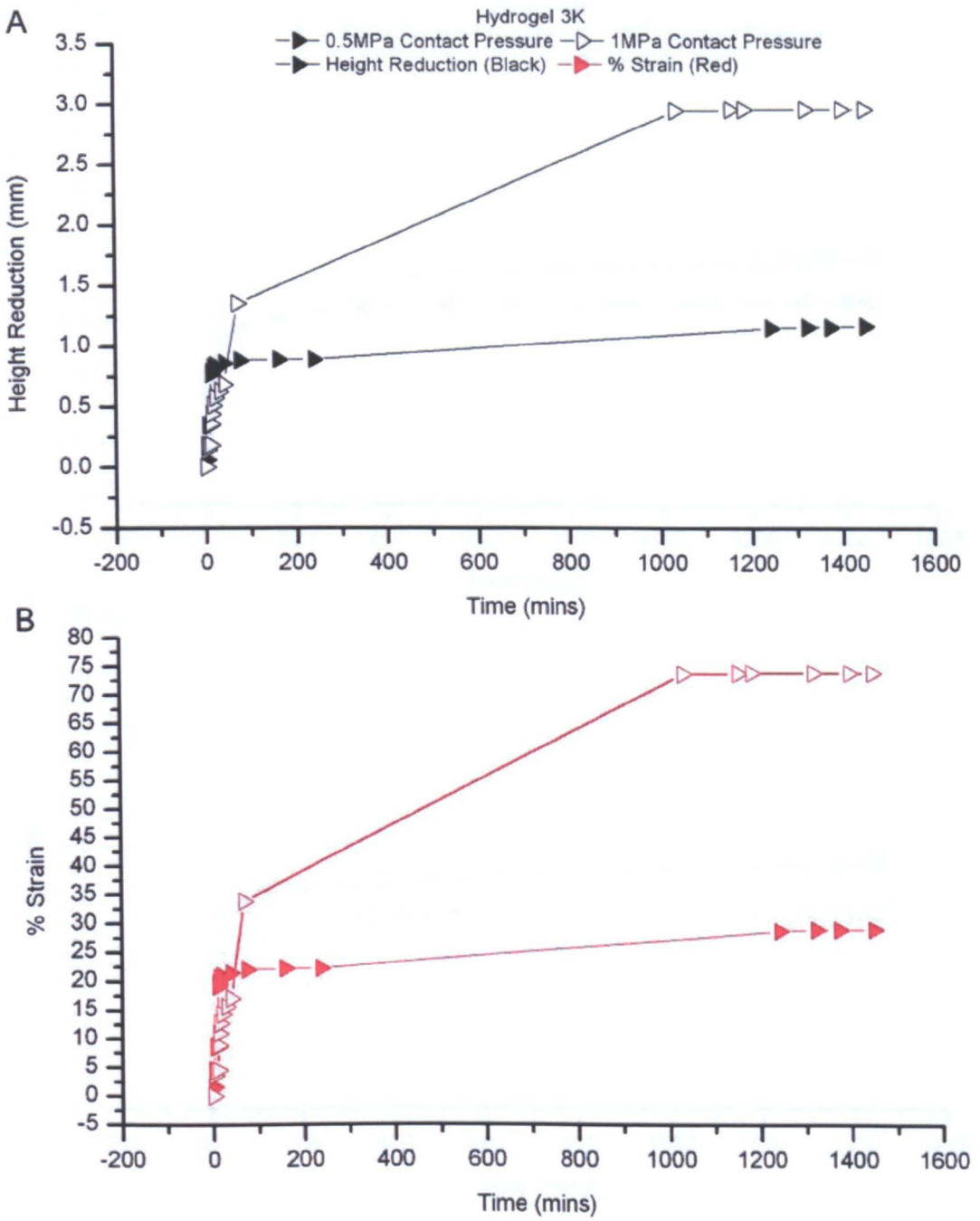

Figure 3-19: Ø5mm by 10mm Bi-material Cement/Hydrogel Height reduction (A) and % Stain (B) for hydrogel Variant 3K

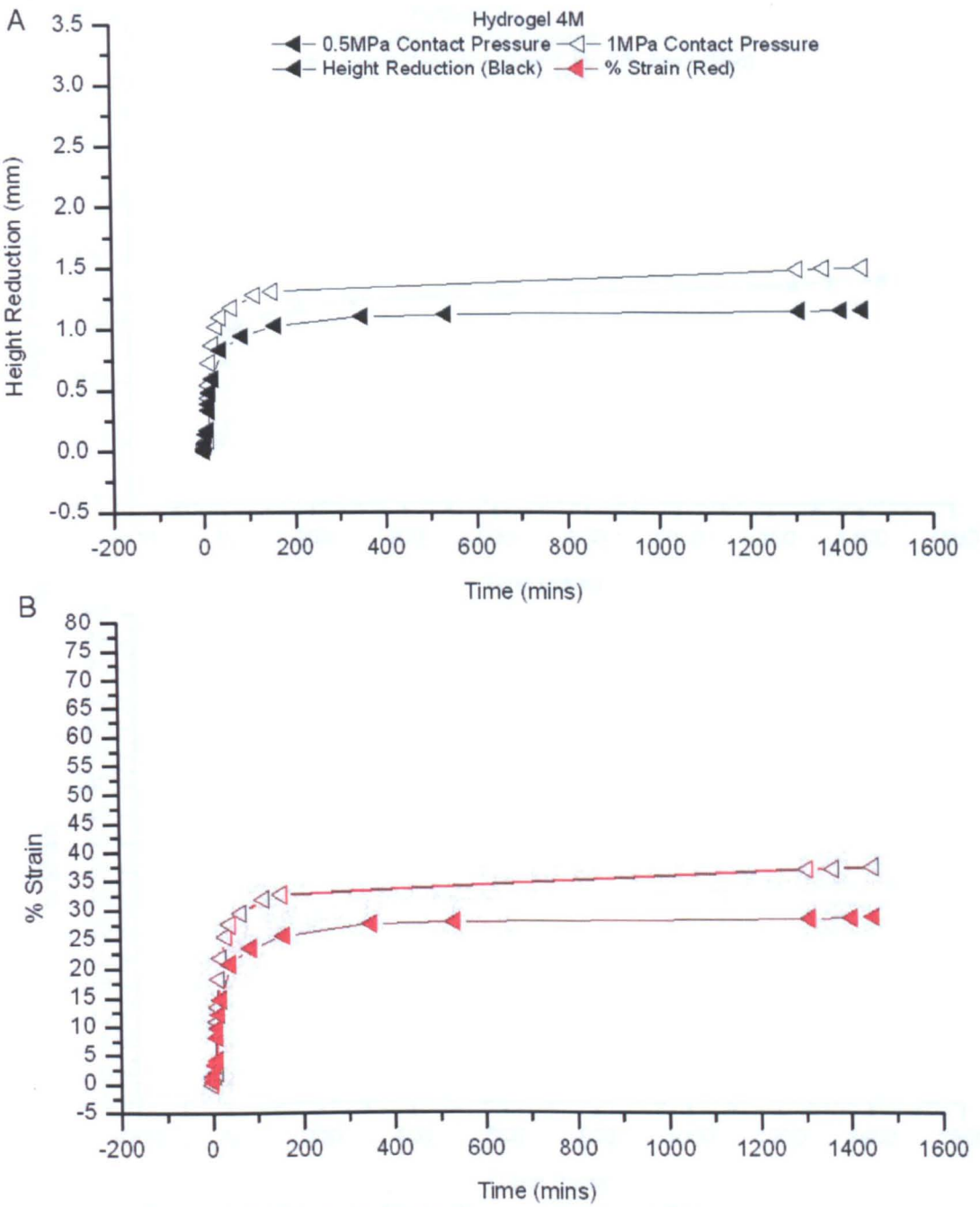

Figure 3-20: Ø5mm by 10mm Bi-material Cement/Hydrogel Height reduction (A) and % Stain (B) for hydrogel Variant 4M

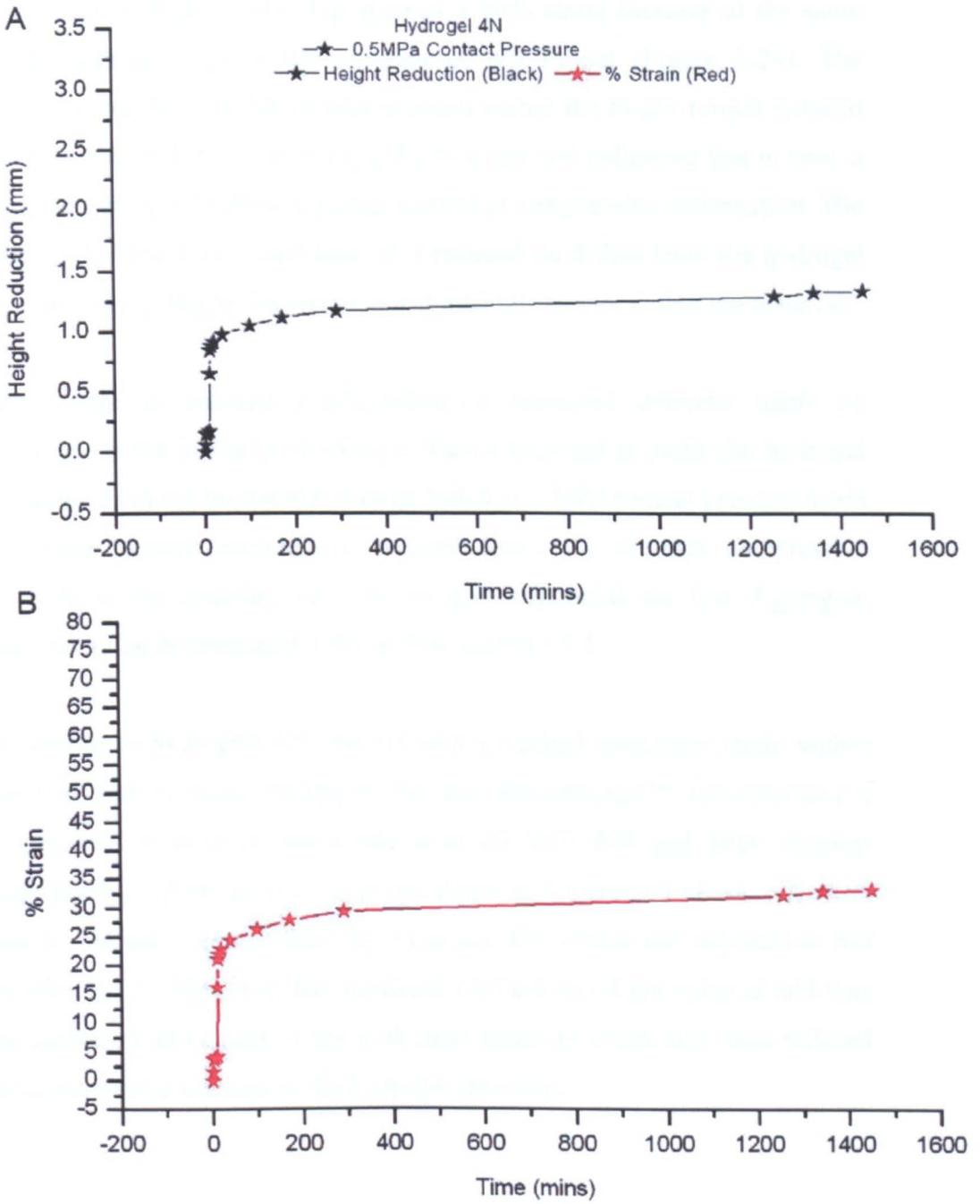

Figure 3-21: Ø5mm by 10mm Bi-material Cement/Hydrogel Height reduction (A) and % Stain (B) for hydrogel Variant 4N

Assuming a constant contact pressure within the uni-material pin compression test, each hydrogel demonstrated a strain increase of between 30-100% when compared with the bi-materials pins. Hydrogel 1D showed little or no increase in deformation between 0.5 MPa and 1 MPa within the

bi-pin format (Figure 3-18) but showed a 60% strain increase at the same contact pressures within the uni-material pin format (Figure 3-24). The reduced percentage of deformable material within the bi-pin format reduced the deformation distance increasing the % strain and indicating that *in vivo*, a composite pin would allow a greater control of compressive deformation. The rigid PMMA backing would have also reduced fluid flow from the hydrogel layer increasing fluid pressurization and internal stresses within the material.

The change in material configuration or increased diameter made no difference to the overall performance of each hydrogel in particular hydrogel 4N which as in the bi-material format, failed at 1 MPa contact pressure again indicating internal compressive stresses above the ultimate compressive strength of the material. This failure also supported the low Aggregate modulus value determined for 4N within section 3.3.1.

In contrast to hydrogels 4N and 1D which reached maximum strain within the first 120 minutes, Hydrogel 4M and Salucartilage™ demonstrated a progressive increase in strain rate over the first 800 and 1600 minutes respectively, indicating a lower permeability and increased phasic response, which was also demonstrated by hydrogel 4M within the indentation test (Section 3.3.1). However, the increased viscoelasity of the material and thus the increased movement of the molecular structure could also have reduced the compressive stresses on the hydrogel structure.

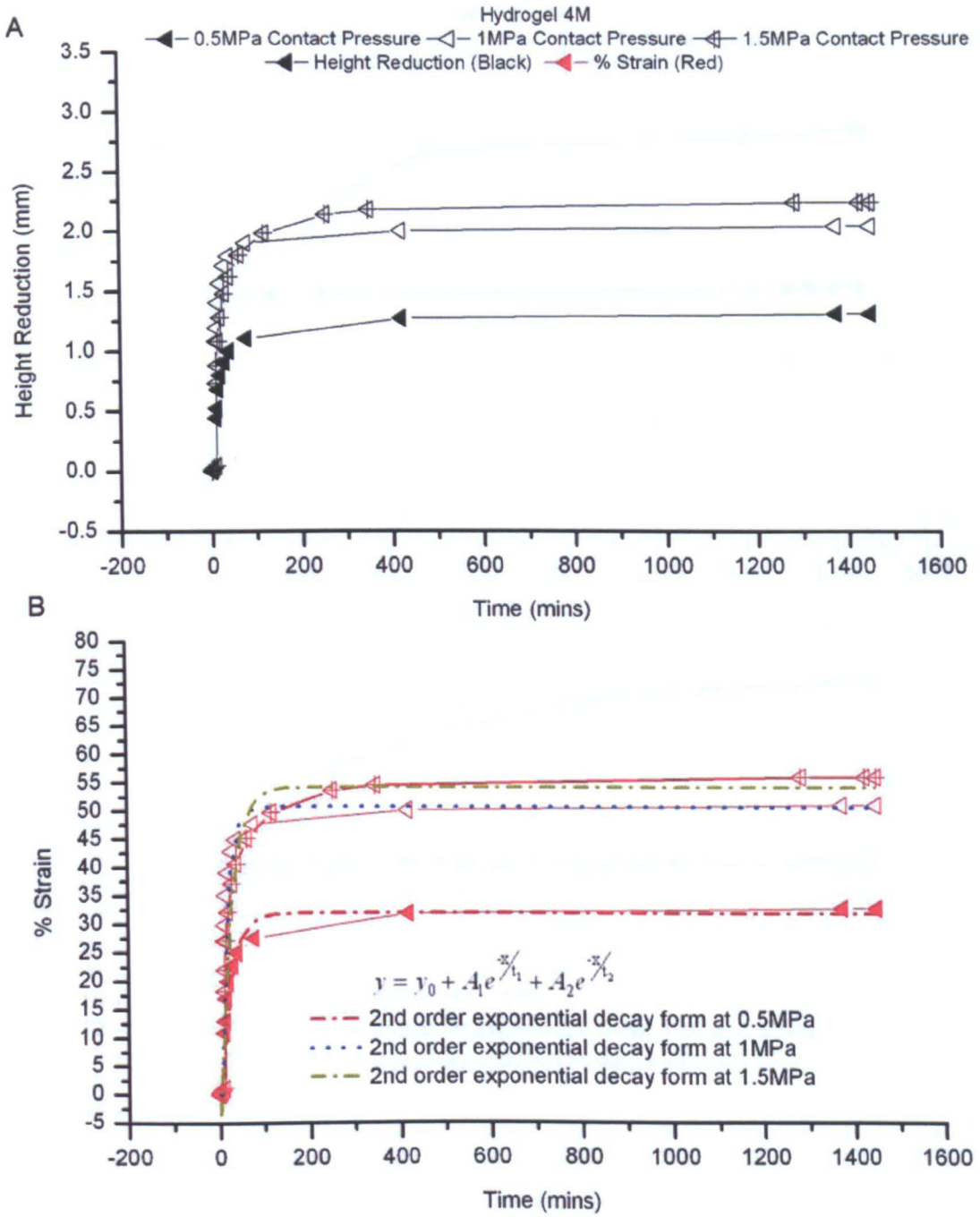

Figure 3-22: Ø10mm by 10mm Uni-material Pin Height reduction (A) and % Stain (B) for Hydrogel Variant 4M

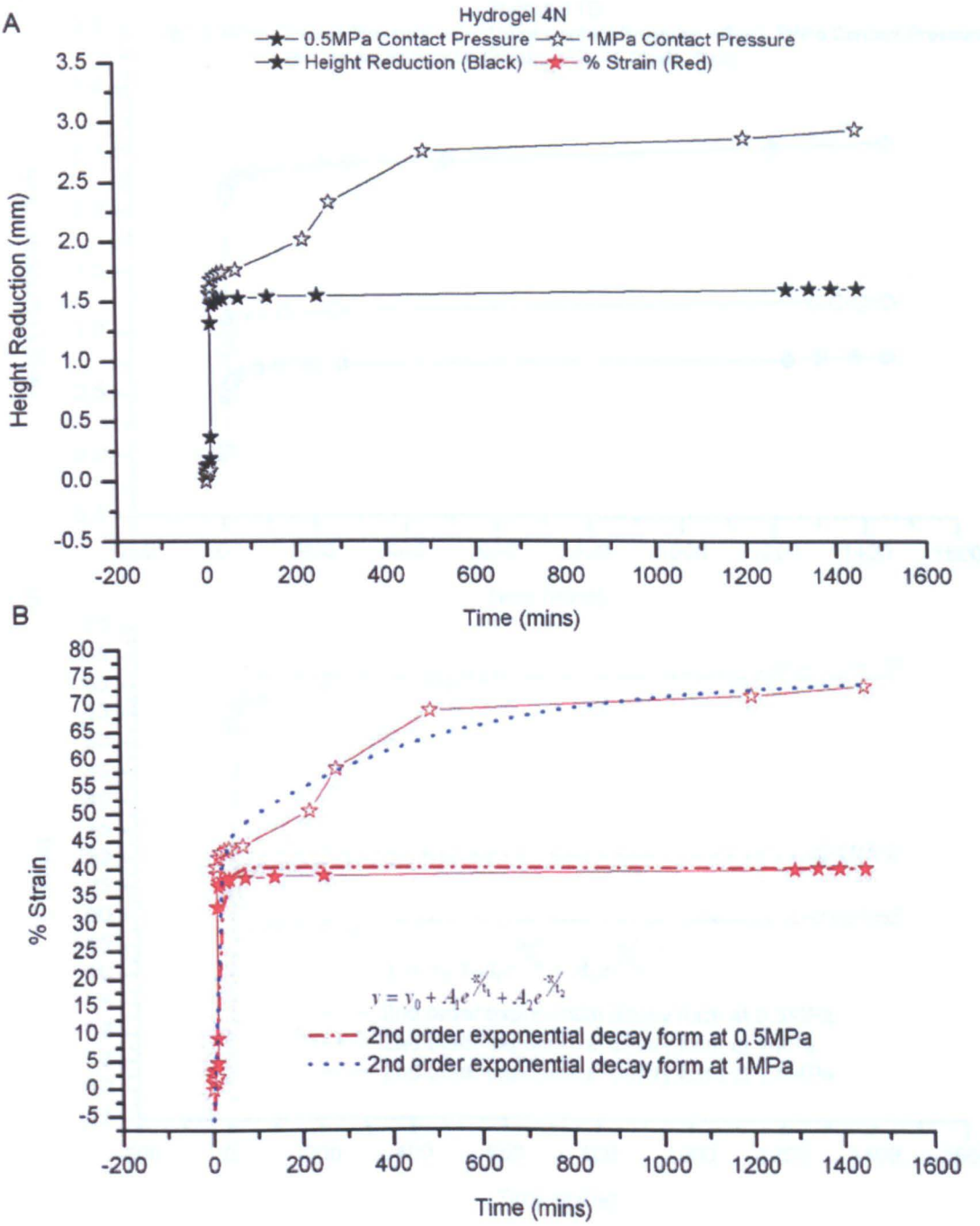

Figure 3-23: Ø10mm by 10mm Uni-material Pin Height reduction (A) and % Stain (B) for Hydrogel Variant 4N

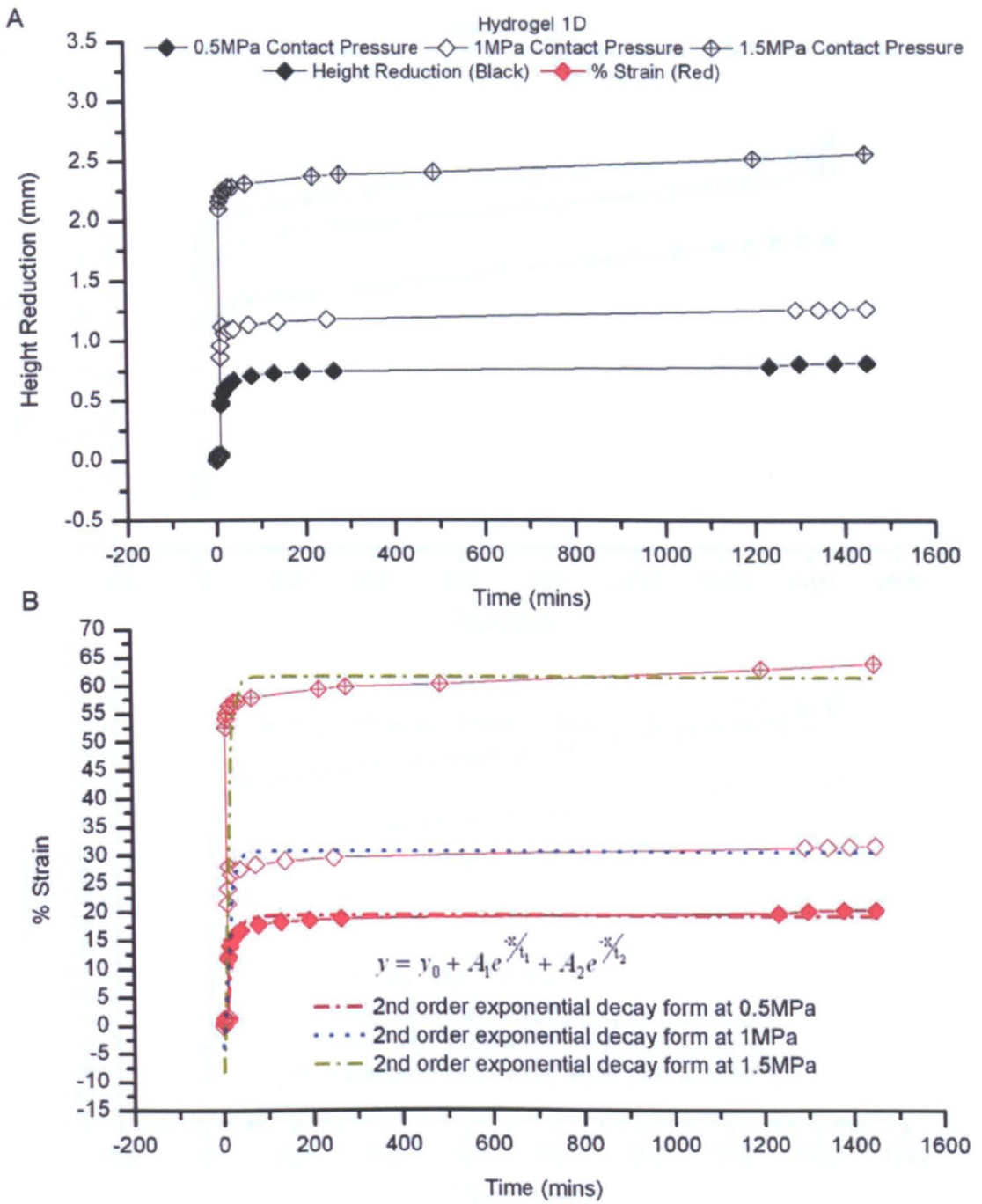

Figure 3-24: Ø10mm by 10mm Uni-material Pin Height reduction (A) and % Stain (B) for Hydrogel Variant 1D

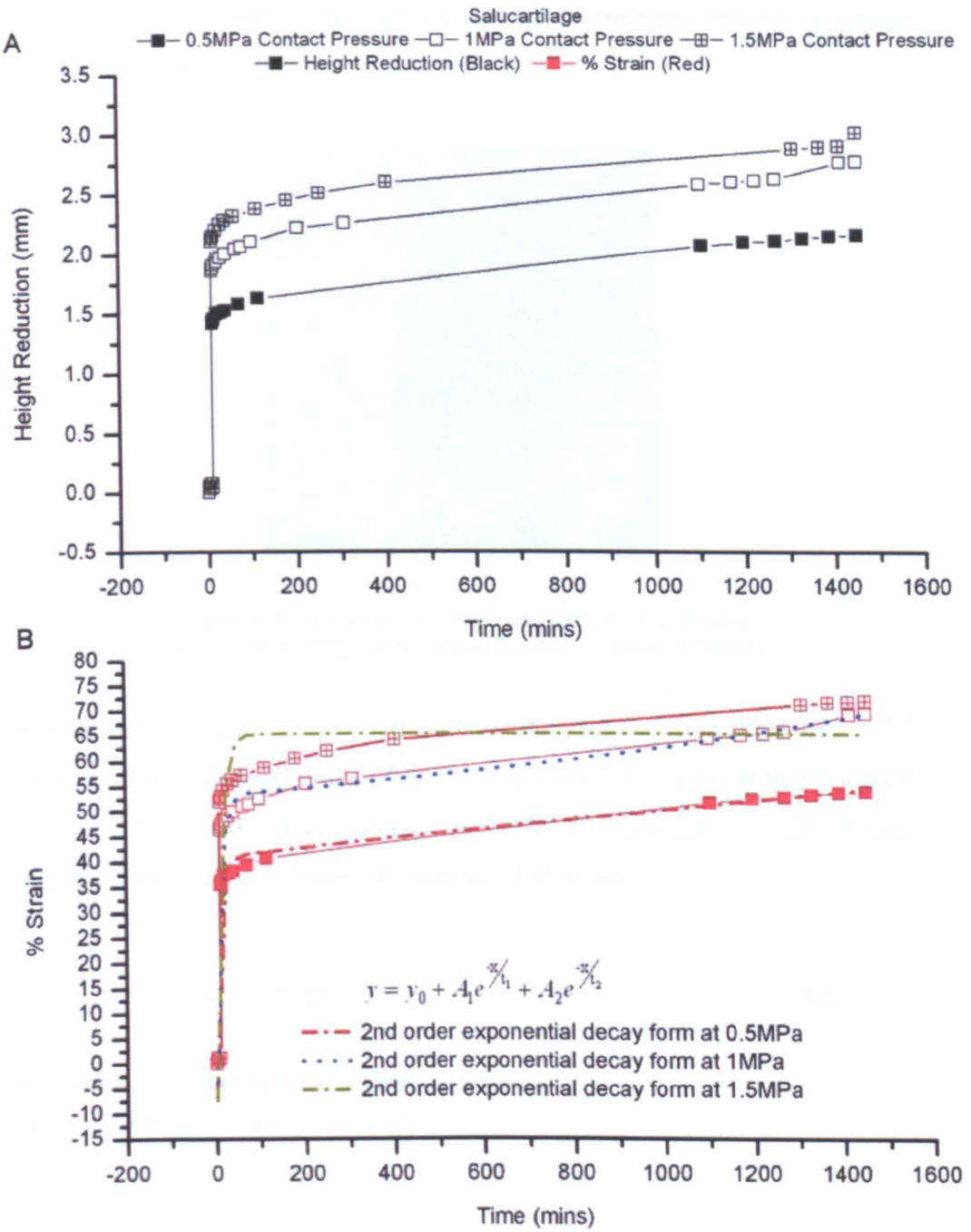

Figure 3-25: Ø10mm by 10mm Uni-material Pin Height reduction (A) and % Stain (B) for Hydrogel Variant SaluCartilage™

At a contact pressure of 1.5 MPa, both Hydrogel 4M and Salucartilage™ again demonstrated an exponential rise in % strain. 1D however, produced a large increase in strain rate between 1 MPa and 1.5 MPa, which indicated a

fundamental change in the compressive strength of the material. Further evaluation of the material showed internal brittle fractures indicating a near catastrophic failure, as shown in Figure 3-26.

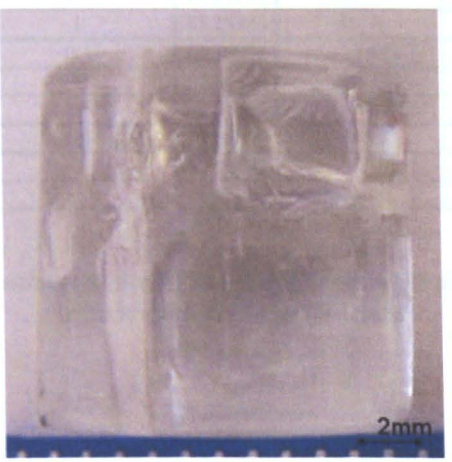

Figure 3-26: Internal fractures to hydrogel 1D following non-confined compressive test at 1.5 MPa Contact Pressure

The uni-material format compression test strain results were fitted with a 2nd order exponential decay form (Origin Laboratory 7.5, USA), with the lowest Chi^2 and highest R^2 value possible as shown in Equation 3-3. The critical constants for each set of data are shown in Table 3-6.

$$y = y_0 + A_1 e^{-x/t_1} + A_2 e^{-x/t_2} \quad \textbf{(3-3)}$$

yo= offset, A1 = Amplitude 1, t1 = decay constant 1,
A2 = Amplitude 2, t2 = decay constant 2

The amplitude and decay constants for each hydrogel showed no relationship between displacement, mechanical properties and final strain value indicating that the constant stress assumptions or complex viscoelastic and biphasic properties of each hydrogel resulted in non-linear deformation performance.

Hydrogel Variant	Contact Pressure (MPa)	Offect (Y_o)	Amplitude (A1)	Decay Constant (t1)	Amplitude (A2)	Decay Constant (t2)
Hydrogel 4M	0.5	31.8177	-17.17	23.81	-17.17	23.81
	1	50.60543	-28.09	16.37	-28.09	16.37
	1.5	54.12265	-28.80	26.32	-28.80	26.32
Hydrogel 4N	0.5	40.22713	-21.91	13.46	-21.91	13.46
	1	75.28923	-49.40	10.26	-31.54	474.48
Hydrogel 1D	0.5	19.30936	-10.42	15.70	-10.42	15.70
	1	30.65623	-17.14	12.25	-17.14	12.24
	1.5	61.55184	-34.84	10.84	-34.84	10.84
Salucartilage™	0.5	1459.833	-1418.83	152184.70	-46.26	10.89
	1	42.36617	-60.10	10.79	10.83	-1587.20
	1.5	65.47389	-36.46	12.78	-36.46	12.78

Table 3-6: Critical constants for the 2nd order exponential decay form fitted to the % Strain of each Hydrogel Variant

3.4 Discussion

The mechanical properties of all hydrogels are dependent on a large number of factors including method of preparation, polymer volume fraction, molecular composition, cross-linking agents and swelling medium *(Peppas, 2004, Corkhill et al., 1990a)*. It was postulated that the biphasic effect resulting from the flow of free water through the hydrogel structure, defined the mechanical response in both the elastic and plastic regions under tensile and compressive forces. The plasticizing effect of free fluid within the hydrogel has been well documented, resulting in increased elongation and a greater ductility *(Corkhill et al., 1990a, Corkhill et al., 1990b)*. However, the EWC showed no relationship with elastic modulus, aggregate modulus and tensile loading response. Hydrogel 4M processed the lowest EWC of 14% and with SaluCartilage which processed the highest EWC value of 75%, were the only two specimens to produce a standard biphasic indentation response, similar to that of natural articular cartilage *(Mow et al., 1989, Mak et al., 1987, Jin et al., 2000, Mow et al., 1980a)*.

The similarity in determined permeability values presented for Hydrogel 4M, SaluCartilage™ and that of natural articular cartilage *(Mow et al., 1989, Swann and Seedhom, 1989, Jin et al., 2000)* indicated similar biphasic responses owing to fluid load support within the hydrogel/cartilage structure. Hydrogel 1D, 3K and 4N produced far higher determined permeability values

indicating low interstitial fluid pressure and a higher level of solid load support during both the indentation and compression testing. The higher solid load support could have resulted in higher internal stresses and the premature failure of these hydrogels.

Hydrogel 4M processes an EWC nearly 6 times lower than the 80% EWC quoted for natural articular cartilage *(Mow and Hayes, 1997, Mow, 1986, Freeman, 1979)* which would result in a lower level of fluid flow through the hydrogel structure. This lower fluid flow could account for the increased time demonstrated by Hydrogel 4M, to reach an equilibrium state of solid load support (150 minutes) compared with Salucartilage (40 minutes) and articular cartilage (45 minutes) *(Jin et al., 2000)*. However, within this study the proportion of the EWC which was active free water and thus able to be pressurised and flow through the molecular structure was not quantified.

Alternatively, the viscous or loss modulus of the hydrogel material could have defined the mechanical response demonstrated within this study. At the constant stresses exerted during the compression and indentation tests, the strain and the viscoelastic response of each material would be dependent on time *(Benham PP et al., 1996)* and molecular motion within the hydrogel structure *(Anseth et al., 1996)*. The realignment of the molecular structure and the highly viscous like behaviour of the hydrogel material regardless of the fluid load support could have resulted in a 'biphasic like' response, independent of free water content.

The maximum loading within the tibial-femoral joint during normal walking can reach up to 3000N *(Lafortune et al., 1992, British Standards, 2004, Mow and Hayes, 1997, Morrison, 1970)* increasing considerably for other activities such as stair climbing, running etc. Which results in contact pressures of between 2- 4 MPa *(Mow and Hayes, 1997, Morrell et al., 2005, Freeman, 1979)*. The unconfined compression test in both the uni-material and bi-material pin formats demonstrated that at 1 MPa contact pressure hydrogel 3K and 4N would fail, demonstrating their unsuitability as chondroplasty

substitution materials. However, with the aim of optimising future hydrogel materials and to understand the biphasic and tribological properties of key monomers and cross-linking agents, hydrogels 3K and 4N were not removed from further tribological studies.

As indicated by the low permeability and a brittle like failure during the compression test (Figure 3-26), hydrogel 1D processed low plasticity resulting in low deformation and catastrophic brittle failure, at contact pressures found *in vivo*. Despite processing a EWC twice that of hydrogel 4M, the higher permeability, fundamental solid structure properties and lower viscoelastic properties of Hydrogel 1D resulted in higher internal stresses and ultimately failure at 1.5 MPa. However, as with hydrogel 3K and 4N, to understand the tribological properties of the key monomers and cross-linking agents, the material was not removed from future studies.

Evaluation of key monomers and cross-linking agents (Table 2-2) demonstrated no distinct relationship between certain monomers and mechanical performance, however, a number of patterns were present. Hydrogels 1D, 3K and 4N all contained hydroxyethyl methacrylate (HEMA) in various percentages (26-88 % dry weight) and demonstrated little phasic response, high permeability and failure at contact pressures below *in vivo* levels. All hydrogels containing 10% dry weight ethylene glycol dimethacrylate (EGMDA) demonstrated an increased elastic modulus and tensile strength but in the case of hydrogel 1D demonstrated brittle failure. Hydrogel 4M was the only hydrogel to process equal amounts of tetrahydrofurfuryl methacrylate (THFMA) and hydroxypropyl methacrylate (HPMA) and demonstrated above average mechanical and biphasic properties. However, it should be noted that further work is required before distinct relationships between the fundamental chemical make up and mechanical properties can be assessed.

3.5 Summary

- A number of experimental methodologies which allowed the effective characterisation of the fundamental mechanical properties processed by 25 hydrogel polymers were developed. This characterisation facilitated the objective selection of key hydrogels for further analysis.

- The further quantification of essential mechanical properties and the objective evaluation of potential chondroplasty materials against a commercially available product.

- The effective characterisation of fundamental mechanical properties will allow the objective evaluation against the tribological performance. Enabling the objective selection of hydrogel properties and critical chemical components within the further development of potential chondroplasty materials.

4 A Simple Geometry Friction Study of Potential Chondroplasty Materials

4.1 Introduction

The aims of this chapter were to investigate the effects of a biomaterial biphasic properties on the dynamic friction response of articular cartilage against a number of potential chondroplasty materials. The friction response of a number of biphasic biomaterials sliding against an articular cartilage pin was studied. The affects of re-hydration on the frictional response and the lubricating effects of a protein enriched lubricant were considered. All friction tests within this chapter were completed using the Short Term Friction Test Apparatus within a mixed boundary lubrication regime as described in Chapter 2.

4.2 Experimental Methodology

4.2.1 Materials

The experimental control materials for the initial dynamic friction test were articular cartilage pins tested against polished stainless steel (positive control) and articular cartilage (negative control) which had previously documented friction responses *(Forster and Fisher, 1999, Bell et al., 2006, Pickard et al., 1998b)*,. Further details of each material and their preparation can be found in Chapter 2.1.

This initial set of experimental tests compared six biphasic hydrogels and four single phasic materials, which are shown in Table 4-1, against the experimental controls (polished stainless steel and articular cartilage). Further information of each biphasic and single phasic material can be found in chapter 2.

Biphasic Materials	Elastic Modulus (MPa)
1D	31.7
4M	140.7
3K	36.9
4N	1.6
4E	31.3
Single Phasic Material	
BS316 Stainless Steel	200000 (standard value)
Ultrahigh Molecular Weight Polyethene GUR1120	600 (standard value)
Delrin	2795 (standard value)
Silicone Elastomer	97
Thermo-Polyetherurethane	3

Table 4-1: Experimental Materials Investigating within the Uni-axial Friction Testing

4.2.2 Method

4.2.2.1 Experimental Positive and Negative Control

Each control material was mounted as the plate specimen and fixed into the bath, filled with 250ml of 100% Ringer's solution. The cartilage pin was inserted into the pin holder with the collagen fibre orientation parallel to the direction of linear motion. The specimens were positioned 1 mm apart and left for 2 minutes to re-hydrate and acclimatise. At this point 30N was applied to the pin, causing the test surfaces to contact. The test surfaces were loaded for 60 seconds following which the reciprocating motion was engaged. The initial start up friction reading was recorded as a zero time reading and readings were taken every 30 seconds up to 120 minutes.

4.2.2.2 Dynamic Friction within a Simple Lubricant

Each test material was again mounted as the plate specimen and tested against a cartilage pin. The mounting, loading and data acquisition were identical to that described in section 4.2.2.1, over the initial 120 minutes. After 120 minutes the rig was stopped at the centre point of oscillation. The load was removed and the contact surfaces separated by 1-2mm, making sure that each specimen was still fully immersed within the hydration medium.

The specimens were then left in this position for a further 120 minutes to allow re-hydration. The 30N load was then re-applied and again left for a further 60 seconds. The friction measurements were then repeated for a further 120 minutes. Once completed cartilage specimens were stored at -20°C and all other specimens were stored at +4°C for further analysis.

4.2.2.3 Dynamic friction study within a Protein Containing Lubricant

The effects of proteins within the lubricant have long been known to affect the friction and wear properties of prostheses *(Ozturk et al., 2004a, Pickard et al., 1998b, Wang et al., 1997, Yao et al., 2003, Cooper et al., 1993)*. Twenty five percent bovine serum containing 16-18 mg/l of protein with 0.1% sodium azide to retard microbiological growth was chosen because of its availability and similar protein concentration to natural synovial fluid *(Wang et al., 1997)*.

Three hydrogel materials were investigated and their properties compared with those of the positive and negative controls. Each test material was again mounted as the plate specimen and fixed into a bath containing 250 ml of the bovine serum. The setup, loading and data acquisition protocols were as described above over a period of 120 minutes, followed by 120 minutes re-hydration time and than a further 120 minutes data acquisition. Once the study was completed, cartilage specimens were stored at -20°C and all other specimens were stored at +4°C for further analysis.

4.3 Dynamic Friction Results

4.3.1 Experimental Positive and Negative Control Results

The frictional response of the single phasic stainless steel plate against a cartilage pin (positive control) (Figures 4-1), demonstrated the effects of fluid pressurisation and a reduction in the fluid load phase at the contact zone *(Forster and Fisher, 1996, Krishnan et al., 2004b)*. Initially the friction was low but progressively increased over the 120 minutes of the test as the fluid within the articular cartilage pin to which a constant load was applied exuded

from the contact zone, reducing the proportion of the fluid load phase and increasing the solid surface to surface contact.

The optimum performance of a biphasic material was shown by the frictional response of a cartilage pin against a cartilage plate (negative control), (Figures 4-1). The interstitial fluid pressure at the contact area maintained a low constant frictional coefficient of 0.03 (±0.01), over the 2 hour test.

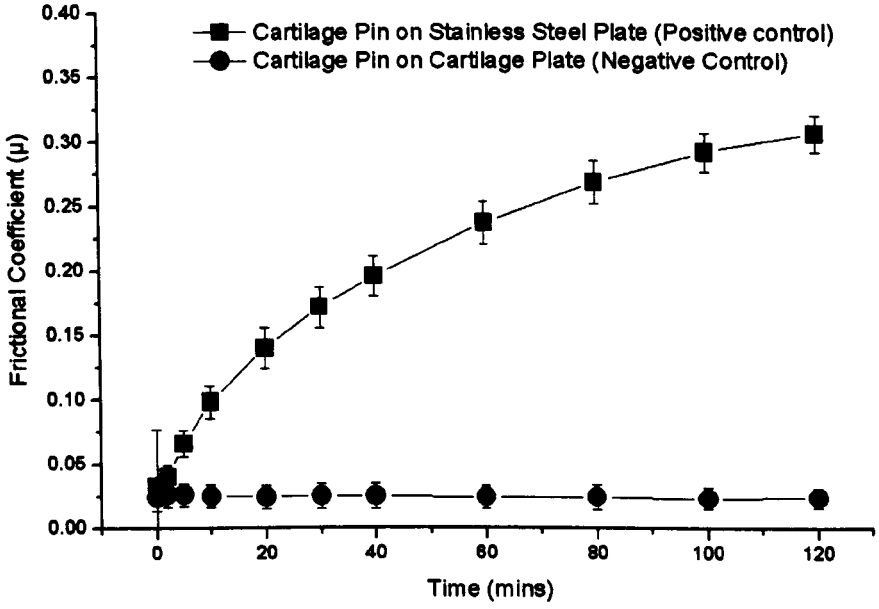

Figure 4-1: Friction Results for the Stainless Steel (Positive Control) and Articular Cartilage (Negative Control). (n=6, Error bars = 95% confidence limit)

4.3.2 Dynamic Friction within a Simple Lubricant

Both the positive and negative controls (Figure 4-2a-d) gave initial friction responses similar to those demonstrated in section 4.3.1. Each single phase polymer material produced very similar frictional traces to the stainless steel positive control. Both the medical grade silicone and medical grade polyetherurethane, as shown in Figure 4-2 a & b, produced a progressive rise in the friction coefficient value over the initial 2 hour period of reciprocating motion. Both the medical grade silicone and medical grade polyetherurethane produced a peak friction coefficient of approximately 0.37(±0.06). Delrin

and GUR1120 UHMWPE produced the initial low value and progressive rise seem in the all single phase materials. However, both the gradient rise and final value were greater than that demonstrated by the positive control and other single phase materials. The cartilage pin against the Delrin specimen was the only single phase material to reached an equilibrium friction value, a steady friction value of 0.5(±0.1) occurred at approximately 30 minutes of the 120 minutes initial trace.

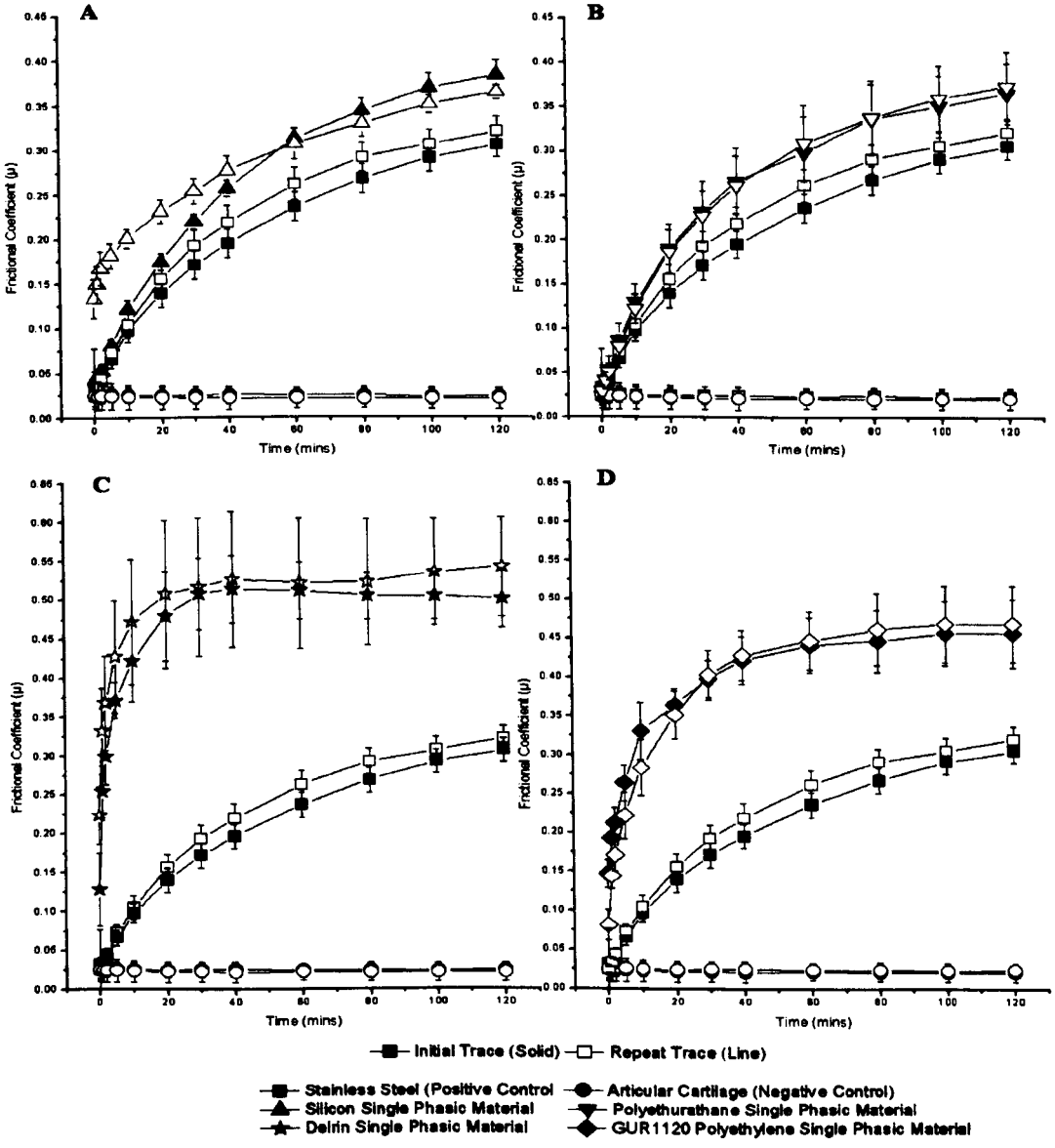

Figure 4-2: Dynamic friction results for Articular Cartilage Pins against Single Phase materials and experimental controls within simple lubrication. (n=6, Error bars = 95% confidence limit)

The frictional responses of biphasic materials 1D and 4E were again similar to the positive control and other single phasic materials, as shown in Figure 4-3 a & h. In contrast, biphasic materials 4M, 3K and 4N (Figures 4-3 b, c and d) produced a statistically significant reduction in the friction coefficient when compared with all the single phasic materials. In particular biphasic materials 4M and 3K, which following an initial steady rise in friction over the first 80 minutes maintained a value approximately 50% of the positive control for the remainder of the test.

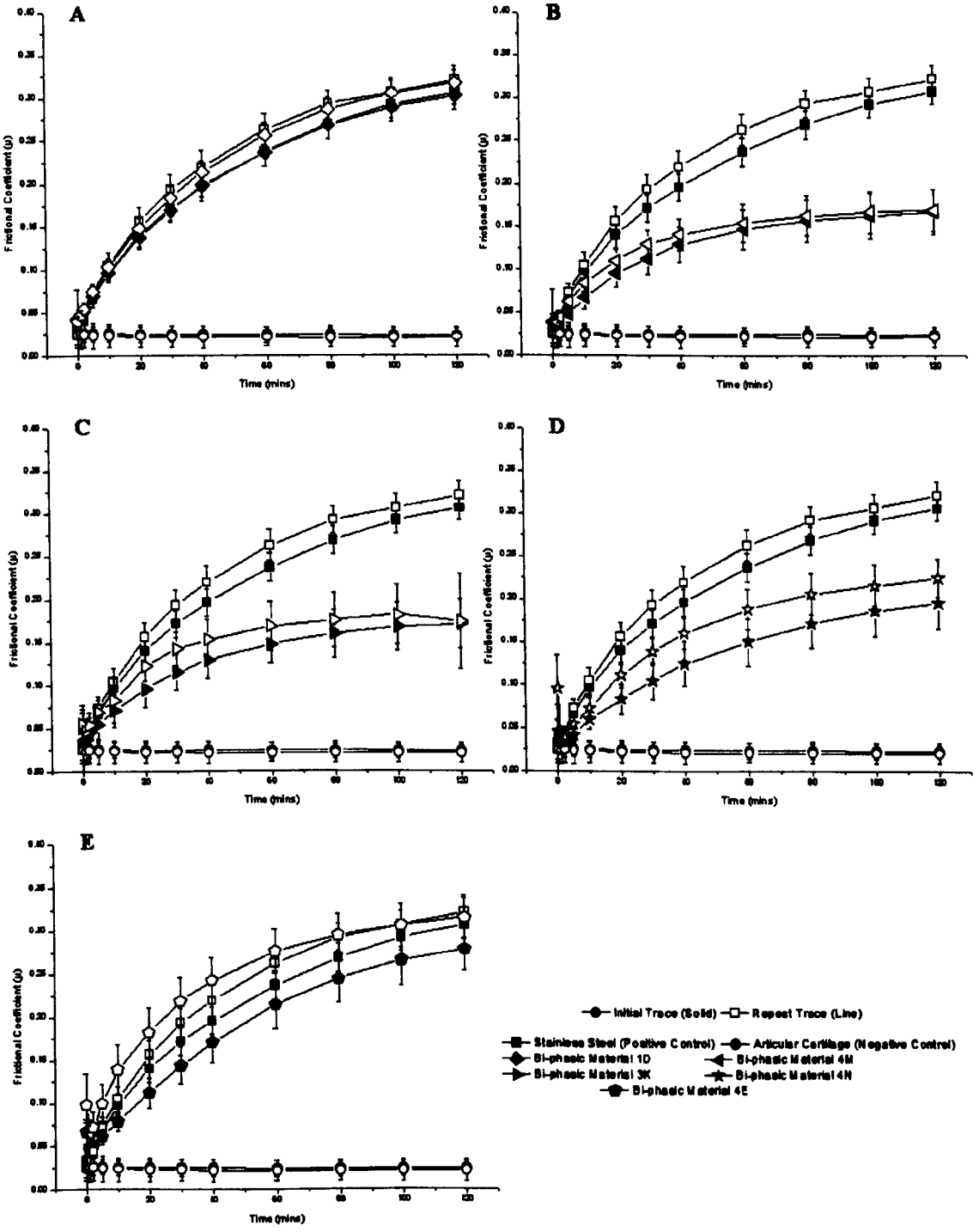

Figure 4-3: Dynamic friction results for Articular Cartilage Pins against Biphasic materials and experimental controls within simple lubrication. (n=6, Error bars = 95% confidence limit)

In all the plate specimens both single phase and biphasic, the first and repeat traces produced very similar starting points and gradient rises. This showed that the re-hydration time of 2 hours between the first and second trace was

sufficient to allow recovery of the dominating factor within the cartilage pin/specimen interface. One exception was the silicone specimen (Figure 4-2 a), which showed a marked increase in friction within the first 20 minutes of the second trace.

4.3.3 Dynamic friction study within a Protein Containing Lubricant

As with the simple lubricant, the single phasic positive control (Figure 4-4a) produced a progressive rise in friction over time in both the initial and secondary results. The addition of proteins to the lubricant resulted in a 26% rise in single phasic positive control when compared with a simple lubrication. The negative control (Figure 4-4a) again demonstrated the optimum performance maintaining a constant friction value over both the initial and repeat traces with no statistical variation when compared with the simple lubricant. All three biphasic specimens (Figure 4-4b-d) tested showed similar characteristics to the simple lubricant demonstrating a statistically significant reduction in the frictional coefficient when compared with all single phasic materials. Hydrogel materials 4M and 3K again produced the initial steady rise over the first 80 minutes and a constant value approximately 50% of the positive control, for the remainder of the test,. However the final value achieved did not show the 26% increase demonstrated by the positive control.

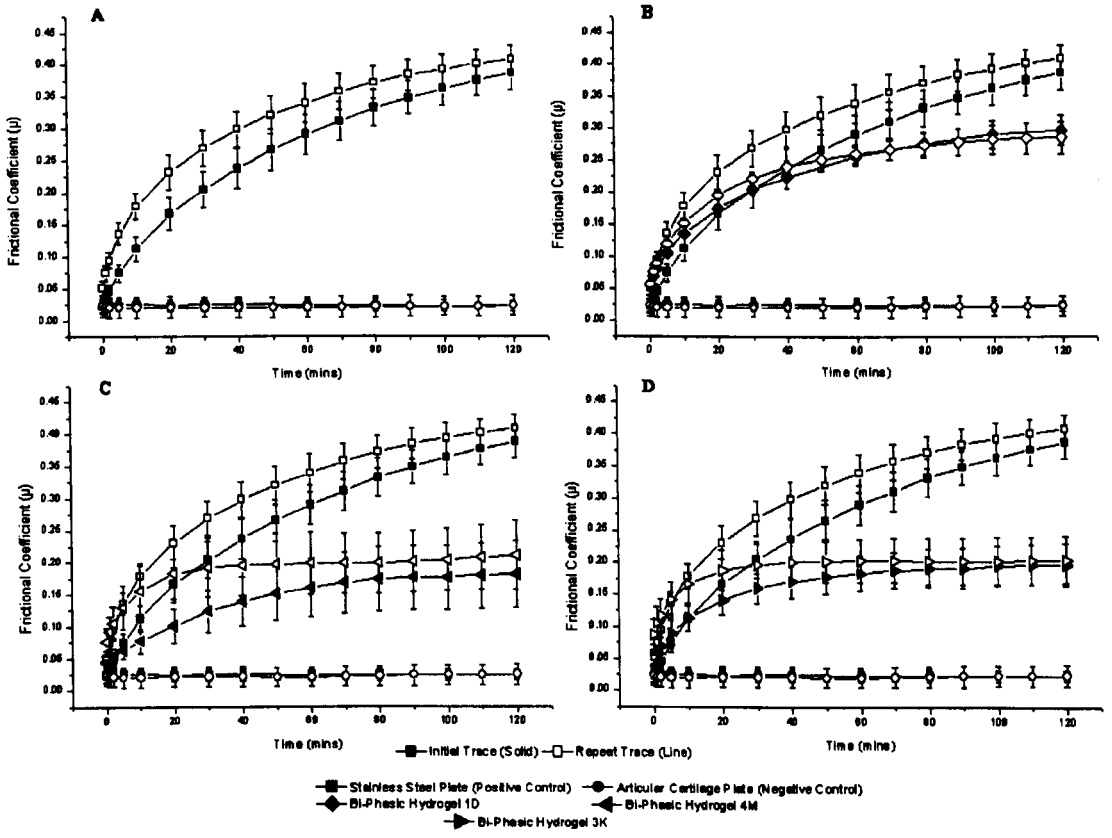

Figure 4-4: Dynamic Friction results for Articular Cartilage Pins against Biphasic materials and experimental controls within a 16g/l Protein Lubricant (n=6, Error bars = 95% confidence limit)

4.4 Discussion

Experimental control

The initial increase in dynamic friction of the positive control with loading time *(Forster and Fisher, 1999, Forster and Fisher, 1996, Bell et al., 2006, Krishnan et al., 2005, Krishnan et al., 2004b, Pickard et al., 1998a, Pickard et al., 2000)*, (Figure 4-1), indicated the loss of the interstitial fluid load support from the cartilage pin as a major factor. This model, as in previous studies *(Pickard et al., 1998a, Pickard et al., 2000, Forster and Fisher, 1996, Forster and Fisher, 1999)* was designed to act within the mixed or boundary lubrication regimes so enabling biomaterial properties to be investigated. The initial friction value of 0.02 -0.03 within the first 60 seconds was similar to the articular cartilage negative control, previous whole joint studies *(Jones, 1934, Roberts et al., 1982, Mabuchi et al., 1994)* and previous small cartilage

specimens studies *(Forster and Fisher, 1999, Forster and Fisher, 1996, Bell et al., 2006, Krishnan et al., 2005, Krishnan et al., 2004b, Pickard et al., 1998a, Pickard et al., 2000)* suggesting a high level of interstitial fluid load support. Alternatively, micro-elastohydrodynamic lubrication (micro-EHL) *(Dowson and Jin, 1986)* which predicts the need for a lower lubrication film thickness owing to flattening of the cartilage asperities could explain or contribute to the initial low friction value. Additionally, boundary lubricants such as lubricin *(Jay, 1992b, Jay et al., 2001b, Jay and Cha, 1999, Swann et al., 1981a)* or phospholipids *(Hills, 2002a, Hills and Crawford, 2003, Hills, 2000)* which have been shown to offer lubricating ability against single phasic materials could also have contributed to the low initial friction. In this study the rate and effect of these boundary lubricants were not taken into account.

During continuous loading, the reduction of the intrinsic fluid load support at the contact zone as fluid is expelled from the constantly loaded pin away from the contact zone, increases the solid to solid contact *(Lewis and McCutchen, 1959, McCutchen, 1969, Mow et al., 1980b)* resulting in a progressive rise of friction as seen in the initial stainless steel control and demonstrated within a number of studies *(Pickard et al., 1998a, Forster and Fisher, 1996, Forster and Fisher, 1999, Bell et al., 2006, Jin et al., 2000, Jin et al., 1991)*. The relationship was quantified by *Krishnan et al (Krishnan et al., 2004b)* through a biphasic model. When considering this reduction in intrinsic fluid load support it should be noted that the experimental geometry would increase the rate of fluid loss away from the contact zone and reduce intrinsic fluid pressure in comparison to *in vivo* situations with time dependent loading.

Articular cartilage surface additives resulting in boundary lubrication have also been shown to maintain low levels of friction over long periods. Removal or wear of the superficial boundary layer *(Stachowiak et al., 1994, Lipshitz and Glimcher, 1979)* may have contributed to the friction rise.

Additionally, the more recent concept of an additional biphasic amorphous layer (BSAL) *(Graindorge et al., 2005)* containing lipids, lubricin and proteoglycans is consistent with the time dependent frictional response.

The low friction value demonstrated by the negative control although similar to the initial positive control value and previous studies *(Jones, 1934, Roberts et al., 1982, Mabuchi et al., 1994, Bell et al., 2006)*, was maintained for the complete initial test. The reciprocating cartilage plate would maintain the intrinsic biphasic load support owing to the low permeability of articular cartilage *(Mow et al., 1984, Ateshian and Wang, 1995)* and re-hydration of the interstitial fluid during the unloaded phase (0.125 – 2.5 seconds dependent on location) of the cycle as recently demonstrated by *Bell et al (Bell et al., 2006)*. The time dependent loading of the plate could also have contributed to maintaining the biphasic surface amorphous layers' lubricating properties thus maintaining the lower friction value.

Dynamic friction study within a simple lubricant

The similar friction response to the positive control, demonstrated by all single phase materials (Figure 4-2 a-d), again demonstrated that the loss of interstitial fluid load support from the constantly loaded cartilage pin was responsible for the rise in friction. While theoretically lower modulus single phasic materials such as polyurethanes can enhance surface fluid film lubrication *(Walker and Gold, 1971, Medley, 1980, Bigsby et al., 1998)*, the mechanics of this experimental set up did not support this mechanism. Theoretically, micro-EHL can enhance surface film thicknesses dependent on the mechanical properties. Thus the similarities in the friction responses between the four single phasic polymers and the positive control indicated this was not a dominant mechanism.

The variation in friction results demonstrated by the biphasic hydrogel specimens indicated different lubrication effects. Hydrogel specimens 1D and 4E produced very similar friction results to the single phasic materials tested,

again showing a lubrication regime dominated by the loss of interstitial fluid load support. Alternatively, hydrogel specimens 4M, 3K and 4N, produced a much lower incremental rise of friction and a significantly lower final friction value after 120 minutes. It is postulated that this reduction can be attributed to their biphasic properties. The fluid phase load support within the articular cartilage/hydrogel interface could be maintained by pressurised interstitial fluid, which resulted in a lower frictional coefficient.

This was highlighted in the friction results for biphasic material 4M which following an initial rise, reached an equilibrium at 50% of the positive control. This equilibrium of fluid load support and solid contact could have been achieved by an influential percentage of fluid load support being maintained as a result of low hydrogel permeability and re-hydration of the interstitial fluid *(Ateshian and Wang, 1995, Bell et al., 2006)* during the unloaded phase of the cycle, thus demonstrating similar, but not as efficient mechanisms, as those shown by the articular cartilage negative control. As with the positive control, articular cartilage surface additive interactions with the biphasic materials could contribute to the lower friction, however, as previously stated, it does not explain the rise in friction seen.

The mechanical properties of both the single and biphasic materials as demonstrated by the elastic modulus and shown in Table 4-1, showed no relationship to the friction response. This again indicated that fluid load support at the cartilage pin/material interface was the influencing factor, independent of mechanical properties.

Repeat Tests

The similarities in the repeat friction trace when compared with the initial friction trace, following 120 minutes of unloaded re-hydration for all specimens, demonstrated a return of the dominating lubrication factor. This recovery has been demonstrated to a lesser extent previously *(McCutchen, 1962, Forster and Fisher, 1996, Forster and Fisher, 1999, Naka et al., 2006)*

and can be explained by re-hydration of interstitial fluid within the cartilage pin. The highly hydrophilic nature of articular cartilage *(Ateshian et al., 1994, Ateshian and Wang, 1995, Jin et al., 2000, Mow et al., 1980a, Mow et al., 1984)* would allow the unloaded cartilage pin to re-hydrate when unloaded. The marked increase in repeat friction rise over the first 40 minutes for the single phasic silicone material (Figure 4-2a) demonstrated increased permeability of the cartilage pin. Cartilage pin degradation following the initial trace could have increased the decline in fluid load support at the contact zone resulting in a higher initial friction value until solid to solid contact became the dominant regime, at which point the trace produced a friction value similar to that of the initial trace.

This study suggested that 120 minutes was long enough to achieve full hydration. Foster et al *(Forster and Fisher, 1999)* investigated load removal for 1 minute and demonstrated some recovery but differences between initial and repeat friction traces. As the lubricant did not contain any boundary lubrication additives, it was unlikely that replenishment of the superficial cartilage layer occurred.

Influence of proteins within the lubricant

It was postulated that the 26% higher friction observed in the positive control using a protein lubricant, with no increase in all other specimens tested, demonstrated a high level of solid to solid contact within the positive control. The addition of proteins to a contact zone with high levels of solid contact might result in the proteins being degraded or denatured, which would result in a greater friction force. This increase could also be due to the adherence of the protein boundary layer to the hydrophilic stainless steel surface.

Previous studies *(Forster and Fisher, 1999, Pickard et al., 1998b, Bell et al., 2006)* have demonstrated the effects of protein content on friction measurements. However, in most cases the removal of proteins from the surface of cartilage produced an increase in friction. Foster et al *(Forster and*

Fisher, 1999) showed a small decrease in friction between a stainless steel plate and cartilage pin, with synovial fluid as a lubricant compared with Ringer's solution, stating replenishment of the boundary layer at the macromolecular level as the reason. The complex chemical interactions between synovial fluid and cartilage, as well as different viscosity and Newtonian behaviour *(Yao et al., 2003, Mazzucco et al., 2002)* of synovial fluid, bovine serum and Ringer's solution, means this study does not question or prove that result. In total joint replacements, friction has been found to both increase and decrease with increased protein concentration, depending on the type of material used *(Williams et al., 2006)*. This demonstrates the importance of macromolecular level lubricant constituents within a high boundary lubrication regime.

The friction value reached at equilibrium for each hydrogel regardless of mechanical properties could be attributed to their biphasic properties. Hydrogel fluid extraction and re-hydration at the contact area would result in lower surface contact. The higher fluid content at the contact area when compared with single phasic materials indicated that the elasto-hydrodynamic effect could have been contributing to the equilibrium response, but the initial friction rise showed a percentage of solid contact, demonstrating that hydrodynamic lubrication is not the dominant lubrication regime.

The tribochemical reactions between proteins present at the contact zone and various hydrogels could have contributed to dynamic friction results demonstrated by different hydrogels. However, these effects were not investigated within this study.

Water Content and Biphasic Properties

The lower levels of dynamic friction produced by Hydrogel variants 4M and 3K were independent of water content and permeability. Both hydrogel variants 4M and 3K process lower EWC values (14% and 19% respectively) when compared with the other hydrogels and articular cartilage (EWC =

80%) *(Freeman, 1979, Mow et al., 1984, Mow, 1986)* indicating a lower level of fluid at the contact zone and increased levels of solid contact. Hydrogel 4E process a similar EWC value of 20% and demonstrated no reduction in friction when compared with the positive control.

The lower permeability and biphasic response of hydrogel 4M as shown in Table 3-5, could indicate a level of interstitial fluid pressure that would maintain fluid load support and reduce the dynamic friction.

However, Hydrogel 3K processed a higher permeability and no biphasic response indicating a lower level of interstitial fluid pressure and thus a reduced level of fluid load support when compared with hydrogel 4M. Therefore it is possible that an alternative lubrication mechanism was dominant at the Hydrogel 3K articular cartilage contact zone. The lower elastic and aggregate moduli values processed by hydrogel 3K when compared with other hydrogels within this study, could have resulted in increased surface conformity and a reduction in the overall surface roughness. The deformation of surface asperities could have increased levels of EHL and Micro-EHL *(Dowson and Jin, 1986, Dowson et al., 1969)*, increasing the level of fluid film lubrication and reducing the final dynamic friction value.

4.5 Summary

- An effective and successful appraisal of the experimental model was achieved by the evaluation of the experimental controls used in previous literature. This allowed the development of an experimental model from which to achieve to aims of the study.

- The dynamic friction response of various single phasic materials independent of their chemical and mechanical properties was established.

- The potential of biphasic materials to reduce friction when compared with the single phase materials was demonstrated.

- Renewal of the dominating factor or factors that influenced the frictional response at the articular cartilage/specimen interface indicated re-hydration of interstitial fluid and recovery of fluid load support.

- The influence of proteins on the dynamic friction response was shown to produce little or no effect within the dynamic friction experimental model.

5 The Development of a Cartilage Surface Topography, Degradation and Wear Model

5.1 Introduction

In order to understand and assess the performance of a potential articular cartilage replacement material, wear of the material and of the opposing articular surface needs to be quantified. As discussed in Section 1.8 wear is defined as the 'progressive loss of material from the surface as a result of mechanical action'*(Ashby and Jones, 1995)*. Both complex chemical and mechanical interactions occur within articular cartilage and to a lesser extent in hydrogel polymers and therefore it is consistent to consider chemical degradation and mechanical wear separately *(Mow and Hayes, 1997)*. This chapter deals with the development of surface topography as a method of quantifying surface fibrillation and its application in the study of mechanical wear in hydrogel polymers and articular cartilage.

5.2 Previous literature

When the surface of healthy articular cartilage was viewed by means of optical or transmission electron microscopy it appeared smooth *(Barnett, 1961, Hunter, 1743)*. However, the use of scanning electron microscopy (SEM) demonstrated a number of pits and ridges on the articulating surface *(Walker et al., 1968, Gardner and McGillivray, 1971, Sayles et al., 1979, Clarke, 1971)*. The causes of these surface features were unclear, explanations such as swelling of the underlying structure in particular chondrocytes *(Clarke, 1971)* or the result of prominent cartilage fibre bundles within the superficial zone *(Walker et al., 1968)* were all suggested. Other studies proposed that the ridges arose from viscoelastic interactions within the cartilage during joint movement *(Mow et al., 1974)* and the so-called 'boosted lubrication theory' *(Dowson et al., 1969)* that ridges were functional, aiding joint lubrication.

The quantification of cartilage surface roughness was limited by the techniques available, as optical microscopy had a limited field of vision and SEM required elaborate and possibly damaging sample preparation. In particular, the vacuum caused dehydration of specimens was seen to produce a shrinkage of up to 19% *(Sayles et al., 1979)*. Further investigations have demonstrated the sensitivity of articular cartilage surface roughness to variations in hydration, revealing an increase in surface roughness with dehydration *(Bloebaum and Wilson, 1980, Speer et al., 1990)*. Separation from the underlying subchondral bone has also been shown to affect the surface topography *(Ghadially et al., 1982)*. More recent studies using methods such as Environmental-SEM, Laser Profilometry, Cyro-SEM and Stylus Profilometry, which involve less destructive specimen preparation have demonstrated a relatively smooth surface, with a stated Ra ~1.6μm *(Forster and Fisher, 1999, Ghadially et al., 1982, Kobayashi et al., 1995, Kobayashi et al., 1996, Graindorge et al., 2005, Sayles et al., 1979)*. A non-collagenous surface amorphous layer of between 1-5μm thick was observed to form part of the quantified surface roughness *(Kobayashi et al., 1995, Kobayashi et al., 1996, Graindorge et al., 2005, Kumar et al., 2001)*.

Varying results have been obtained between direct contact measurement and so-called reverse moulding methodology, where a mould is taken of the surface and the surface topography of the mould is examined. The use of different materials and moulding techniques could have led to the reported variations in the results *(Sayles et al., 1979)*. However, recent studies have demonstrated that direct surface measurement using a variety of techniques achieves an acceptable level of consistency in results without causing surface damage or degradation *(Krishnan et al., 2004a, Forster and Fisher, 1999, Sayles et al., 1979)*.

The variation in surface topography resulting from joint and articular cartilage degradation is not indentfied. Cartilage fibrillation, defined as structural abnormalities characterized by splitting or fraying of the tissue

(Freeman, 1979) has been observed within diseased joints *in vitro (Freeman, 1979, Ghadially et al., 1982, Meachim and Fergie, 1975, Emery and Meachim, 1973, Meachim, 1975)* but little or no quantitative surface topography values have been recorded. Where the surface topography variation of articular cartilage within osteoarthritic joints has been studied, a surface roughness of 4-5μm has been reported *(Forster, 1996, Gardner et al., 1997)*. However, the complex chemical and physical alterations present in osteoarthritic cartilage, such as increased osmotic swelling *(Maroudas, 1976)* and inflammation *(Felson et al., 2000)* means caution should be used when comparing quantitative surface roughness measurements from osteoarthritic joints and those from *in vitro* mechanically degraded specimens.

5.3 Experimental Methodology and Procedure

5.3.1 Validation of the Method

Two direct quantitative methods were proposed for the presented study, Stylus Profilometry (Taylor-Hobson) and White Light Interferometry (WLI) (Veeco Instruments). Further information about each process can be found in chapter 2.4. To define the most appropriate technique, each quantitative method was investigated within an initial study to define the optimum time of measurement, repeatability and influence of the contact probe on the cartilage surface.

5.3.1.1 Time of measurement study

Six non-tested articular cartilage pins extracted and stored as described in Chapter 2, were defrosted overnight and stored at 21°C within 100% Ringer's solution. Each pin was placed, with the cartilage side up, into a custom made jig and bath filled with 100% Ringer's solution to a level just below the cartilage surface, making sure the surface was not submerged.

To investigate the influence of measurement time and the effects of dehydration on the surface topography, each cartilage pin was positioned and four traces taken, as shown in Figure 5-1, taking a total of 3.5 minutes. Each

8mm long trace was acquired using a 0.8mm Gaussian filter cut-off and fitted to a least square arc, which allowed the calculation of an overall radius. The sample was then left exposed to the environment and further sets of traces taken after 2, 5 and 10 minutes. The custom made jig allowed controlled rotation and parallel motion allowing the set of four traces to be repeated.

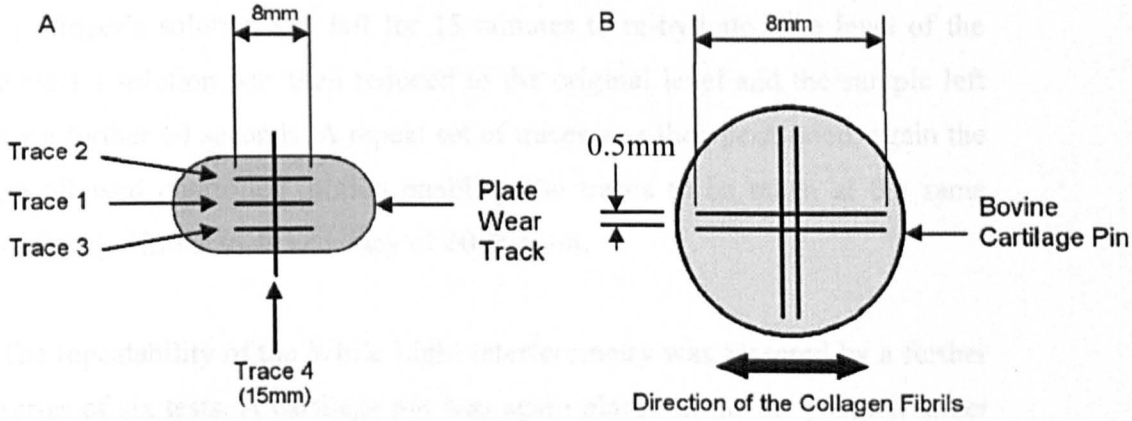

Figure 5-1: Stylus Profilometry traces taken on hydrogel plate specimens (A) and articular cartilage pins (B)

For consistency a maximum time constraint of 4 minutes was set for each measurement on the WLI. This placed limitations on the available scan area, magnification setting and scanning depth. Following an initial investigation using donor cartilage pins, the following variables were used.

Magnification	25.96X
Measurement Mode	Vertical Scanning Interferometry (VSI)
Sampling Area	647.11nm
Sample Size	300x300μm
Data Restore	Off
Back Scan Distance	50μm

The study was then repeated as six articular cartilage pins were placed into the jig and bath which was placed in a known position under the optical lens of the WLI. The lens was moved to the correct height and the measurement taken. Further measurements were again taken after 2, 5 and 10 minutes respectability.

5.3.1.2 Repeatability Study

To assess the repeatability of the Stylus Profilometry technique on the articular cartilage surface, a total of six articular cartilage pins were again placed into the custom made jig and bath and left for 60 seconds. Four initial traces were taken as shown in figure 5-1, the specimen was then submerged by Ringer's solution and left for 15 minutes to re-hydrate. The level of the Ringer's solution was then reduced to the original level and the sample left for a further 60 seconds. A repeat set of traces was then performed, again the jig allowed controlled motion enabling the traces to be taken at the same surface positions to an accuracy of ±0.005mm.

The repeatability of the White Light Interferometry was assessed by a further series of six tests. A cartilage pin was again placed in the set position under the lens and a measurement taken. Without moving the sample the pin was submerged within 100% Ringer's solution and left for 15 minutes. The level of Ringer's solution was again reduced and the sample left for 60 seconds, when a second measurement was then taken.

5.3.1.3 Effects of Surface Profilometry Probe on Articular Cartilage and Hydrogel Surface

The direct measurement Stylus Profilometry technique required a diamond-tipped hemispherical shaped probe to be drawn across the surface of the material. The probe has a 2.5μm radius and exerted a force of 0.85mN. The effects of this contact on the surface of both the articular cartilage and hydrogel specimens were investigated. The surface profile as obtained by the Stylus Profilometry technique was compared with that of a non-contacting laser profilometry method (USB Messtechnik), which has a wide field of vision within the time constraints allowing a high percentage of the surface area to be studied (More information regarding the process can be found in chapter 2-4). In order to reduce hydration effects, a time limit of 2 minutes was set for each measurement. The critical parameters used were dependent on the reflective properties of the surface, as with the WLI an initial

comparison study using donor specimens was performed and the critical parameter used for the study are shown in table 5-1.

	Hydrogel	Cartilage
Resolution (points/mm)	500 x 8	400 x 40
Specimen Area (mm^2)	25	16
Vertical Resolution	10nm	10nm

Table 5-1: Laser Profilometry critical parameters used

Hydrated samples of each selected hydrogel and six bovine articular cartilage pins were placed into the custom-made jig, and a measurement taken using the laser profilometer. The bath was then filled to maintain hydration and the specimens transferred to the stylus profilometry apparatus. The Ringer's solution was then reduced to below the surface and each specimen left for 60 seconds. Four traces were taken on each specimen as shown in figure 5-1. The specimen was then re-transferred to the laser profilometry and a further optical measurement taken.

5.4 Surface Topography Methodology Results

A good reproducibility was achieved with each technique. The mean average of all four surface profilometry traces for any given sample, regardless of collagen fibril direction are presented within this thesis. The surface topography metrics used within this thesis are stated below;

Ra - the arithmetic average value of the departure of the profile from the centre line over a sample length.

Rq - the root mean square (RMS) value of the depart of the profile from the centre line over a sample length. This value is less affected by the electrical filters used during data processing and allows a validation of the Ra value *(Dagnall, 1986)*.

Rz - The arithmetic mean distance between the five highest peaks and five lowest valleys over a sample length. By averaging the 5 highest peaks

and lowest valleys, the value gives a proportional view of the data distribution *(Dagnall, 1986)*.

5.4.1 Effects of Time of Measurement and Hydration

Surface profilometry data as shown in Figure 5-2 and associated data files were produced from each specimen. The data was exported into Excel (Microsoft, US) and the mean average of all four traces calculated. Figure 5-2 shows a typical trace for articular cartilage presented with the 0.8mm cut off. At this cut off all surface variation with a wavelength above this value was removed and the trace appears flat for ease of analysis, however it should be noted that the trace is not a true representation of the surface profile. The trace depicts peaks and valleys along side smoother more consistence areas, which could possibly be the 5µm thick non-collagenous surface amorphous layer coating the articular cartilage surface *(Graindorge et al., 2005, Kobayashi et al., 1995, Kobayashi et al., 1996)*.

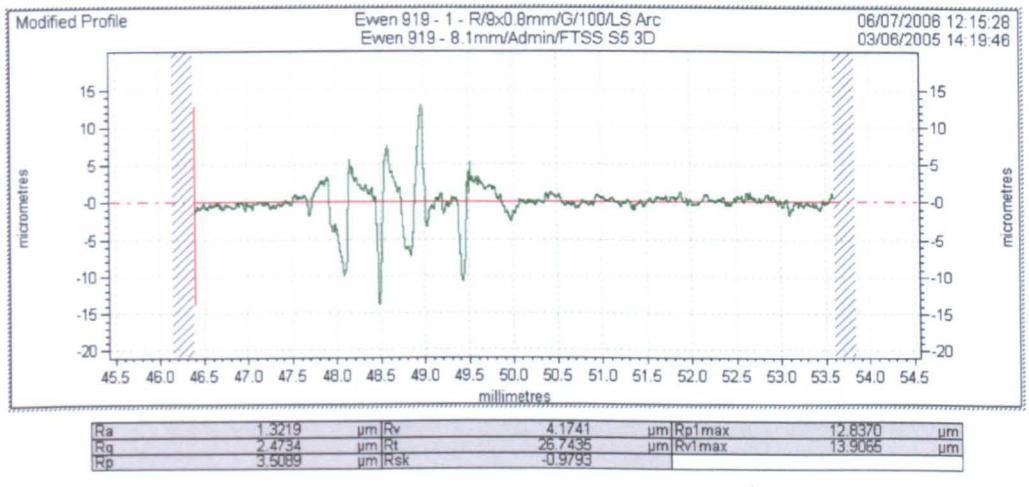

Figure 5-2: Example of a Surface Profilometry trace for an initial pin at 0 minutes

The WLI technique produced a three dimensional image of the surface as well as the relevant metrics. Figure 5-3 and 5-4 show a set of images for a single pin at 0, 2, 5 and 10 minute time intervals. The relatively high resolution initial image (figure 5-3A) shows a surface of peaks, undulations and valleys. The presented surface form could be due to either collapsed superficial chondrocytes *(Clarke, 1971)* or exposure of the collagen bundles

(Walker et al., 1969). However, the samples were not worn or damaged before testing and that initial surface Ra value, of between 1.3-1.9μm was consistent with previous literature investigating intact non-worn cartilage samples *(Sayles et al., 1979, Forster and Fisher, 1999)*. Over the four images shown in figures 5-3 and 5-4, the peak and valleys increase in size slightly but the average Ra value only increased by 13% demonstrating no large increase in surface roughness over the 10 minute exposure period.

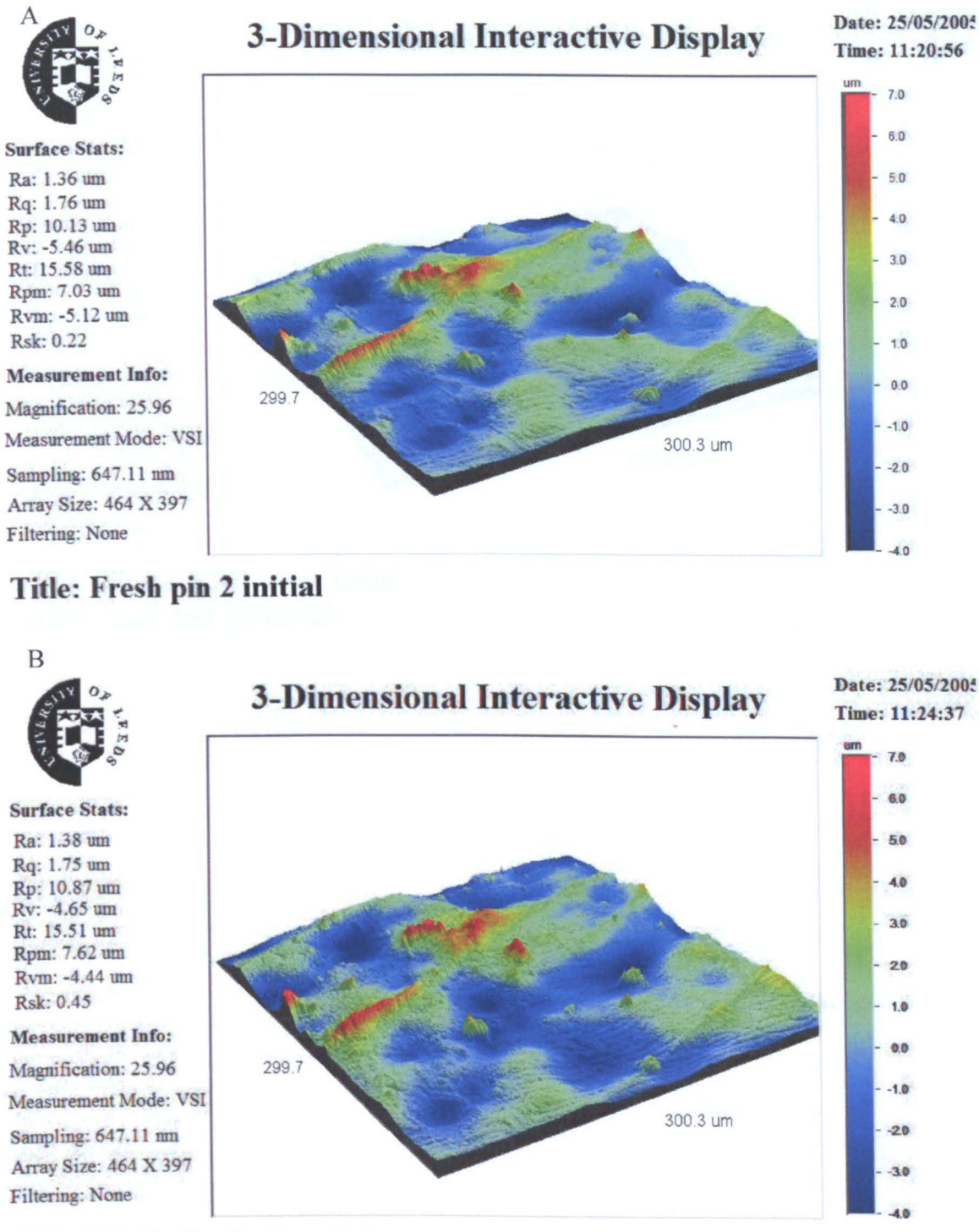

Figure 5-3: The White Light Interferometry results for a single cartilage specimen at 0 (A) and 2 (B) minutes

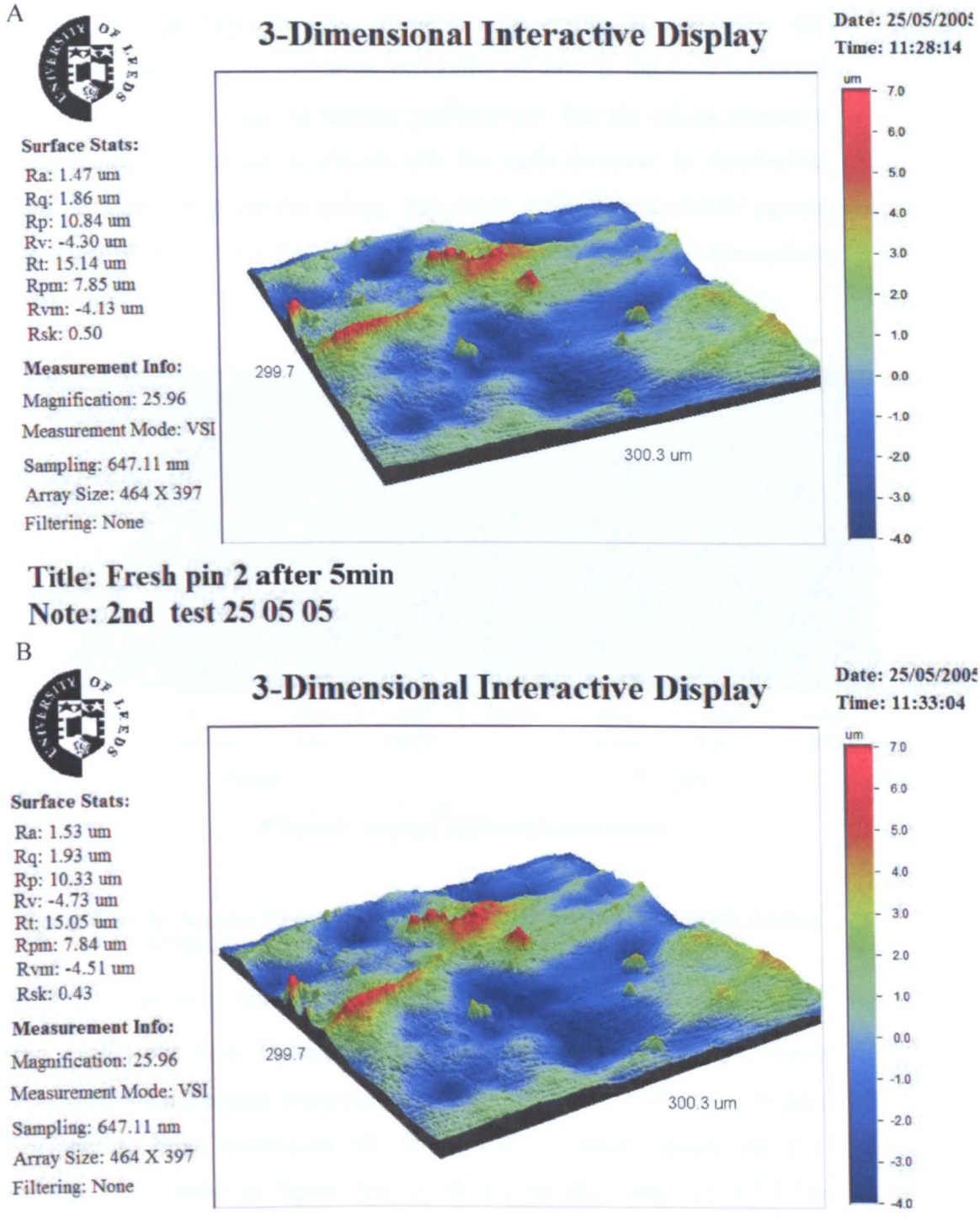

Figure 5-4: The White Light Interferometry results for a single cartilage specimen at 5 (A) and 10 (B) minutes.

For both techniques an average surface roughness for all pins at each time point was calculated, as shown in Figure 5-5. The results show no increase in

surface roughness, with an average Ra value of between 1- 2μm remaining constant over the exposure time. However, the results do show that the optical WLI produced an increased variability of data as the time increased compared with the contacting surface profilometry. The Rq values showed a slight increase in surface roughness and the same increase in distribution when compared with the Ra values. The small increase and similar pattern demonstrated by both the Ra and Rq indicate a similar picture for the surface profilometer.

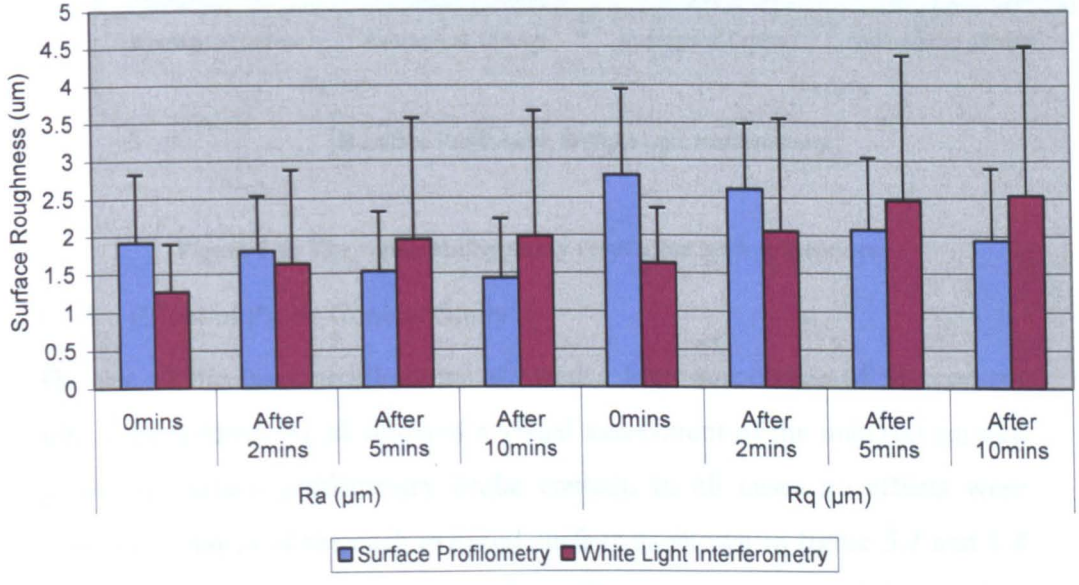

Figure 5-5: The Average Ra and Rq roughness over 10 minutes for both the Surface Profilometry and White Light Interferometry techniques.

5.4.2 Repeatability Study

The results for both techniques again showed little variability between individual measurements allowing an average for each set of pins to be used. Considering both techniques the initial and secondary results after 15 minutes, as shown in figure 5-6, produced an Ra value of 1.5-1.7μm demonstrating good repeatability for both measurement techniques and consistency with the previous results and current literature *(Sayles et al., 1979, Forster and Fisher, 1999, Longfield et al., 1969)*. The Rq values were also consistent over the 15 minutes independent of measurement technique.

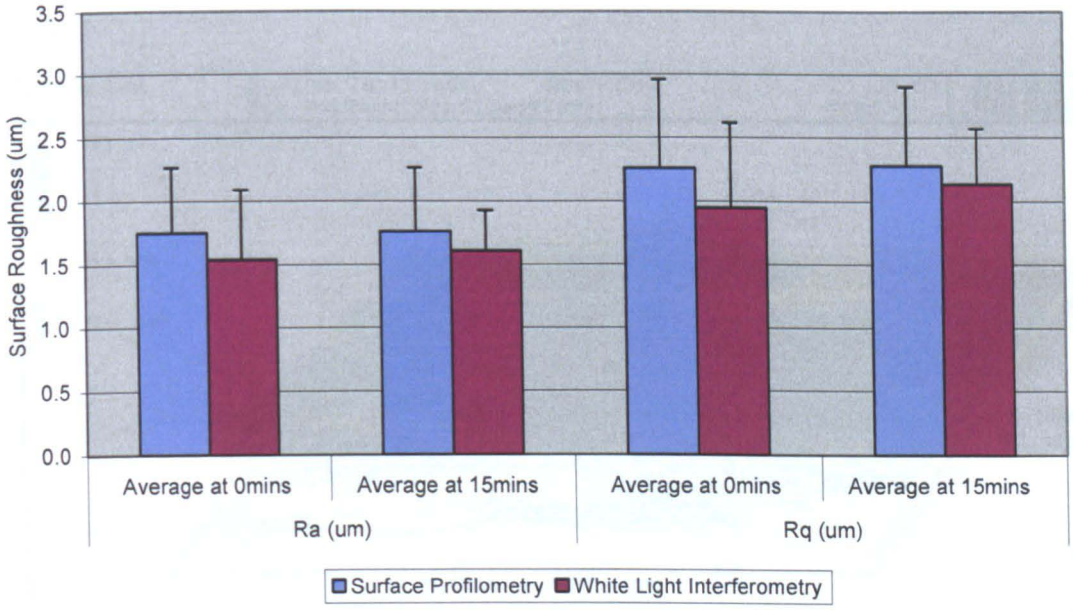

Figure 5-6: The repeatability study results for both techniques

5.4.3 Effect of Probe Contact Study

The use of the laser profilometry allowed a high percentage of the contact area to be studied, which allowed a visual assessment of the material surface following surface profilometry probe contact. In all cases no effects were seen. The images of the each material surface as shown in figure 5.7 and 5.8 clearly showed no undulations and trenching as a result of the surface profilometry probe travelling across the surface. All materials produced consistence surface roughness results between each technique and each measurement.

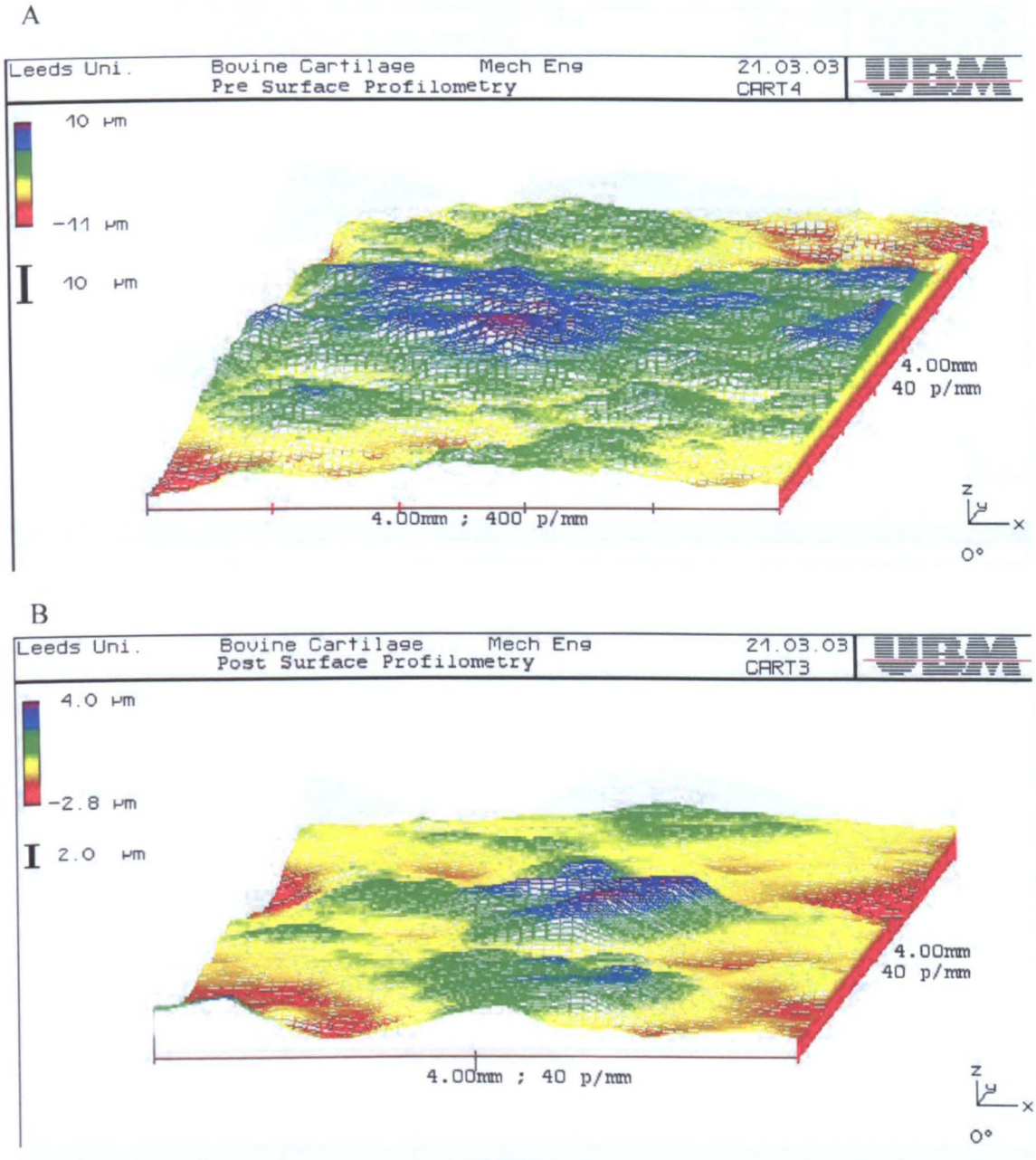

Figure 5-7: Laser profilometry images of bovine articular cartilage before (A) and after (B) surface profilometry traces.

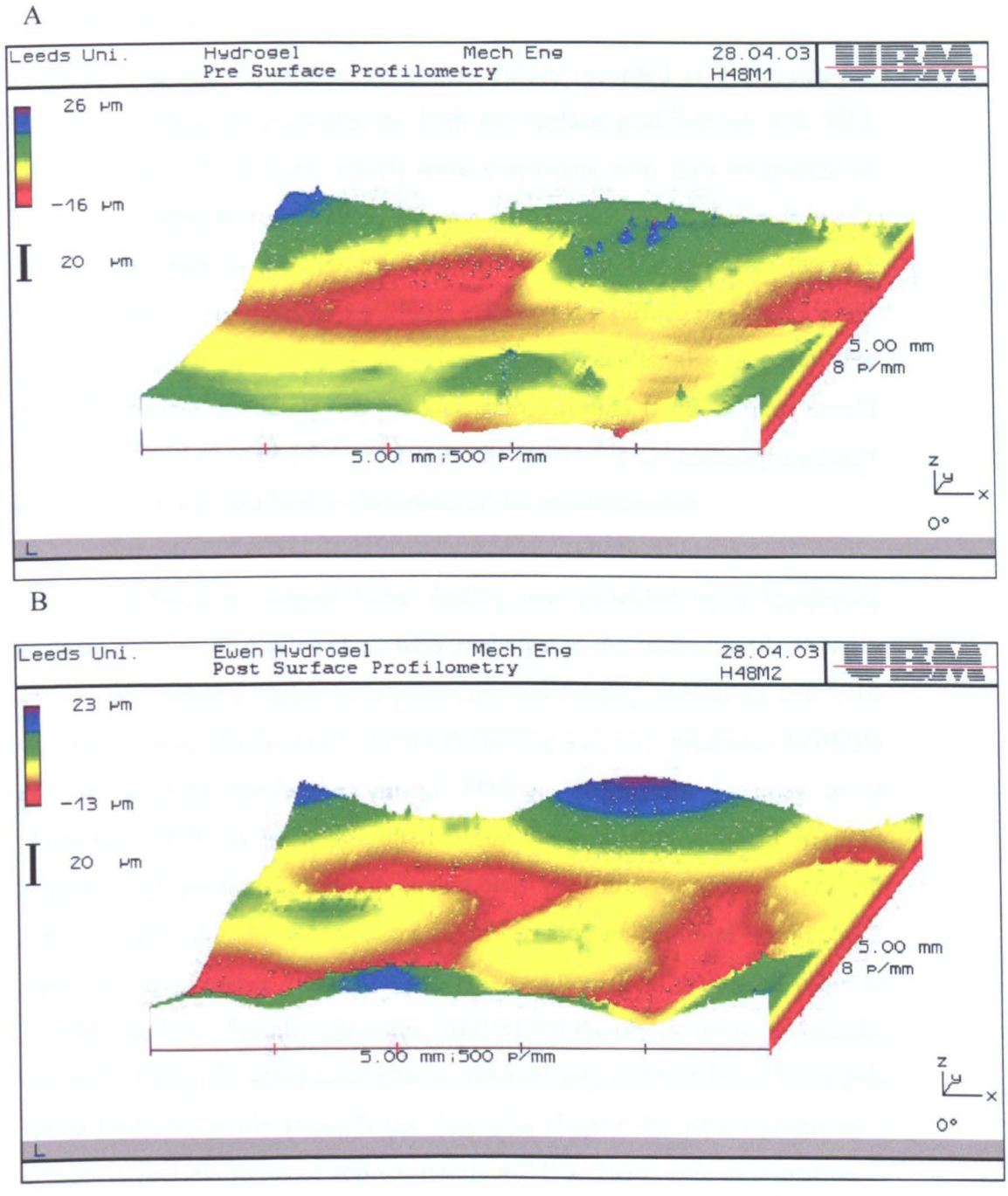

Figure 5-8: Laser profilometry images of an hydrogel variant 4M before (A) and after (B) surface profilometry traces.

5.5 Discussion

The initial Ra and Rq surface roughness values recorded at 0 minutes for articular cartilage, as quantified by both the surface profilometry and WLI ranged between 1.3-1.9μm, which were consistent with data in published literature *(Longfield et al., 1969, Forster and Fisher, 1999, Schmidt et al., 1990)*. This supports the viability of each technique and indicates that the contacting probe produces no additional effect on the surface roughness when compared to the optical method. These initial results also suggest that although reverse moulding can produce viable results if the correct mould material is used *(Longfield et al., 1969)*, the method is unnecessary as direct stylus contact does not lead to distortion of the measurements.

Further evidence to support these finding was provided by a theoretical analysis perform by Sayles et al, who investigated the interaction between a surface profilometry stylus with geometry and loading similar to that used within this study *(Sayles et al., 1979)*. Purposing a contact pressure of 40MPa and an uniaxial tensile strength of 34MPa, taken from Freeman et al *(Freeman, 1979)* as an approximation for the compressive yield strength Sayles et al predicted that the indentation pressure or Meyer Hardness *(Meyer, 1908)* for an homogenous, elastic, isotropic material would be 3 times the compressive yield strength. This resulted in an estimated value of 100MPa for the indentation pressure, well within the elastic range of articular cartilage. Using the same assumptions, the majority of short-listed hydrogels had a ultimate tensile strength (as shown in chapter 3), which predicted a compressive yield stress of approximately 40MPa. The elastic deformation of the articular cartilage during stylus contact was reported to be a maximum of ~0.4μm *(Sayles et al., 1979)*, which accounts for between 20-30% of the overall surface roughness. Thus the Ra values were deemed acceptable. The absence of trenching or undulations in the laser profilometry images following stylus contact, provided further support for these calculations and demonstrated no damage to the surface of the articular cartilage following the proposed set of surface profilometry traces.

WLI and Laser Profilometry techniques both provide 3D images of the cartilage surface but both techniques rely on the reflection of light, which is highly sensitive to the reflectivity of the material and surface water. The acquisition of detailed images over a larger surface area using both techniques can be time consuming, in particular the focusing setup required for the WLI on articular cartilage can lead to large variation in setup time. The laser profilometry can be used to examine larger areas than the WLI but this is achieved by a loss in measurement accuracy.

The average Ra and Rq values for each time interval show small variations which are due to the internal filtering process of the measuring technique and the underlying mathematical calculations used to determine each value. For standard machining processes an Rq value of between 10-20% greater than that Ra value is acceptable; however for non machined surfaces this can increase to 50% *(Dagnall, 1986)*. With variations of between 20-30% between Ra and Rq, therefore the Rq values within this study provided a clear validation for the Ra value calculated.

Both techniques showed no statistical variation in results over the 10 minutes exposure to air at room temperature. However, the WLI produced a noticeable increase in the variability of the data distribution on measurements taken following 5 minutes of air exposure, which are indicated by the increased confidence limits shown on Figure 5-5. This indicated that the WLI technique is influenced to a greater extent by the time of measurement than the surface profilometry.

Good repeatability was achieved regardless of measurement technique again demonstrating the consistency of each method and the suitability of direct measurement, as opposed to reverse mould measurement.

However, the increased consistency in the data distribution shown by the surface profilometry measurement technique over time as compared with the

WLI suggested that the surface profilometry technique was the most suitable technique to use in further analysis of both cartilage and hydrogel specimens.

5.6 Summary

- Two surface topography quantification techniques were investigated and the experimental data obtained was compared with that reported within the literature. This allowed the identification of the most appropriate technique for future work.

- The optimisation of both optical and direct contact quantification methods for the surface topography of articular cartilage was achieved. This lead to the formulation of an experimental method by which the aims of this thesis could be achieved.

- The appraisal of the effect of stylus contact on the surface of both bovine articular cartilage and a number of potential chondroplasty materials provided evidence for the suitability of direct measurement techniques.

6 An Extended Simple Geometry Wear Study of Potential Chondroplasty Materials

6.1 Introduction

The aims of this study were to further investigate the potential of single phasic and biphasic materials to reduce friction and surface degradation of both bearing surfaces. The friction model described in Chapter 4 was developed to maintain a constant clinically relevant load and contact pressure for an extended period. The model was also developed to allow the quantification of surface topography alterations following the dynamic testing, thus allowing the tribological effects of each potential chondroplasty material to be evaluated. All friction tests reported in this chapter were completed using the simple geometry wear simulator within a mixed boundary lubrication regime as described in Chapter 2.

6.2 Experimental Methodology

6.2.1 Materials

The experimental control materials for all dynamic friction tests were articular cartilage pins tested against polished stainless steel (positive control) and articular cartilage (negative control), the friction response of which had previously been investigated *(Forster and Fisher, 1999, Bell et al., 2006, Pickard et al., 1998b)*. In addition, a Ø9 mm flat-bottomed stainless steel pin was tested against an articular cartilage plate. The pin shown schematically in Figure 6-1, had a polished contact surface with an average surface roughness Ra value of 0.02 (±0.005) μm.

This initial set of experimental tests compared three biphasic hydrogels, which are listed in Table 6-1, against the experimental controls (polished stainless steel and articular cartilage). Further information on each biphasic and single phasic material can be found in chapter 2.1.

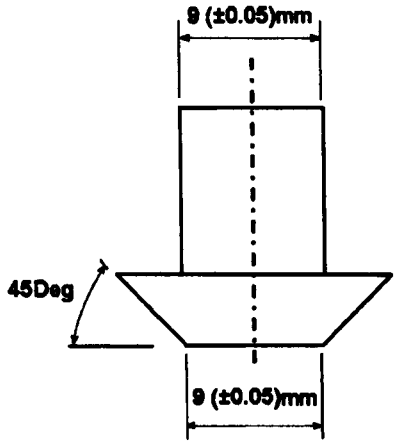

Figure 6-1: Schematic diagram of the stainless steel pin

	Biphasic Hydrogel Specimen		
	4M	1D	3K
Elastic Modulus (MPa)	140.67	31.67	36.90
Uniaxial Tensile Strength (MPa)	9.63	2.90	6.46
1% Proof Stress (MPa)	6.77	2.92	5.02
% Strain @ Failure	56.75	14.20	91.00
Water Content (%Mass alteration)	14	37	19

Table 6-1: Experimental materials investigated within the Extended Friction and Degradation Study

6.2.2 Method

6.2.2.1 Dynamic Friction Study

6.2.2.1.1 Experimental Positive and Negative Control

Each control material was mounted as the plate specimen and fixed into the bath, which was filled with 25% bovine serum containing 0.1% sodium azide to reduce bacterial growth. The cartilage or stainless steel pin was inserted

into the pin holder with the collagen fibre orientation parallel to the direction of linear motion. The specimens were positioned 1 mm apart and left for 2 minutes to re-hydrate and acclimatise. At this point either 30N or 127N was applied to the pin resulting in a contact pressure of 0.5 MPa or 2 MPa respectively, bringing the pin and plate surfaces into contact. The test surfaces were loaded for 60 seconds following which the reciprocating motion was engaged and the friction recorded every 30 seconds for 8 hours (28,800 cycles).

6.2.2.1.2 Eight hour study with a Protein Lubricant

Three hydrogel materials were investigated when subjected to a contact pressure of 0.5 MPa (30N load) and 2 MPa (127N load) respectively and the response compared with that of the positive and negative controls. Each test material was again mounted as the plate specimen and fixed into a bath containing 250 ml of 25% bovine serum with 0.1% sodium azide. The setup and data acquisition protocols were as described above. Once the study was completed, cartilage specimens were stored at -20°C and all other specimens at +4°C for further analysis.

6.2.2.2 Surface Degradation and Quantification of Wear

Quantification of specimen surface alteration was used as the method to infer material wear on all materials. Following the evaluation process as described in Chapter 5, surface profilometry was deemed the most appropriate method for quantifying surface topography changes as it produced no detectable surface damage, showed good repeatability, produced the least variability in results and allowed a large enough area to be quantified within a suitably short time, reducing the risk of tissue dehydration.

Before and after each dynamic friction test, all test specimens had the surface topography quantified using the surface profilometer with a 0.8 mm cut off and Gaussian filter (further information on the method used can be found in Chapter 5). To prevent any potential surface damage to the cartilage pins before testing, the pre-tested cartilage surface topography was quantified

using a number of non-tested controls (n=10). All other pin and plate specimens were quantified using the trace pattern shown in Figure 5-1. The number and position of traces were chosen in order to quantify degradation in both the parallel and perpendicular directions and to keep within a set time limit for measurements, as identified during the technique validation describe in Chapter 5.

Following the friction testing, each specimen was re-measured using the trace positions shown in Figure 5-1. Articular cartilage pin and plate specimens were defrosted at 20°C for 12 hours before being mounted within a custom made jig. Following surface topography quantification all specimens were stored in 100% Ringer's solution at -20°C.

6.3 Results

6.3.1 Experimental Positive and Negative Dynamic Friction Controls

Over the 8 hour test, the positive control of a cartilage pin against a stainless steel plate demonstrated, an equilibrium of fluid load support and solid to solid contact (shown in Figure 6-2). Within the first 250 minutes at 0.5 MPa contact pressure (30N load) and 150 minutes at 2 MPa contact pressure (127N load), the initially low frictional value progressively increased with the gradient of friction rise decreasing over time until it reached about zero. The friction value then remained approximately constant for the concluding section of the test. The final value reached was dependent upon loading, a contact pressure of 0.5 MPa produced a peak friction value of 0.7 (± 0.08) and a contact pressure of 2 MPa produced a peak friction value of 0.4 (± 0.04) for the positive control. While for the negative control, friction levels remained low 0.06 (± 0.01) and 0.032 (± 0.01) for 0.5 MPa and 2 MPa respectively.

The relationship between dynamic friction and contact pressure has been previously investigated by Pickard et al *(Pickard et al., 1998a)*. Using bovine articular cartilage pins on cobalt chromium plates, Pickard et al observed an

almost linear relationship between contact pressure and peak dynamic friction coefficient. By varying the contact pressure from 0.5 MPa to 4 MPa over a 45 minute time period the proposed relationship suggested that as the contact pressure increased by a factor of 2, the friction coefficient decreased by 1.25.

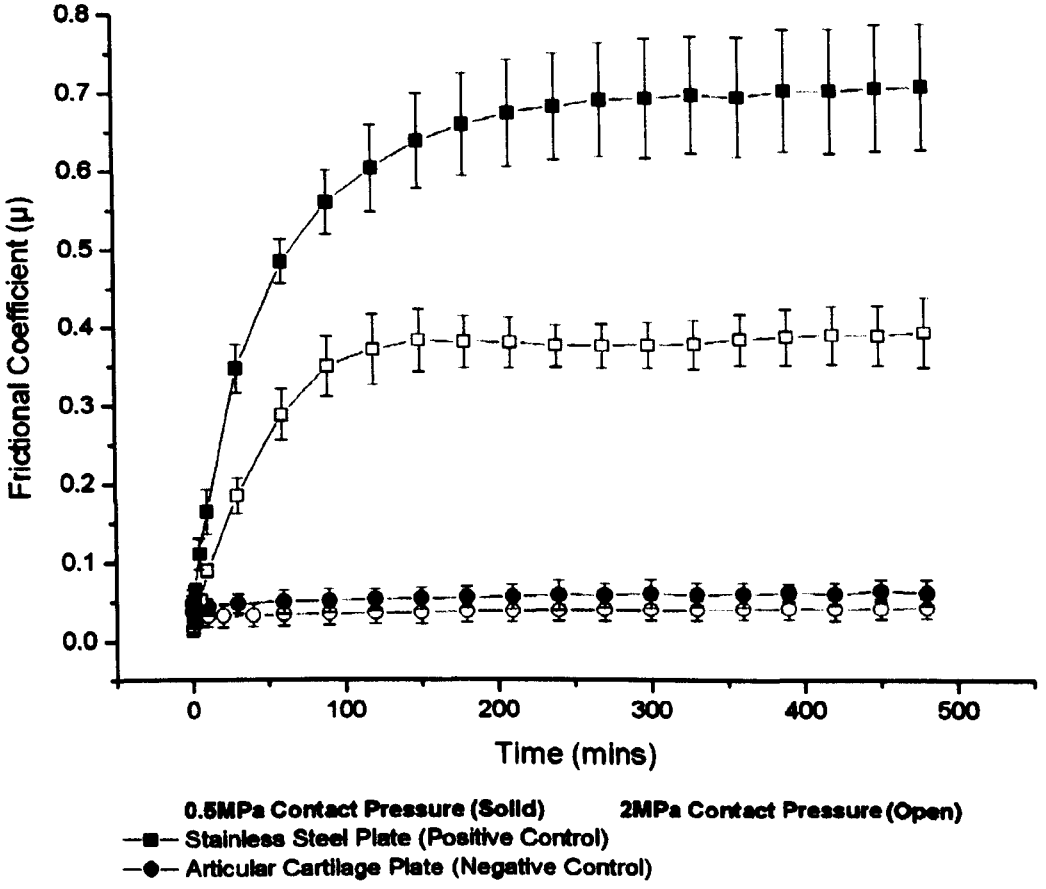

Figure 6-2: Dynamic friction results for Positive and Negative control eight hour tests within a high protein containing lubricant. (n=6, Error bars = 95% confidence limit)

It was found that the optimum performance of a cartilage pin against a cartilage plate (negative control) previously shown over a 2 hour period (see Chapter 4) was in fact maintained for 8 hours. In each loading case the interstitial fluid pressure at the contact area maintained a constant frictional coefficient of 0.04-0.05(±0.015) again regardless of loading or increase contact pressure.

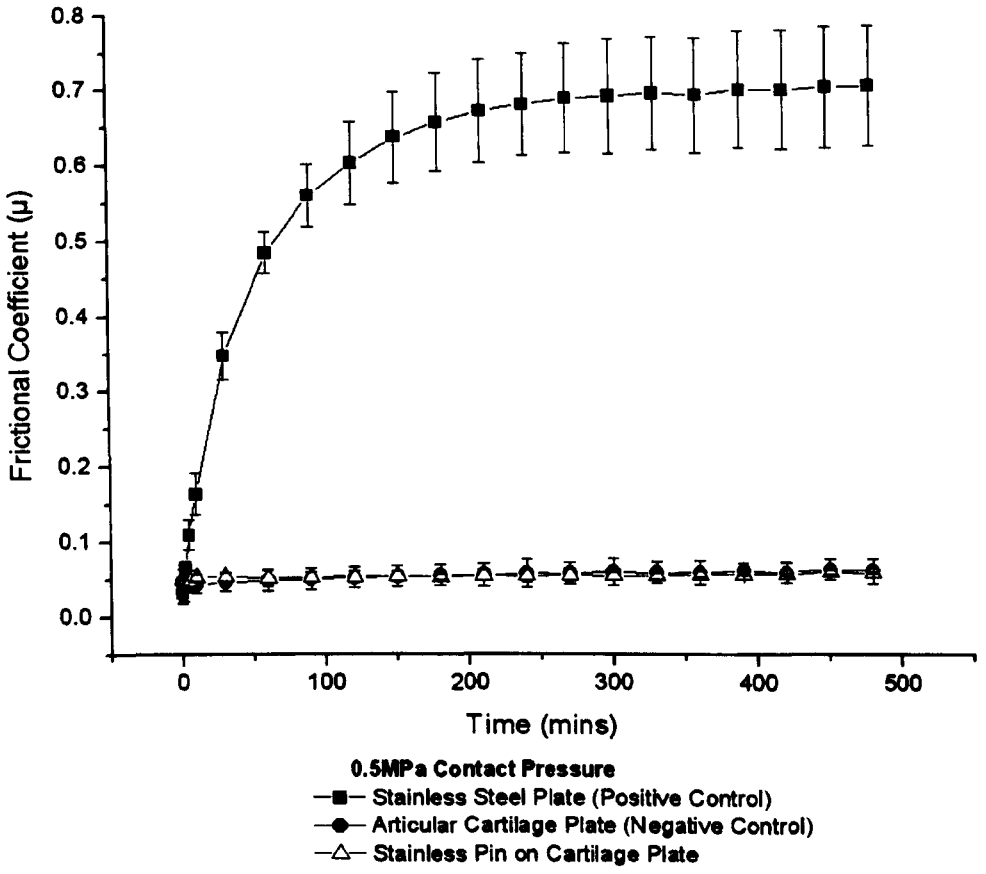

Figure 6-3: Dynamic friction results for Stainless Steel Positive and Negative control eight hour tests within a high protein containing lubricant. (n=6, Error bars = 95% confidence limit)

The additional control of a stainless steel pin against an articular cartilage plate produced a level of dynamic friction similar to the negative control, again demonstrating the continued influence and maintenance of interstitial fluid pressure over the 8 hour test. The similar dynamic friction performance regardless of pin material also indicated the dominant influence of interstitial fluid within the articular cartilage plate.

6.3.2 Eight hour Dynamic Friction within a Protein Containing Lubricant

The frictional responses of each biphasic material and associated experimental controls when tested at 0.5 MPa contact pressure (30N load) are shown in Figures 6-3, 6-4 and 6-5. Each biphasic material again using a one-way ANOVA statistical test, showed a statistically significant reduction in the frictional coefficient when compared with the single-phase positive

control. As in the 2 hour study pin on plate study within a protein lubricant presented in chapter 4.3.3, each hydrogel material produced a steady rise in friction over the initial 100 to 150 minutes, demonstrating a 50% reduction in friction compared with the positive control 150 minutes into the test. Each material then maintained the friction value for the remainder of the test giving a 40% reduction in the final value friction coefficient when compared with the positive control.

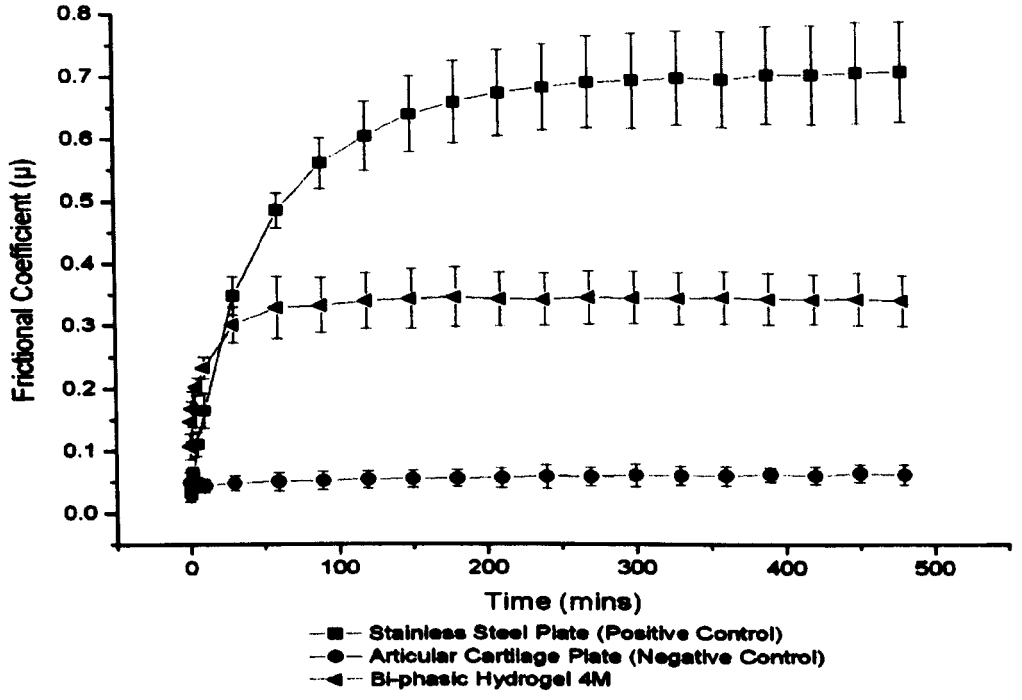

Figure 6-4: Dynamic friction results for Biphasic hydrogel 4M and experimental controls, following the extended friction and wear study within a high protein containing lubricant at 0.5MPa contact pressure. (n=6, Error bars = 95% confidence limit)

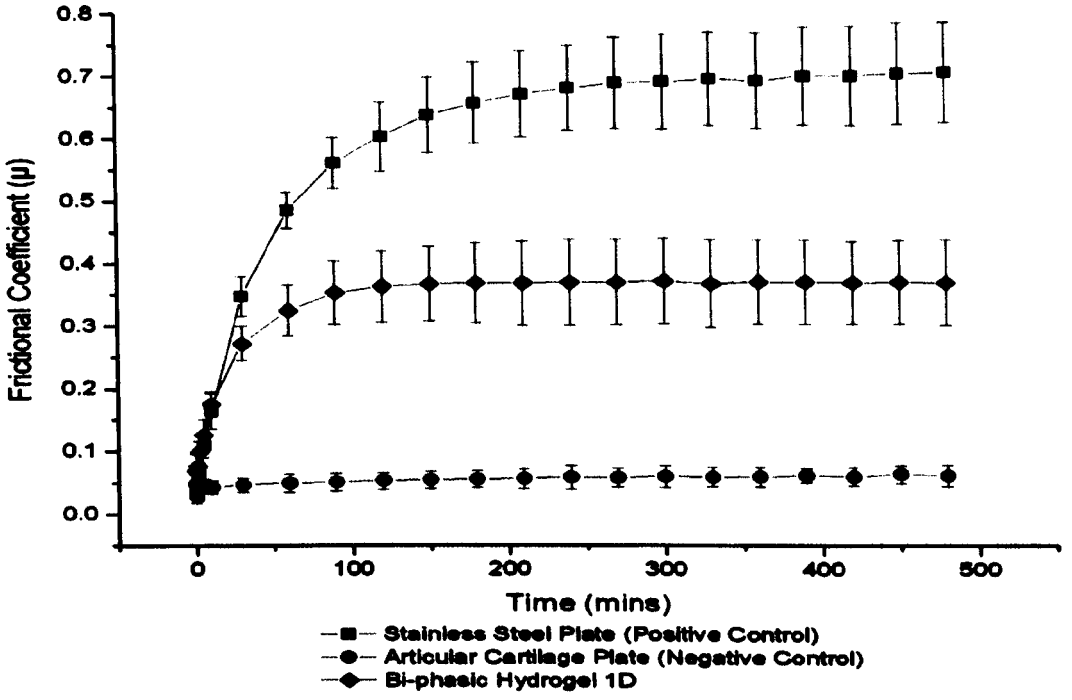

Figure 6-5: Dynamic friction results for Biphasic hydrogel 1D and experimental controls, following the extended friction and wear study within a high protein containing lubricant at 0.5MPa contact pressure. (n=6, Error bars = 95% confidence limit)

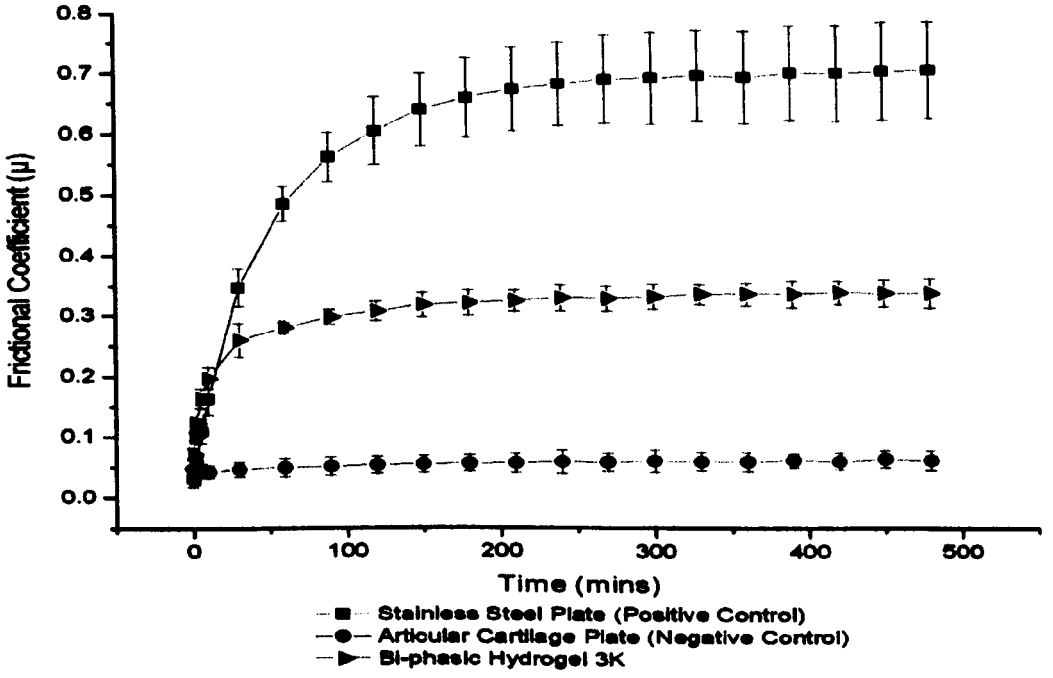

Figure 6-6: Dynamic friction results for Biphasic hydrogel 3K and experimental controls, following the extended friction and wear study within a high protein containing lubricant at 0.5MPa contact pressure. (n=6, Error bars = 95% confidence limit)

When tested at a contact pressure of 2 MPa (127N load), hydrogel materials 1D and 3K failed during testing. In each case a catastrophic failure occurred between 2 and 6 hours of the 8 hour test. Figure 6-7 shows an example of the failure demonstrated by hydrogel 3K. However, both the positive controls, negative controls and hydrogel 4M showed no signs of damage and degradation and a complete set of friction tests were performed. Figure 6-8 shows the frictional coefficients for biphasic hydrogel 4M at both 0.5 MPa and 2 MPa contact pressures with associated controls.

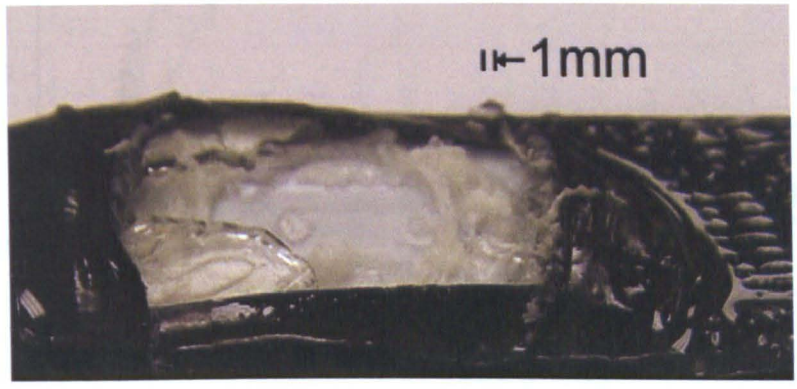

Figure 6-7: Example of catastrophic failure experienced by hydrogel 3K following 8 hour friction test at a contact pressure of 2MPa

As with the experimental controls, the increase in contact pressure resulted in a decrease in friction coefficient with hydrogel 4M producing a steady rise in friction for the first 90 minutes of the test and maintaining a constant frictional coefficient value of 0.16 for the remainder of the test. When compared with the friction value at 0.5 MPa contact pressure, the observed relationship between contact pressure and friction coefficient varied from that proposed by Pickard et al *(Pickard et al., 1998a)*, who indicated that as the contact pressure increased by 2 times, the frictional coefficient reduced by a factor of 1.55 times. However, to determine a statistical significant relationship further data will be required.

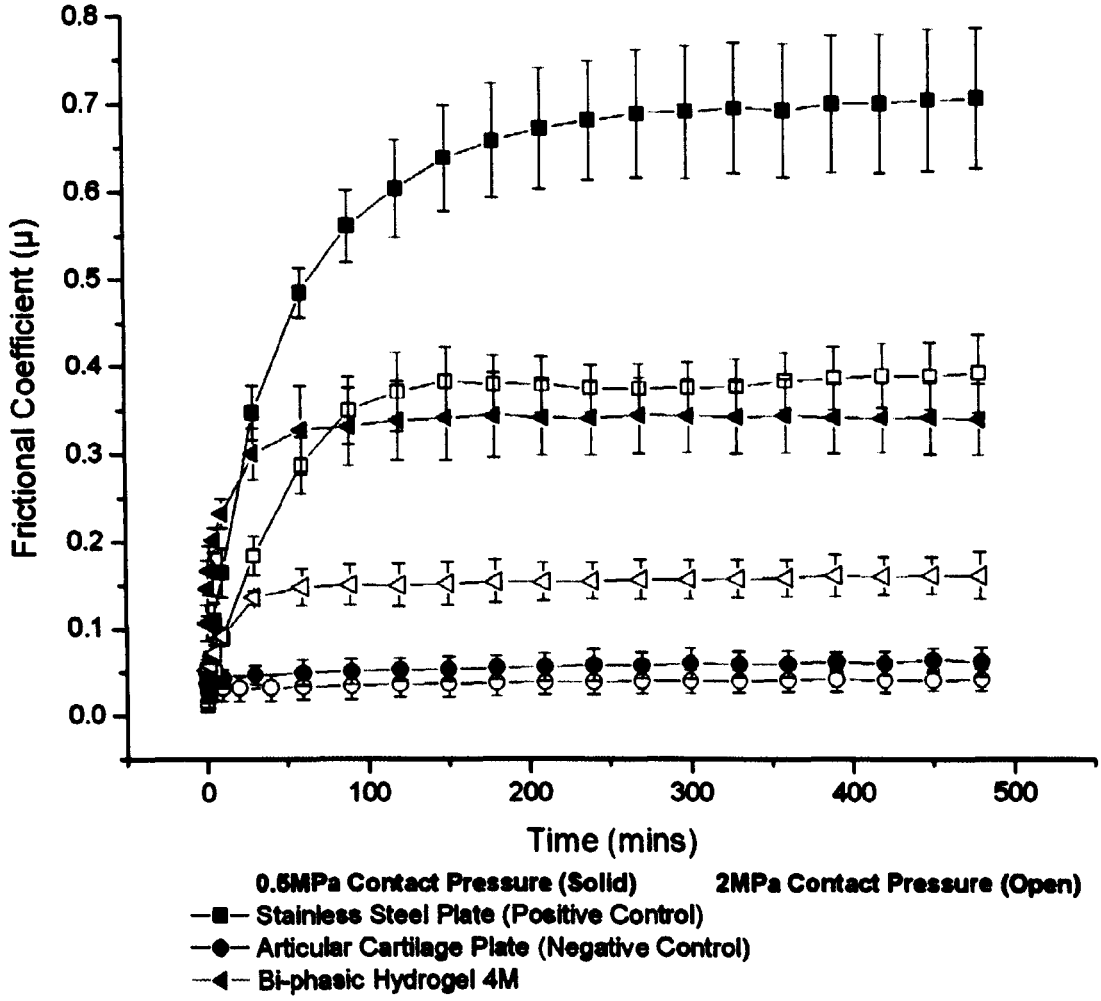

Figure 6-8: Dynamic friction results for experimental controls and biphasic hydrogel 4M at 0.5MPa and 2MPa contact pressure, within a high protein containing lubricant. (n=6, Error bars = 95% confidence limit)

6.3.3 Surface Degradation and Wear

The damage and wear of both surfaces after the 8 hour friction study were investigated using analysis of the surface topography. In all cases, no variation in directionality of the surface traces was found, so all results presented within this section are an average of all four traces taken.

6.3.3.1 Wear and Damage to the Opposing Cartilage Surface Model

Figure 6-9 shows the average surface topography measurements on each cartilage pin as the opposing surface model, following testing at 0.5 MPa contact pressure (30N loading). Using a one-way ANOVA statistical test, the cartilage pins which had been tested against stainless steel (positive control)

showed a statistically significant ($P<0.05$) increase of 75% in the Ra value compared with un-tested articular cartilage samples. The increase in Ra indicated a change in the mechanical structure of the cartilage surface. The articular cartilage pins tested on articular cartilage plates (negative control) were not statistically difference from that of untested articular cartilage pins, which showed no variation in the surface structure.

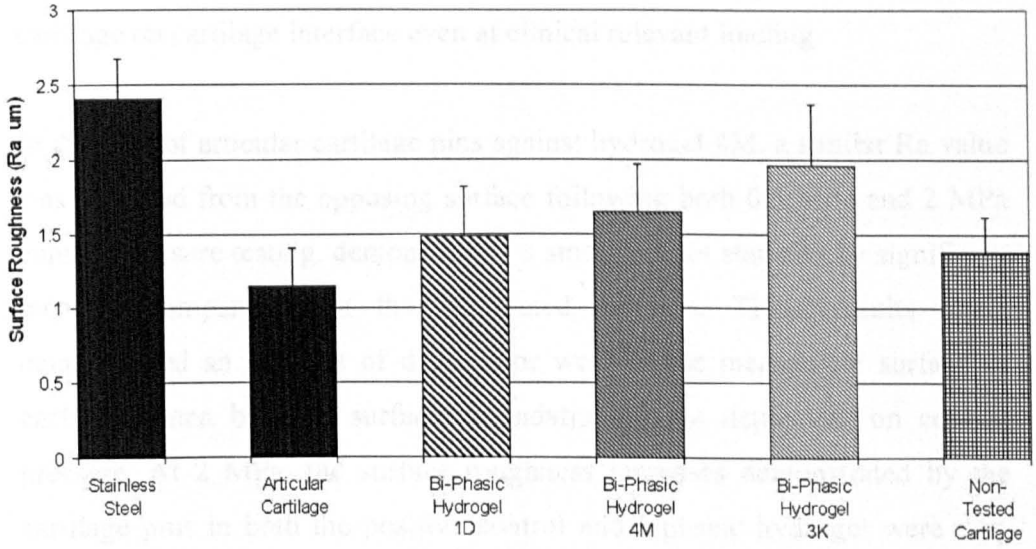

Figure 6-9: The surface variation of cartilage pins following testing at 0.5 MPa contact pressure (n=6, Error bars = 95% confidence limit)

The surface topography alterations to cartilage pins after testing against each biphasic hydrogel produced values between that of the positive and negative controls. In each case, the cartilage pins demonstrated a non statistically significant increase in surface roughness when compared with non-tested cartilage. This indicated an element of damage or wear to the mechanical surface of each specimen. However, regardless of which material the results showed a marked reduction in surface roughness alteration when compared with the positive control, which clearly demonstrated a reduced amount of surface fibrillation to the cartilage surface.

The effects of the higher contact pressure of 2 MPa is shown in Figure 6-10. The articular cartilage pins tested at the 2 MPa positive control again showed a marked increase in surface roughness, when compared with non-tested

articular cartilage. However, using a one-way ANOVA statistical test this increase was not statistically significant. The 2 MPa control cartilage pins also showed a marked but not statistically significant decrease in surface roughness alteration when compared with the 0.5 MPa positive control cartilage pins. The 2 MPa negative control pins produced little variation when evaluated against the 0.5 MPa negative control pins or the non-tested articular cartilage specimens, indicating no surface alterations between the cartilage on cartilage interface even at clinical relevant loading.

In the case of articular cartilage pins against hydrogel 4M, a similar Ra value was recorded from the opposing surface following both 0.5 MPa and 2 MPa contact pressure testing, demonstrating a small but not statistically significant increase compared with the non-tested controls. These results again demonstrated an element of damage or wear to the mechanical surface of each specimen but any surface degradation is not dependent on contact pressure. At 2 MPa, the surface roughness increases demonstrated by the cartilage pins in both the positive control and biphasic hydrogel were very similar in value suggesting a similar amount of surface degradation to the opposing surface at increased loading.

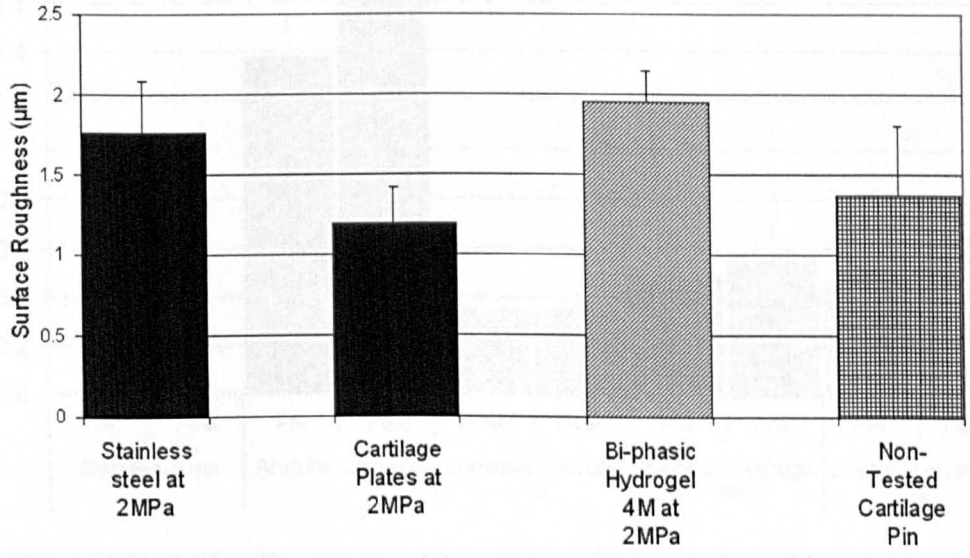

Figure 6-10: The surface variation of cartilage pins following testing at 0.5 MPa and 2 MPa contact pressure (n=6, Error bars = 95% confidence limit)

6.3.3.2 Degradation and Wear of Potential Biphasic Polymers

Figures 6-11 and 6-12 show surface topography alterations for each plate specimen pre- and post-eight hour testing at 0.5 MPa and 2 MPa contact pressure respectively. In each case, both the positive and negative controls produced no statistically significant change in surface roughness following the longer term friction tests. This indicated no mechanical damage or deposit of material to the control specimen's surface.

At a contact pressure of 0.5 MPa, biphasic hydrogel specimens 1D and 4M showed no change in surface roughness, which again indicated no mechanical change in the surface structure. In contrast, biphasic hydrogel specimen 3K demonstrated an increase in the surface roughness. It is unlikely that this alteration to the mechanical structure was the result of material deposit as this was not seen on any other test specimens. The increase in surface roughness seen was either the result of material loss or fibrillation of the material surface and indicated that the biphasic hydrogel specimen 3K had a lower wear resistance then the other biphasic hydrogel specimens.

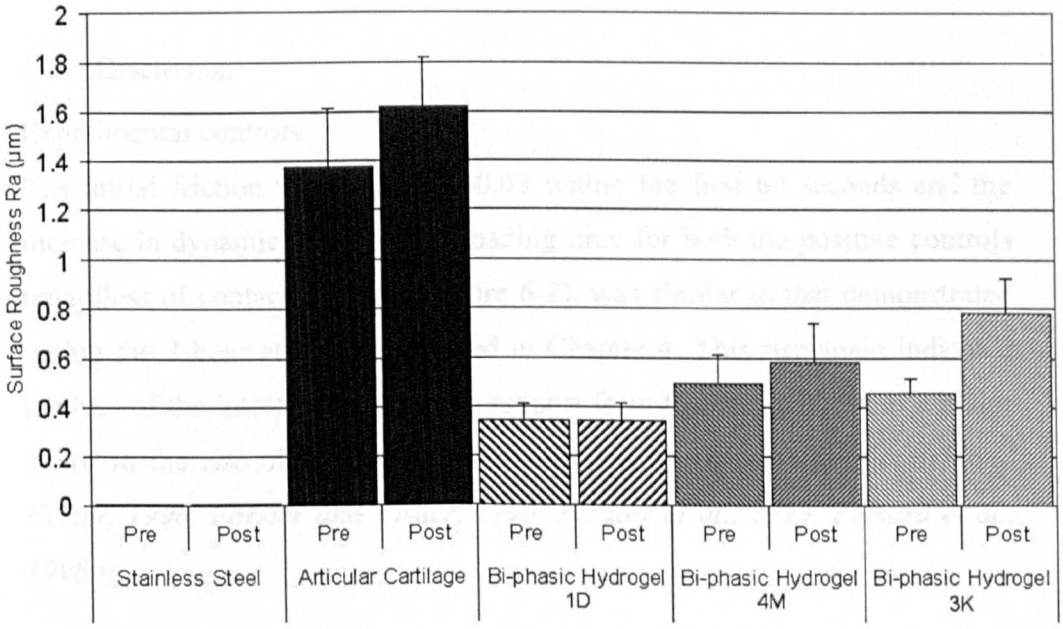

Figure 6-11: Surface Topography of Sample materials pre and post 8 hours wear testing at 0.5MPa contact pressure (n=6, Error bars = 95% confidence limit)

At a contact pressure of 2 MPa, the positive control produced little variation in surface roughness following testing. Both the negative control and hydrogel 4M showed a small increase in surface roughness following testing as shown in figure 6-12. However using a one-way ANOVA statistical test, any increase was not statistically significant.

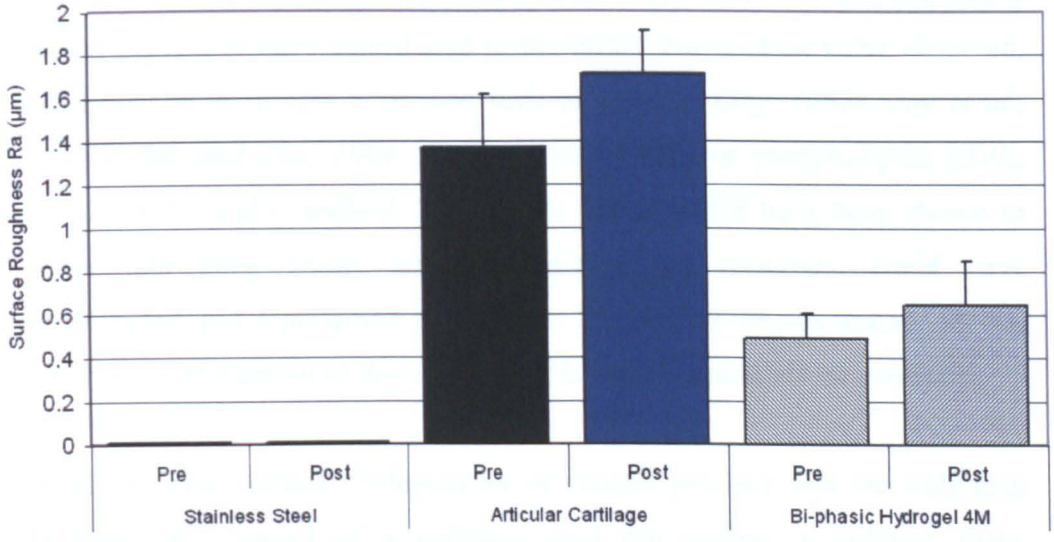

Figure 6-12: Surface Topography of Sample materials pre- and post- 8 hours wear testing at 2 MPa contact pressure (n=6, Error bars = 95% confidence limit)

6.4 Discussion

Experimental controls

The initial friction value of 0.02 -0.03 within the first 60 seconds and the increase in dynamic friction with loading time for both the positive controls regardless of contact pressure (Figure 6-2), was similar to that demonstrated within the 2 hour study as described in Chapter 4. This rise again indicated the loss of the interstitial fluid load support from the cartilage pin as a major factor in the rise of dynamic friction *(Krishnan et al., 2004b, Forster and Fisher, 1996, Forster and Fisher, 1999, Forster et al., 1995, Pickard et al., 1998a)*.

Extending the test duration to 8 hours allowed the friction for all material specimens to reach and maintain a friction equilibrium at 200 to 250 minutes

which was maintained for the remainder of the test. In the case of the both positive controls the interstitial fluid load support had reached its equilibrium, with solid to solid contact and boundary lubrication being the dominating effects.

Alternatively, as in the 2 hour models, micro-EHL *(Dowson and Jin, 1986)* could explain or have contributed to the initial low friction value observed. Additionally, boundary lubricants such as lubricin *(Jay, 1992b, Jay et al., 2001b, Jay and Cha, 1999, Swann et al., 1981a)* or phospholipids *(Hills, 2002a, Hills and Crawford, 2003, Hills, 2000)* which have been shown to offer lubricating ability against single phasic materials, could have contributed and maintained the friction equilibrium demonstrated. In this study the contribution of these boundary lubricants could not be assessed.

Both negative controls, independent of contact pressure and the additional experimental control of a stainless steel pin against a cartilage plate, maintained the initial low friction value for the entire 8 hour test. Again it is postulated that this low friction value, independent of reciprocating pin material, was maintained by cartilage plate permeability and re-hydration of the interstitial fluid during unloaded periods of the cycle *(Bell et al., 2006)*. However, the biphasic amorphous layer (BSAL) of articular cartilage *(Graindorge et al., 2005, Kobayashi et al., 1995, Kobayashi et al., 1996)* containing lipids, lubricin and proteoglycans could also have influenced the result, by transferring the load from the solid phase to the fluid phase and 'shielding' the solid cartilage structure from elevated stresses, thus maintaining the structural integrity, which is vital to maintaining the water content and permeability of articular cartilage *(Maroudas, 1976, Mow and Hayes, 1997, Freeman, 1979, Armstrong and Mow, 1982)* and thus maintaining the interstitial fluid load support.

Articular cartilage surface additives resulting in boundary lubrication have also been shown to maintain low levels of friction but not for the length of

time demonstrated in this study *(Jay, 1992b, Jay et al., 2001b, Jay and Cha, 1999, Swann et al., 1981a);(Hills, 2002a, Hills and Crawford, 2003, Hills, 2000)*. However as with the positive control, the contribution of boundary layer lubrication could not be assessed.

Biphasic Hydrogel Materials

At a contact pressure of 0.5 MPa, the friction value reached at equilibrium by each hydrogel, regardless of mechanical properties, could be attributed to their biphasic properties. Hydrogel fluid extraction and re-hydration at the contact area would result in lower surface contact. An increased level of fluid at the contact zone could possibly indicate the contribution of EHL to the equilibrium response. However, the initial friction rise showed a percentage of solid contact, thus suggesting that EHL was not the dominant lubrication regime.

The catastrophic failure of hydrogel 3K and 1D at the higher contact pressure of 2 MPa was supported by the unconfined creep test, shown in Chapter 3. 10mm diameter pins of Hydrogel 3K and 1D failed at compressive stresses of 1 MPa and 1.5 MPa respectively demonstrating an ultimate compressive stress well below 2 MPa. As in the unconfined creep test, biphasic hydrogel 4M performed at the higher contact pressure maintaining a friction value well below the positive control. The small initial rise to a peak friction value of 0.15 was maintained for the reminder of the test indicating the material's potential to resist higher forces and perform at clinically relevant loading.

As discussed in Chapter 3, the performance of hydrogel 4M also assisted in the identification of key monomers and cross-linking agents in order to optimise a potential chondroplasty material. The failure of both 3K and 1D at 2 MPa contact pressure would indicate that hydroxyethyl methacrylate (HEMA) at any percentage volume is not a suitable monomer for use within a potential chondroplasty material. The influence of each monomer and their critical percentages within a composite hydrogel was also demonstrated by

the variation in performance of 3K and 4M. The only difference between each hydrogel is that 3K contains 39% of HEMA and 4M 39% of hydroxypropyl methacrylate (HPMA). This difference brought about a diverse range in mechanical and physical properties with 4M possessing an elastic modulus four times that of 3K. However, hydrogel 4N which contains 29% of HPMA possessed an elastic modulus below that of hydrogel 3K.

The relationship between friction and contact pressure within the positive control results showed a degree of consistency with that reported by Pickard et al, with a variation of only +5% *(Pickard et al., 1998a)*. The extend period of testing and the variation in metallic material in our study could explain this small difference. However, the relationship is less consistent when applied to hydrogel 4M. With a +24% error, the biphasic nature, possible plastic deformation, increased conformity at the contact zone and surface reactivity, could have influenced the friction value and contributed to the difference. It should be noted that with only two data points it is not possible to confirm a relationship linear or otherwise, between contact stress and friction within this study.

All hydrogels, regardless of permeability and equilibrium water content (EWC), demonstrated similar maximum friction results, indicating high levels of solid-to-solid contact and boundary lubrication at the contact zone. The rate of friction rise was also independent of permeability, with all three hydrogels showing similar rates of friction rise and all reaching equilibrium after approximately 100 minutes. The survival of hydrogel 4M at the higher contact pressure was independent of aggregate modulus. However, the increased phasic response demonstrated by 4M (see Chapter 3) and not the flow of free water could have contributed to the higher load performance. The plastic flow of 4M's molecular structure could have resulted in a reduction of peak internal stresses and survival of the material.

Surface roughness alterations

As shown in previous studies *(Forster and Fisher, 1999, Stachowiak et al., 1994, Graindorge and Stachowiak, 2000)* the articular cartilage pin surface within the positive control subject to a contact pressure of 0.5 MPa (30N) (figure 6-11) showed a statistically significant increase in mechanical degradation to the surface layer. At the higher contact pressure of 2 MPa a non statistically significant yet relevant increase in surface roughness was demonstrated. Stachowiak et al *(Stachowiak et al., 1994)* suggested wear of the superficial boundary layer resulted in this increase. This was disputed by Foster et al *(Forster and Fisher, 1999)* who demonstrated a decline in the fluid load phase as the major factor.

In these preliminary studies, a connection between friction, loss of fluid load support and increasing surface roughness was demonstrated by positive and negative control specimens. No statistically significant surface roughness change in the negative control pins regardless of contact pressure demonstrated the high level of load support and low solid contact. The increased solid contact found in the positive control could have contributed to the increase in surface roughness and thus indicates a potential higher wear rate for the opposing surface following implantation within a synovial joint.

At a contact pressure of 0.5 MPa the cartilage pins from each biphasic material showed less increase in surface roughness than the 0.5 MPa positive control. It is postulated that through maintaining a higher proportion of the fluid load support, a lower rate of opposing surface degradation was achieved. However, the interaction between surface additives present on the articular cartilage surface and the biphasic monomer could have had a role in the final roughness of the cartilage pin surface.

The lower surface roughness value demonstrated by the 2 MPa positive control compared with the 0.5 MPa positive control indicated that a loss of interstitial fluid and an increase in solid to solid contact was not the only

lubrication mechanism present. As shown in Appendix A, the influence of load on fluid film thickness is small, but higher load could have resulted in an increase in either elastic or plastic surface deformation which reduced the surface roughness of each surface under load. Elastic deformation could have reduced the level of extremity contact between both surfaces resulting in a lower contact. The increased load and possible increased fluid pressure could have increased plastic deformation of each material, resulting in a permanent 'polishing effect' to the cartilage surface thus lowering the overall surface roughness at higher loading.

The higher load could have also increased the influence of the Biphasic-SAL *(Kobayashi et al., 1995, Kobayashi et al., 1996, Graindorge et al., 2005)* by increasing the proportion of stress shielding to the underlying solid structure and increasing the fluid pressure at the surface reducing the percentage of solid to solid contact. Also the higher load could have resulted in an increased influence of boundary lubrication through a form of boosted lubrication *(Walker et al., 1968, Longfield et al., 1969)* increasing the concentration of boundary lubricants at the surface.

At 0.5 MPa contact pressure the only biphasic material to show a variation in surface roughness was hydrogel 3K (Figure 6-11). This had little correlation with the friction results as hydrogel 3K produced a friction response similar to hydrogel 4M. It did identify the low wear resistance of material 3K when compared with material 1D which possessed a lower elastic modulus and ultimate tensile strength. It is the understanding of such differences that is vital for the successful development of new cartilage substitution materials.

At the increased contact pressure biphasic hydrogel 4M showed no variation in surface roughness when compared with the 0.5 MPa contact pressure result or the 2 MPa positive control, again demonstrating a consistent level of surface degradation independent of a lower friction coefficient value. This result showed no relationship between overall friction value and level of

surface degradation. The increased contact pressure could have increased the conformity of elastic hydrogel material, thereby increasing the effects of EHL and micro-EHL *(Hamrock and Dowson, 1978, Dowson et al., 1969, Dowson and Jin, 1986)* and reducing the amount of solid to solid contact.

6.5 Summary

- An experimental model which allowed the appraisal of each potential chondroplasty material at extended time periods and clinically relevant loading was developed.

- The potential of biphasic materials to reduce and maintain a low friction value for extended periods at clinical relevant loading was demonstrated.

- An experimental model to evaluate the frictional properties and surface degradation of potential chondroplasty materials and the opposing cartilage joint surface was developed, which can be used to aid in the prediction of *in vivo* performance.

- The complex interactions between various lubrication and tribological regimes present with synovial joint lubrication were demonstrated. As was the importance of understanding not only friction but material wear on each contacting surface in the development of potential chondroplasty materials.

7 The Effects of Multi-directional Motion on Friction and Wear

7.1 Introduction

Natural joint kinematics consist of multi-directional forces and movements including elements of rotation and cross shear *(Lafortune et al., 1992, Levens, 1948, Paul, 1966, Freeman and Pinskerova, 2005, Iwaki et al., 2000)*. Multi-directional motion has been shown to increase wear rates within traditional orthopaedic polymers *(Tandon et al., 1983, Joyce, 2005, Galvin et al., 2006, Wang, 2001)* with Briscoe et al demonstrating a linear relationship between angular rotation of the pin and wear rate for polytetrafluoroethylene (PTFE) within a pin on plate configuration *(Briscoe and Stolarski, 1985)*. The aims of this study were to further develop the simple geometry friction and wear model to include multi-directional motion and investigate the effects of this increased complexity of motion on a number of potential chondroplasty implant materials. The model was applied to compare friction and wear under uni-directional motion (reciprocating) and multi-directional (reciprocating and rotation) motion over an eight hour period.

The model was also used quantify surface roughness as discussed in Chapter 5, in order to evaluate the tribological performance of each chondroplasty material. The friction and wear tests within this chapter were completed using the simple geometry wear simulator within a mixed boundary lubrication regime as described in Chapter 2.

7.2 Experimental Methodology

7.2.1 Materials

The experimental control materials for this experimental model were articular cartilage pins tested against polished stainless steel (positive control) *(Forster and Fisher, 1999, Pickard et al., 1998b)* and articular cartilage (negative control) *(Bell et al., 2006)*. The experimental model presented in this chapter was used to compare three biphasic hydrogels, which are shown in Table 6-1, against the experimental controls (polished stainless steel and articular

cartilage). Further information of each biphasic and single phasic material can be found in chapter 2.1.

7.2.2 Method

7.2.2.1 Dynamic Friction Study

7.2.2.1.1 Experimental Positive and Negative Control

Each control material was mounted as described in the uni-directional study described in Chapter 6. The cartilage pin was again inserted into the pin holder with the collagen fibre orientation parallel to the direction of linear motion. In the multi-directional configuration, the multi-directional attachment was fitted and the pin holder inserted into the polymer plain bearing and multi-directional attachment as shown in Figure 7-1. The multi-directional attachment resulted in an additional rotation of $\pm 10^{\circ}$ about the vertical axis of the cartilage pin as shown in Figure 7-2.

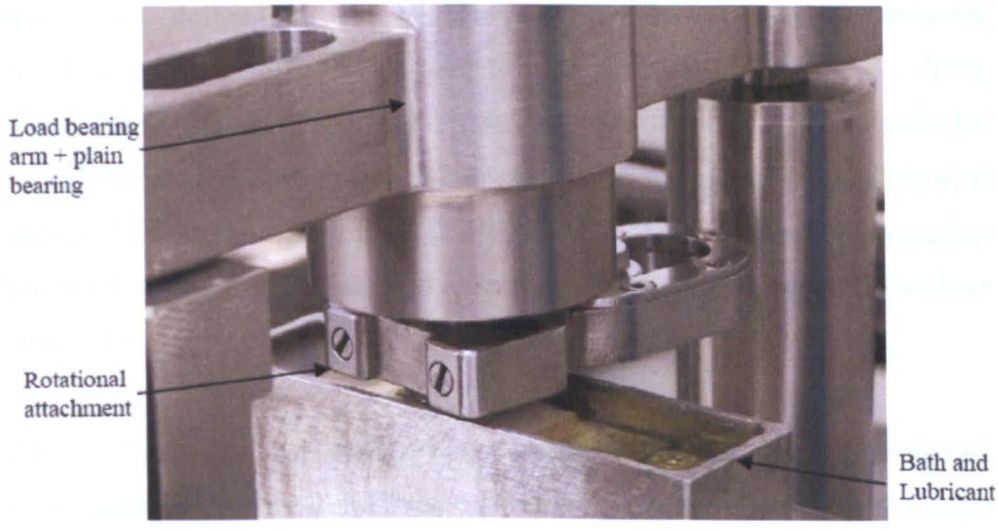

Figure 7-1: The multi-directional attachment when fitted to the simple geometry wear simulator

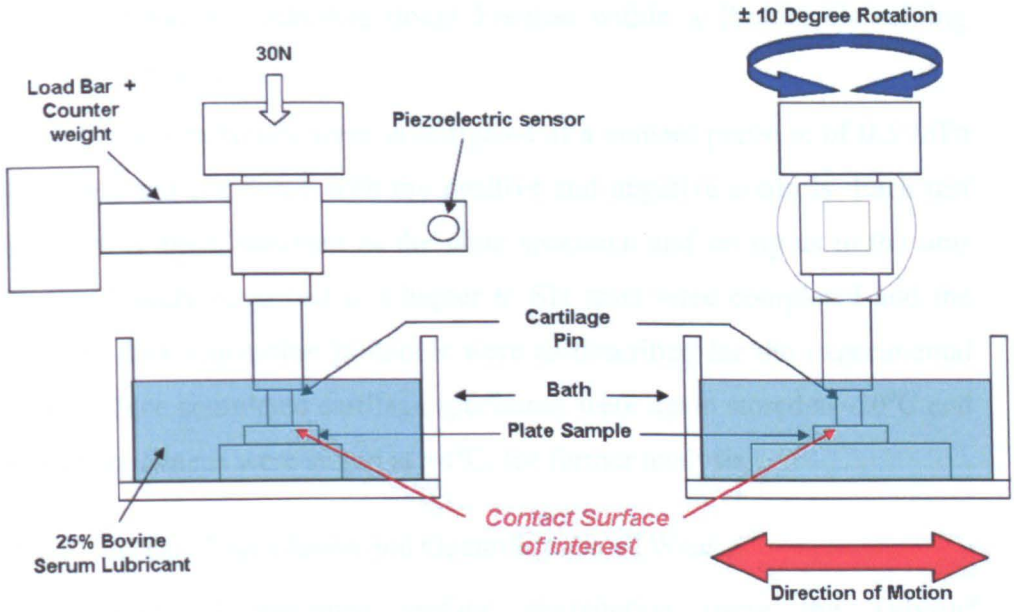

Figure 7-2: A schematic diagram showing the motion applied during the multidirectional testing

Multi-directional motion resulted in the frictional force constantly changing direction with respect to the linear reciprocating direction. These continuously variable cross shear forces were assessed by defining the cross shear ratio, defined by the frictional work released in the cross-shear direction over that in the linear reciprocating direction *(Galvin et al., 2006, Wang, 2001)*. The quantitative analysis used to define a cross-shear ratio for the experimental geometry used within this study was taken from Galvin et al and can be found in Appendix B *(Galvin et al., 2006)*. A linear reciprocation length of 10mm and $\pm 10^0$ degree rotation resulted in an average cross-shear ratio of 0.01.

Within all experimental configurations, the specimens were again positioned 1 mm apart and left for 2 minutes to re-hydrate and acclimatise. At this point 30N was applied to the pin resulting in a contact pressure of 0.5 MPa which brought the test surfaces into contact. The test surfaces were loaded for 60 seconds, following which the reciprocating motion was engaged and the friction recorded every 30 seconds for 8 hours (28,800 cycles).

7.2.2.1.2 Dynamic Multi-directional Friction within a Protein Containing Lubricant

Three hydrogel materials were investigated at a contact pressure of 0.5 MPa (30N load) and compared with the positive and negative controls. Each test material was again mounted as the plate specimen and set-up as in the uni-directional study described in Chapter 6. Six tests were completed and the setup and data acquisition protocols were as described for the experimental controls. Once completed cartilage specimens were again stored at -20°C and all other specimens were stored at +4°C, for further analysis.

7.2.2.2 Surface Degradation and Quantification of Wear

Quantification of specimen surface degradation using the Talysurf profilometer was again used as an indication of material damage and wear on all materials before and after testing, further information can be found in Chapter 5.

7.3 Results

7.3.1 Dynamic Friction and Wear Study

7.3.1.1 Experimental Positive and Negative Dynamic Friction Controls

The uni-directional positive control of a cartilage pin against a stainless steel plate showed an initial rise in friction until equilibrium of fluid load support and solid to solid contact was reached. As shown in Figure 7-3, within the first 250 minutes at 0.5 MPa contact pressure the initially low friction value progressively increased with the gradient of rise decreasing over time until it reached zero, remaining approximately constant at the peak value of 0.7 for the concluding section of the test.

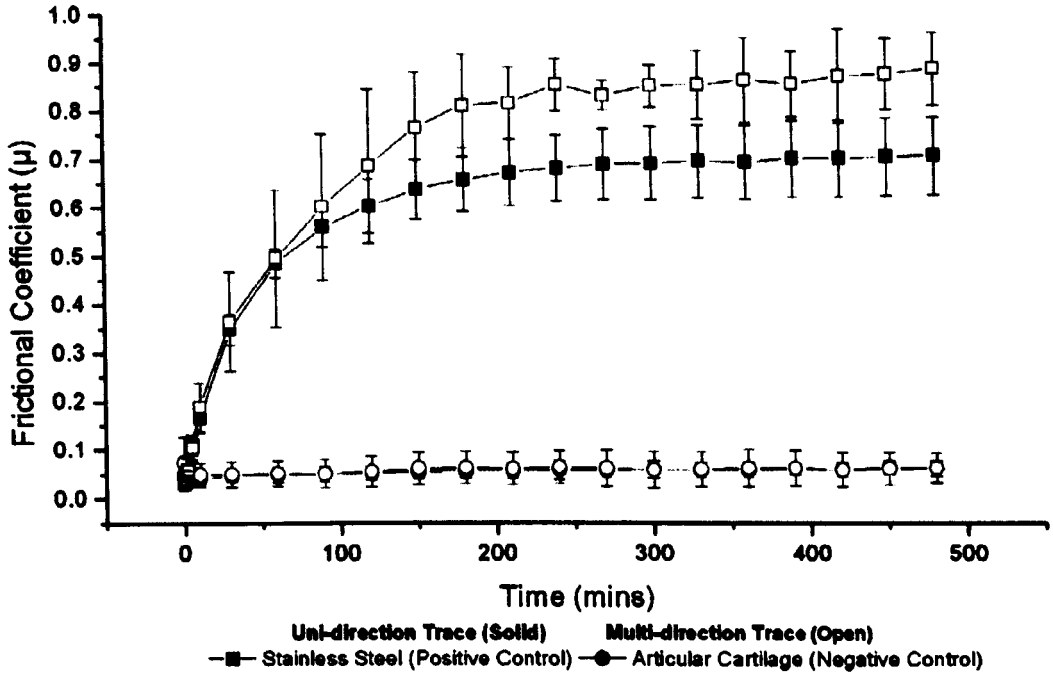

Figure 7-3: Uni-directional and Multi-directional dynamic friction results for Positive and Negative controls within a high protein containing lubricant. (n=6, Error bars = 95% confidence limit)

The addition of rotational motion within the multi-directional positive control produced an initial low value and progressive rise in friction similar to that seen in the uni-directional positive control. However, the rate of gradient decrease was lower than that in the uni-directional study, resulting in a peak friction coefficient value of 0.88 at 250 minutes which was again maintained for the reminder of the test. Using a one-way ANOVA statistical test, the additional rotation produced a statistically significant increase in the peak positive control dynamic friction coefficient.

Regardless of pin rotation, the cartilage pin against a cartilage plate again produced the optimum performance shown in the uni-directional studies. In each case the interstitial fluid pressure at the contact area maintained a constant frictional coefficient of 0.04-0.05(±0.015) with no statistically significant variation in frictional coefficient.

7.3.1.2 Multi-directional Dynamic Friction within a Protein Containing Lubricant

The effects of multidirectional motion on the frictional responses of each biphasic material are shown in Figures 7-4, 7-5 and 7-6. Using a one-way ANOVA statistical analysis, the addition of rotation produced no statistically significant variation in dynamic friction for each biphasic polymer. As in the uni-directional test, each hydrogel material exhibited a similar frictional response composed of an initial steady rise over the first 100 minutes, demonstrating a 50% reduction in friction compared with the positive control at this point in the test. Hydrogel 4M reached a slightly lower maximum friction value when compared with 1D and 3K. Each material then maintained the friction value for the remainder of the test giving a 65% reduction in the final value friction coefficient when compared with the multi-directional positive control. This was greater than the 50% reduction shown by each biphasic hydrogel within the uni-directional study.

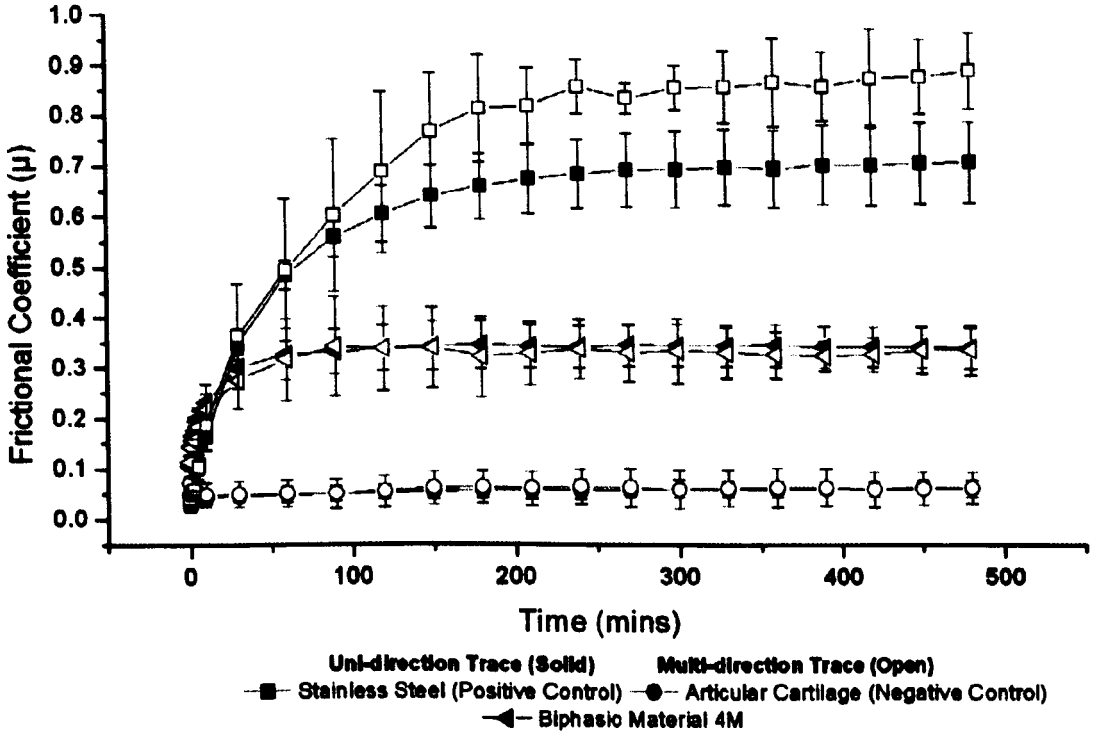

Figure 7-4: The effect of multi-directional motion on the dynamic friction results for Biphasic hydrogel 4M and experimental controls, following an eight hour tests within a high protein containing lubricant. (n=6, Error bars = 95% confidence limit)

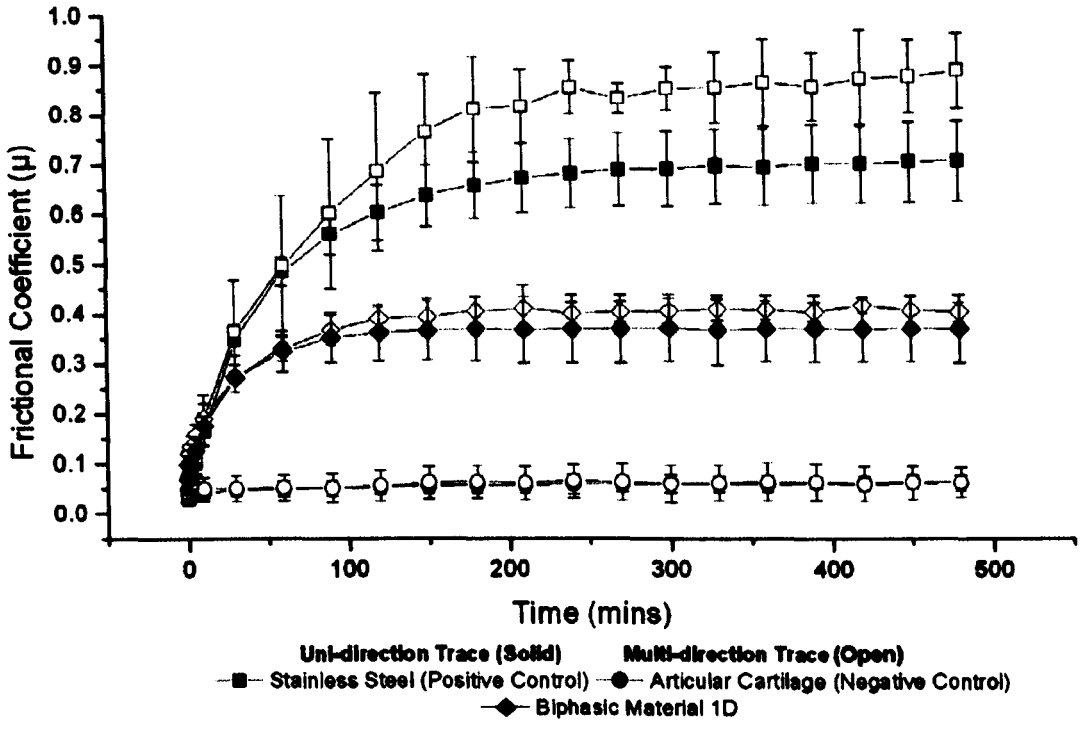

Figure 7-5: The effect of multi-directional motion on the dynamic friction results for Biphasic hydrogel 1D and experimental controls, following an eight hour tests within a high protein containing lubricant. (n=6, Error bars = 95% confidence limit)

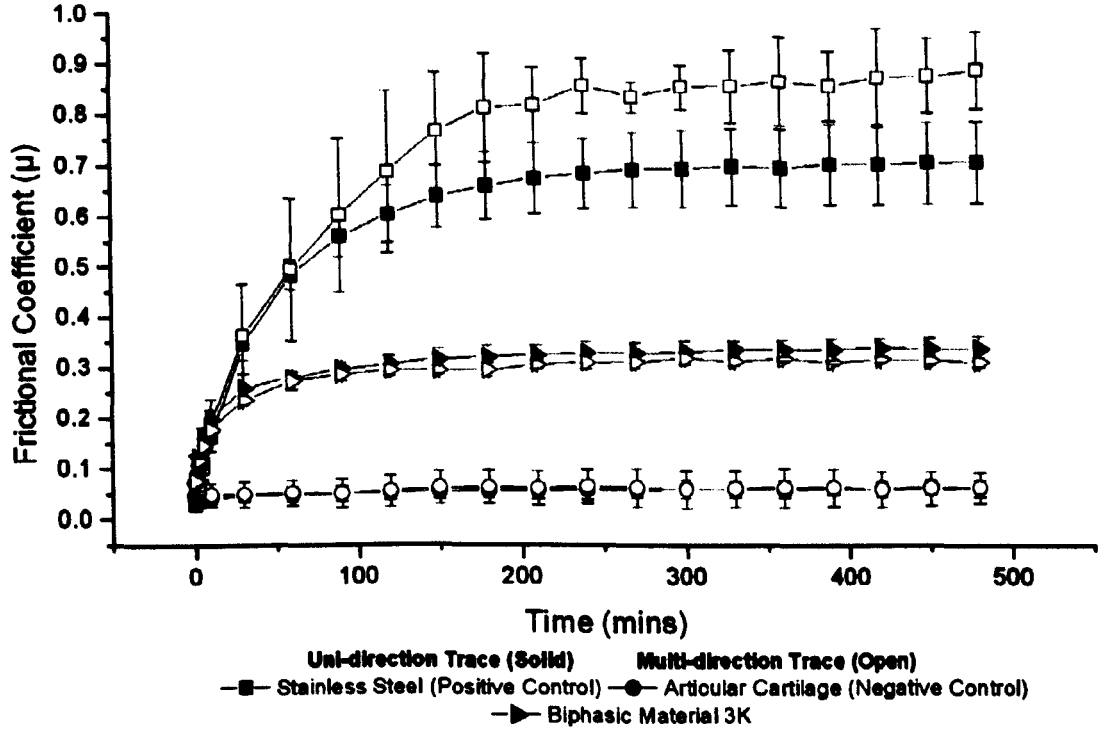

Figure 7-6: The effect of multi-directional motion on the dynamic friction results for Biphasic hydrogel 3K and experimental controls, following an eight hour tests within a high protein containing lubricant. (n=6, Error bars = 95% confidence limit)

7.3.2 Multi-directional Surface Degradation and Wear

The damage and wear of both surfaces after the multi-directional friction study was again investigated using surface topography and compared with the results obtained within the uni-directional study presented in Chapter 6. In all cases, no variation in surface trace directionality was found so all results presented within this section are an average of all four traces taken.

7.3.2.1 Damage and Wear to the Opposing Cartilage Surface Model

Figure 7-7 shows the average surface roughness (Ra) measurement of each cartilage pin as the opposing surface model, following testing at 0.5 MPa contact pressure. As described in Chapter 6, the uni-directional stainless steel positive control produced a statistically significant increase of 75% in the Ra value when compared with none tested articular cartilage.

However, using a one-way ANOVA statistical test, the inclusion of rotation within the multi-directional positive control produced no statistically significant increase in the surface roughness value, compared with the non-tested control. This result would suggest that the multi-directional motion either prevented the surface damage which was present in the uni-directional study or the multi-directional motion had an additional 'polishing' effect on the articular cartilage surface as previously shown in metal on metal pin on plate studies *(Tipper et al., 1999, Scholes and Unsworth, 2001)*.

The negative control produced a statistically significant rise of 40% in the surface roughness when compared with the non-tested control. This was in contrast with the uni-directional results as discussed in Chapter 6, which indicated no increase in Ra value following the 8 hour test. The increased damage demonstrated by the multi-directional negative control indicated the presence of different wear mechanisms when compared with the positive control, which showed a reduction in surface fibrillation with multi-directionality.

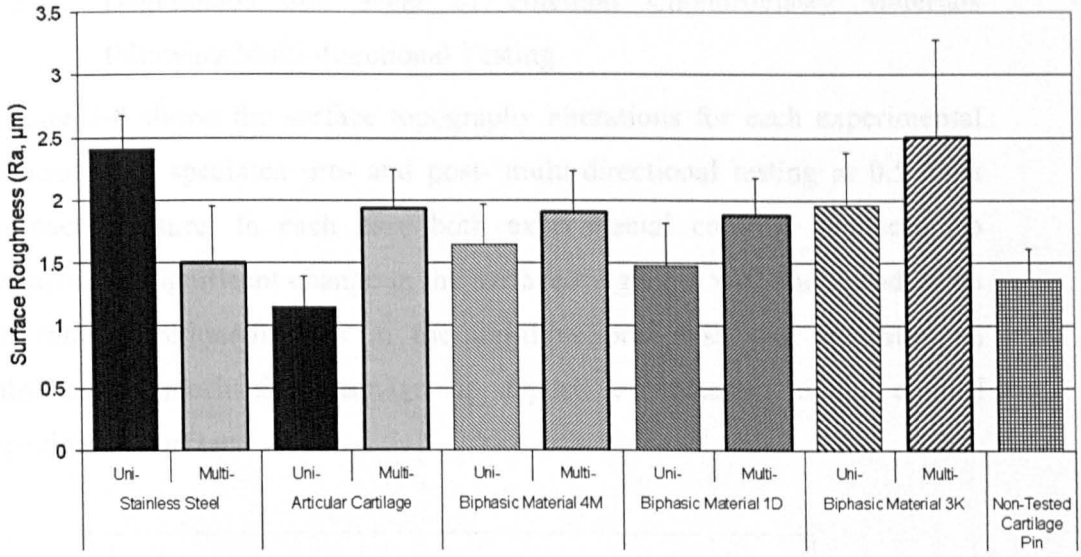

Figure 7-7: The surface roughness of articular cartilage pins following Uni-directional and Multi-directional testing at 0.5 MPa contact pressure (n=6, Error bars = 95% confidence limit)

The surface topography alterations to the articular cartilage pins after multi-directional testing against each biphasic hydrogel produced a small but not statistically significant increase in surface roughness values when compared with the uni-directional testing. When compared with the non-tested articular cartilage control, the hydrogels 4M and 1D produced no statistically significant increase in surface roughness. However, using a one-way ANOVA statistical test at 95% confidence limits, the addition of rotation produced a statistically significant increase in the surface roughness of articular cartilage when tested against biphasic material 3K.

The small increase in surface roughness exhibited by each hydrogel following multi-directional testing indicated that multi-directional motion resulted in surface damage to the articular cartilage pin as found in the negative control result. However, the percentage rise in articular cartilage pin surface roughness was far lower when tested against hydrogels (15-27%) than that shown by the articular cartilage negative control (69%).

7.3.2.2 Degradation and Wear of Potential Chondroplasty Materials following Multi-directional Testing

Figure 7-8 shows the surface topography alterations for each experimental control plate specimen pre- and post- multi-directional testing at 0.5 MPa contact pressure. In each case both experimental controls produced no statistically significant change in the surface roughness with the introduction of multi-directionality. As in the uni-directional test, this indicated an absence of mechanical damage or deposit of material to the control specimen's surface.

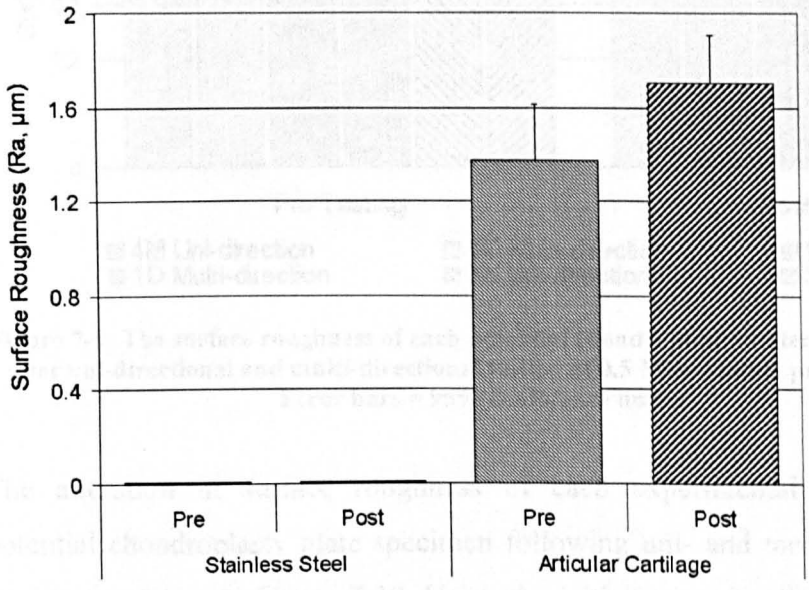

Figure 7-8: The surface roughness measurement of both experimental control plate specimens before and after Multi-directional testing at 0.5 MPa contact pressure (n=6, Error bars = 95% confidence limit)

Figure 7-9 shows the surface roughness of each potential chondroplasty material before and after uni-directional and multi-directional testing at 0.5 MPa contact pressure. In both the uni- and multi-directional studies, hydrogel materials 1D and 4M produced no statistically significant increase in surface roughness. However, in both the uni- and multi-directional studies, hydrogel material 3K produced a statistically significant rise in the average surface roughness value. It is again unlikely that this alteration in surface roughness was the result of material deposit, thus suggesting that either material loss or surface fibrillation to the material surface were the cause. This would indicate

hydrogel specimen 3K had a lower wear resistance then the other biphasic hydrogel specimens (as shown in Chapter 6).

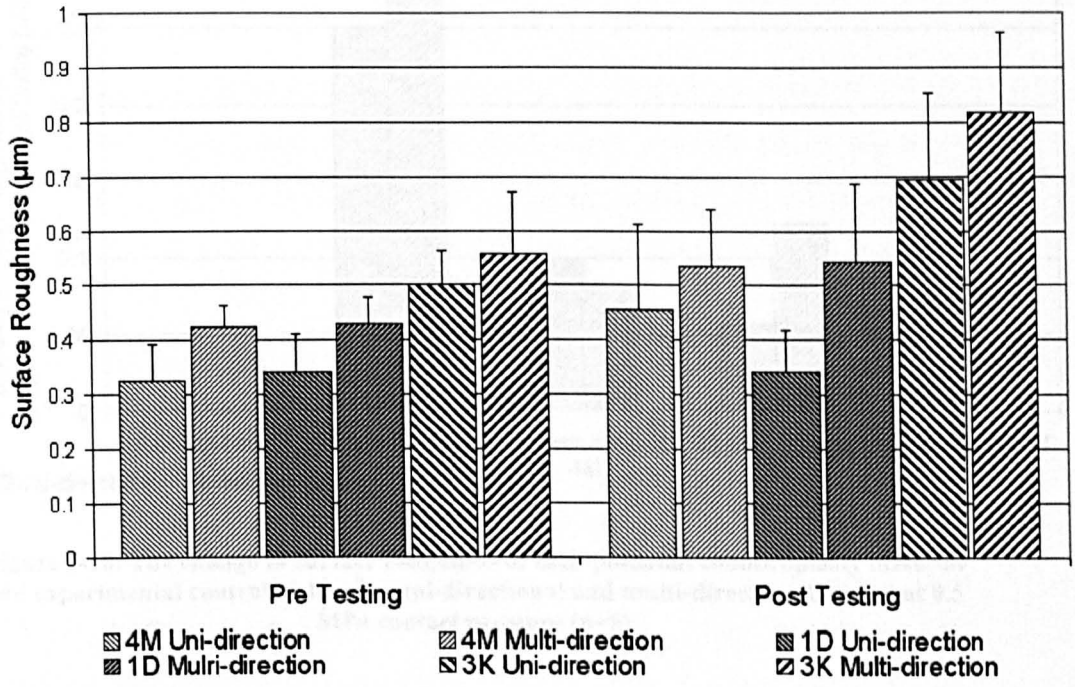

Figure 7-9: The surface roughness of each potential chondroplasty material before and after uni-directional and multi-directional testing at 0.5 MPa contact pressure (n=6, Error bars = 95% confidence limit)

The alteration in surface roughness of each experimental control and potential chondroplasty plate specimen following uni- and multi-directional testing are shown in Figure 7-10. Using the initial pre-test surface roughness measurement for each surface as the start point, the relative increase following each test is shown. The stainless steel plate (positive control) showed no change in Ra following testing. However, hydrogels 3K, 1D and the articular cartilage negative control all showed that multi-directional motion resulted in an additional increase in surface roughness when compared with uni-directional motion, indicating additional surface degradation. However, hydrogel 4M showed little or no variation in Ra between uni-directional and multi-directional motion which would indicate that hydrogel 4M processes an increased wear resistance when compared with the other hydrogels tested.

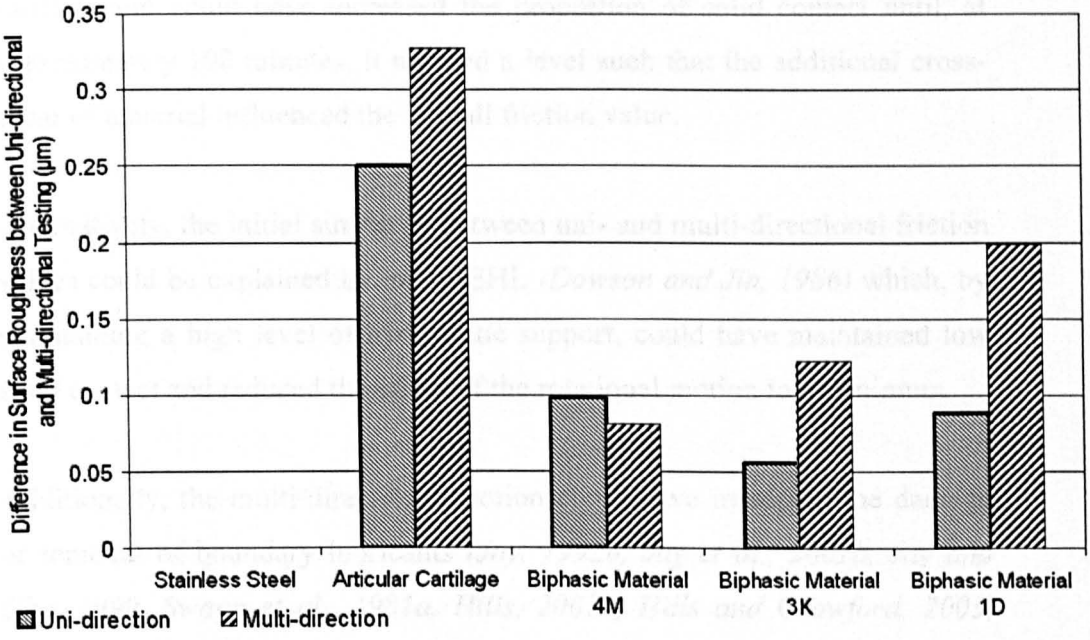

Figure 7-10: The change in surface roughness of each potential chondroplasty material and experimental controls following uni-directional and multi-directional testing at 0.5 MPa contact pressure (n=6)

7.4 Discussion

Experimental Controls

The initial friction value of 0.02 to 0.03 and the increase in dynamic friction with loading time produced by the multi-directional positive control, (Figure 7-3), was similar to that demonstrated within the 2 hour study (Chapter 4) and unidirectional study (Chapter 6). This increase again indicated the loss of the interstitial fluid load support from the cartilage pin to be a major factor *(Krishnan et al., 2004b, Forster and Fisher, 1996, Forster and Fisher, 1999, Forster et al., 1995, Pickard et al., 1998a)*. The similarity in friction rise gradient between uni- and multi-directional studies within the first hour of the positive control also indicated a high level of fluid load support at the contact zone. With a low solid contact and high material separation, rotation of one bearing surface would have little or no effect on the overall friction. However, at about 100 minutes the multi-directional motion increased the overall friction and rise gradient indicating an increased influence of the additional cross shear motion. The continued lose of interstitial fluid from the

cartilage pin could have increased the proportion of solid contact until, at approximately 100 minutes, it reached a level such that the additional cross-shear of material influenced the overall friction value.

Alternatively, the initial similarity between uni- and multi-directional friction values could be explained by micro-EHL *(Dowson and Jin, 1986)* which, by maintaining a high level of hydrostatic support, could have maintained low solid contact and reduced the effect of the rotational motion to a minimum.

Additionally, the multi-directional motion could have increased the damage or removal of boundary lubricants *(Jay, 1992b, Jay et al., 2001b, Jay and Cha, 1999, Swann et al., 1981a, Hills, 2002a, Hills and Crawford, 2003, Hills, 2000)* and/or the BSAL, *(Graindorge et al., 2005, Kobayashi et al., 1995, Kobayashi et al., 1996)* from the bearing surface, reducing their lubricating effect and increasing the overall friction. However, the continued influence of boundary lubricants does not explain the initial rise in friction over time.

The negative control produced no frictional variation when compared with the unidirectional testing discussed in Chapter 6. The negative control again demonstrated the optimum performance of interstitial fluid load support maintaining the initial low friction value for the entire 8 hours test. Again it was postulated that this low friction value was maintained by cartilage permeability and re-hydration of the interstitial fluid during unloaded periods of the cycle *(Bell et al., 2006)*.

However, as in the uni-directional test the effects of the BSAL *(Graindorge et al., 2005, Kobayashi et al., 1995, Kobayashi et al., 1996)* and boundary lubricating surface additives *(Jay et al., 2000, Jay et al., 2001a, Hills, 2000, Hills and Thomas, 1998, Foy et al., 1999, Forster, 1996, Pickard et al., 1998b, Pickard et al., 1998a, Swann et al., 1981a)* cannot be ruled out. The

contribution of boundary layer lubrication could not be assessed within this study.

Biphasic Hydrogel Materials

Multi-directional motion resulted in no statistically significant variation in friction values between the three hydrogels tested when compared with the uni-directional study, regardless of mechanical properties. This result could again be attributed to their biphasic properties maintaining a lower element of solid contact than the positive control, thus reducing the effects of rotational motion and overall friction. The initial rise in friction did again indicate a reduction in the proportion of the fluid load support. As in the uni-directional study, EHL could have contributed to the equilibrium response but the initial rise would indicate that it is not the dominant lubrication regime.

As in the unidirectional study no relationship between dynamic friction, permeability and EWC was demonstrated as all hydrogel variants produced similar friction results.

Surface roughness alterations

Within the multi-directional test, the positive control opposing surface cartilage pin model showed no increase in surface roughness despite producing the highest level of friction. The addition of rotation cross shear forces and the removal of uni-directionality at the contact zone could have resulted in compression or removal of the articular cartilage surface fibrillations caused by solid to solid contact. This 'polishing' effect could have been the result of the uniform highly polished stainless steel plate specimen acting as an ultra fine abrasive thus reducing the overall surface roughness.

Alternatively, it is possible that the higher levels of multi-directional shear and tensile stresses on the positive control removed fluid from the contact zone. This would have increased the level of non lubricating additives and

proteins on the cartilage surface and reduced the level of surface fibrillation, thus the overall surface roughness.

Additionally, the higher multi-directional shear and tensile stresses experienced by the positive control pin could have damaged the solid cartilage tissue structure. Any increased damage could have resulted in a higher level of tissue deformation under the contact pressure exerted by the contacting probe on the surface profilometer and the increased deformation could have resulted in the lower surface roughness reading.

The multi-directional negative control produced no change in friction but the opposing surface model produced a statistically significant rise in cartilage surface roughness. The multi-directional result does not support the connection shown in the uni-directional model between friction, loss of fluid load support and surface roughness increase. The increase in surface roughness demonstrated by the negative control, but not by the positive control, could be explained by the uniformity of the plate surface structure. While the stainless steel plates were polished to a surface roughness of 0.02 (±0.002) μm with no directionality, articular cartilage has been shown to process collagen fibril direction *(Bullough and Goodfellow, 1968, Meachim et al., 1974, Freeman, 1979)* and mechanical property directionality *(Lewis and McCutchen, 1959, Freeman, 1979, Buckwalter, 1983, Moss and Moss, 1983, Mow and Hayes, 1997)*. Although within this study the collagen fibril orientation of the cartilage pins was controlled, this was not the case for the plate specimens and therefore it is possible that an unnatural misalignment of cartilage structure between both contacting surfaces was present. Therefore, although the solid contact present within the negative control was lower than in the positive control resulting in the lower friction result, the rotation of the two misaligned cartilage structures could have increased the surface roughness. This misalignment in surface structure would not be present in the positive control owing the smoothness and uni-directionality of the stainless steel plate.

Alternatively, the differences within the experimental controls could have been the result of natural biological variation within the tissue, although a minimum of 6 specimens of each material were tested, the inherent variation of biological tissue could have been an additional factor.

Using a one-way ANOVA statistical test, the cartilage pins from biphasic materials 1D and 4M again showed a small but not statistically significant increase in surface roughness compared with non-tested cartilage and the uni-directional test results, thus indicating a small variation in surface damage experienced by the opposing surface model. It was again postulated that by maintaining a higher proportion of the fluid load support and the structural uniformity of the biphasic plate surface, a lower rate of opposing surface degradation was achieved.

However, as in the unidirectional study the interaction between surface additives present on the articular cartilage surface and each biphasic monomer could have had an influential role in the final roughness of the cartilage pin surface.

In the multi-directional study, 3K, 1D and the negative control plate specimens all showed a non statistically significant increase in surface roughness compared with the result of the uni-directional study. It is postulated that this additional surface degeneration was the result of the extra multi-directional shear and tensile stresses applied. Previous experimental studies performed on single phasic orthopaedic polymers against metallic plates have shown not only increased wear under multi-directional contact *(Galvin et al., 2006, Joyce, 2005)* but a linear relationship between rotation angle and polymer wear rate *(Briscoe and Stolarski, 1985)* .

Hydrogel 4M showed little or no increase in surface roughness with the addition of rotation, demonstrating an improved level of wear resistance

when compared with the other biphasic hydrogel polymers tested. Hydrogel 4M possessed a higher elastic modulus and ultimate tensile strength than the other hydrogels tested however, the chemical interactions between hydrogel 4M and the articular cartilage surface could have contributed to the lower wear rates demonstrated.

The lower permeability demonstrated by hydrogel 4M could have resulted in an increased level of fluid load support, which while not altering dynamic friction results, could have reduced the solid to solid contact and surface degradation compared with the other hydrogel variant. Alternatively, the plastic flow of the molecular structure could have increased the conformity of the material at the contact zone, reducing solid-to-solid contact and the overall increase in surface roughness.

7.5 Summary

- An experimental model was developed which allowed the appraisal of each potential chondroplasty material under more realistic motion compared with *in vivo* kinematics.

- The experimentally model was the first to be applied to and evaluate the effect of multi-directional motion on the frictional properties and surface degradation of potential chondroplasty materials and the opposing cartilage joint surface, improving predictions of potential *in vivo* performance.

- The potential of biphasic materials to reduce and maintain low friction values under multi-directional motion for extended periods was demonstrated.

- The no linear interactions between friction and surface degradation resulting from the complex lubrication and tribological regimes present with synovial joint lubrication were demonstrated.

8 Clinical Defect Repair Friction and Wear Study

8.1 Introduction

Spontaneous *in vivo* repair of chondral lesions or trauma damage is considered inadequate, retaining little or no functionality of healthy articular cartilage *(Hunziker, 2002, Robert, 2001)*. Four main techniques are currently used in the treatment of these lesions or articular cartilage damage, autologous chondrocyte implantation (ACI), microfracture, osteochondral grafts, and grafts of chondrocytes *(Hunziker, 2002, Robert, 2001)*. The implantation of both carbon-hydrate-based polymers to act as cellular scaffolds or synthetic polymers such as carbon fibre, Teflon and hydrogel polymers have offered the potential for additional clinical solutions *(Oka et al., 1990, Oka et al., 2000, Stammen et al., 2001, Hunziker, 2002)*. The *in vivo* implantation of a potential chondroplasty material as a clinical repair would result in different contact mechanics and potentially different tribological conditions from the *in vitro* model used within this study. An aim of this study was to develop the experimental model to mimic an *in vivo* clinical defect repair as closely as possible within an *in vitro* pin on plate experimental configuration. The implantation of the defect repair material within the articular cartilage plate when tested against an articular cartilage pin allowed the further development of the *in vitro* model and the continued assessment of a number of potential chondroplasty material.

The model again utilised the quantification of surface roughness as discussed in Chapter 5, and all friction tests within this chapter were completed using the simple geometry wear simulator within a mixed boundary lubrication regime as described in Chapter 2.

8.2 Experimental Methodology

8.2.1 Materials

The positive control defect repair was a Ø6mm by 10mm polished stainless steel pin (Figure 8-1) inserted into the centre position of the articular cartilage plate. The stainless steel pin bearing surface was polished to an average surface roughness value (Ra) = 0.02 (±0.003)μm. The negative control was an articular cartilage plate with no defect repair again tested against an articular cartilage pin, as described in Chapter 6.

The experimental model presented within this chapter was used to evaluate biphasic hydrogels 4M and 1D as a defect repair solution, against the experimental controls (polished stainless steel defect repair and articular cartilage plate). The defect repair consisted of Ø6 mm by 10mm hydrogel/PMMA composite pins manufactured as described in Chapter 2.2.2. Further information on each biphasic and single phasic material can be found in Chapter 2.

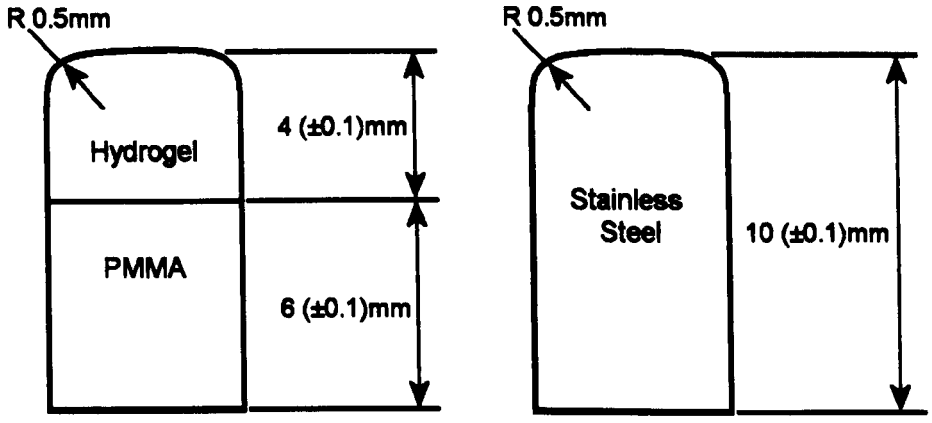

Figure 8-1: A schematic diagram showing both the hydrogel and stainless steel Ø6mm by 10mm defect repairs

8.2.2 Method

8.2.2.1 Dynamic Friction Study

During the dynamic friction study two loading protocols were used. Firstly an initial unidirectional configuration, as described in Chapter 6 was used to

investigate the frictional response at a contact pressure of 0.5 MPa. A second multi-directional configuration as described in Chapter 7, was also completed at a contact pressure of 2 MPa.

8.2.2.1.1 Experimental Positive and Negative Control

Following attachment of the articular cartilage plate to a polymethylmethacrylate (PMMA) backing plate, a Ø6.1 mm hole was drilled vertically into the centre point of the cartilage plate to a depth of 12 mm and the Ø6 mm by 10 mm defect repair inserted such that the bearing surface of the defect repair was 0.5 mm below the surrounding cartilage surface. The pin was held in place by 1g of PMMA bone cement inserted into the drilled hole before fixation of the pin. Care was taken to maintain articular cartilage hydration and surface integrity throughout the process by the application of 100% Ringer's solution every 30 seconds and a total air exposure time of 1 minute. For experimental consistency, the negative control plates without a defect repair were exposed to air at room temperature for the same time as articular cartilage plates fitted with a defect repair.

Following fixation of the defect repair, the uni-directional study controls were mounted as described in Chapter 6. In the multi-directional configuration, the multi-directional attachment was fitted and the pin holder inserted as described in Chapter 7. Again, multi-directional attachment resulted in an additional rotation of $\pm 10^{\circ}$ about the vertical axis of the cartilage pin (Figure 7-2) and again a frictional cross shear ratio of 0.01, further details of which can be found in Chapter 7 and Appendix B.

Within all experimental configurations, the specimens were positioned 1 mm apart and left for 2 minutes to re-hydrate and acclimatise. At this point, the relevant load was applied to the pin resulting in a contact pressure of either 0.5 MPa or 2 MPa. The test surfaces were loaded for 60 seconds, after which the reciprocating motion was engaged and the friction recorded every 30 seconds for 8 hours (28,800 cycles).

8.2.2.1.2 Dynamic Friction of the Defect Repair Model

Hydrogels 4M and 1D defect repairs were investigated and compared with the positive and negative controls. Each composite hydrogel/PMMA defect repair (Figure 8-1) was inserted and mounted as described for the positive control defect repair (Section 8.2.2.1.1). Six tests were completed on each variant and the setup and data acquisition protocols were as described for the experimental controls. Once completed cartilage specimens were again stored at -20°C and all other specimens were stored at +4°C, for further analysis.

8.2.2.2 Surface Degradation and Quantification of Wear

Quantification of opposing surface degradation using the surface profilometer was again used as an indication of opposing surface damage. (Further information on the method used can be found in Chapter 5.)

8.3 Results

8.3.1 Experimental Positive and Negative Dynamic Friction Controls

Within the unidirectional study at a contact pressure of 0.5 MPa, the articular cartilage pin against the stainless steel defect repair (positive control) produced a far lower frictional response when compared with the articular cartilage pin against a stainless steel plate, also shown in Figure 8-2. The defect repair produced a similar initial low level of friction but a far lower gradient of friction rise, reaching a peak friction level five times lower than that of the stainless steel plate configuration. This lower friction rise rate and final value indicated a far lower reduction in the fluid load support and lower solid contact at the contact zone. However, the stainless steel defect repair produced a progressive rise in friction and a final value higher than the negative control cartilage plate, which maintained a low constant friction level for the 8 hour test.

The lower progressive increase in friction demonstrated by the stainless defect repair indicated lower interstitial fluid loss at the contact zone than that shown by the cartilage pin on stainless steel plate configuration *(Forster and*

Fisher, 1999, Krishnan et al., 2004b, Bell et al., 2006) but greater than that demonstrated by the negative control. Over the 8 hour test, the progressive rise demonstrated by the positive control defect repair did not reach a constant value, unlike the equilibrium reached by the stainless steel plate configuration at approximately 300 minutes. This would indicate a higher level of fluid load support present after the 8 hour test.

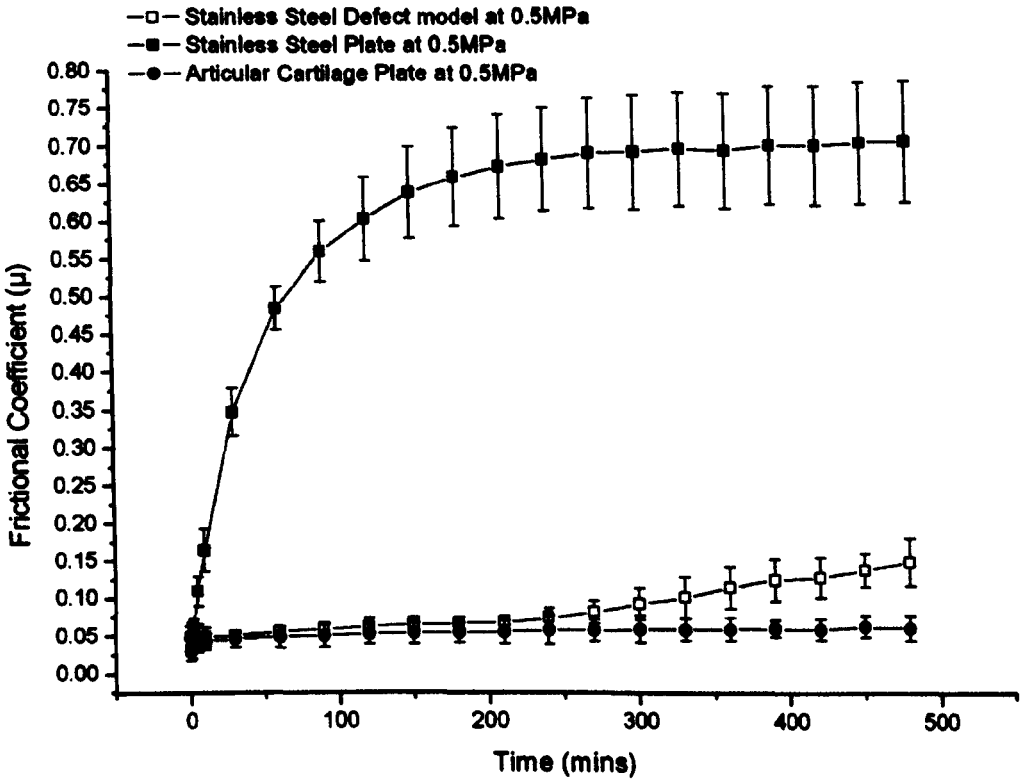

Figure 8-2: The uni-directional experimental controls friction results at a contact pressure of 0.5MPa (n=6, Error bars = 95% confidence limit)

In the 2 MPa contact pressure multidirectional friction study, the positive control defect repair and negative control produced no frictional increase (Figure 8-4). In contrast with the unidirectional configuration, the stainless steel defect repair produced a constant low level of friction which was maintained for the entire eight hour test indicating a continued high level of fluid load support and low solid to solid contact.

Using a one-way ANOVA statistical test at 95% confidence limits, the stainless steel plate against cartilage pin configuration produced no

statistically significant change in friction when compared with the 2 MPa uni-directional positive control described in Chapter 6, indicating little or no effect of multidirectional cross shear on the overall frictional response at higher contact pressures. As described in Chapter 7, this was not the case at the lower contact pressure of 0.5 MPa, which produced a statistically significant rise in friction with the addition of multi-directional motion.

8.3.2 Defect Repair Dynamic friction within a protein containing lubricant

At a contact pressure of 0.5 MPa, the implantation of hydrogels 4M (Figure 8-3) and 1D (Figure 8-4) as defect repairs produced only a small increase in dynamic friction when compared with the negative control. Hydrogel 4M produced a linear increase in dynamic friction very similar to that produced by the positive control defect repair. This similar initial friction value and dynamic frictional response when compared with the defect repair positive control indicated similar levels of fluid load support at the contact area resulting in a friction value independent of repair material. As in the positive control, the steady rise demonstrated by 4M also indicated a steady decline in fluid load support over the 8 hours thus indicating that at an increased time constant, an eventual solid to solid contact dominant regime would be reached.

Hydrogel 1D (Figure 8-4) produced a constant friction value of 0.1 demonstrating a 100% increase when compared with the negative control. The constant dynamic friction value, in contrast with that of hydrogel 4M, indicated a constant level of fluid load support at the contact zone, maintained by re-hydration and fluid pressurization of the surrounding cartilage tissue and to a lesser extent the hydrogel material. This is in contrast to the behaviour of the articular cartilage pin against a hydrogel 1D plate dynamic friction result (Figure 8-4) which demonstrated an increase in friction over the first 150 minutes reaching an equilibrium value of 0.35 ($\pm$0.02) for the remainder of the test.

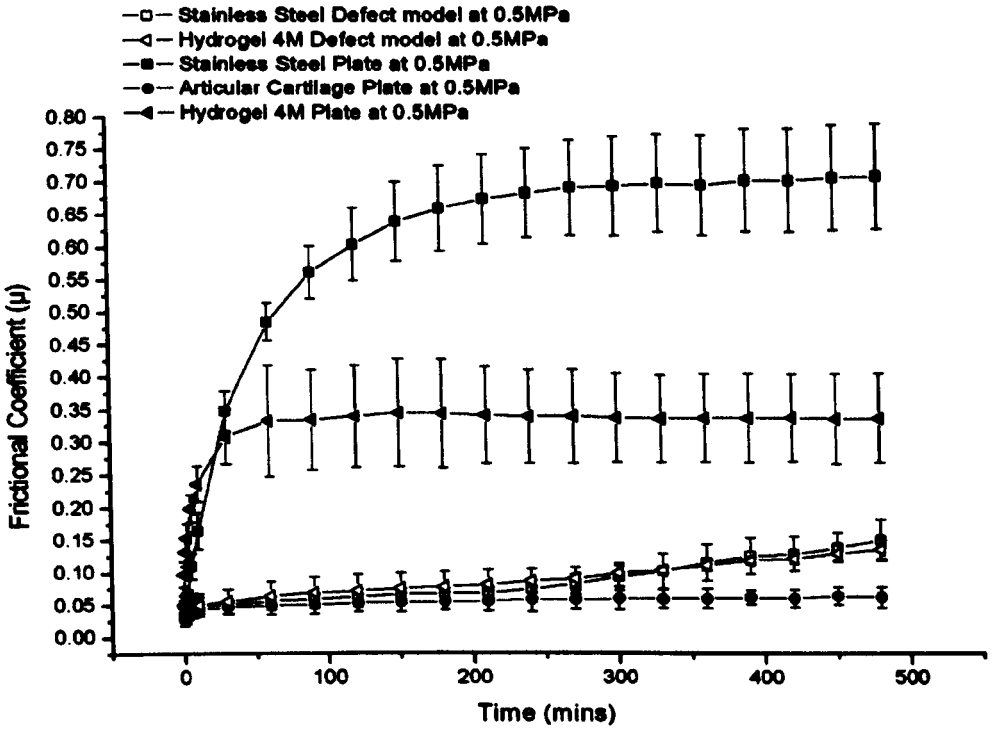

Figure 8-3: The uni-directional friction results at a contact pressure of 0.5MPa for Hydrogel 4M as a defect repair and plate specimens with experimental controls. (n=6, Error bars = 95% confidence limit)

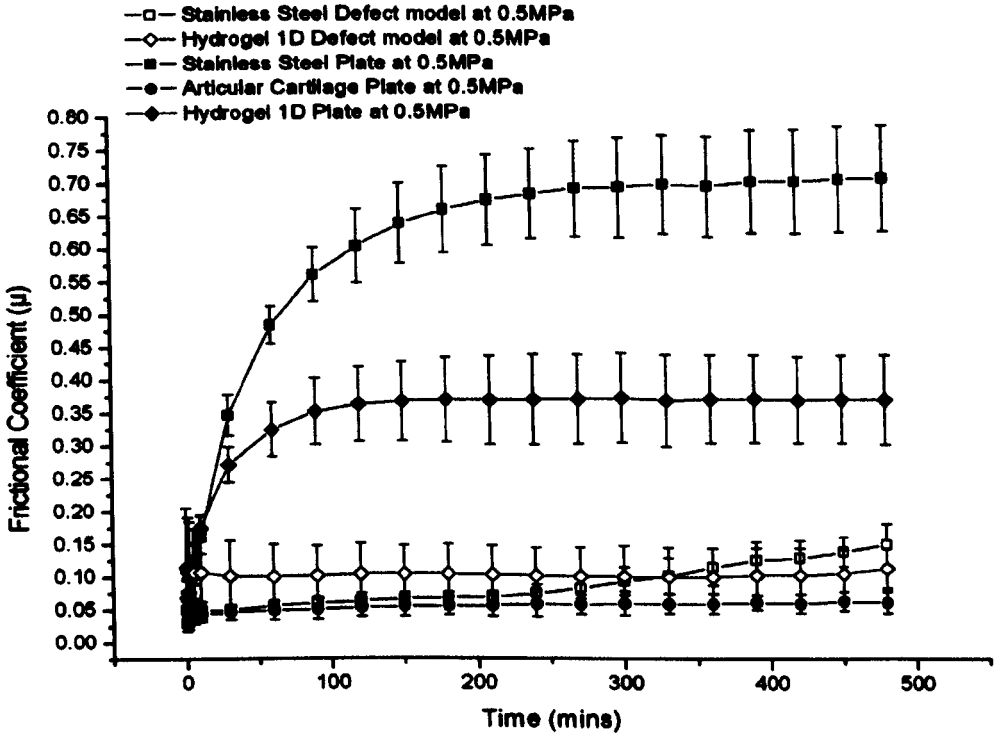

Figure 8-4: The uni-directional friction results at a contact pressure of 0.5MPa for Hydrogel 1D as a defect repair and plate specimens with experimental controls. (n=6, Error bars = 95% confidence limit)

As shown in Figure 8-5, the introduction of multidirectional motion and an increased contact pressure of 2 MPa resulted in a small increase in friction for the hydrogel 4M defect repair when compared with the negative control. Despite an initial small rise in friction over the first 50 minutes, the hydrogel 4M defect repair produced a constant value for the remainder of the test. When compared with the stainless steel positive control, hydrogel 4M produced increased variability within the dynamic friction results and a non statistically significant increase in the final value. However, the overall constant value again indicated a continued high level of interstitial load support previously demonstrated within the uni-directional defect repair test.

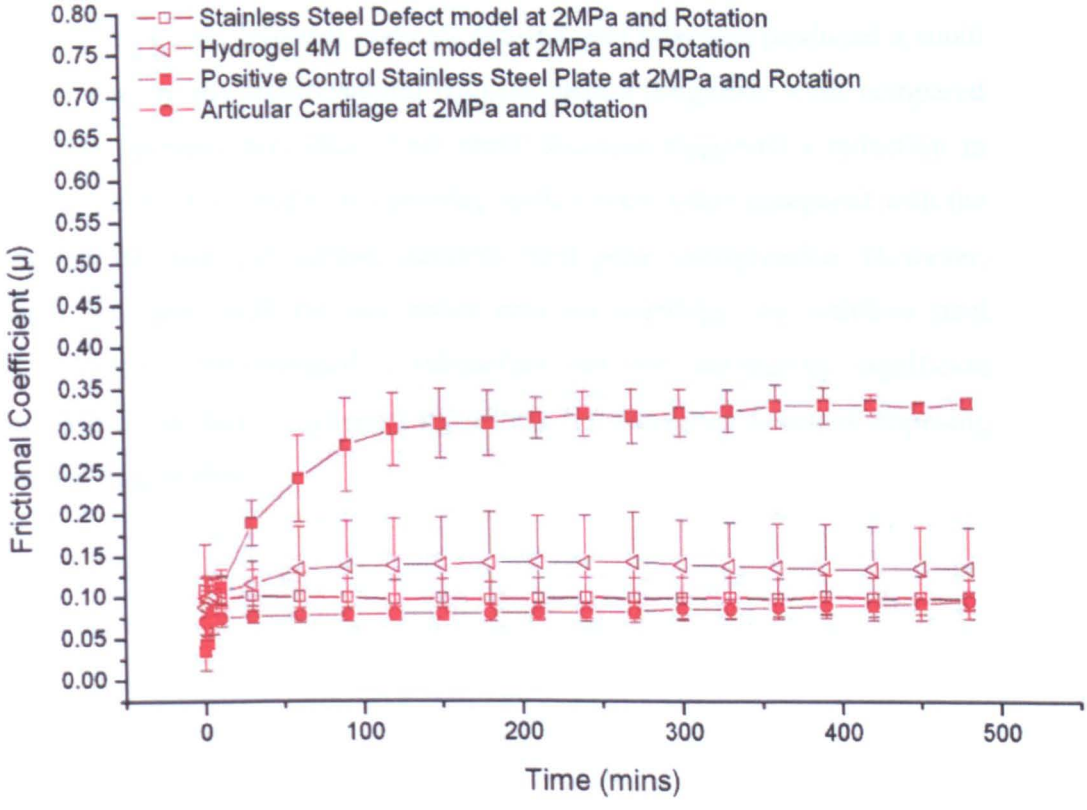

Figure 8-5: The multi-directional friction results at a contact pressure of 2MPa for Hydrogel 4M as a defect repair with experimental controls. (n=6, Error bars = 95% confidence limit)

Comparison between the uni-directional articular cartilage pin against a hydrogel 4M plate test at a contact pressure of 2 MPa, described in Chapter 6.3.2, and the 4M defect repair demonstrated that the 4M defect repair produced a non statistically significant lower final value. This indicated little

or no effect was demonstrated by the addition of multi-directionality or the change in contact geometry resulting from the defect repair experimental configuration.

8.3.3 Defect Repair Surface Degradation and Wear Results

Figure 8-6 shows the average surface roughness (Ra) measurement of each cartilage pin following the uni-directional dynamic friction tests at 0.5 MPa contact pressure. As described in Chapter 6, the uni-directional stainless steel plate produced a statistically significant increase of 75% in the Ra surface roughness value when compared with none-tested articular cartilage, indicating an increased level of surface degradation and wear.

The stainless steel (positive control) defect repair however produced a small but not statistically significant reduction in surface roughness when compared with the stainless steel plate. This small decrease suggested a reduction in surface degradation and thus opposing surface wear when compared with the articular cartilage pin against stainless steel plate configuration. However, when compared with the non-tested articular cartilage, the stainless steel defect repair demonstrated a substantial but not statistically significant increase in surface roughness suggesting an increased level of opposing surface degradation.

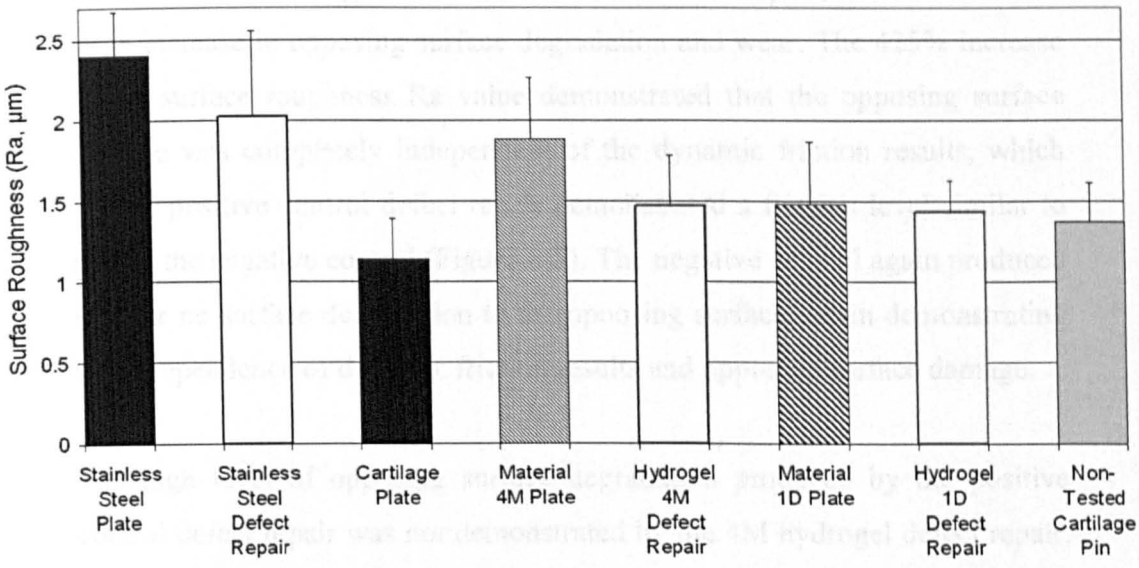

Figure 8-6: The surface roughness variation of cartilage pin following tested unidirectional testing at 0.5MPa (n=6, Error bars = 95% confidence limit)

Again as shown in Chapter 6, the articular cartilage pins tested against articular cartilage plate (negative control) showed no statistically significant difference in surface roughness when compared with the untested articular cartilage pins, demonstrating no variation in the opposing surface structure and again indicating an increased level of fluid load support.

Unlike the stainless steel defect repair, hydrogel 4M and 1D defect repairs produced no variation in opposing surface roughness when compared with non-tested articular cartilage, indicating little or no surface degradation resulting from the defect repair. Compared with the hydrogel 4M plate, the hydrogel 4M defect repair produced a small but not statistically significant reduction in Ra value (Figure 8-6), suggesting a reduced level of surface degradation if the material is used as a clinical implant. Hydrogel 1D produced little or no variation in opposing surface roughness when compared with the cartilage pin on hydrogel 1D plate configuration (Figure 8-6), again indicating little or no effect on opposing surface wear.

The introduction of multidirectional motion and increased contact pressure (Figure 8-7) resulted in a large surface roughness increase for the opposing

surface when tested against the stainless steel defect repair, which indicated a large increase in opposing surface degradation and wear. The 425% increase in the surface roughness Ra value demonstrated that the opposing surface damage was completely independent of the dynamic friction results, which for the positive control defect repair demonstrated a friction level similar to that of the negative control (Figure 8-5). The negative control again produced little or no surface degradation to the opposing surface, again demonstrating the independence of dynamic friction results and opposing surface damage.

The high level of opposing surface degradation produced by the positive control defect repair was not demonstrated by the 4M hydrogel defect repair, which produced an opposing surface roughness similar to that demonstrated by the hydrogel 4M plate, within the unidirectional 2 MPa contact pressure configuration (Figure 6-10) and the multidirectional 0.5 MPa contact pressure configuration (Figure 7-7). The combination of multi-directionality and increased contact pressure produced only a small but not statistical significant increase in surface roughness when compared with the non-tested cartilage specimens. Again independent of dynamic friction results, the hydrogel 4M defect repair demonstrated a reduced level of opposing surface degradation compared with the positive control stainless steel defect repair.

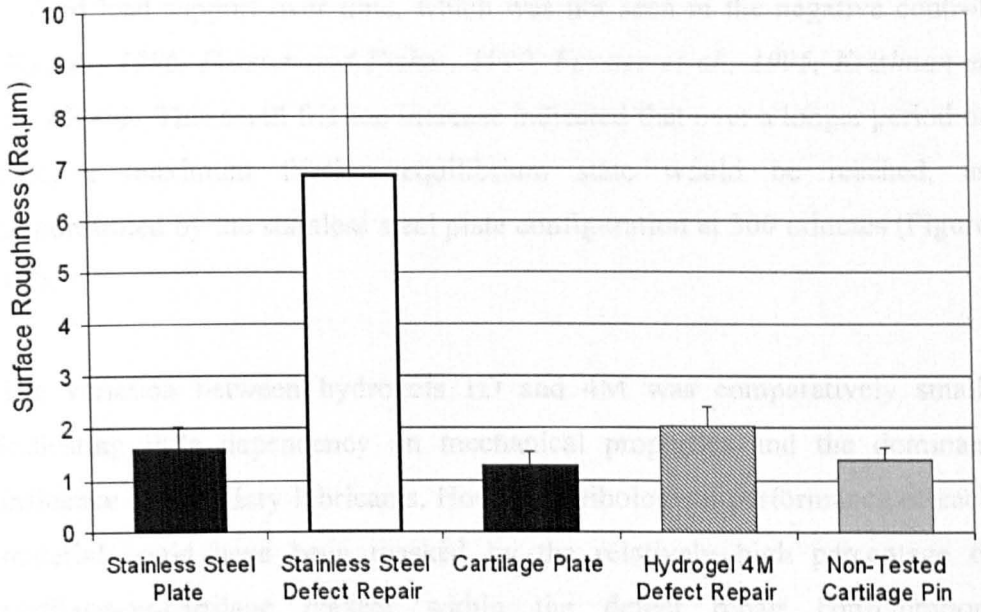

Figure 8-7: The surface roughness variation of cartilage pin following tested multidirectional testing at 2MPa (n=6, Error bars = 95% confidence limit)

8.4 Discussion

Dynamic friction

The variation in experimental contact geometry resulting from defect repair implantation produced a large variation in the dynamic friction results, as compared with the previous cartilage pin against plate configuration (shown in chapter 4, 6 and 7). The 10 mm diameter cartilage pin reciprocating over the centrally located Ø6 mm defect repair meant that the percentage area of the cartilage pin in continued contact with the articular cartilage material of the plate, and not the defect repair, influenced the dynamic friction response. This cartilage-on-cartilage contact, as demonstrated in the negative control, produced higher levels of fluid pressurisation, re-hydration and interstitial fluid load support compared with the articular cartilage pin on a plate configurations, thus producing a far lower level of dynamic friction *(Forster and Fisher, 1999, Krishnan et al., 2004b, Bell et al., 2006).*

Although less than that demonstrated by the stainless steel plate configuration, the small rise in dynamic friction demonstrated by the positive control defect repair over the 8 hour test would indicate a continued reduction

in fluid load support over time, which was not seen in the negative control *(Forster, 1996, Forster and Fisher, 1999, Forster et al., 1995, Krishnan et al., 2004b)*. This small friction increase indicated that over a longer period of time, a maximum friction equilibrium state would be reached, as demonstrated by the stainless steel plate configuration at 300 minutes (Figure 8-2).

The variation between hydrogels 1D and 4M was comparatively small, indicating little dependency on mechanical properties and the dominant influence of boundary lubricants. However, tribological performance of each material could have been masked by the relatively high percentage of cartilage-on-cartilage present within the defect repair configuration. Therefore, the small variation in dynamic friction rise could have been caused by the difference in mechanical properties. The higher permeability of 1D, as discussed in Chapter 3, compared with 4M would suggest a lower level of internal fluid pressurisation and fluid load support within the hydrogel structure. This could have increased the level of solid to solid contact and boundary lubrication, thus resulting in the higher initial value being maintained for the remainder of the test. In contrast, the lower permeability of 4M could have produced an increased level of initial fluid load support, which resulted in the low initial friction value and the progressive friction rise seen, as the fluid load support declined over the 8 hours test *(Forster and Fisher, 1999, Krishnan et al., 2004b)*.

Alternatively, the increased viscoelastic behaviour of 4M compared with 1D could have resulted in an increased level of plastic deformation and hydrogel molecular flow as the opposing cartilage pin traversed over the defect repair. This increased level of deformation could have reduced the level of resistance between the hydrogel defect repair and opposing surface reducing the friction coefficient. However, this would not explain the similar initial friction values and gradient rise demonstrated by the positive control and 4M defect repairs.

The introduction of multi-directionality and increased contact pressure resulted in no statistically significant variation in the final dynamic friction value, for either the positive control or the hydrogel 4M defect repair models. However, unlike the unidirectional low contact pressure configuration, no progressive friction rise was demonstrated, indicating the continued maintenance of fluid load support through fluid pressurisation and re-hydration as demonstrated by the negative control *(Forster, 1996, Forster and Fisher, 1999, Forster et al., 1995, Krishnan et al., 2004b).*

Additionally, the increased contact pressure could have resulted in a higher percentage of surface deformation, resulting in a lower overall surface roughness. This reduced surface roughness could have increased the percentage of fluid film lubrication with the overall mixed lubrication regime, reducing the overall friction coefficient *(Hutchings, 1992).*

Alternatively, the constant friction value demonstrated by both experimental controls and the hydrogel 4M defect repair also could have indicated the increased influence of boundary lubricants. The higher contact pressure and multi-directional motion could have increased the percentage of boundary lubrication within the contact zone through fluid expulsion and increased boundary lubricant infusion, from the cartilage surfaces into the contact zone. This increase in surface additives *(Hills, 2000, Jay and Cha, 1999, Swann et al., 1981b, Jay, 1992b, Jay et al., 2001a, Bell et al., 2006)* or higher levels of surface amorphous layer contact *(Kobayashi et al., 1995, Kobayashi et al., 1996, Graindorge et al., 2005)* resulting from the increased cartilage on cartilage contact, could have maintained an influential level of boundary lubrication and thus maintained a constant dynamic friction level over the 8 hour test.

At 2 MPa contact pressure, the introduction of multidirectional motion within the cartilage pin against stainless steel plate configuration produced no dynamic friction variation, again producing a progressive rise until an

equilibrium friction level was reached at approximately 150 minutes into the test. This is in contrast to the application of rotation at the lower contact pressure of 0.5 MPa which demonstrated a statistically significant increase in friction when compared with the unidirectional configuration (Figure 7-3). As previously discussed, the increased contact pressure could have resulted in higher levels of fluid pressurisation, surface deformation or boundary lubrication, all of which could have influenced the dynamic friction result.

Surface damage and wear of the opposing surface model

As reported in Chapter 6 and 7, the negative control regardless of contact pressure or directional motion, showed no alteration in surface roughness compared with non tested articular cartilage, indicating no surface degradation and demonstrating the optimum bearing response.

As discussed in Chapter 6, the cartilage pin on stainless steel plate configuration demonstrated a statistically significant increase in surface roughness demonstrating increased levels of degradation and surface wear, resulting from increase levels of solid to solid contact *(Stachowiak et al., 1994, Forster and Fisher, 1999, Graindorge and Stachowiak, 2000)*. At a contact pressure 0.5 MPa the positive control defect repair produced a non-significant rise in surface roughness when compared with the non-tested articular cartilage, indicating increased levels of opposing surface degradation and wear. However, this result demonstrated no connection with dynamic friction results as the positive control defect repair demonstrated similar dynamic friction results to both hydrogel defect repairs.

At both contact pressures, each hydrogel defect repair produced no variation in surface roughness of the opposing cartilage surface, indicating no opposing surface degradation or wear. As demonstrated within the cartilage pin on hydrogel plate configuration (Chapter 6), when compared with the positive control this would indicate a higher level of fluid load support reducing the level of solid to solid contact and thus the degradation and wear of the

opposing surface. However, the similar dynamic friction results shown by both the experimental controls and hydrogel defect repairs was in contrast to the large variation in opposing surface degradation demonstrated at the higher contact pressure, indicating the presence of further wear mechanisms.

It is postulated that the fundamental mechanical properties of the stainless steel pin increased the level of opposing surface wear. Care was taken to implant the defect repair below the surface of the cartilage plate. However, owing to the different mechanical properties of stainless steel and articular cartilage, under loading the articular cartilage would deform to a greater extent than the stainless steel pin, resulting in the top surface of the defect repair becoming proud of the surrounding cartilage tissue. This change in geometry would result in increased levels of abrasive wear as the harder stainless steel material contacted the opposing articular cartilage surface. This was demonstrated to a greater extent at the higher contact pressure resulting in a large statistically significant increase in opposing surface wear when compared with the viscoelastic softer hydrogel material.

The increased level of plastic deformation present within the hydrogel defect repair could also have contributed to the lower opposing surface degradation. Under loading, the viscoelastic molecular flow of hydrogel 4M and to a less extent hydrogel 1D (Chapter 3) could have resulted in a smoother bearing surface reducing the level of solid contact with the opposing cartilage surface. The smoother surface and increase plasticity could have reduced solid to solid contact and thus abrasive wear of the opposing articular cartilage surface.

The interaction between the boundary layer lubricants *(Hills, 2000, Jay and Cha, 1999, Swann et al., 1981b, Jay, 1992b, Jay et al., 2001a, Bell et al., 2006)* and the individual materials used as the defect repair was not quantified within this study. The porous hydrogel defect repair could have

absorbed or interacted with the boundary layer lubricants reducing the potential for opposing cartilage surface degradation.

8.5 Summary

- An experimental model which evaluated the tribological performance of each potential chondroplasty material and related opposing surface wear within a proposed clinical defect repair, was demonstrated for the first time.

- Independence between the dynamic friction response of a potential chondroplasty material and opposing cartilage surface degradation was demonstrated.

- The benefits of using viscoelastic phasic materials such as Hydrogel 4M to reduce opposing surface degradation was demonstrated.

9 Final Discussion and Conclusion

9.1 Key Objectives

The development of multi-disciplined *in vitro* cartilage friction and wear models and the development of novel clinical solutions for articular cartilage defect repair will increase availability and efficacy of solutions within the clinical community and improve patient care. The key objectives of the study were threefold, to design and develop an *in vitro* evaluation protocol, which would allow the objective assessment of natural joint lubrication within a mixed lubrication regime and potential chondroplasty materials. The study also aimed to characterise and evaluate a number of potential chondroplasty materials. Thirdly, the study aimed to objectively assess the tribological performance of a number of potential chondroplasty materials and their impact on the opposing joint surface.

9.2 Selection of Hydrogel Material

In this study, the mechanical properties of a range of hydrogel materials were objectively quantified and evaluated. The results revealed a range of fundamental mechanical properties which as discussed in previous literature are dependent on factors such as method of preparation, type of cross-linking agent and hydration medium *(Corkhill et al., 1990a, Peppas, 2004)*. Evaluation of mechanical properties under various loading protocols demonstrated time dependent mechanical properties, which as postulated in Chapter 3, were the effect of fluid pressurisation and fluid dissipation through the structure. By producing a high ultimate tensile strength, high aggregate modulus, low permeability and a biphasic response, hydrogels such as 4M demonstrated a range of suitable mechanical properties indicating both a viable solid structure and the internal fluid pressurisation required by a potential chondroplasty material. Additionally, survival of the material following long term testing at contact pressures found *in vivo* also indicated the potential of hydrogel 4M for this purpose.

Under both uni-directional and multi-directional testing, all biphasic hydrogels demonstrated reduced dynamic friction and opposing surface degradation compared with single phasic controls, indicating an increased level of fluid pressurisation and reduced solid to solid contact. No relationship could be discerned between the type of monomer and cross-linking agent used and the tribological performance. Hydrogels such as 4M, which processed high elastic modulus and ultimate tensile strength values demonstrated strong solid structure which as in articular cartilage would allow high levels of internal fluid pressurisation without failure of the solid structure. Hydrogel 4M also possessed an experimentally-derived permeability value similar to that of natural articular cartilage. This low permeability value indicated the potential for pressurisation of the internal fluid under loading, maintaining a high level of fluid load support and a biphasic response.

However, 4M processed an EWC of 14% net weight, 6 times lower than that of natural articular cartilage. Although the proportion of 'free' water was not quantified, the relatively small percentage of water does raise questions regarding the role of biphasic lubrication. Alternatively, the viscous or loss modulus of the hydrogel material could have determined the tribological response observed. As discussed in Chapter 3, the realignment of the molecular structure and highly viscous behaviour of some hydrated hydrogel materials, regardless of the fluid load support, could have resulted in a 'biphasic like' response, independent of free water content. During the friction and degradation studies, this viscoelastic behaviour could have increased surface conformity at the contact zone resulting in a higher proportion of EHL and micro-EHL *(Hamrock and Dowson, 1978, Dowson and Jin, 1986)* assisting the natural lubricating properties of the opposing articular cartilage surface. As discussed in previous chapters, the chemical interaction between the opposing cartilage surface and each hydrogel could not be quantified. Naturally occurring boundary lubricants interacting with

the hydrogel surface could have contributed significantly to the tribological performance. These interactions should be investigated in future work.

9.3 Cartilage lubrication and tribology

In this present work, the experimental model of biphasic theory and loss of interstitial fluid load support first demonstrated by Forster et al *(Forster and Fisher, 1996, Forster et al., 1995)* has been further developed. The presented friction and degradation model provided reliable friction data for a cartilage pin against a number of single and biphasic materials under *in vivo* loading, time and multi-directional motion. The reduced rate of increase and final dynamic friction values demonstrated by biphasic hydrogel materials when compared with single phasic materials, plus the repeatability of the friction traces following re-hydration, demonstrated the influence of interstitial fluid load support over time. The ability of the cartilage plate to maintain a low dynamic friction value over 8 hours was also demonstrated by the evaluation of a stainless steel pin against a cartilage plate, which maintained similar dynamic friction values compared with the cartilage against cartilage negative control. This demonstrated that the plate was able to maintain the fluid load support for up to eight hours, through low internal permeability resulting in internal fluid pressurisation and re-hydration of the interstitial fluid.

The incorporation into the test medium of 25% bovine serum with a protein concentration similar to that of natural synovial fluid *(Wang et al., 1997)* gave an *in vitro* experimental model, with lubrication more similar to that of the natural synovial joint. The use of a protein-containing lubricant increased the final dynamic friction by between 2% and 26%, with single phasic materials demonstrating the greatest rise. This rise in dynamic friction within the cartilage single phasic material interface would indicate that the combination of increased solid contact and protein chains within the lubricant resulted in the higher friction value observed.

The eight hour wear model developed within this study was the first to demonstrate the loss of interstitial fluid and the increased influence of boundary lubrication until an equilibrium was reached between each potential chondroplasty replacement material and articular cartilage. The large variation in dynamic friction values following this equilibrium suggested the importance of permeability and re-hydration of interstitial fluid within the potential chondroplasty material. Additionally, the extended model using contact pressures found *in vivo* created more realistic *in vitro* conditions with which to evaluate the resultant dynamic friction and degradation of the tribological system. Natural articular cartilage demonstrated the optimum response by maintaining a high level of fluid load support through internal fluid pressurisation and fluid re-hydration. A number of hydrogels indicated the potential to maintain a higher proportion of natural biphasic lubrication *in vivo* through internal fluid pressurisation and reduced solid contact at the contact zone when compared to single phasic polymers. However, as discussed previously, the influence of viscoelastic properties and boundary lubricant interactions within articular cartilage need to be investigated further before final conclusions can be made regarding the dominant lubrication regime present.

At the extended time periods and contact pressures investigated in this study, the model would suggest that natural joint lubrication maintains a low dynamic friction value. Although static friction has been demonstrated to produce higher friction values *(Pickard et al., 2000, Bell et al., 2006)*. These fall instantaneously following relative motion of one or both articulating surfaces. Therefore high friction values found in arthritic synovial joints are likely to be the result of one or more factors including;

a) Fundamental cartilage fatigue following sustained loading at undetermined rates and levels.
b) Biochemical alterations within the tissue (e.g. loss of natural boundary lubricants or proteoglycans)

c) Trauma damage resulting in failure of the cartilage matrix or the increased onset of factors a or b.

The experimental loading protocol used in this series of studies was harsh when compared with physiological loading regimes. The oscillation of only one surface and the unnatural geometry of the cartilage pin increased surface area and fluid exudation away from the contact zone, which in turn increased the dynamic friction values compared with synovial joints. However, complete joint studies would not have allowed the systematic evaluation of dynamic friction and tribological properties of various materials. The clinical defect model using a protein-rich lubricant, multi-directional motion and extended evaluation time was considered most likely to mimic the situation where a defect repair material is inserted into a synovial joint. The model clearly showed that the dynamic friction of the implant material was unrelated to the degradation experienced by the opposing articular cartilage surface. It is vital that this interdependence between friction and degradation is evaluated in the development of artificial articular cartilage materials as in the majority of previous studies, friction and wear were evaluated independently *(Freeman et al., 2000, Caravia et al., 1995, Katta et al., 2004, Bavaresco et al., 2004, Stammen et al., 2001).*

However, it should be noted that the presented model did possess a number of limitations, including the geometry of the pin on plate configuration, continual loading of pin and a lack of metabolic activity within the articular cartilage. Also bovine serum, used as the lubricant, possesses different rheology and lubricating properties compared with synovial fluid *(Schmidt and Sah, 2006, Cooke et al., 1978).* Additionally, the model used healthy bovine articular cartilage instead of arthritic or damaged human articular cartilage. Although previous literature has stated that bovine and human cartilage are of similar thickness and chemical composition, and possess similar mechanical and physiological properties, *(Athanasiou et al., 1991)* variation in the materials could have influenced the results.

9.4 Surface Degradation and Wear

As discussed in Chapter 5, in order to satisfactorily assess the tribological performance of a potential chondroplasty material, quantification of wear on both of the bearing surfaces was necessary. This study evaluated and optimised a number of techniques using alterations in surface topography of both contacting surfaces as an indication of wear. Surface profilometry was used to measure loss of material and alterations to both surfaces at the contact zone. It was found that direct contact of the surface profilometer produced no damage to the surface of either articular cartilage or the hydrogels tested and confirmed previous reports that the use of direct contact surface profilometer is a suitable technique for the quantification of soft tissue surface topography *(Sayles et al., 1979).*

It must be pointed out, however, that surface topography measurements cannot provide a complete picture of material wear. Measurements of a single parameter such as surface roughness cannot provide a comprehensive picture of the complex chemical and biological interactions resulting from the wear of a natural tissue, nor does it allow the prediction of material failure such as that demonstrated by hydrogel 3K (Figure 6-7). The use of surface profilometry was however a useful indicator of wear which for the first time allowed objective comparisons to be made between different materials and, equally importantly as shown in chapter 8, the assessment of these materials within a purposed clinical chondroplasty solution. Additionally, the results demonstrated that evaluation of frictional properties alone is not a reliable guide to the wear characteristics of any tribological system. In the clinical defect model both stainless steel and hydrogel 4M produced similar dynamic frictional responses but large variations in opposing surface wear, predicting significant differences between the performance of the two materials *in vivo.*

The series of unidirectional dynamic friction studies presented supported biphasic theory and the predictable relationship between equilibrium dynamic friction, interstitial fluid pressurization and re-hydration which reduces

surface to surface contact and material degradation at the contact zone *(Mow et al., 1980a, Forster and Fisher, 1999, Krishnan et al., 2005)*. The introduction of multi-directional contact demonstrated similar dynamic frictional results but the surface degradation of each experimental control material did not conform to the predictable relationships demonstrated in the unidirectional model. This suggested alternative or additional tribological mechanisms are present within the multi-directional contact model.

9.5 Hydrogels as Potential Chondroplasty Materials

The use of hydrogels or elastic polymers as articular cartilage replacement has been an area of research for many years *(Bavaresco et al., 2000, Freeman et al., 2000, Oka et al., 1990, Medley, 1980, Corkhill et al., 1990a)*. However, this study was the first to objectively assess the fundamental mechanical properties of a large number of potential chondroplasty materials and evaluate and quantify their tribological performance against natural articular cartilage within both non-clinical and purposed clinical solutions. The results demonstrated the potential of hydrogel materials to replicate natural biphasic lubrication to a considerable extent, and to reduce opposing joint damage. When used as a defect repair material a number of viscoelastic biphasic hydrogel materials demonstrated similar low levels of dynamic friction and opposing surface degradation to that of the natural articular cartilage control.

The large variation in opposing surface degradation within the defect model also demonstrated the importance of matching the mechanical properties of the implant material and those of natural articular cartilage. The viscoelastic and elastic properties of hydrogel 4M increased the level of compliance between the contacting surfaces and reduced degradation from edge effects as the opposing articular surface oscillated over the defect repair, when compared with the stainless steel defect repair. The implantation of a material which is compatible with articular cartilage and complements not only the natural lubrication regimes but also conformity and stress distribution is vital for the long term clinical success of a chondroplasty material.

Using the results of this study as a foundation, further work is required to optimise the mechanical properties of hydrogel materials such that natural articular cartilage is replicated as closely as possible. In order to develop an ideal product for clinical use a number of key areas require future investigation, these include;

a) Long term durability of the implant material under regular cyclic loading.
b) The effect of implant size variation.
c) Possible calcification of the implant material.
d) The immunogenic activity resulting from both the implant and the resultant wear particles.

9.6 Final Conclusions

The major findings of this research project are;

Further evidence was obtained demonstrating fluid load support resulting from 'biphasic lubrication' *(Mow et al., 1980a, Forster and Fisher, 1996, Forster and Fisher, 1999)* as the major lubrication regime present within natural joint lubrication.

The renewal of low friction values following unloaded re-hydration, independent of the plate material, demonstrated re-hydration of the interstitial fluid as the dominant factor in dynamic friction values.

The consistently lower dynamic friction values produced by either a cartilage or hydrogel biphasic plate demonstrated the ability of a biphasic material to maintain fluid load support through low permeability and re-hydration of the interstitial fluid.

The potential of biphasic hydrogels as a chondroplasty material was demonstrated through both tribological and mechanical testing.

The continued reduction in dynamic friction and surface degradation resistance demonstrated compatibility between articular cartilage and certain hydrogels following implantation as a defect repair.

This study demonstrated that the degradation of the opposing surface, and thus the long term clinical success of any chondroplasty material, depends on not just dynamic friction results but compatibility of tribological and mechanical properties.

Appendices

Appendix A

A Lubrication Film Thickness Predictions

Film thickness was calculated in two stages. Section A.i defined the fundamental interactions and geometry of two deformable materials, allowing definition of all the parameters required to calculate the minimum film thickness. Section A.ii completes the necessary calculations required to model the minimum film thickness (h_{min}) using Hertzian contact analysis *(Hertz, 1890, Hutchings, 1992)*. The minimum film thickness could then be compared to the combined surface roughness of each tribological system to define the lubrication regime present. Where appropriate the initial parameter values used within the calculations were consistence with previous studies.

A.i Combined Radius and Elastic Modulus Calculations

A.i.i Combined Elastic Modulus Calculations

Elastic modulus (E) of each material was determined as the gradient of the stress verses strain curve within the linear elastic region, up to the yield point. Each stress verses strain curve was produced from the dimensions, load and displacement quantified during the uniaxial tensile test, further information of which can be found in Chapter 3. An average of three specimens was used to calculate the final elastic modulus value. Poisson Ratio was assumed to be -0.5 giving the worst case situation. The maximum and minimum elastic modulus from the range of hydrogels under investigation were used to represent the maximum variation in elastic contact. Within the current literature study values for the elastic modulus and Poisson's ratio of articular cartilage are extensive, with stated elastic modulus values ranging from 5 to 20MPa. The in-homogeneity of cartilage has also caused a range of published Poisson's Ratio values within the literature from -0.3 to -0.5. It was deemed appropriate to used a figure of 10MPa for the elastic modulus and a Poisson's ratio of -0.4 *(Freeman, 1979)* within the initial calculations. The combined Elastic Modulus (E′) range was calculated using Equation A-i. Experimental

constants and the resultant range of values achieved can be seen in Tables A-i and A-ii respectively.

$$1/E' = \frac{(1-\upsilon_1^2)}{E_1} + \frac{(1-\upsilon_2^2)}{E_2} \qquad \text{(A-i)}$$

Combined Elastic Modulus =E'. E1,E2 = Minimum and Maximum Elastic Modulus of each material under investigation (MPa). υ1,υ2= Minimum and Maximum Poisson's Ratio of each material under investigation.

Hydrogel Parameters used	Values	
	Minimum Value	Maximum Value
Hydrogel Elastic Modulus Range - (E_1) (MPa)	0.95	140.67
Hydrogel Poisson Ratio Range - (υ_1)	-0.5	-0.5
Parameters for Articular Cartilage	**Values**	
Elastic Modulus value (E_2) (MPa)	10	
Poisson Ratio value (υ_2)	-0.4	

Table A-i: Input values used within the Elastic Modulus Calculations

	Minimum Value	Maximum Value
Combined Elastic Modulus Range (MPa)	1.14	11.19

TableA-ii: Results of the Combined Elastic Modulus Calculation

A.i.ii Combined Radius Calculations

As part of this study the surface topography for each pin or plate specimen was recorded using surface profilometry (Rank-Taylor-Hobson, Leicester, UK), more detail of the process can be found in Chapter 2 and 5. As part of the surface quantification process, the surface profilometer can calculate the concave or convex radius of each specimen. The radius of a random set of plate samples (n=20) were recorded and an average radius value for the hydrogel plate specimens was derived. An identical process was used on a random sample (n=10) of bovine cartilage pins. Bovine cartilage pins (R_{pin})

produced a convex radius averaging 85mm. Hydrogel specimens produced an average radius of 500mm with 9 concave and 11 convex. Owing to the variation in geometry and far higher value when compared with the R_{pin} value, it was deemed appropriate to define the hydrogel radius (R_{plate}) as a plate with an infinite radius. The combined radius ($R_{combined}$) could now be calculated from the equation A-ii and is shown in table A-iii.

$$1/R_{Combined} = 1/R_{pin} + 1/R_{Plate}$$
$$1/R_{Combined} = 1/R_{pin} \qquad \text{(A-ii)}$$

Combined radius = $R_{combined}$. R_{plate} = infinity, therefore $R_{combined} = R_{pin}$

	Value
Combined Radius ($R_{combined}$) (m)	0.085

Table A-iii: Table showing the combined Radius value

A.ii Static and Dynamic Fluid Film Thickness Calculations

It is now possible to calculate the static and dynamic fluid film thicknesses.

A.ii.i Static Fluid Film Thickness Calculations

To model the static film thickness of the cartilage pin normal to the plate specimen, smooth surfaces were assumed and Equation A-iii *(Dowson et al., 1991)* was used.

$$h_S = a^2\sqrt{\frac{3\pi\eta}{4Wt}} \qquad \text{(A-iii)}$$

h_S= Squeeze film thickness, a = contact area radius (m), W = load (N), η = Viscosity of 100% Ringers Solution and t = Squeeze film time

A.ii.ii Dynamic Fluid film thickness Calculations

To model the fluid film thickness during dynamic motion, the standard Elasto-hydrodynamic (EHL) Lubrication formula was used *(Hamrock and Dowson, 1978)*, this can be seen in Equation A-iv.

$$\frac{h_D}{R_{combined}} = 2.789\left(\frac{\eta u}{E' R_{combined}}\right)^{0.65}\left(\frac{W}{E' R_{combined}^{\ 2}}\right)^{-0.21} \qquad \text{(A-iv)}$$

h_D = Squeeze film thickness, u = Relative surface velocity, η = Viscosity of 100% Ringers Solution and W = load (N).

Film Thickness Calculations Parameters	
Viscosity as water (η)	0.001 Pas
velocity (u)	0.004m/s
Force (W)	30N
Contact Radius (a)	0.0045m
Time (t)	60sec

Static Film Thickness (hs)	
Film Thickness after Static Loading (hs)	0.0023μm
Dynamic Film Thickness Range (hd)	
Dynamic Film Thickness Range - Maximum Value	0.1369μm
Dynamic Film Thickness Range - Minimum Value	0.0502μm

Table A-iv: Static and Dynamic Film thickness Parameters and Calculated Results

The calculation variables and results of both the static and dynamic calculations can be seen in table A-iv. These results can be compared with the combined root mean square surface roughness (R_{com}) calculated using equation A-v. The surface roughness (Ra) values for both articular cartilage and biphasic specimens were calculated from a random set (n=20) of surface profilometry measurements obtained using the process described in Chapter 2.

$$R_{com} = \sqrt{R_1^2 + R_2^2} \qquad \text{(A-v)}$$

R_1 = Average Cartilage Surface Roughness, R_2 = Average Biphasic Specimen Surface Roughness

Surface Roughness Parmeters	
Articular Cartilage Surface Roughness Value (R_1)	1.37μm
Average Hydrogel Surface Roughness Value (R_2)	0.343μm
Combine Surface Roughness Range	
Combine Surface Roughness (R_{Com})	1.412μm

Table A-v: Combined Surface Roughness Input Parameters and Calculated Range

The combined surface roughness (R_{com}) value (shown in table A-v) is greater than the maximum fluid film thickness value calculated thus it is reasonable to assume that all friction studies presented within this study act within a mixed or boundary lubrication regime.

Appendix B

B Cross Shear Ratio Calculation

Determination of the cross shear ratio was completed using the method as described by Galvin et al, which analysed the wear of cross-linked polyethylene under various tribological conditions *(Galvin et al., 2006)*. The addition of pin rotation to a reciprocating pin on plate experimental configuration, results in different points of the pin surface experiencing different relative motion, directional friction forces and thus different principle molecular orientation (PMO). Calculation of the PMO initially required the determination of the sliding track between a fixed point on the cartilage pin surface and plate specimen as shown schematically in Figure B-i. For each fixed element on the pin surface, the PMO direction was calculated as the slope average of the sliding track from the x-axis at the mid stroke with zero rotation (γ) as shown in Figure B-ii. A separate coordinate system (x',y') was allocated to the pin relative to the PMO.

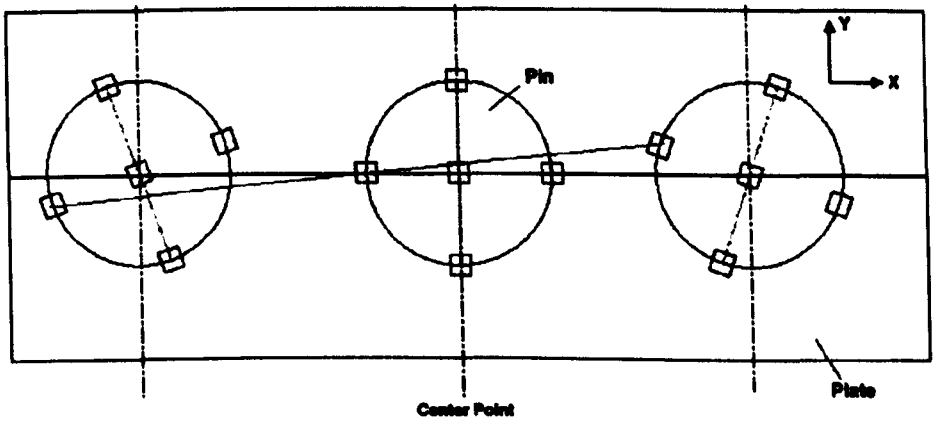

Figure B-i: Schematic Diagram demonstrating sliding track for a fixed point on the Cartilage pin surface

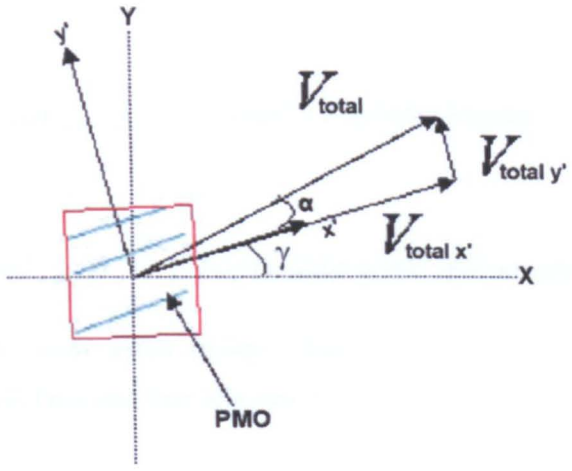

Figure B-ii: Principal molecular orientation (PMO) relative to the horizontal axis at the mid stroke (γ) for a fixed point on the polymer pin.

At any given point within the cycle, the total resultant velocity (V_{total}) between a fixed point on the cartilage pin and the plate specimen was determined from the individual rotation and reciprocating motions. The resultant velocity vector allowed the determination of frictional force direction (α), measured relative to the PMO (x',y') (Figure B-ii). This allowed both the resultant frictional force (F) and V_{total} to be resolved parallel and perpendicular to the PMO, thus taking into account the cartilage pin rotation. The frictional work (γw) was then calculated using Equations B-i.

$$d\gamma\omega_{x'} = F_{x'}V_{totalx'}.dt$$

$$d\gamma\omega_{y'} = F_{y'}V_{totaly'}.dt \qquad \textbf{(B-i)}$$

Frictional force = F, Total resultant velocity V_{total},

Frictional work = γw

At half a cycle ($^t/_2$), the frictional work corresponding to a pin rotational angle between $-\beta_o$, and β_o, which in this case were -10° and +10°, was integrated as shown in Equations B-ii.

$$\gamma\omega_{x'} = \int_0^{\frac{T}{2}} -F\cos\alpha V_{totalx'}\,dt \qquad \textit{- Parallel to the PMO direction}$$

$$\gamma\omega_{y'} = \int_0^{\frac{T}{2}} -F\sin\alpha V_{totaly'}\,dt \qquad \textit{- Perpendicular to the PMO direction} \qquad \textbf{(B-ii)}$$

Frictional force = F, Total resultant velocity = V_{total},

Frictional work =γw, Frictional force direction =α

A constant frictional force of 0.02 was assumed to represent articular cartilage on articular cartilage and for ease of calculation. The cross-shearing effect was assessed by defining the cross-shear ratio (*Cw*), based on the frictional work released perpendicular to and along the PMO. The corresponding equation (Equation B-iii) was evaluated numerically. The numbers of divisions in one cycle were finally chosen as 41 and 401 for determining the PMO and *Cw* respectively after mesh sensitivity checks. All the numerical analyses were carried out using Matlab7.0 (The Mathworks Inc, USA).

$$Cw = \frac{\int_0^{\frac{T}{2}} \sin\alpha V_{totaly'}\,dt}{\int_0^{\frac{T}{2}} \cos\alpha V_{totalx'}\,dt} \qquad \textbf{(B-iii)}$$

Cross-shear ratio =Cw, Total resultant velocity = V_{total},

Frictional force direction =α

For the experimental configuration within this study, both the PMO and the sliding track were mainly in the reciprocating direction. Therefore, the angle (α) between the PMO and the V_{total} was approximately the same as the rotation angle of the pin. This assumption allowed the simplification of Equation B-iii creating Equation B-iv which was presented by Wang et al but in a different form *(Wang, 2001)*. The average cross shear ratio for the whole cartilage pin was calculated by the averaging of 17 points distributed evenly

over the pin contact area. For a track length of 10 mm and overall rotation angle of $\pm 10^{o}$, the average cross shear ratio was 0.01.

$$Cw = \frac{\int_{0}^{\frac{T}{2}} \sin \alpha V_{totaly} \cdot dt}{\int_{0}^{\frac{T}{2}} \cos \alpha V_{totalx} \cdot dt} = \frac{2\beta_o - \sin(2\beta_o)}{2\beta_o + \sin(2\beta_o)} \qquad \textbf{(B-iv)}$$

Cross-shear ratio =Cw, Total resultant velocity = V_{total},

Frictional force direction =α, Range of pin rotational angle= β_o

Publications, Presentations and Awards

Publications

Title: Investigation of the friction and surface degradation of innovative chondroplasty materials against articular cartilage

Journal: Proceedings of the Institution of Mechanical Engineers, Part H, Journal of Engineering in Medicine.

Authors: E Northwood, R Kowalski and J Fisher

Status; Accepted and In Press

Title: A multi-directional *in vitro* investigation into friction, damage and wear of innovative chondroplasty materials against articular cartilage

Journal: Clinical Biomechanics

Authors: E Northwood and J Fisher,

Status; Accepted and In Press

Presentations

Title: An investigation of friction and wear of cartilage defect chondroplasty biomaterials in a cartilage on cartilage simulation model.

Orthopedic Research Society 2007

Authors: E Northwood, R Kowalski and J Fisher

Poster Presentation

Title: *In vitro* investigation into the effects of uni and multi-directional motion on the friction, damage and wear of innovative chondroplasty materials against articular cartilage

5th World Congress of Biomechanics in Munich

Authors: E Northwood and J Fisher

Podium Presentation

Winner of the European Society of Biomaterials Clinical Award 2006

Title: An *in vitro* investigation of wear and friction between two bi-phasic biomaterials and articular cartilage.
International Cartilage Repair Society Symposium
Authors: E Northwood, R Kowalski and J Fisher
Podium Presentation

Title: An *in vitro* investigation of wear and friction between a biphasic biomaterial and articular cartilage.
Orthopedic Research Society 2006
Authors: E Northwood, R Kowalski and J Fisher
Poster Presentation

Title: An *in vitro* investigation the Influence of Sliding Friction between biomaterials for Cartilage Substitution and Articular Cartilage
World Tribology Conference 2005
Authors: E Northwood, R Kowalski and J Fisher
Podium Presentation

Title: A Investigation into the Frictional Properties of Innovative Chondroplasty Materials
Institute of Mechanical Engineering Tribology 2005
Authors: E Northwood and J Fisher
Podium Presentation

References

Adams, M. E. (1993) An analysis of clinical studies of the use of crosslinked hyaluronan, hylan, in the treatment of osteoarthritis. *J Rheumatol Suppl,* 39, 16-8.

Anseth, K. S., Bowman, C. N. & Brannon-Peppas, L. (1996) Mechanical properties of hydrogels and their experimental determination. *Biomaterials,* 17, 1647-1657.

Armstrong, C. G. & Mow, V. C. (1982) Variations in the intrinsic mechanical properties of human articular cartilage with age, degeneration, and water content. *J Bone Joint Surg Am,* 64, 88-94.

Ashby, M. & Jones, D. (1995) *Engineering Materials 1*, Butterworth-Heinemann Ltd

Ateshian, G. A. (1997) A theoretical formulation for boundary friction in articular cartilage. *J Biomech Eng,* 119, 81-6.

Ateshian, G. A., Lai, W. M., Zhu, W. B. & Mow, V. C. (1994) An asymptotic solution for the contact of two biphasic cartilage layers. *J Biomech,* 27, 1347-60.

Ateshian, G. A. & Wang, H. (1995) A theoretical solution for the frictionless rolling contact of cylindrical biphasic articular cartilage layers. *J Biomech,* 28, 1341-55.

Athanasiou, K. A., Rosenwasser, M. P., Buckwalter, J. A., Malinin, T. I. & Mow, V. C. (1991) Interspecies comparisons of in situ intrinsic mechanical properties of distal femoral cartilage. *J Orthop Res,* 9, 330-40.

Barbucci, R., Lamponi, S., Borzacchiello, A., Ambrosio, L., Fini, M., Torricelli, P. & Giardino, R. (2002) Hyaluronic acid hydrogel in the treatment of osteoarthritis. *Biomaterials,* 23, 4503-13.

Barnett, C. H. D., D.V. Macconaill, M.V. (1961) *Synovial joints : their structure and mechanics,* London, Longmans.

Basalo, I. M., Mauck, R. L., Kelly, T. A., Nicoll, S. B., Chen, F. H., Hung, C. T. & Ateshian, G. A. (2004) Cartilage interstitial fluid load support in

unconfined compression following enzymatic digestion. *J Biomech Eng,* 126, 779-86.

Bavaresco, V. P., De Carvalho Zavaglia, C. A., De Carvalho Reis, M. & Malmonge, S. M. (2000) Devices for use as an artificial articular surface in joint prostheses or in the repair of osteochondral defects. *Artif Organs,* 24, 202-5.

Bavaresco, V. P., Zavaglia, C. A. C., Reis, M. C. & Gomes, J. R. (2004) Swelling and tribological properties of poly (HEMA) hydrogels. *Advanced Materials Forum II: proceedings of the II International Materials Symposium: Materials 2003 and XI Encontro Sociedade Portugesa de Materials, 2003 ATERIAIS, Apr 14-16 2003.* Caparica, Portugal, Trans Tech Publications Ltd, Zurich-Ueticon, Switzerland.

Bell, C. J., Ingham, E. & Fisher, J. (2006) Influence of hyaluronic acid on the time-dependent friction response of articular cartilage under different conditions. *Proc Inst Mech Eng [H],* 220, 23-31.

Benham Pp, Crawford Rj & Cg, A. (1996) *Mechanics of Engineering Materials,* Addison Wesley Longman Limited.

Bentley, G., Biant, L. C., Carrington, R. W., Akmal, M., Goldberg, A., Williams, A. M., Skinner, J. A. & Pringle, J. (2003) A prospective, randomised comparison of autologous chondrocyte implantation versus mosaicplasty for osteochondral defects in the knee. *J Bone Joint Surg Br,* 85, 223-30.

Berrien, L. S., Furey, M. J. & Veit, H. P. (2000) Tribological study of joint pathology. *Crit Rev Biomed Eng,* 28, 103-8.

Bigsby, R. J., Auger, D. D., Jin, Z. M., Dowson, D., Hardaker, C. S. & Fisher, J. (1998) A comparative tribological study of the wear of composite cushion cups in a physiological hip joint simulator. *Journal of Biomechanics,* 31, 363-9.

Bloebaum, R. D. & Wilson, A. S. (1980) The morphology of the surface of artcular cartilage in adult rats. *J Anat,* 131, 333-46.

Brandt, K. D., Smith, G. N., Jr. & Simon, L. S. (2000) Intraarticular injection of hyaluronan as treatment for knee osteoarthritis: what is the evidence? *Arthritis Rheum,* 43, 1192-203.

Briscoe, B. J. & Stolarski, T. A. (1985) Transfer wear of polymers during combined linear motion and load axis spin. *Wear,* 104, 121-37.

British Standards (1996) BS EN ISO 527-2:1996: Plastics. Determination of tensile properties. Test conditions for moulding and extrusion plastics.

British Standards (2004) BS ISO 14243-3:2004: Implants for surgery. Wear of total knee-joint prostheses. Loading and displacement parameters for wear-testing machines with displacement control and corresponding environmental conditions for test.

British Standards (2006) BS ISO 21509:2006: Plastics and ebonite. Verification of Shore durometers.

Broom, N. D. (1977) The stress/strain and fatigue behaviour of glutaraldehyde preserved heart-valve tissue. *Journal of Biomechanics,* 10, 707-24.

Brown, S., Worsfold, M. & Sharp, C. (2001) Microplate assay for the measurement of hydroxyproline in acid-hydrolyzed tissue samples. *Biotechniques,* 30, 38-40, 42.

Buckwalter, J. A. (1983) Articular cartilage. *Instr Course Lect,* 32, 349-70.

Buckwalter, J. A. (2002) Articular cartilage injuries. *Clin Orthop Relat Res,* 21-37.

Bullough, P. & Goodfellow, J. (1968) The significance of the fine structure of articular cartilage. *J Bone Joint Surg Br,* 50, 852-7.

Caravia, L., Dowson, D. & Fisher, J. (1993a) A Comparsion of friction in hydrogel and polyurathane materials for cushion-form joints. *Journal of Materials Science: Materials in Medicine,* 4, 515-520.

Caravia, L., Dowson, D. & Fisher, J. (1993b) Start up and steady state friction of thin polyurethane layers. *Wear,* 160, 191-197.

Caravia, L., Dowson, D., Fisher, J., Corkhill, P. H. & Tighe, B. J. (1995) Friction of hydrogel and polyurethane elastic layers when sliding

against each other under a mixed lubrication regime. *Wear,* 181-183, 236-240.

Chan, B., Donzelli, P. S. & Spilker, R. L. (2000) A mixed-penalty biphasic finite element formulation incorporating viscous fluids and material interfaces. *Ann Biomed Eng,* 28, 589-97.

Cherin, E., Saied, A., Laugier, P., Netter, P. & Berger, G. (1998) Evaluation of acoustical parameter sensitivity to age-related and osteoarthritic changes in articular cartilage using 50-MHz ultrasound. *Ultrasound Med Biol,* 24, 341-54.

Clar, C., Cummins, E., Mcintyre, L., Thomas, S., Lamb, J., Bain, L., Jobanputra, P. & Waugh, N. (2005) Clinical and cost-effectiveness of autologous chondrocyte implantation for cartilage defects in knee joints: systematic review and economic evaluation. *Health Technol Assess,* 9, iii-iv, ix-x, 1-82.

Clark, I. (2000) *Matrix Metalloproteinase, Methods in Molecular Biology, 151,* Humana Press.

Clarke, I. C. (1971) Articular cartilage: a review and scanning electron microscope study. 1. The interterritorial fibrillar architecture. *J Bone Joint Surg Br,* 53, 732-50.

Cooke, A. F., Dowson, D. & Wright, V. (1978) The pressure-viscosity characteristics of synovial fluid. *Biorheology,* 15, 129-35.

Cooper, J. R., Dowson, D. & Fisher, J. (1993) The effect of transfer film and surface roughness on the ear of lubricated ultra-high molecular weight polyethylene. *Clinical Materials,* 14, 295-302.

Corkhill, P. H., Hamilton, C. J. & Tighe, B. J. (1990a) The Design of Hydrogels for Medical Applications. 5, 363-436.

Corkhill, P. H., Trevett, A. S. & Tighe, B. J. (1990b) The potential of hydrogels as synthetic articular cartilage. *Proc Inst Mech Eng [H],* 204, 147-55.

Dagnall, H. (1986) *Exploring Surface Texture,* Leiester, Rank Taylor Hobson Limited.

Donnan, F. G. (1924) The theory of membrane equilibria. *Chem, Rev,* 1, 73-90.

Dowson, D., Fisher, J., Jin, Z. M., Auger, D. D. & Jobbins, B. (1991) Design considerations for cushion form bearings in artificial hip joints. *Proc Inst Mech Eng [H],* 205, 59-68.

Dowson, D. & Jin, Z. M. (1986) Micro-elastohydrodynamic lubrication of synovial joints. *Eng Med,* 15, 63-5.

Dowson, D., Wright, V. & Longfield, M. D. (1969) Human joint lubrication. *Biomed Eng,* 4, 160-5.

Edwards, J. (1966) Physical characteristics of articular cartilage. *Institution of Mechanical Engineers -- Proceedings,* 181, 16-24.

Ellis, A. J., Curry, V. A., Powell, E. K. & Cawston, T. E. (1994) The prevention of collagen breakdown in bovine nasal cartilage by TIMP, TIMP-2 and a low molecular weight synthetic inhibitor. *Biochem Biophys Res Commun,* 201, 94-101.

Elmore, S. & Sokoloff, L. (1963) Nature of impact elasticity of articular cartilage. *J.Appl. Physiology,* 18, 393,396.

Emery, I. H. & Meachim, G. (1973) Surface morphology and topography of patello-femoral cartilage fibrillation in Liverpool necropsies. *J Anat,* 116, 103-20.

Eyre, D. R. (1980) Collagen: molecular diversity in the body's protein scaffold. *Science,* 207, 1315-22.

Eyre, D. R. & Wu, J. J. (1995) Collagen structure and cartilage matrix integrity. *J Rheumatol Suppl,* 43, 82-5.

Felson, D. T., Lawrence, R. C., Dieppe, P. A., Hirsch, R., Helmick, C. G., Jordan, J. M., Kington, R. S., Lane, N. E., Nevitt, M. C., Zhang, Y., Sowers, M., Mcalindon, T., Spector, T. D., Poole, A. R., Yanovski, S. Z., Ateshian, G., Sharma, L., Buckwalter, J. A., Brandt, K. D. & Fries, J. F. (2000) Osteoarthritis: new insights. Part 1: the disease and its risk factors. *Ann Intern Med,* 133, 635-46.

Ferrandez, W. & Graindorge, S. L. (2003) Biphasic Surface Layer Lubrication of Cartilage, Surface Characterisation - A Presentation.

Flores, R. H. & Hochberg, M. C. (1998) Definition and Classification of Osteoarthritis. IN BRANDT, K. D. & LOHMANDER, L. S. (Eds.) *Osteoarthritis.* Oxford, Oxford Medical Press.

Forsey, R. (2003) Development of cartilage models for a tribological investigation of therapeutic lubricants in osteoarthritis *School of Mechanical Engineering Department.* Leeds University of Leeds

Forster, H. (1996) Mixed and Boundary Lubrication in Natural Synovial Joints. *Department of Mechanical Engineering.* Leeds, University of Leeds.

Forster, H. & Fisher, J. (1996) The influence of loading time and lubricant on the friction of articular cartilage. *Proc Inst Mech Eng,* 210, 109-119.

Forster, H. & Fisher, J. (1999) The influence of continuous sliding and subsequent surface wear on the friction of articular cartilage. *Proc Inst Mech Eng [H],* 213, 329-45.

Forster, H., Fisher, J., Dowson, D. & Wright, V. (1995) The effect of stationary loading on the friction and boundary lubrication of articular cartilage in the mixed lubricant regime. *Lubricants and Lubrication,* 71-83.

Foy, J. R., Williams, P. F., 3rd, Powell, G. L., Ishihara, K., Nakabayashi, N. & Laberge, M. (1999) Effect of phospholipidic boundary lubrication in rigid and compliant hemiarthroplasty models. *Proc Inst Mech Eng [H],* 213, 5-18.

Freeman, M. A. & Pinskerova, V. (2005) The movement of the normal tibio-femoral joint. *J Biomech,* 38, 197-208.

Freeman, M. A. E. A. (1979) *Adult Articular Cartilage,* London, Tunbridge Wells, Eng. : Pitman Medical.

Freeman, M. E., Furey, M. J., Love, B. J. & Hampton, J. M. (2000) Friction, wear, and lubrication of hydrogels as synthetic articular cartilage. *Wear,* 241, 129-135.

Galvin, A., Kang, L., Tipper, J., Stone, M., Ingham, E., Jin, Z. & Fisher, J. (2006) Wear of crosslinked polyethylene under different tribological conditions. *J Mater Sci Mater Med,* 17, 235-43.

Gardner, D. L. & Mcgillivray, D. C. (1971) Surface structure of articular cartilage. Historical review. *Ann Rheum Dis,* 30, 10-4.

Gardner, D. L., Salter, D. M. & Oates, K. (1997) Advances in the microscopy of osteoarthritis. *Microsc Res Tech,* 37, 245-70.

Gent, A. N. (1958) On the relation between Indentation Hardness and Young's Modulus. *Transactions I.R.I,* 34, 46-57.

George, A. F., Strozzi, A. & Rich, J. I. (1987) STRESS FIELDS IN A COMPRESSED UNCONSTRAINED ELASTOMERIC O-RING SEAL AND A COMPARISON OF COMPUTER PREDICTIONS AND EXPERIMENTAL RESULTS. *Tribology International,* 20, 237-247.

Ghadially, F. N., Yong, N. K. & Lalonde, J. M. (1982) A transmission electron microscopic comparison of the articular surface of cartilage processed attached to bone and detached from bone. *J Anat,* 135, 685-706.

Graindorge, S., Ferrandez, W., Jin, Z., Ingham, E., Grant, C., Twigg, P. & Fisher, J. (2005) Biphasic surface amorphous layer lubrication of articular cartilage. *Med Eng Phys,* 27, 836-44.

Graindorge, S. L. & Stachowiak, G. W. (2000) Changes occurring in the surface morphology of articular cartilage during wear. *Wear,* 241, 143-150.

Gray, H. (1918) *Anatomy of the Human Body*, PHILADELPHIA: LEA & FEBIGER.

Gross, A. E. (2003) Cartilage resurfacing: filling defects. *J Arthroplasty,* 18, 14-7.

Hamrock, B. & Dowson, D. (1978) Elastohydrodynamic Lubrication of Ellpitical Contacts for Materials of Low Elastic Modulus I - Fully Flooded Conjunction. *Journal of Lubrication Technology,* 100, 236-245.

Hangody, L., Feczko, P., Bartha, L., Bodo, G. & Kish, G. (2001) Mosaicplasty for the treatment of articular defects of the knee and ankle. *Clin Orthop Relat Res,* 2, S328-36.

Hardingham, T. E., Beardmore-Gray, M., Dunham, D. G. & Ratcliffe, A. (1986) Cartilage Proteoglycans. IN EVARED, D. & WHELAN, J. (Eds.) *Functions of the Proteoglycans.* London, John Wiley and Sons.

Harkness, R. D. (1968) Mechanical Properties of Collagen Tissues. IN GOULD, B. S. (Ed.) *Biology of Collagen.* London, New YOrk, Academic Press.

Hayes, A., Harris, B., Dieppe, P. A. & Clift, S. E. (1993) Wear of articular cartilage: the effect of crystals. *Proc Inst Mech Eng [H],* 207, 41-58.

Hertz, H. (1890) Electro dynamics of stationary bodies. *Electrical World.*

Higaki, H. & Murakami, T. (1994) Role of constituents in synovial fluid and surface layer of the articular cartilage in joint lubrication (part 1): Experimental study in application of enzyme digestion. *Japanese Journal of Tribology,* 39, 859 - 869.

Higaki, H. & Murakami, T. (1995) Role of constituents in synovial fluid and surface layer articular cartilage in joint lubrication (part2): The boundary lubricating ability of proteins. *Japanese Journal of Tribology,* 40, 691-700.

Higaki, H., Murakami, T., Nakanishi, Y., Miura, H., Mawatari, T. & Iwamoto, Y. (1998) The lubricating ability of biomembrane models with dipalmitoyl phosphatidylcholine and gamma-globulin. *Proc Inst Mech Eng [H],* 212, 337-46.

Hills, B. A. (1988) *The Biology of Surfactant,* Cambridge, Cambridge University Press.

Hills, B. A. (1990) Oligolamellar nature of the articular surface. *J Rheumatol,* 17, 349-56.

Hills, B. A. (2000) Boundary lubrication in vivo. *Proc Inst Mech Eng [H],* 214, 83-94.

Hills, B. A. (2002a) Identity of the joint lubricant. *J Rheumatol,* 29, 200-1.

Hills, B. A. (2002b) Surface-active phospholipid: a Pandora's box of clinical applications. Part I. The lung and air spaces. *Intern Med J,* 32, 170-8.

Hills, B. A. & Butler, B. D. (1984) Surfactants identified in synovial fluid and their ability to act as boundary lubricants. *Ann Rheum Dis,* 43, 641-8.

Hills, B. A. & Crawford, R. W. (2003) Normal and prosthetic synovial joints are lubricated by surface-active phospholipid: a hypothesis. *J Arthroplasty,* 18, 499-505.

Hills, B. A. & Thomas, K. (1998) Joint stiffness and 'articular gelling': inhibition of the fusion of articular surfaces by surfactant. *Br J Rheumatol,* 37, 532-8.

Hou, J. S., Holmes, M. H., Lai, W. M. & Mow, V. C. (1989) Boundary conditions at the cartilage-synovial fluid interface for joint lubrication and theoretical verifications. *J Biomech Eng,* 111, 78-87.

Hunter, W. (1743) Of the structure and disease of articulaing cartilage. *Philos Trans R Soc Lond,* 42, 514-521.

Hunziker, E. B. (2002) Articular cartilage repair: basic science and clinical progress. A review of the current status and prospects. *Osteoarthritis and Cartilage,* 10, 432-463.

Hutchings, I. M. (1992) *Tribology: Friction and wear of engineering materials,* Oxford, Butterworth-Heinemann.

Ikeuchi, K. (1995) The role of synovial fluid in joint lubrication. *Lubricants and Lubrication,* 30, 65-69.

Iwaki, H., Pinskerova, V. & Freeman, M. A. (2000) Tibiofemoral movement 1: the shapes and relative movements of the femur and tibia in the unloaded cadaver knee. *J Bone Joint Surg Br,* 82, 1189-95.

Jaffre, B., Watrin, A., Loeuille, D., Gillet, P., Netter, P., Laugier, P. & Saied, A. (2003) Effects of antiinflammatory drugs on arthritic cartilage: a high-frequency quantitative ultrasound study in rats. *Arthritis Rheum,* 48, 1594-601.

Jay, G. D. (1992a) Characterization of a bovine synovial fluid lubricating factor. I. Chemical, surface activity and lubricating properties. *Connect Tissue Res,* 28, 71-88.

Jay, G. D. (1992b) Characterization of a bovine synovial fluid lubricating factor. I. Chemical, surface activity and lubricating properties. *Connect Tissue Res,* 28, 71-88.

Jay, G. D., Britt, D. E. & Cha, C. J. (2000) Lubricin is a product of megakaryocyte stimulating factor gene expression by human synovial fibroblasts. *J Rheumatol,* 27, 594-600.

Jay, G. D. & Cha, C. J. (1999) The effect of phospholipase digestion upon the boundary lubricating ability of synovial fluid. *J Rheumatol,* 26, 2454-7.

Jay, G. D., Haberstroh, K. & Cha, C. J. (1998) Comparison of the boundary-lubricating ability of bovine synovial fluid, lubricin, and Healon. *J Biomed Mater Res,* 40, 414-8.

Jay, G. D., Harris, D. A. & Cha, C. J. (2001a) Boundary lubrication by lubricin is mediated by O-linked beta(1-3)Gal-GalNAc oligosaccharides. *Glycoconj J,* 18, 807-15.

Jay, G. D., Tantravahi, U., Britt, D. E., Barrach, H. J. & Cha, C. J. (2001b) Homology of lubricin and superficial zone protein (SZP): products of megakaryocyte stimulating factor (MSF) gene expression by human synovial fibroblasts and articular chondrocytes localized to chromosome 1q25. *J Orthop Res,* 19, 677-87.

Jin, Z. M., Dowson, D. & Fisher, J. (1991) Stress analysis of cushion form bearings for total hip replacements. *Proc Inst Mech Eng [H],* 205, 219-26.

Jin, Z. M., Pickard, J. E., Forster, H., Ingham, E. & Fisher, J. (2000) Frictional behaviour of bovine articular cartilage. *Biorheology,* 37, 57-63.

Jones, E. S. (1934) Joint lubrication. *The Lancet,* 223, 1426-1427.

Jones, E. S. (1936) Joint lubrication. *The Lancet,* 227, 1043-1045.

Joyce, T. J. (2005) The wear of two orthopaedic biopolymers against each other. *Journal of biomaterials and biomechanics,* 3, 141-146.

Katta, J. K., Jin, Z., Ingham, E. & Fisher, J. (2006) Effect of Glycosaminoglycan (GAG) Depletion on Cartilage Friction under

Various Tribological Conditions. *World Congress of Biomechanics.* Munich.

Katta, J. K., Marcolongo, M. S., Lowman, A. M. & Mansmann, K. A. (2004) Friction and wear characteristics of PVA/PVP hydrogels as synthetic articular cartilage. *Bioengineering Conference, 2004. Proceedings of the IEEE 30th Annual Northeast.*

Kingston, B. (2000) *Understanding Joints: A practical guide to thier structure and function*, Stanley Thornes Ltd.

Kobayashi, S., Yonekubo, S. & Kurogouchi, Y. (1995) Cryoscanning electron microscopic study of the surface amorphous layer of articular cartilage. *J Anat,* 187 (Pt 2), 429-44.

Kobayashi, S., Yonekubo, S. & Kurogouchi, Y. (1996) Cryoscanning electron microscopy of loaded articular cartilage with special reference to the surface amorphous layer. *J Anat,* 188 (Pt 2), 311-22.

Korossis, S. A., Booth, C., Wilcox, H. E., Watterson, K. G., Kearney, J. N., Fisher, J. & Ingham, E. (2002) Tissue engineering of cardiac valve prostheses II: biomechanical characterization of decellularized porcine aortic heart valves. *J Heart Valve Dis,* 11, 463-71.

Korossis, S. A., Wilcox, H. E., Watterson, K. G., Kearney, J. N., Ingham, E. & Fisher, J. (2005) In-vitro assessment of the functional performance of the decellularized intact porcine aortic root. *J Heart Valve Dis,* 14, 408-21; discussion 422.

Krishnan, R., Caligaris, M., Mauck, R. L., Hung, C. T., Costa, K. D. & Ateshian, G. A. (2004a) Removal of the superficial zone of bovine articular cartilage does not increase its frictional coefficient. *Osteoarthritis Cartilage,* 12, 947-55.

Krishnan, R., Kopacz, M. & Ateshian, G. A. (2004b) Experimental verification of the role of interstitial fluid pressurization in cartilage lubrication. *Journal of Orthopaedic Research,* 22, 565-570.

Krishnan, R., Mariner, E. N. & Ateshian, G. A. (2005) Effect of dynamic loading on the frictional response of bovine articular cartilage. *Journal of Biomechanics,* 38, 1665-1673.

Kumar, P., Oka, M., Toguchida, J., Kobayashi, M., Uchida, E., Nakamura, T. & Tanaka, K. (2001) Role of uppermost superficial surface layer of articular cartilage in the lubrication mechanism of joints. *J Anat,* 199, 241-50.

Kuster, M. S., Podsiadlo, P. & Stachowiak, G. W. (1998) Shape of wear particles found in human knee joints and their relationship to osteoarthritis. *Br J Rheumatol,* 37, 978-84.

Lafortune, M. A., Cavanagh, P. R., Sommer, H. J., 3rd & Kalenak, A. (1992) Three-dimensional kinematics of the human knee during walking. *J Biomech,* 25, 347-57. Show: 5 10 20 50 100 200 500 Sort Author Journal Pub Date Text File.

Lai, W. M., Hou, J. S. & Mow, V. C. (1991) A triphasic theory for the swelling and deformation behaviors of articular cartilage. *J Biomech Eng,* 113, 245-58.

Levens, A. I., Ts. Blosser, Ja (1948) Transverse rotation of the segments of the lower extremity in locomotion. *Journal of bone and joint surgery. American volume,* 30-A, 859.

Lewis, P. R. & Mccutchen, C. W. (1959) Experimental evidence for weeping lubrication in mammalian joints. *Nature,* 184, 1285-1285.

Linn, F. C. (1967) Lubrication of animal joints. I. The arthrotripsometer. *J Bone Joint Surg Am,* 49, 1079-98.

Linn, F. C. (1968) Lubrication of animal joints. II. The mechanism. *J Biomech,* 1, 193-205.

Linn, F. C. & Radin, E. L. (1968) Lubrication of animal joints. 3. The effect of certain chemical alterations of the cartilage and lubricant. *Arthritis Rheum,* 11, 674-82.

Lipshitz, H., Etheredge, R., 3rd & Glimcher, M. J. (1976) Changes in the hexosamine content and swelling ratio of articular cartilage as functions of depth from the surface. *J Bone Joint Surg Am,* 58, 1149-53.

Lipshitz, H., Etheredge, R., 3rd & Glimcher, M. J. (1980) In vitro studies of the wear of articular cartilage--III. The wear characteristics of

chemical modified articular cartilage when worn against a highly polished characterized stainless steel surface. *J Biomech,* 13, 423-36.

Lipshitz, H. & Glimcher, M. J. (1979) In vitro studies of the wear of articular cartilage. II. Characteristics of the wear of articular cartilage when worn against stainless steel plates having characterized surfaces. *Wear,* 52, 297-339.

Longfield, M. D., Dowson, D., Walker, P. S. & Wright, V. (1969) "Boosted lubrication" of human joints by fluid enrichment and entrapment. *Biomed Eng,* 4, 517-22.

Lotz, M. (2001) Cytokines in cartilage injury and repair. *Clin Orthop,* S108-15.

Lyyra, T., Arokoski, J. P., Oksala, N., Vihko, A., Hyttinen, M., Jurvelin, J. S. & Kiviranta, I. (1999) Experimental validation of arthroscopic cartilage stiffness measurement using enzymatically degraded cartilage samples. *Phys Med Biol,* 44, 525-35.

Mabuchi, K., Tsukamoto, Y., Obara, T. & Yamaguchi, T. (1994) The effect of additive hyaluronic acid on animal joints with experimentally reduced lubricating ability. *J Biomed Mater Res,* 28, 865-70.

Macconaill, M. A. (1932) The Function of Intra-Articular Fibrocartilages, with Special Reference to the Knee and Inferior Radio-Ulnar Joints. *J Anat,* 66, 210-227.

Macirowski, T., Tepic, S. & Mann, R. W. (1994) Cartilage stresses in the human hip joint. *J Biomech Eng,* 116, 10-8.

Mak, A. F., Lai, W. M. & Mow, V. C. (1987) Biphasic indentation of articular cartilage--I. Theoretical analysis. *J Biomech,* 20, 703-14.

Mankin, H. J. & Thrasher, A. Z. (1975) Water content and binding in normal and osteoarthritic human cartilage. *J Bone Joint Surg Am,* 57, 76-80.

Maroudas, A. & Holborow, E. (1980) *Studies in Joint Disease Vol 1.*

Maroudas, A. I. (1976) Balance between swelling pressure and collagen tension in normal and degenerate cartilage. *Nature,* 260, 808-9.

Massey, B. S. (1968) *Mechanics of fluids,* London: Princeton, N.J, Chapman and Hall.

Mazzucco, D., Mckinley, G., Scott, R. D. & Spector, M. (2002) Rheology of joint fluid in total knee arthroplasty patients. *J Orthop Res,* 20, 1157-63.

Mccutchen, C. W. (1959) Sponge hydrostatic and weeping bearings. *Nature,* 184, 1284-1285.

Mccutchen, C. W. (1962) The frictional properties of animal joints. *Wear,* 5, 1-17.

Mccutchen, C. W. (1966) Boundary lubrication by synovial fluid demonstration and possible osmiotic explantion. *Fed Proc,* 25, 1061-1068.

Mccutchen, C. W. (1969) More on Weeping Lubrication:Experiments with Hydron, A Microporous Polyhydroxyalkylacrylic Ester Resin. IN WRIGHT, V. (Ed.) *In 'Lubrication and Wear in Joints'.* Sector.

Meachim, G. (1975) Cartilage fibrillation at the ankle joint in Liverpool necropsies. *J Anat,* 119, 601-10.

Meachim, G., Denham, D., Emery, I. H. & Wilkinson, P. H. (1974) Collagen alignments and artificial splits at the surface of human articular cartilage. *J Anat,* 118, 101-18.

Meachim, G. & Fergie, I. A. (1975) Morphological patterns of articular cartilage fibrillation. *J Pathol,* 115, 231-40.

Medley, J. (1980) Hydrophillic polyurethane elastomers for hemiarthroplasty:a preliminary in virtro wear study. *Eng Med,* 9, 59-65.

Meyer, E. (1908) Hardness testing and hardness. *Zeitschrift des Vereines Deutscher Ingenieure,* 52, 645-654.

Minas, T. & Nehrer, S. (1997) Current concepts in the treatment of articular cartilage defects. *Orthopedics,* 20, 525-38.

Morrell, K. C., Hodge, W. A., Krebs, D. E. & Mann, R. W. (2005) Corroboration of in vivo cartilage pressures with implications for synovial joint tribology and osteoarthritis causation. *PNAS,* 102, 14819-14824.

Morrison, J. B. (1970) The mechanics of the knee joint in relation to normal walking. *Journal of Biomechanics,* 3, 51-61.

Moss, M. L. & Moss, S. L. (1983) Cartilage Structure, Function and Biochemistry. IN HALL, B. K. (Ed.) *Cartilage.* New York, Accademic Press.

Mow, V. C. (1986) Biomechanics of articular cartilage. IN FRANKEL, N. A. (Ed.) *Basic Biomechanics of the Musculo-Skeletal system.* London, Leafebeyer.

Mow, V. C., Gibbs, M. C., Lai, W. M., Zhu, W. B. & Athanasiou, K. A. (1989) Biphasic indentation of articular cartilage--II. A numerical algorithm and an experimental study. *J Biomech,* 22, 853-61.

Mow, V. C. & Hayes, W. C. (1997) Basic Orthopeadic Biomechanics. 2nd ed., Lippincott-Raven.

Mow, V. C., Holmes, M. H. & Lai, W. M. (1984) Fluid transport and mechanical properties of articular cartilage: a review. *J Biomech,* 17, 377-94.

Mow, V. C., Kuei, S. C., Lai, W. M. & Armstrong, C. G. (1980a) Biphasic creep and stress relaxation of articular cartilage in compression? Theory and experiments. *J Biomech Eng,* 102, 73-84.

Mow, V. C. & Lai, W. M. (1980) Recent developments in synovial joint biomechanics. *SIAM Review,* 22, 275-317.

Mow, V. C., Lai, W. M. & Redler, I. (1974) Some surface characteristics of articular cartilage--I. A scanning electron microscopy study and a theoretical model for the dynamic interaction of synovial fluid and articular cartilage. *Journal of Biomechanics,* 7, 449-456.

Mow, V. C., Proctor, C. S. & Kelly, M. A. (1980b) Biomechanics of Articular Cartilage. IN NORDIN, M. & FRANKEL, V. H. (Eds.) *Basic Biomechanics of the Musculoskeletal System.* second ed. Philadelphia, Lea & Febiger.

Mow, V. C., Ratcliffe, A. & Poole, A. R. (1992) Cartilage and diarthrodial joints as paradigms for hierarchical materials and structures. *Biomaterials,* 13, 67-97.

Mow, V. C., Ratcliffe, A. & S.L.Y, W. (1990a) *Biomechanics of Diarthrodial Joints - Vol 2*, New York ; London : Springer.

Mow, V. C., Ratcliffe, A. & S.L.Y, W. (1990b) *Biomechanics of Diarthrodial Joints -Vol 1, London : Springer.*

Mow, V. C., Ratcliffe, A. & S.L.Y, W. (1990c) *Biomechanics of Diarthrodial Joints -Vol 1*, New York ; London : Springer.

Mow, V. C., Wang, C. C. & Hung, C. T. (1999) The extracellular matrix, interstitial fluid and ions as a mechanical signal transducer in articular cartilage. *Osteoarthritis Cartilage,* 7, 41-58.

Muir, H. (1983) Proteoglycans as organizers of the intercellular matrix. *Biochem Soc Trans,* 11, 613-22.

Muir, I. H. (1980) Biochemistry of articular cartilage in rheumatic diseases. *Scand J Rheumatol Suppl,* 38, 25-9.

Murakami, T., Sawae, Y. & Ihara, M. (2003) Protective Mechanism of articular cartilage to Severe Loading : Roles of Lubricants Cartilage Surface Layers, Extracellular matrix and Chondrocytes. *JSME,* 46, 594-603.

Naka, M. H., Hattori, K. & Ikeuchi, K. (2006) Evaluation of the superficial characteristics of articular cartilage using evanescent waves in the friction tests with intermittent sliding and loading. *J Biomech,* 39, 2164-70.

Newman, A. P. (1998) Articular cartilage repair. *Am J Sports Med,* 26, 309-24.

Nimni, M. E. (1988) The cross-linking and structure modification of the collagen matrix in the design of cardiovascular prosthesis. *J Card Surg,* 3, 523-33.

Norkin, C. C. & Levingie, P. K. (1983) *Joint Structure and Function: A comprehensive analysis,* Philadelphia, Philadelphia : F.A. Davis, c1983.

Obrink, B. (1973) A study of the interactions between monomeric tropocollagen and glycosaminoglycans. *Eur J Biochem,* 33, 387-400.

Oka, M. (2001) Biomechanics and repair of articular cartilage. *J Orthop Sci,* 6, 448-56.

Oka, M., Noguchi, T., Kumar, P., Ikeuchi, K., Yamamuro, T., Hyon, S. H. & Ikada, Y. (1990) Development of an artificial articular cartilage. *Clin Mater,* 6, 361-81.

Oka, M., Ushio, K., Kumar, P., Ikeuchi, K., Hyon, S. H., Nakamura, T. & Fujita, H. (2000) Development of artificial articular cartilage. *Proc Inst Mech Eng [H],* 214, 59-68.

Oka, Y. I., Sakohara, S., Gotoh, T., Iizawa, T., Okamoto, K. & Doi, H. (2004) Measurements of mechanical properties on a swollen hydrogel by a tension test method. *Polymer Journal,* 36, 59-63.

Ozturk, H. E., Stoffel, K. K., Jones, C. F. & Stachowiak, G. W. (2004a) The Effect of Surface-Active Phospholipids on the Lubrication of Osteoarthritic Sheep Knee Joints: Friction. *Tribology Letters,* 16, 283-289.

Ozturk, H. E., Stoffel, K. K., Jones, C. F. & Stachowiak, G. W. (2004b) The effect of surface-active phospholipids on the lubrication of osteoarthritic sheep knee joints: friction. *Tribology Letters,* 16, 283-9.

Panayi, G. (1982) *Scientific Basis of Rheumatology*, Churchill Livingstone.

Patwari, P., Cook, M. N., Dimicco, M. A., Blake, S. M., James, I. E., Kumar, S., Cole, A. A., Lark, M. W. & Grodzinsky, A. J. (2003) Proteoglycan degradation after injurious compression of bovine and human articular cartilage in vitro: interaction with exogenous cytokines. *Arthritis Rheum,* 48, 1292-301.

Paul, J. P. (1966) Forces transmitted by joints in human body. *Institution of Mechanical Engineers -- Proceedings of Lubrication and Wear in Living and Artificial Human Joints,* 181, 8-15.

Pawaskar, S. S. (2006) Contact mechanics modelling of articular cartilage and applications. *Institute of Biological and Medical Engineering, School of Mechanical Engineering.* Leeds, The University of Leeds.

Pellaumail, B., Watrin, A., Loeuille, D., Netter, P., Berger, G., Laugier, P. & Saied, A. (2002) Effect of articular cartilage proteoglycan depletion

on high frequency ultrasound backscatter. *Osteoarthritis Cartilage,* 10, 535-41.

Peppas, N. A. (2004) Hydrogels. IN RATNER, B. D., HOFFMAN, A., SCHOEN, F. & LEMONS, J. (Eds.) *Biomaterials Science: An Introduction to Materials in Medicine.* 2nd ed. London, Elsevier Academic Press.

Pickard, J., Fisher, J., Ingham, E., Egan, J. & Hallett, J. (2000) Investigation into the tribological condition of acetabular tissue after bipolar joint replacement hip surgery. *Proc Inst Mech Eng [H],* 214, 361-70.

Pickard, J., Ingham, E., Egan, J. & Fisher, J. (1998a) Investigation into the effect of proteoglycan molecules on the tribological properties of cartilage joint tissues. *Proc Inst Mech Eng [H],* 212, 177-82.

Pickard, J. E., Fisher, J., Ingham, E. & Egan, J. (1998b) Investigation into the effects of proteins and lipids on the frictional properties of articular cartilage. *Biomaterials,* 19, 1807-12.

Pratta, M. A., Yao, W., Decicco, C., Tortorella, M. D., Liu, R. Q., Copeland, R. A., Magolda, R., Newton, R. C., Trzaskos, J. M. & Arner, E. C. (2003) Aggrecan protects cartilage collagen from proteolytic cleavage. *J Biol Chem,* 278, 45539-45.

Reimann, I., Stougaard, J., Northeved, A. & Johnsen, S. J. (1975) Demonstration of boundary lubrication by synovial fluid. *Acta Orthop Scand,* 46, 1-10.

Reynolds, O. (1886) On the Theory of Lubrication and Its Application to Mr. Beauchamp Tower's Experiments, Including an Experimental Determination of the Viscosity of Olive Oil. *Philosophical Transactions of the Royal Society of London (1776-1886),* 177, 157-234.

Robert, H. (2001) Techniques of chondral and osteochondral repair in the knee. *European Journal of Orthopaedic Surgery & Traumatology,* 11,, 97-102.

Roberts, B. J., Unsworth, A. & Mian, N. (1982) Modes of lubrication in human hip joints. *Ann Rheum Dis,* 41, 217-24.

Rosenberg, L. (1975) Structure of Cartilage Proteoglycans. IN BURLEIGH, P. M. C. & POOLE, A. R. (Eds.) *Dynamics Of Connective Tissue Macromolecules.* Amsterdam, North Holand Publishing.

Saarakkala, S., Laasanen, M. S., Hirvonen, J., Nieminen, H. J., Jurvelin, J. S. & Toyras, J. (2004) Ultrasound backscatter detects sensitively early degeneration of cartilage surface. *ORS 2004 Presentation.*

Sarma, A. V., Powell, G. L. & Laberge, M. (2001) Phospholipid composition of articular cartilage boundary lubricant. *J Orthop Res,* 19, 671-6.

Sasada, T., Takahashi, M., Watakabe, M., Mabuchi, K., Tuskamoto, Y. & Nanba, M. (1985) Frictinoal behaviour of a total hip prosthesis containing artificial articular cartilage. *Journal of Japanese Society of Biomaterials,* 3, 151-157.

Sayles, R. S., Thomas, T. R., Anderson, J., Haslock, I. & Unsworth, A. (1979) Measurement of the surface microgeometry of articular cartilage. *J Biomech,* 12, 257-67.

Schmidt, M. B., Mow, V. C., Chun, L. E. & Eyre, D. R. (1990) Effects of proteoglycan extraction on the tensile behavior of articular cartilage. *J Orthop Res,* 8, 353-63.

Schmidt, T. A. & Sah, R. L. (2006) Effect of synovial fluid on boundary lubrication of articular cartilage. *Osteoarthritis Cartilage,* 15, 35-47.

Scholes, S. C. & Unsworth, A. (2001) Pin-on-plate studies on the effect of rotation on the wear of metal-on-metal samples. *J Mater Sci Mater Med,* 12, 299-303.

Schwalbe, H. J., Bamfaste, G. & Franke, R. P. (1999) Non-destructive and non-invasive observation of friction and wear of human joints and of fracture initiation by acoustic emission. *Proc Inst Mech Eng [H],* 213, 41-8.

Shepherd, D. E. T. (1997) The compressive modulus of human articular cartilage in joints of the lower limb determined under physiological loading conditions. *Research School of Medicine.* Leeds, University of Leeds.

Shibakawa, A., Aoki, H., Masuko-Hongo, K., Kato, T., Tanaka, M., Nishioka, K. & Nakamura, H. (2003) Presence of pannus-like tissue on osteoarthritic cartilage and its histological character. *Osteoarthritis Cartilage,* 11, 133-40.

Speer, K. P., Callaghan, J. J., Seaber, A. V. & Tucker, J. A. (1990) The effects of exposure of articular cartilage to air. A histochemical and ultrastructural investigation. *J Bone Joint Surg Am,* 72, 1442-50.

Stachowiak, G. W., Batchelor, A. W. & Griffiths, L., J (1994) Friction and Wear changes in synovial joints. *Wear,* 171, 135-142.

Stachowiak, G. W. & Podsiadlo, P. (1997) Analysis of wear particle boundaries found in sheep knee joints during in vitro wear tests without muscle compensation. *J Biomech,* 30, 415-9.

Stammen, J. A., Williams, S., Ku, D. N. & Guldberg, R. E. (2001) Mechanical properties of a novel PVA hydrogel in shear and unconfined compression. *Biomaterials,* 22, 799-806.

Staubli, H.-U., Durrenmatt, U., Porcellini, B. & Rauschning, W. (1999) Anatomy and surface geometry of the patellofemoral joint in the axial plane

10.1302/0301-620X.81B3.8758. *J Bone Joint Surg Br,* 81-B, 452-458.

Stockwell, R. A. (1979) *Biology of Cartilage Cells,* Cambridge, New York, Cambridge University Press.

Swann, A. C. & Seedhom, B. B. (1989) Improved techniques for measuring the indentation and thickness of articular cartilage. *Proc Inst Mech Eng [H],* 203, 143-50.

Swann, D. A., Hendren, R. B., Radin, E. L., Sotman, S. L. & Duda, E. A. (1981a) The lubricating activity of synovial fluid glycoproteins. *Arthritis Rheum,* 24, 22-30.

Swann, D. A., Silver, F. H., Slayter, H. S., Stafford, W. & Shore, E. (1985) The molecular structure and lubricating activity of lubricin isolated from bovine and human synovial fluids. *Biochem J,* 225, 195-201.

Swann, D. A., Slayter, H. S. & Silver, F. H. (1981b) The molecular structure of lubricating glycoprotein-I, the boundary lubricant for articular cartilage. *J Biol Chem,* 256, 5921-5.

Tandon, P. N., Gupta, R. S., Dwivedi, A. P., Banerjee, M. B. & Dube, S. N. (1983) Effect of rotation in the lubrication of a short porous journal bearing: a simple model for hip joints. . *Wear,* 87, 123-131.

Tipper, J. L., Firkins, P. J., Ingham, E., Fisher, J., Stone, M. H. & Farrar, R. (1999) Quantitative analysis of the wear and wear debris from low and high carbon content cobalt chrome alloys used in metal on metal total hip replacements. *J Mater Sci Mater Med,* 10, 353-62.

Toyras, J., Laasanen, M. S., Saarakkala, S., Lammi, M. J., Rieppo, J., Kurkijarvi, J., Lappalainen, R. & Jurvelin, J. S. (2003) Speed of sound in normal and degenerated bovine articular cartilage. *Ultrasound Med Biol,* 29, 447-54.

Unsworth, A. (1987) Soft layer lubrciaotin of artifical hip joints. *Proc. of Int'l Conference on 'Tribology - friction, lubrication and wear: Fifty year on',* C219/87.

Unsworth, A. (1991) Tribology of human and artificial joints. *Proc Inst Mech Eng [H],* 205, 163-72.

Unsworth, A., Dowson, D. & Wright, V. (1975) Some new evidence on human joint lubrication. *Ann Rheum Dis,* 34, 277-85.

Urban, J. P. (1994) The chondrocyte: a cell under pressure. *Br J Rheumatol,* 33, 901-8.

Vynios, D. H., Papageorgakopoulou, N., Sazakli, H. & Tsiganos, C. P. (2001) The interactions of cartilage proteoglycans with collagens are determined by their structures. *Biochimie,* 83, 899-906.

Wachtel, E. & Maroudas, A. (1998) The effects of pH and ionic strength on intrafibrillar hydration in articular cartilage. *Biochim Biophys Acta,* 1381, 37-48.

Walker, P. S., Dowson, D., Longfield, M. D. & Wright, V. (1968) "Boosted lubrication" in synovial joints by fluid entrapment and enrichment. *Ann Rheum Dis,* 27, 512-20.

Walker, P. S., Dowson, D., Longfield, M. D. & Wright, V. (1969) Lubrication of human joints. *Ann Rheum Dis,* 28, 194.

Walker, P. S. & Gold, B. L. (1971) The tribology (friction, lubrication and wear) of all-metal artificial hip joints. *Wear,* 285-299.

Walker, P. S., Unsworth, A., Dowson, D., Sikorski, J. & Wright, V. (1970) Mode of aggregation of hyaluronic acid protein complex on the surface of articular cartilage. *Ann Rheum Dis,* 29, 591-602.

Wang, A. (2001) A unified theory of wear for ultra-high molecular weight polyethylene in multi-directional sliding. *Wear,* 248, 38-47.

Wang, A., Essner, A., Polineni, V., Sun, D., Stark, C. & Dumbleton, J. (1997) Lubrication and wear of ultra-high molecular weight polyethylene in total joint replacements. *Howmedica, Inc. Pfizer Medical Technology Group, Rutherford, New Jersey, USA.*

Weidow, J., Pak, J. & Karrholm, J. (2002) Different patterns of cartilage wear in medial and lateral gonarthrosis. *Acta Orthop Scand,* 73, 326-9.

Weightman, B. O., Freeman, M. A. R. & Swanson, S. A. V. (1973) Fatigue of Articular Cartilage. 244, 303-304.

Wells, T., Davidson, C., Morgelin, M., Bird, J. L., Bayliss, M. T. & Dudhia, J. (2003) Age-related changes in the composition, the molecular stoichiometry and the stability of proteoglycan aggregates extracted from human articular cartilage. *Biochem J,* 370, 69-79.

Williams, S., Jalali-Vahid, D., Brockett, C., Jin, Z., Stone, M. H., Ingham, E. & Fisher, J. (2006) Effect of swing phase load on metal-on-metal hip lubrication, friction and wear. *Journal of Biomechanics,* 39, 2274-2281.

Wright, V. & Dowson, D. (1976) Lubrication and cartilage. *J Anat,* 121, 107-18.

Wright, V. & Radin, E. L. (1993) *Mechanics of Human Joints*, New York : Marcel Dekker.

Wyke, B. (1967) The neurology of joints. *Ann R Coll Surg Engl,* 41, 25-50.

Yao, J. Q., Laurent, M. P., Johnson, T. S., Blanchard, C. R. & Crowninshield, R. D. (2003) The influences of lubricant and material on polymer/CoCr sliding friction. *Wear,* 255, 780-784.